SELECTIVE HYDROGENATION OF α,β-UNSATURATED ALDEHYDES TOWARDS CLEAN SYNTHESIS OVER NOBLE METAL CATALYSTS IN MASS TRANSFER EFFICIENT THREE PHASE REACTORS

By

LAIQI ZHANG

A Thesis Submitted to The Faculty of Engineering of The University of Birmingham for the Degree of DOCTOR OF PHILOSOPHY

School of Chemical Engineering
The University of Birmingham
Edgbaston
Birmingham B15 2TT
United Kingdom

October 1997

Synopsis

The hydrodynamics and mass transfer characteristics of a cocurrent downflow contactor (CDC) are studied in this work in order to investigate the viability of this bubble column as a catalytic reactor for the hydrogenation of α,β-unsaturated aldehydes. Oxygen/water was used as the system throughout. In order to obtain reproducible results, a very effective gas-liquid separation method was conceived and developed after much trial and error work. Shutdown and deadleg gas holdup measuring methods were compared and it was found that the shutdown method is more reliable than the deadleg method.

The hydrogenation of cinnamaldehyde using both in-house-prepared and commercial palladium, platinum and ruthenium catalysts was carried out in stirred tank reactors and cocurrent downflow reactors in order to study the kinetics and mass transfer characteristics and the selectivity towards the corresponding desired product, hydrocinnamaldehyde or cinnamyl alcohol.

When palladium catalysts were used the desired product was hydrocinnamaldehyde. The effects of homogeneous reactions, type of solvent, catalyst loading, temperature, pressure, reactant concentration and the effects of promoter or poison on the selectivity towards hydrocinnamaldehyde were investigated systematically. Aldehyde acetals were produced in polar solvents, but not in non-polar solvents. Two methods can be used to obtain hydrocinnamaldehyde selectively without reduction of the carbonyl double bond: (1) by using non-polar solvents such as toluene; (2) by

incorporating poisons or promoters into the reactant solution or onto the surface of the catalysts. 97% selectivity to hydrocinnamaldehyde was achieved. The effects of the solvent, temperature, pressure, catalyst loading, promoters, and reactant concentration on the kinetics were studied and the following reaction kinetics are proposed for the hydrogenation of cinnamaldehyde over non-modified palladium/charcoal catalysts in propan-2-ol and in toluene:

$$Ra = kC_{Cat}C_{H_2}C^0_{CAL}$$

The apparent activation energy varies with themperature range in propan-2-ol and is 65 ± 5 kJ.mol^{-1} in toluene.

When platinum catalysts were used the desired product was cinnamyl alcohol. The effects of solvent, catalyst loading, temperature, pressure and promoter on the selectivity to cinnamyl alcohol were investigated. The selectivity can be improved significantly by the addition of a base to the reaction system, and it was found that the selectivity was dependent on the base concentration. The selectivity effect of a solvent is strong and it was found that when toluene/water was used as the solvent at the optimal ratio over 96% selectivity towards cinnamyl alcohol was achieved. This aqueous medium provides a good environment for producing potassium ions, and cinnamaldehyde has high solubility in toluene. High temperature does not favour the selective hydrogenation of cinnamaldehyde towards cinnamyl alcohol. The reaction rate increased considerably with increase in the base concentration (or PH values).

This work is dedicated to

my parents, my wife, my brother and my sisters.

Acknowledgements

I should like to express my sincerest thanks to Dr J. M. Winterbottom and Dr A. P. Boyes for their constant supervision, guidance, help, encouragement and advice during all stages of this work; I should like to thank Professor A. J. Biddlestone, Head of the School of Chemical Engineering, for the provision of the research facilities.

I should like to thank the Government of The People's Republic of China, the Foundation of Sir Y. K. Pao and the British Council for the studentship of the Sino-British Friendship Scholarship Scheme, and Northwestern University (China) and my friends for their support and assistance. I should also like to thank Dr J. M. Winterbottom for his support during the later stage of this work.

I should like to express my thanks to Mr G. Titmus for his kind help especially for valuable proof reading, to Ms Ming Sun and Mr Xingwang Liu for the analysis and identification of the products in polar solvents using NMR and to all members of the Catalysis and Reaction Engineering Group for their companionship and assistance; Grateful thanks are extended to Ms G. Wheeler for the production of the photographs, to Mr S. Clabon for the manufacture and maintenance of the glassware, and to Mr D. Boylin for the mechanical work.

A very special thanks is extended to Dr. Z. Khan for his advice, support, help and companionship throughout this research.

Contents

Chapter 1. Introduction

Effective contact between gas, liquid, and solid phases is very important throughout the chemical industry for several processes, including absorption (Astarita, 1967; Dankwerts, 1970), absorption with chemical reaction (Shah, 1979; Shah et al, 1982; Patterson, 1983; Ramachandran and Chaudhari, 1983; Doraiswamy and Sharma, 1984; Jiang et al, 1990; Deckwer, 1992), fermentation processes (Bailey and Ollis, 1986; Chisti, 1989), coal liquefaction (Mangold, 1982) and waste water treatment (Ram et al, 1990). Many devices are available for three-phase chemical processing, ranging from simple stirred-tank reactors to complex multistage packed bubble columns. The means to develop more efficient reactors and to improve the existing well-established reactor technology are in great demand. It is very important to improve mass transfer performance in the case of mass transfer being the limiting step. Mass transfer limitation hinders reactor performance and productivity due to inefficient catalyst utilization.

The Cocurrent Downflow Contactor (CDC), developed by Boyes and Ellis (1976) as a new type of bubble column, is a highly efficient mass transfer gas-liquid and three phase chemical reactor. Liquid is introduced at the top of the CDC column through a restriction device such as an orifice to create a high velocity liquid stream in the column. The gas stream can be introduced cocurrently into the column at any point. The high velocity liquid stream creates a vigorously and turbulently agitated gas-liquid dispersion in the upper entry zone. This vigorous agitation and turbulence by the incoming liquid stream generates and maintains a gas-liquid dispersion matrix of densely packed bubbles extending downwards in the column. This allows coalescence

of the bubbles in the lower section of the column, which leads to large bubbles rising in the column towards the highly agitated region where re-dispersion occurs due to the breakup of large bubbles by the incoming liquid stream. Bubble shear created by the high velocity liquid stream leads to good gas-liquid-solid contacting in the upper section of the column. The CDC offers several advantages over stirred tank reactors in which it allows a close approach to gas-liquid equilibrium in a short time, provides 100% gas utilization and results in a very high mass transfer coefficient and a large specific interfacial area.

Previous applications of the use of the CDC to study chemical reactions focused on model reactions (Lu, 1988; Raymahasay, 1989; Tilston, 1990; Chughtai, 1993) and oxidation of organic waste water (Sulidis, 1995; Khan, 1996) and demonstrated that the CDC is an efficient mass transfer reactor. The purpose of this study is to extend the application of the CDC for the commercially important but complex consecutive-parallel reactions for the selective hydrogenation of cinnamaldehyde towards the clean synthesis of cinnamyl alcohol or hydrocinnamaldehyde.

In order to provide basic information for selective hydrogenation in the CDC, stirred tank reactors were used to study the kinetics, selectivity and mass transfer. In this particular case stirred tank reactors offer some advantages. Stirred tank reactors allow the use of small amounts of reactants, including the catalyst, so that costs can be reduced. Stirred tank reactors allow straightforward analysis of the reaction kinetics and mass transfer characteristics because the flow pattern in the reactor can be treated as that of perfect mixing. The intensive and turbulent agitation in stirred reactors allows fine catalysts to be suspended completely in a solvent with gas bubbles and

facilitates good heat transfer control in the case of an exothermic reaction such as hydrogenation. In this work stirred tank reactors were used only to obtain basic information due to scaleup and sealing problems. Pilot scale experiments were carried out in the CDC.

Cinnamaldehyde and its corresponding unsaturated alcohol (cinnamyl alcohol), saturated aldehyde (hydrocinnamaldehyde), and saturated alcohol (3-phenyl propanol) are very important in the fine chemicals industry. A considerable range of products, including flavours, fragrances, agrochemicals, pharmaceuticals and polymers, has been developed using these chemicals as either synthetic intermediates or ingredients (Schröder and Verdier, 1993; Eilerman, 1979). The selective hydrogenation of α,β-unsaturated aldehydes is a difficult problem in heterogeneous catalysis and has led to attempts to develop a suitable catalytic system (Tuley and Adams, 1925; Rylander, 1963; Rylander and Hilmestein, 1969; Millman and Smith, 1977; Rylander, 1979; Poscoe and Stenberg, 1980; Poltarzewski et al, 1986; Galvagno et al, 1986; Goupil et al, 1987; Giroir-Fendler et al, 1988; Galvagno et al, 1989; Vannice and Sen, 1989). The widespread use of cinnamic derivatives has led to the pursuit of reliable methods for their direct synthesis.

In this work, cinnamaldehyde was hydrogenated in various solvents over noble-metal catalysts for the clean synthesis of the desired product, for example, hydrocinnamaldehyde or cinnamyl alcohol. The selectivity is the important issue in this study. It has been reported that almost all noble metal catalysts can hydrogenate both olefinic and carbonyl groups simultaneously, resulting in a lower selectivity; but the addition of promoters can significantly change the activity, and can alter the

reaction route so that a higher selectivity can be achieved (Rylander, 1967). In this work, various operating parameters such as temperature, pressure, catalyst, solvents, promoters and poisons were examined to achieve the main research aim of clean synthesis. The kinetics and mass transfer characteristics also were investigated.

Use of the basic information obtained in the stirred tank reactors, the optimal conditions were tested in the CDC for the production of cinnamyl alcohol or hydrocinnamaldehyde.

The aims of this study are: (1) to investigate hydrodynamics and mass transfer of the CDC; (2) to examine the activity of the catalysts for the hydrogenation of cinnamaldehyde; (3) to investigate the kinetic characteristics of the hydrogenation of cinnamaldehyde as a model system for study in the CDC; (4) to study the selectivity with respect to the desired products, such as hydrocinnamaldehyde or cinnamyl alcohol, as an example of hydrogenation of α,β-unsaturated aldehydes to decide the optimum reaction conditions for clean synthesis; (5) to evaluate the relative importance of liquid-solid mass transfer and reaction kinetics; (6) to determine the optimum combination of catalysts and reaction conditions for the clean synthesis towards the desired products and to provide the basic information for economic industrial production.

Chapter 2 Literature Survey

Catalytic hydrogenation is one of the most widely used steps in organic synthesis. The scope of the reaction is very broad. The hydrogen atom can be made to react readily with most functional groups, and is more selective in high yield, often under mild conditions, to any of several possible products. In addition, hydrogenation often turns out to be the most economical reduction method, and this appears to be true for all scales of production.

Catalytic hydrogenations are carried out usually in multiphase reactors, with most applications involving dissolving hydrogen and liquid reactant in the presence of a solid catalyst. In the fine chemical industry, use of catalytic hydrogenation, in particular batch slurry hydrogenation, seems to be the accepted practice. However, the major disadvantage of catalytic hydrogenation is its complexity, such as the problem of the catalyst choice, the arbitrariness of the operating conditions and of catalyst preparation and the uncertainty of the catalyst performance (Rylander, 1979, 1990; Richardson, 1989). In this chapter various important aspects of liquid-phase hydrogenation processes will be reviewed briefly in order to shed light on a new project, the selective hydrogenation of cinnamaldehyde.

2.1 Catalytic Hydrogenation

2.1.1 General Considerations

2.1.1.1 Solvents

Although it is preferred that no solvents be used during hydrogenation for clean synthesis, solvents are often used in catalytic hydrogenation for several purposes, namely, (1) to aid catalyst handling and recovery; (2) to moderate exothermic reactions by dilution; (3) to increase rate and selectivity; and (4) to permit easier hydrogenation of solid materials.

Solvents ideally should meet as many as possible of the following criteria, namely, (1) inertness to the hydrogenation system; (2) environmental acceptability; (3) non-ignition in the presence of the catalyst; (4) inertness to the catalyst; (5) easy removal from solids. The catalytic products should dissolve hot and precipitate cold from the solvent.

Most liquids that are stable under the hydrogenation conditions and do not inactivate the catalyst can be used as solvents. Among them, water is the ideal solvent. Possible organic solvents that can be used are short-chain alcohols, ethers, aliphatic and aromatic hydrocarbons, and short-chain aliphatic acids. When organic solvents are used one should be aware of the possible ignition of their vapours in the presence of the catalyst and of possible ignition during the catalyst filtration operation at the end of the hydrogenation. It is also important to note that the formation of products insoluble in the solvent used could cause catalyst agglomeration. The environmentally

unacceptable solvents (such as chlorinated hydrocarbons, carbon disulphide, and dioxane) and catalyst-deactivating solvents (for example, pyridine and sulphur compounds) must be avoided if at all possible.

2.1.1.2 Catalysts and Supports

A hydrogenation catalyst should (1) have sufficient active surface area, (2) adsorb hydrogen and the reducible functional group in reactive forms, (3) spatially orient adsorbed reactants for forming the desired product, (4) be sufficiently stable, (5) contain minimum poisons itself, unless incorporated intentionally for controlling selectivity, and (6) allow easy desorption of the product from the catalyst surface.

Hydrogenation catalysts vary widely in activity and selectivity. Functionality depends on crystal structure, electronic configuration and surface atomic orbital occupancy. The catalytic characteristics are determined mainly by the major metal component. Support and catalyst preparation usually have secondary influences compared to the metal (Rylander, 1990). For selective reduction of bifunctional molecules, the desirably reducible function group should occupy preferentially most of the active catalyst sites.

Most hydrogenation catalysts are heterogeneous catalysts, highly dispersed forms of transition metals although Wilkinson's catalyst ($Rh[PPh_3]_3Cl$) is homogeneous. Two main sub-categories of heterogeneous catalysts are widely used. One group is the precious metals (also called noble metals), such as platinum, palladium, ruthenium, rhodium, osmium, iridium, silver and gold; the other the base metals such as nickel,

cobalt, copper and iron. For efficient use of the metal (especially if a noble metal) various materials such as carbon, alumina, silica, zeolite and calcium carbonate are used as supports. In addition, the structure and the pore size of a support play an important role in activity and selectivity. As a compromise between the most efficient use of the metal and the economic need to minimize the amount of catalyst a frequently-used metal loading for batch-type noble metal catalysts is 5% (w/w). Supported base-metal catalysts, because they are less active, usually contain much more metal than do noble-metal catalysts,.

2.1.1.3 Promoters and Poisons

A material which has favourable effects on activity, selectivity or catalyst life can be used as a promoter (Innes, 1954). Promoter action is not an intrinsic property of a modifier or a catalyst; it depends also on the reaction in which the catalyst is used. The effects of a promoter are sometimes remarkable. In some cases the promoter effects are equal to or even more important than the catalytic function.

A poison can be anything that inactivates the catalyst partially or completely. Poisons vary from reaction to reaction. A small amount of a substance may be beneficial to catalyst functioning but larger amounts may be poisonous. Poisons may be the impurities present in the catalyst, hydrogen gas, the solvent, the reactants, or in the pipelines or in the reactor systems. Poisons include heavy metal cations, halides, sulphur compounds, carbon monoxide, amines and phosphines (Maxted, 1951; Baltzly, 1976; Rylander, 1979). Although impurities should be reduced to a minimal

level, in some situations a poison is intentionally incorporated into the reaction system in order to improve its selectivity.

2.1.2 Reaction Conditions

In a catalytic hydrogenation process the catalyst dominates the reaction mechanism. However, an optimal combination of the catalyst, reaction conditions and the reactor would result in a desired outcome. Temperature, pressure, and agitation can affect both activity and selectivity in catalytic hydrogenation. It is noted that hydrogenation rates may decrease with increasing temperature due to the lower solubility of hydrogen, or cease completely at the boiling point of the solvent (Cowan and Eisenbraun, 1976), and rates may be maximal at intermediate pressures (Rylander and Greenfield, 1977).

The rate may be limited partially or wholly by the hydrogen transfer rate to the catalyst surface. The more active the catalyst, the more likely it is that mass transfer will be a limiting factor. If the reciprocal of the hydrogenation rate is plotted against the reciprocal of the catalyst loading the intercept will be equal to the rate that would exist if the reaction were controlled by gas-liquid hydrogen transport. The slope of the line is related to resistances due to liquid-solid mass transfer plus the chemical reaction and pore diffusion (Rylander, 1979; Shah, 1979; 1983; Ramachandran and Chaudhari, 1983; Doraiswamy and Sharma, 1984).

The effects of reaction conditions on selectivity are often linked with hydrogen availability at the catalyst surface. If the desired product is favoured by a hydrogen-

rich catalyst (high hydrogen availability at the catalyst surface), the hydrogen concentration can be increased by various means for achieving higher selectivity, such as more intensive agitation, decreased catalyst loading, higher pressure, or using a hydrogen-rich solvent. For a complex reaction it is very difficult to predict the effects of reaction conditions on selectivity but an easy method to probe the possible effect of hydrogen availability on the selectivity is to measure selectivity under two widely different degrees of agitation with the rest of the process conditions unchanged.

2.1.3 Hydrogenation Reactors

Hydrogenation reactors have been reviewed by Rylander (1990). Catalytic hydrogenation reactors widely used can be divided into liquid-phase reactors and vapour-phase reactors. Fluidized-bed and fixed-bed reactors are used in vapour phase reactions. Gas-phase reactions take place in shell and tube reactors (for example ammonia synthesis) or in multi-stage reactors. Compared with liquid-phase reactors, the masses of the reactants and the products are very small in gas-phase reactors. Liquid-phase hydrogenation reactors can be classified into three categories: slurry reactors (such as bubble columns and stirred vessels), ebullating beds and fixed beds/trickle beds.

In a slurry reactor gas is either bubbled through the suspension of fine catalyst particles or entrained by the action of agitation. Mechanically stirred tank reactors (Figure 2.1) and bubble columns (Figure2.2) are used widely in slurry reaction systems and loop reactors (Figure 2.4) are modified bubble column reactors. A

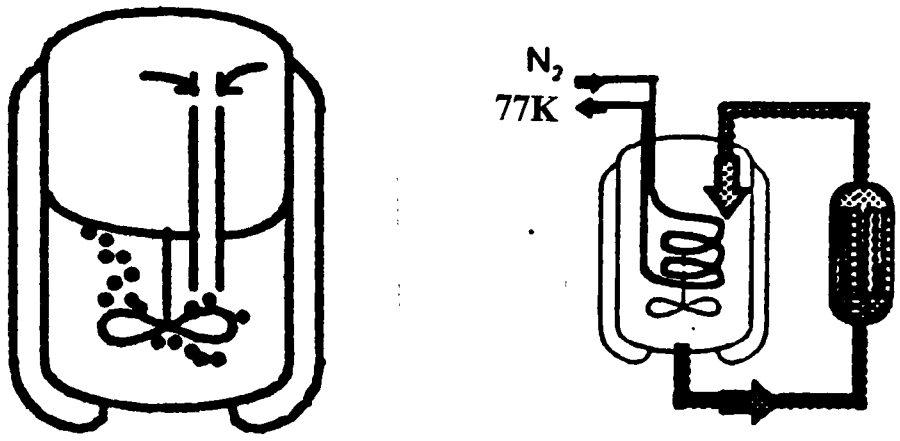

Without Extra Cooling With Extra Cooling

Figure 2.1 Stirred Tank Reactor

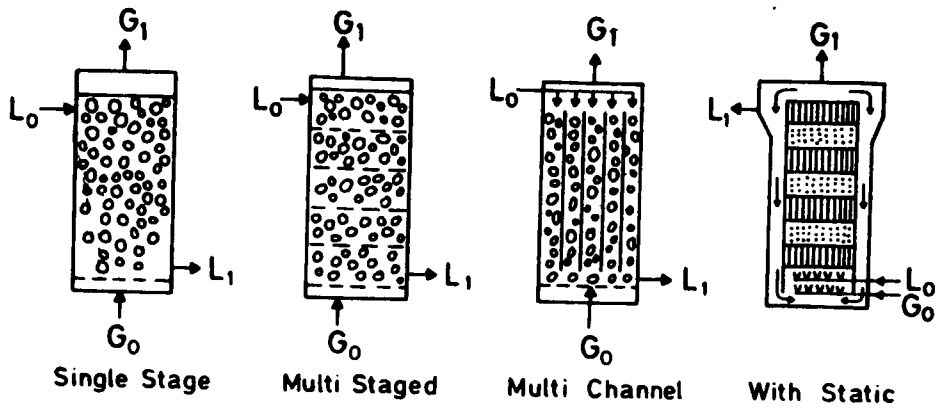

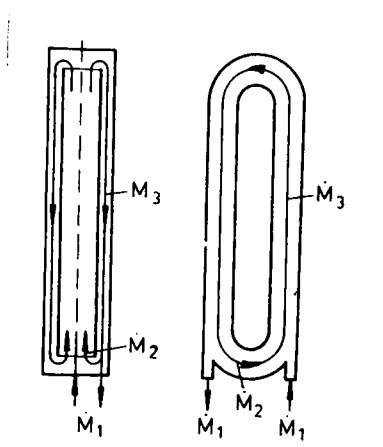

Gas-lift Loop Reactor (GLR)

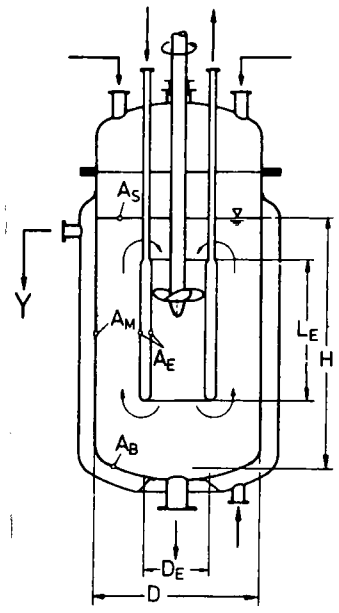

Propeller Loop Reactor (PLR)

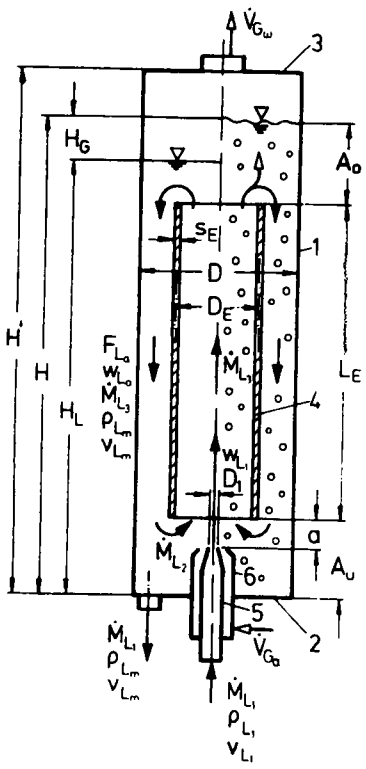

Jet Loop Reactor (JLR) with Aeration

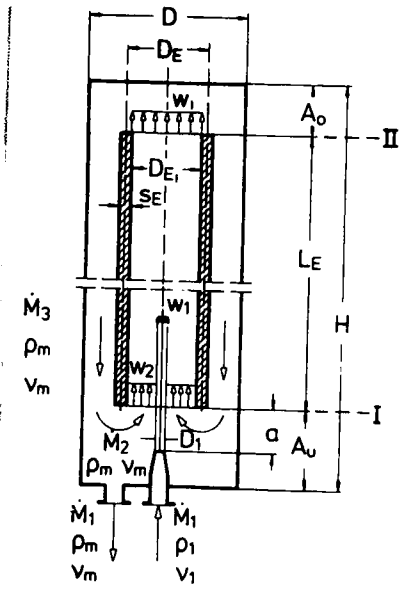

Jet Loop Reactor (JLR) without Aeration

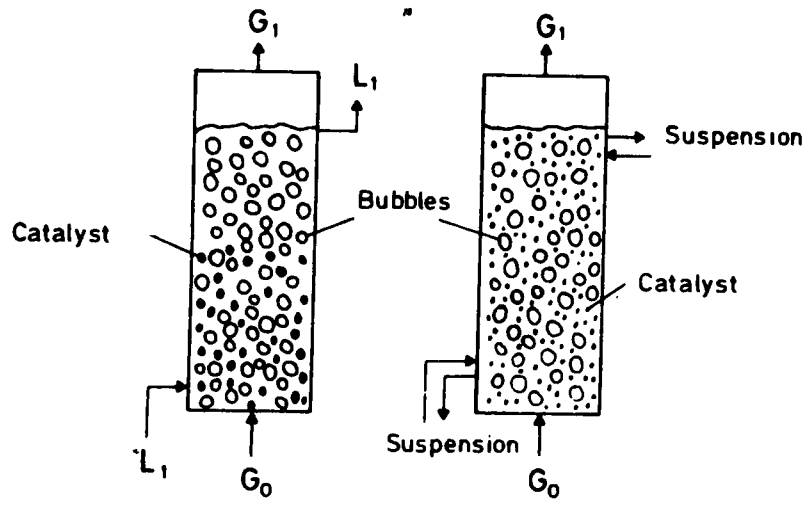

Figure 2.2 Bubble Column Reactors and Modifications

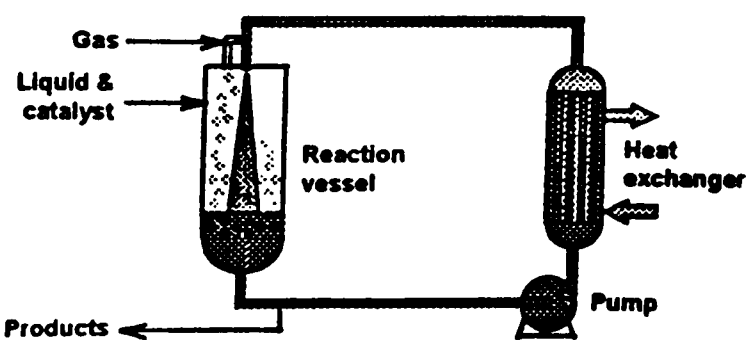

Figure 2.3 BUSS Loop Reactor

D : internal diameter of loop reactor
H : filling hight of reaction system
D_E: mean diameter of draft tube
D_{E_i}: internal diameter of draft tube
L_E: length of draft tube
A_u: distance of draft tube from bottom
A_o: distance of draft tube from surface
a : distance of draft tube from liquid nozzle
D_1: diameter of liquid nozzle and liquid jet
$\dot{M}_1$: liquid mass trough flow
$\dot{M}_2$: liquid circulation mass flow
$\dot{M}_3$ total mass flow of liquid

1 external tube
2 bottom
3 top plate
4 draft tube
5 liquid-jet nozzle
6 air sparger

Figure 2.4 Principles of Loop Reactors

particular type of loop reactor, the BUSS loop reactor (Figure 2.3), is a downflow bubble column reactor with a specialised gas-liquid distributor. Stirred tank reactors, bubble columns and loop reactors are related to this research project and will be reviewed briefly.

2.2 Stirred Tank Reactors

Mechanically agitated slurry reactors are widely used. They are convenient for use in batch processes. They offers some advantages (Holfman, 1983; L'Homme, 1983; Shah, 1979). High efficiency of mass transfer and heat transfer can be achieved. The utilization of the catalyst can be maximised because small particle sizes can be used and the intraparticle diffusional resistance is smaller. Due to the higher mass transfer and heat transfer rates stirred tank reactors are most suitable for kinetic studies in the laboratory and are more flexible for batch processes due to the ease of charging and discharging the reactor contents. However, larger power consumption, significant liquid backmixing and difficult separation of the catalyst in continuous operations are major disadvantages.

Batch hydrogenations are carried out in a single stirred vessel. Usually, the rate-determining step in the early stages of the cycle is mass transfer. Kinetics become more important towards the end of the reaction (Murthy, 1993). A series of gas-sparged agitated reactors is used for continuous hydrogenation. The design procedure involves system design and reactor design. System design consists of (1) the selection of the number and the size of the reactor vessels, (2) the selection of process logic such as flow schemes for the organic liquid and hydrogen-containing

gases, (3) the determination of optimal catalyst loading, (4) the determination of optimal pressure and temperature for each reaction vessel, (5) catalyst recycle and regeneration and (6) the development of an overall control strategy. Reactor design constitutes (1) the estimation of the extent of the reactions taking place in each vessel, (2) the estimation of the distribution of the various species between the gas and the liquid streams in the reactor, (3) the design of the agitation system to achieve the expected mass transfer in each vessel and (4) the design of the cooling/heating system to provide good heat transfer in each vessel. The performance of three-phase reactors depends on the extent of mixing in the gas-liquid phases (Middleton, 1985; Joshi et al, 1992). Agitators used in the stirred tank reactors dominate the mixing. Nagata (1975) proposed optimal ratios for vessels with different shapes: for a flat-bottom vessel d_I/d_T = 0.45-0.5; for a dished-bottom vessel d_I/d_T = 0.4; and for a spherical-bottom vessel d_I/d_T = 0.35. The use of baffles is also very important for proper distribution of the gas, uniform suspension of the catalyst particle, and help in avoiding the formation of vortices at the free surface of the liquid. The standard baffles are 1/10-1/12 of the vessel diameter and four baffles are commonly used.

2.2.1 Suspension of Catalyst Particles

In order to maximise the utilization of the catalyst it is essential to keep all the catalyst particles suspended in liquid phase. A certain minimal degree of agitation is required to achieve this. Zwietering (1958) investigated the conditions for complete suspension and proposed the following equation to predict the minimal speed required:

$$N_m = \frac{\beta\, d_p^{0.2} \mu_L^{0.1} g^{0.45} (\rho_p - \rho_L)^{0.45} W^{0.13}}{\rho_L^{0.55} d_I^{0.85}} \qquad (2.2.1)$$

where W = the percentage catalyst loading, g/100g solution

N_m = the minimum stirrer speed required for complete suspension, rev/s

β= a parameter.

Zwietering (1958) obtained a graph of β against d_T/d_I for various agitator arrangements. Alternatively β values can be estimated for a disc turbine by the following equation (Nienow 1975):

$$\beta = 2\left(\frac{d_T}{d_I}\right)^{1.33} \qquad (2.2.2)$$

Subba Rao and Taneja (1979) studied the minimal gas sparging needed to settle the solid completely in a three phase system and proposed the following limiting values of sparging rates as functions of the impeller speed:

for a complete suspension $$\frac{Q_G}{(N_{stir} - N_c)D^3} < 0.5\times10^{-2} \qquad (2.2.3)$$

for a partial suspension $$0.5\times10^{-2} < \frac{Q_G}{(N_{stir} - N_c)D^3} < 5\times10^{-2} \qquad (2.2.4)$$

for a total sedimentation $$\frac{Q_G}{N_{stir} D^3} > 5\times10^{-2} \qquad (2.2.5)$$

The position of an impeller from the bottom for the minimal power consumption to maintain complete suspension lies in the range $0.25 < H_i/d_T < 0.75$ depending on the solid loading (Wiedmann et al, 1980).

2.2.2 Power Consumption for Agitation

Stirred tank reactors are usually baffled vessels with turbine agitators. The gas is introduced below the impeller by a gas distributor. Agitation promotes (1) gas-liquid mass transfer by increasing gas-holdup and creating small bubbles, (2) liquid-solid mass transfer by keeping the catalyst particles well dispersed and (3) uniformity of heat transfer and temperature by maintaining high internal circulation rate. The effectiveness of agitation is measured by the circulation rate, the maximum shear rate generated and power input per unit volume of the reactor.

For a disc turbine the impeller moves liquid radially towards the wall. Near the wall the motion is parallel to the wall both upward and downward away from the impeller level. At the top and bottom of the liquid-phase the flow is radial towards the centre. The shear is proportional to the velocity gradient. The maximum fluid shear is proportional to the tip velocity $N_{stir}d_I$ of the turbine. The velocity head H developed by the agitator is proportional to the square of the tip velocity, $N_{stir}^2 d_I^2$. Shear is also very important as it breaks up large hydrogen bubbles into small and thereby maintains a high interfacial area for gas-liquid mass transfer. The power input P into the liquid phase by the agitator is determined by

$$P = \rho_L Q H \qquad (2.2.6)$$

where Q = the pumping capacity of the impeller and $Q \propto N_{stir}d_I$. Therefore power input is proportional to $N_{stir}^3 d_I^3$.

Power consumption for agitation of a liquid free from gas and solid is often correlated in terms of the power number N_P:

$$N_P = \frac{P_o}{\rho_L N_{stir}^3 d_I^5} \qquad (2.2.7)$$

and the hydrodynamic state of the system given by the impeller Reynolds Number

$$\mathrm{Re} = \frac{\rho_L N_{stir} d_I^2}{\mu_L} \qquad (2.2.8)$$

If the Reynolds Number (Re) is greater than 10000, N_p is a constant equal to 6.3 for a flat-blade turbine and 4.0 for a curved-blade turbine. If the impeller Reynolds Number is less than 10000 the power number can be estimated by a equation developed by Bates et al (1963).

For gas-liquid systems the power consumption is reduced. The value of N_P seems to be a minor function of catalyst loading at high Reynolds Numbers (Wiedmann et al, 1980). Chapman et al (1983) found that N_P generally increases as particle concentration increases at the just-suspended condition. However, if the system is well mixed, the effect of the particles on the gas-liquid hydrodynamics is virtually negligible. Luong and Volesky (1979) proposed a equation for a gas-liquid system

$$\frac{P}{P_o} = 0.497\left(\frac{Q_G}{N_{stir} d_I^3}\right)^{-0.38}\left(\frac{N_{stir}^2 d_I^3 \rho_L}{\sigma}\right)^{-0.18} \qquad (2.2.9)$$

Nagata (1975) suggested that the power consumption for agitated slurries should be taken as $P\rho_{S\text{-}L}/\rho_L$, where $\rho_{S\text{-}L}$ is the density of the slurry defined as:

$$\rho_{S-L} = w + \rho_L\left(1 - \frac{w}{\rho_p}\right) \qquad (2.2.10)$$

However, for low catalyst loading and catalysts with low densities the effect of the catalyst on power consumption is not significant.

2.2.3 Gas Holdup

Various equations of gas holdup in stirred tank reactors are available from literature. Gas holdup is a function of power consumption and the superficial gas velocity. Yung et al (1979) proposed the following equation

$$\varepsilon_g = 6.8 \times 10^{-3}\left(\frac{Q_G}{N_{stir} d_I^3}\right)^{0.5}\left(\frac{\rho_L N_{stir}^2 d_I^3}{\sigma}\right)^{0.65}\left(\frac{d_I}{d_T}\right)^{1.4} \qquad (2.2.11)$$

Although various equations are available it is better to consult a equation obtained under similar conditions to predict the gas holdup.

2.2.4 Bubble Diameter

There is little consistency in the literature about the variation of bubble diameter with stirring speed. However, the average bubble diameter can be estimated by the following equation (Calderbank, 1958):

$$d_b = 4.15\frac{\sigma^{0.6}\varepsilon_g^{0.5}}{(P/V_L)^{0.4}\rho_L^{0.2}} + 0.09 \qquad (2.2.12)$$

2.2.5 Gas-Liquid Mass Transfer

Most studies on k_La are reported on gas-liquid systems in a continuous operation mode. Several equations to estimate the k_La value can be found in the literature (Ramachandran and Chaudhari, 1983). Calderbank (1958) proposed a equation of gas-liquid interfacial area:

$$a = 1.44 \frac{\left(\frac{P}{V_L}\right)^{0.4} \rho_L^{0.2}}{\sigma^{0.6}} \left(\frac{u_G}{u_b}\right)^{0.5} \qquad (2.2.13)$$

Calderbank and Moo-Yong (1961) developed a liquid-side mass transfer coefficient (k_L) equation for an average bubble swarm diameter greater than 2.5mm:

$$k_L = 0.42 \left(\frac{(\rho_L - \rho_g)\mu_L g}{\rho_L^2}\right)^{\frac{1}{3}} \left(\frac{D_A \rho_L}{\mu_L}\right)^{\frac{1}{2}} \qquad (2.2.14)$$

Yagi and Yoshida (1975) proposed a equation for k_La in an agitated contactor based on the physical properties of the liquid:

$$\frac{k_L a d_I^2}{D_A} = 0.060 \left(\frac{d_I^2 N_{stir} \rho_L}{\mu_L}\right)^{1.5} \left(\frac{d_I N_{stir}^2}{g}\right)^{0.19} \left(\frac{\mu_L}{\rho_L D_A}\right)^{0.5} \left(\frac{\mu_L u_G}{\sigma}\right)^{0.6} \left(\frac{N_{stir} d_I}{u_G}\right)^{0.32} \qquad (2.2.15)$$

The values of k_La increased slightly with the increase in the solid loading but the effect can be ignored at low solid loading (Ramachandran and Chaudhari, 1983). Since the catalyst loading used in practice is usually less than 10% (w/w) the

equations proposed for gas-liquid systems can be used for three-phase systems without significant deviation.

2.2.6 Liquid-Solid Mass Transfer

Levins and Glastonbury (1972) developed a equation based on Kolmogoroff's theory for liquid-solid mass transfer in agitated vessels:

$$\frac{k_s d_p}{D_A} = 2 + 0.47\left(\frac{d_p^{4/3} e^{1/3} \rho_L}{\mu_L}\right)^{0.62}\left(\frac{d_I}{d_T}\right)^{0.17}\left(\frac{\mu_L}{\rho_L D_A}\right)^{0.36} \qquad (2.2.16)$$

This equation is valid when the density difference between the liquid and solid is not large.

The equation of liquid-solid mass transfer for flow around a spherical pellet is analogous to that given for heat transfer (Fogler, 1986) leading to a general expression:

$$Sh = \frac{k_s d_p}{D_A} = 2 + \alpha\, \mathrm{Re}^m\, Sc^n \qquad (2.2.17)$$

where α, m and n are parameters and vary with different workers and conditions.

The stated effect of particle size on k_s varies in the literature. Doraiswamy and Sharma (1984) claimed that in the turbulent region the value of k_s becomes independent of particle size and is substantially affected by the hydrodynamics. No

effect of particle size was observed by Barker and Treybal (1960) and Johnson and Hung (1965) whereas a k_s increase with decrease in particle size was reported by Hughmark (1969) and Lewins and Glastonbury (1972). Harriot (1962) reported that particles greater than 200μm in diameter did not affect k_s, but for particles less than 200μm in diameter k_s increased with decrease in particle size. Nagata (1975) observed a similar effect but the critical size is 40-50μm instead of 200μm.

2.2.7 Dead-end Agitated Reactors

A dead-end agitated reactor is a system in which no components leave the reactor and an amount of gas corresponding to the consumption rate is supplied continuously. The advantage of this system is that recycling of the unreacted gas is not necessary in cases where there is no significant build-up of by-product gases. This operation is suitable mainly for pure gas feeds.

The mass transfer coefficients (gas-liquid) for dead-end reactors are generally lower than for systems where the gas is sparged at reasonable rates into the reactor. To improve the mass transfer efficiency it may be desirable to recirculate the gas from the head space back into the liquid phase. This can be achieved either by using a gas-induced agitator (Martin, 1972) or by using a dual agitator system (Oldshue, 1980).

2.3 Upflow Bubble Columns

Bubble columns are contactors in which a discontinuous gas phase in the form of bubbles moves relative to a continuous phase. The continuous phase can be a liquid or a homogeneous slurry. Bubble columns can be single-staged or multi-staged, batch or

continuous, and can be operated cocurrently or countercurrently (Shah et al, 1982). Bubble columns can be divided into two types: upflow bubble columns and downflow bubble columns.

The literature available concerning the diverse aspects of bubble columns is quite extensive. Several reviews and books provide easy approaches to various features of bubble columns. A detailed discussion into the design parameters in bubble columns is presented by Shah et al (1982) and Deckwer (1992).

Bubble columns are widely used in the chemical and biochemical industries because of the simple configuration and the low cost of manufacture needed to achieve effective contact between the continuous phase and the dispersed gas phase. Some advantages of bubble columns over other multi-phase contactors are as follows:

1. Higher values of effective interfacial areas and overall mass transfer coefficients can be achieved.

2. Higher heat transfer rates per unit volume of the reactors can be obtained.

3. Solids can be handled without any erosion or plugging problems and no fouling problems exist.

4. Slow reactions can be carried out due to high liquid residence-time.

5. Simpler design and construction can be easily used for higher temperature and higher pressure processes.

6. Fewer sealing problems exist and less maintenance is required due to the absence of internal moving parts.

7. Less floor space is occupied and bubble column reactors are less costly.

However, some disadvantages also exist. Poor reactor performance can occur when considerable backmixing occurs in the liquid phase or in both gas and liquid phases.

If the gas flow used is at atmospheric pressure additional energy is required to overcome the column pressure drop. When the ratio of length to diameter is greater than 10, there is a rapid decrease in the specific interfacial area and mass transfer coefficient due to the sharp increase of bubble coalescence.

Bubble columns have been modified in many ways to suit particular applications to give types such as single stage reactors, multi-stage reactors, multi-channel reactors, loop reactors, jet reactors, downflow bubble columns, bubble columns with static mixers, three-phase fluidized bed reactors and slurry reactors.

2.3.1 Hydrodynamics

2.3.1.1 Flow Regimes

The hydrodynamics, transport and mixing properties such as pressure drop, holdup of various phases, fluid-fluid interfacial areas and interphase mass and heat transfer coefficients depend strongly on the prevailing flow regime. Although different criteria are proposed to differentiate flow regimes (Govier and Aziz, 1972; Lockett and Kirpatrick, 1975; Wallis, 1969; Hills, 1976; Miller, 1980), it is commonly accepted that the following three flow regimes occur in the order of increasing gas flowrate:

1. Bubbly flow or quiescent bubbling This regime is characterised by almost uniformly sized bubbles with equal radial distribution and occurs if the superficial gas velocity is less than $0.05 m.s^{-1}$ (Fair, 1967) and the rise velocity of the bubbles lies between $0.18 m.s^{-1}$ and $0.30 m.s^{-1}$ (Levich, 1962). However these data should be regarded only as guidelines which are valid only for the aeration of water.

2. Churn turbulent regime or heterogeneous regime At higher gas velocities the homogeneous gas-in-liquid dispersion cannot be maintained and an unsteady flow regime pattern with channelling occurs. The heterogeneous flow regime is characterised by large bubbles moving with high rise velocities in the presence of small bubbles (Hills and Darton, 1976). The large bubbles take the form of spherical caps with very mobile and flexible interfaces. These large bubbles can grow to a diameter of about 150mm.

3. Slug flow In columns of all diameters at high gas flowrates, large bubbles are stabilised by the column wall, leading to the formation of bubble slugs. Bubble slugs can be observed in columns of diameters up to 150mm (Hills, 1976; Miller, 1980).

2.3.1.2 Bubble Dynamics

Bubble size, bubble rise velocity, bubble size distribution and liquid and bubble velocity profiles have direct influences on the performance of bubble columns. Many methods are available to determine bubble sizes. Photography is widely used although light scattering, light reflection, depolarisation, and various optical and electrical probes have been developed. Though the original bubble size distributions observed by various techniques differ markedly, the volume-to-surface mean bubble diameters d_{vs} differ only slightly:

$$d_{vs} = \frac{\sum n_i d_{bi}^3}{\sum n_i d_{bi}^2} \qquad (2.3.1)$$

Akita and Yoshida (1974) proposed the following equation

$$\frac{d_{vs}}{D_c} = 26\left(\frac{D_c^2 g\rho_L}{\sigma}\right)^{-0.5}\left(\frac{gD_c^3}{\nu_L^2}\right)^{-0.12}\left(\frac{u_G}{\sqrt{gD_c}}\right)^{-0.12} \qquad (2.3.2)$$

It is reported that the orifice diameter has an effect on the bubble size in a bulk region away from the sparger (Akita and Yoshida, 1974; Deckwer et al, 1978) because of a balance between coalescence and breakup rate which controlled bubble sizes.

It is found that bubble diameter depends on the specific gas-liquid system and its properties with respect to coalescence. Coalescence is influenced significantly by the physical properties of the liquid. A high bubble coalescence rate in highly viscous liquid bubble breakup is due to disturbance at the interface caused by external factors (Calderbank, 1967, Vasalos et al, 1980), and low viscosity liquid systems showed significant bubble breakup. The addition of alcohols lowers the surface tension and suppresses the coalescence.

Gas distribution plays an important role in coalescence. Small bubbles are generated over the entire column if sintered plates of high porosity and two-phase injector or ejector nozzles are used. In practice small bubbles are desirable because they result in large interfacial areas, which more than offsets the decrease in k_L with decreasing bubble diameter. Kolbel et al (1961) reported that there was no effect on gas holdup and mean bubble diameter if the gas velocity is corrected to take into account the pressure in the column.

2.3.1.3 Gas Holdup

The importance of gas holdup is multifold. Gas holdup determines the residence time of the gas in the liquid, and in combination with the bubble size it influences the gas-liquid interfacial area available for mass transfer. Gas holdup influences reactor design also because the total volume of the reactor for any range of operating conditions depends on the maximum holdup that must be accommodated. The commonly encountered techniques of gas holdup measurements have been reviewed by Merchuk (1986) and Nottenkamper et al (1983).

When the column diameter is greater than 100mm its effect is negligible (Miyauchi and Shyu, 1970; Kato et al, 1973; Akita and Yoshida, 1973; Hills, 1974; Hikita et al, 1980). The dependence of gas holdup on gas velocity can be expressed by $\varepsilon_g \propto u_G^n$, where n is the function of the flow regime. For a bubbly flow regime, the value of n ranges from 0.7 to 1.2 (Reith et al, 1968; Miyauchi and Shyu, 1970; Deckwer et al, 1980). In the churn turbulent or transition regime, the effect of u_G is less pronounced and the exponent n takes values from 0.4 to 0.7.

The physical properties of the system and their effect on gas holdup were investigated extensively and many equations have been developed by different workers (Shah et al, 1982), but due to the significant dependence of the system on physical properties and the existence of trace impurities there is no equation for general use. It is strongly recommended that in order to predict the gas holdup an equation for the conditions be used which is very close to the real situation.

Quicker and Deckwer (1981) studied the gas holdup for hydrocarbon liquids (xylene, decalin, C_{10} to C_{14} alkane mixture, molten hard wax) at 333-543K but failed to correlate their data. Zhang et al (1988, 1990) studied the effect of the temperature on the gas holdup from 293-393K using water, ethanol and various aqueous metal salt solutions as the liquid phase and air as the gas phase, and developed a equation by introducing the vapour pressure to correlate the relationship between gas holdup and temperature. Deckwer et al (1980) and Kölbel et al (1961) claimed that there was no effect of pressure on gas holdup for the pressure range 0.1-1.7MPa, but further investigation needs to be carried out.

Hikita et al (1980) compared their data with other data and concluded that at low gas velocities the single nozzle gas sparger gives lower values of gas holdup than are given by a multi-nozzle or a porous plate sparger. Zahrandnik and Kastanek (1979) observed that the critical gas hole velocity corresponding to the onset of stable

performance of a sieve plate depends on the plate hole diameter. The presence of solids does not affect the gas holdup significantly (Begovich and Watson 1978).

2.3.1.4 Gas-Liquid Interfacial Area

The gas-liquid interfacial area is an important design variable which depends on the geometry of the apparatus, the operating conditions and the physical properties of the liquid media. The mass transfer rate, which is determined by the volumetric mass transfer coefficient $k_L a$, can be influenced easily by varying the interfacial area. Physical and chemical methods are used to measure the interfacial area. The physical methods to determine the interfacial area are through gas holdup and mean bubble diameter d_{vs}:

$$a = \frac{6\varepsilon_g}{d_{vs}} \qquad (2.3.3)$$

Akita and Yoshida (1974) developed a relation for the interfacial area per unit volume. This is recommended as a conservative estimate of a at low gas velocities (Shah et al, 1982):

$$aD_c = \frac{1}{3}\left(\frac{gD_c^2\rho_L}{\sigma}\right)^{0.5}\left(\frac{gD_c^3}{\nu_L^2}\right)^{0.1}\varepsilon_g^{1.13} \qquad (2.3.4)$$

If a chemical method is used to determine gas-liquid interfacial area a, a suitable reaction should have a clear reaction mechanism. The usual reactions are sulphite oxidation and carbon dioxide absorption in alkali. The possible gas-phase conversion $X_{conv.}$ at the reactor outlet is a function of the Stanton Number and depends on the reactor model applied and the reaction order:

$$St_m = K_m^*(aH_d / u_G) = K_m^*(6\tau / d_{vs}) \qquad (2.3.5)$$

where the absorption-reaction parameters K_m^* is defined as

$$K_m^* = \left(\frac{2k_m D_A}{(m-1)H^{m+1}} \right)^{0.5} RTP^{(m-1)/2} \qquad (2.3.6)$$

It should be noticed that interfacial areas determined by physical and chemical methods may vary by more than 100% (Weiseiler and Rösch, 1978). For homogeneous bubbly flow Schumpe and Deckwer (1980) reported

$$a_{photo}=1.35\ a_{sulfite} \qquad (2.3.7)$$

For churn-turbulent flow the difference is even larger. For the measurement of interfacial area the use of sulphite oxidation with low conversion is recommended.

2.3.2 Mass Transfer Characteristics

2.3.2.1 Volumetric Gas-Liquid Mass Transfer Coefficients

To determine the volumetric mass transfer coefficient k_La knowledge of the residence time distribution is necessary for obtaining the flow pattern. When the column diameter is large enough ($D_c \geq$ 100mm) the complete mixing model may be applicable, but in tall and small diameter bubble columns the calculation of k_La should be based on the concentration profiles along the column (Deckwer et al, 1974).

Volumetric mass transfer coefficients are dependent on gas velocity and sparger design and are sensitive to physico-chemical properties, particularly to those which promote or prevent coalescence. The column diameter has some influence if it is small but in large diameter reactors the value of k_La does not depend on the column

diameter. The dependence of k_La on the gas velocity can be expressed as $k_La \propto u_G^n$ and the value of n varies from 0.78 to 0.82 (Kastanek et al, 1977).

In three-phase bubble column reactors k_La can be affected by the presence of solids, and the degree of dependence on k_La for suspended particles was determined by the particle size, the liquid-solid density difference, the geometrical sizes and the operating conditions. A summarised list of equations was presented by Shah et al (1982).

2.3.2.2 Liquid-Solid Mass Transfer Coefficient

In three-phase bubble column slurry reactors the mass transfer from bulk liquid to the solid surface can play an important role in the overall apparent reaction rate (Chaudhari and Ramchandran, 1980). According to the slip velocity between the two phases the liquid-solid mass transfer expression was developed as follows:

$$Sh = 2.0 + \alpha\, Re^m Sc^n \qquad (2.3.8)$$

Frössling (1938) and Ranz and Marshall (1952) showed that m=1/2 and n=1/3, although m can have values other than 1/2.

2.3.3 Backmixing

The performance of a chemical reactor with respect to conversion and selectivity depends not only upon the intrinsic kinetics of the various chemical reactions but also on various physical rate processes such as interphase, interparticle and intraparticle heat and mass transfer. The effects of these physical rate processes on the reactor performance have been shown to depend upon the dynamics of the various phases involved. Backmixing is a specific case of axial mixing in which random movement of fluid is superimposed on and is in the direction of the main flow stream, and where

the transverse mixing is complete. Backmixing in the various phases in a multiphase reactor can have significant effects on the reaction rates, conversion and product selectivity. The backmixing characteristics of various phases in a multiphase reactor are evaluated from the residence time distribution of a tracer injected into the phase of interest. The tracer techniques usually involve the injection of a tracer at one or more locations in the system and detection of its concentration as a function of time at one or more downstream positions.

Various models were developed to determine the degree of the backmixing in bubble column reactors but the axial dispersion model was widely used due to its simplicity. This model characterises the backmixing by a simple, one dimensional, Fick's Law type of diffusional equation. The constant in this model is known as the axial dispersion coefficient E_{ZL}. The dispersion coefficient is expressed in the dimensionless form as the Peclet Number ($Pe = uL / E_{ZL}$). If Pe = 0, backmixing is complete, and for Pe = ∞, plug flow prevails. Shah et al (1978) reviewed various residence time distribution measurement methods. In a bubble column reactor, the backmixing in the fast-moving gas phase is considerably smaller than in the slow-moving liquid phase. In small-scale reactors, the gas phase is usually assumed to move in plug flow. In a bubble column reactor, significant backmixing in the liquid phase is caused by the gas flow and the extent of backmixing increases with the diameter of the reactor. The degree of backmixing in the liquid phase depends on the column diameter, gas velocity and the nature of the gas distributor. Although there are some discrepancies, it appears that the axial dispersion coefficient in a vertical cylindrical bubble column is essentially independent of liquid velocity and the liquid properties such as viscosity, surface tension and density but in rectangular and helical bubble columns the liquid phase dispersion coefficient depends on the liquid flowrate. For a given gas velocity, a rectangular bubble column gives considerably larger axial dispersion coefficients than a cylindrical column of the equivalent diameter possibly due to corner effects on the mixing characteristics within the column. The liquid

backmixing coefficient was a strong function of liquid velocity in a helical bubble column. At low liquid flowrates two phase flow gave higher liquid axial dispersion than single phase flow, whereas at a high liquid Reynolds Number (Re = 400-2000) both single liquid phase and gas-liquid phase flow gave the same degree of liquid phase axial mixing. The design of a bubble column reactor always requires consideration of backmixing in the liquid phase. For vertical bubble columns Joshi and Sharma (1976) developed a general equation for the literature data using the energy balance approach:

$$E_{ZL} = 0.31 D_c^{1.5} u_c \qquad (2.3.9)$$

where u_c is the circulation velocity and dependent upon the dispersion condition. Deckwer et al (1974) correlated the literature data and proposed a general equation for prediction of the liquid phase dispersion coefficient:

$$E_{ZL} = 0.678 D_c^{1.4} u_G^{0.3} \qquad (2.3.10)$$

2.4 Downflow Bubble Columns

The residence time of a gas in an upflow bubble column reactor is a function of reactor length and bubble rise velocity, with the latter value between 0.2 $m.s^{-1}$ and 0.3 $m.s^{-1}$ (homogeneous flow) for bubbles between 3mm and 10mm in diameter. Hence gas residence times are short even in tall columns. This is a great disadvantage in many cases and could be overcome by a gas recycle but for the fact that the resultant intermixing due to extension of the residence time distribution is undesirable. The downflow bubble column, in which a choice of suitable liquid and gas throughput rates permits gas residence times to be adjusted within certain limits up to a maximum gas content, presents a neat solution (Freidal et al, 1980, Shah et al,

1983 and Deckwer, 1992). The liquid must be moving at a minimum rate of $0.2m.s^{-1}$ so that no gas cushion forms at the column head as a result of bubble rise and coalescence. A high gas content up to a maximum of 20% is obtained even at low gas flowrates (Deckwer, 1992).

Downflow bubble columns are efficient gas-liquid contacting devices. In these columns, gas is injected from the top of the column into a liquid stream flowing cocurrently downwards, so that the bubbles are forced to move in a direction opposite to their buoyancy. A state of near suspension of gas bubbles can be obtained by manipulating the liquid flowrate in the column. As a result the mean residence time of the gas can be increased. This is especially favourable for heterogeneous reactions requiring high conversions (Kulkarni et al, 1983). The advantages of a downflow bubble column are in its low capital cost and in the high gas residence times which give rise to high conversion in the gas phase (Deckwer, 1992).

Under cocurrent downflow conditions, the mean residence time of the gas bubbles can be extended to the maximum where a state of suspension is reached by imposing the condition that the liquid superficial velocity must be similar to the bubble swarm rise velocity. There is no upper limit for the liquid superficial velocity. However, with the increase in the liquid throughput, the advantage of the extended bubble residence time diminishes, leading to a decrease in the value of the mean gas holdup and hence in the interfacial area available for mass transfer (Herbrechtsmeier et al, 1981; Steiner, 1987).

Downflow bubble columns provide novel means of contacting and reacting gas-liquid and gas-liquid-solid phases. In downflow bubble columns higher contact efficiency between the phases can be obtained than that observed in upflow columns under similar operation conditions (Ohkawa et al, 1987; Herbrechtsmeier et al, 1985; Clark and Flemma, 1984; Fujie et al, 1980; Friedel et al, 1980). The gas-liquid contact

mechanisms proposed for downflow bubble columns are basically the same, although different methods of supplying the gas phase (aiming mainly to improve both the range of downflow bubble column stable operation and contact efficiency) have been reported. Downflow bubble columns can be classified as follows according to the methods of introducing the gas phase into the liquid phase:

1. Sparging type: The gas phase is dispersed into the column through a sparging device or a sintered disc, perforated plate, tube, or ring (Friedel et al, 1980; Fujie et al, 1980; Herbrechtsmeier et al, 1981, 1982, 1985); Shah et al, 1983; Kulkarni et al, 1983 and 1984).

2. Entrainment type: The gas phase is entrained from the atmosphere by a liquid jet from a nozzle (Ohkawa et al, 1985, 1987; Yamagiwa et al, 1990).

3. Jet type: The gas and liquid phases are introduced into the column by means of a simultaneous two-phase jet (Brien et al, 1992; Bando et al, 1988; Boyes, 1987; Boyes and Ellis, 1976).

The maximum attainable mass transfer rate in a downflow bubble column, as for many other gas-liquid contactors in which the two phases flow cocurrently, corresponds to a single theoretical stage. This basic characteristic of downflow bubble columns is the greatest disadvantage of such gas-liquid contactors, especially for physical absorption processes (Steiner, 1987; Herbrechtsmeier and Schafer, 1982). To overcome this disadvantage of the downflow bubble column, Steiner (1987) and Herbrechtsmeier and Schafer (1982) developed a cascade downflow reactor which combines cocurrent and counter-current flow of the two phases.

Despite these attractive features, the literature available concerning the hydrodynamics and mass transfer in downflow bubble columns is quite limited.

2.4.1 Hydrodynamics

2.4.1.1 Flow Regime

The nature of the flow regime developed in this sort of gas-liquid contactor is at least non-uniform bubbly flow in which a rather narrow heterogeneity in bubble size (d_b = 3-5mm) can be observed. The flow scheme in downflow bubble columns with a sintered disc, porous plate or ring-type gas sparger varies along the flow direction in the column. Violent turbulence occurs in the vicinity of the gas distributor, where frequent coalescence and breakup of bubbles can be seen. As the liquid flows downwards the column, bubble diameters become more uniform. However, bubbles with diameters larger than some critical value were found to rise through the column to the gas distributor where they may be split into smaller bubbles and again flow down into the bulk of the column (Fujie et al, 1980, Shah et al, 1983, and Kulkami et al (1983). Based on the drift flux approach, Shah et al (1983) confirmed that the flow pattern developed in the downflow bubble column was bubble flow.

Ohkawa et al (1985) investigated the variation in gas holdup in a downflow bubble column with gas entrainment by a liquid jet. The results were compared with those in a bubble column with gas sparger. Four types of flow regimes were observed during the operation of the column using an air/water system:

1. **Regime A**: bubble stagnant flow.
2. **Regime B:** non-uniform bubbling flow.
3. **Regime C:** uniform bubbling flow.
4. **Regime D:** churn turbulent flow.

Regime C was used to compare the results with those from other bubble columns. The results indicated that gas holdup varied considerably compared with that from upflow gas systems, but was consistent with that from downflow bubble columns with gas spargers. Using identical apparatus, Ohkawa et al (1987) determined bubble

size, gas-liquid interfacial area and k_La using the absorption of oxygen from air into water. The mass transfer coefficient k_La was evaluated using the following assumptions:

1. Liquid phase resistance controls the rate of mass transfer;
2. Plug flow occurs in the liquid phase;
3. Mass transfer through the free jet and liquid surface is small;
4. Henry's Law is applied to determine the equilibrium concentration of oxygen.

Based on the above assumptions the following equation was developed for estimation of k_La value:

$$k_L a = \frac{u_L (C_o - C_i)}{\Delta C_L H_d} \qquad (2.4.1)$$

From this analysis, k_La ($0.02\text{-}0.07 s^{-1}$) was found to increase with increasing jet velocity, liquid jet length and diameter and decreasing column diameter.

When gas and liquid were injected simultaneously into the column, Bando et al (1988) observed two different flow patterns. A spouting section developed near the nozzle exit where the gas and liquid were violently mixed, and a calm section of uniform bubbly downflow appeared at some distance below the nozzle. They claimed that the patterns were similar to those observed in a cocurrent upflow bubble column with simultaneous gas-liquid injection nozzle (Bando et al, 1987; Nishikawa et al, 1976).

2.4.1.2 Bubble Formation and Bubble Size

The performance of a downflow bubble column is limited by the formation of a gas pocket at the top of the column. When the gas velocity exceeds the critical velocity for a given state gas will accumulate at the top of the column to form a gas pocket.

The breakdown of the stable downflow operation is the shift of both the magnitude and the direction of the resultant force acting on the bubble. This is due to the formation of bubbles larger than the critical equilibrium size for a gas-liquid system, leading to high turbulence when the bubble density increases and the gas holdup exceeds a critical value. Under cocurrent downflow operation, when the buoyancy force exceeds the drag force acting on the bubble the bubble rises counter-currently to the top of the column. At the top of the column the large bubbles can be either redispersed by the action of the higher turbulence in the vicinity of the distributor and so return to the bulk of the column, or can accumulate there gradually to form a gas pocket, so creating unfavourable conditions and the breakdown of the stable downflow operation.

Shah et al (1983) showed that the range of stable downflow operation in two-phase flow can be extended considerably by preventing coalescence by the addition of a surface-active agent into the system, since surface-active agents can reduce the surface tension so that smaller and more stable bubbles are formed. Another improvement of gas-liquid contact and extension of stable operation of the downflow bubble column is to use a simultaneous gas-liquid injector nozzle to form small bubbles (Bando et al, 1988). The liquid downflow velocity can be increased and bubble coalescence can be suppressed considerably under simultaneous gas-liquid injection, so the range of stable operation of the downflow bubble column is much higher. Stable operation of this sort of column could be extended further by increasing the liquid velocity in the column and decreasing the nozzle diameter, so increasing the liquid injection velocity.

When the gas entrainment method was used in a downflow bubble column the application of high liquid throughput to disperse the bubbles uniformly without coalescence can expand the range of stable operation (Yamagiwa et al, 1990).

Bubble size depends on the gas introduction method. By using a sparging device under stable downflow conditions gas bubbles with larger diameters than a critical value rise to the diffuser position and are split into smaller bubbles of d_b = 3-5mm (Fujie et al, 1980; Herbrechtsmeier et al, 1981). When entrainment or simultaneous gas-liquid methods were used to introduce the gas into the liquid phase, Ohkawa et al (1988) observed that uniform bubbles were found along the column length independently of the gas rate. Bando et al (1988) observed two distinct regions. In the upper section violent agitation leads to the formation of small bubbles with low gas holdup but in the lower less turbulent section uniformly-sized bubbles are produced with high gas holdup. It was found that bubble size was determined also by the physical characteristics of the liquid (Kulkarni et al, 1983a, 1983b; Shah et al, 1982).

2.4.1.3 Gas Holdup Characteristics

Gas holdup is determined by many factors. Gas holdup increases with increasing gas velocity and decreasing liquid velocity (Friedel et al, 1980; Fujie et al, 1980; Herbrechtsmeier et al, 1981,1985; Kularni et al, 1983; Shah, et al, 1983; Ohkawa et al, 1985; Bando et al, 1988; Yamagiwa et al, 1990). Gas holdup increases with a higher jet velocity and with an increase in the length of the jet due to the amount of gas entrained, and a decrease in the nozzle diameter at a constant jet velocity since the liquid superficial velocity decreases (Ohkawa et al, 1985; Yamagiwa et al, 1990). Since more than one region exists in a downflow bubble column the gas holdup varies from zone to zone along the length of the column.

Ohkawa et al (1985) compared the range of gas holdup in a downflow bubble column with the range for upflow bubble columns, and concluded that the relationship between the gas superficial velocity and gas holdup in the downflow system differed markedly from that in the gas upflow system. Shah et al (1983) and Ohkawa et al (1985) reported that higher values of gas holdup could be obtained in the downflow

system with a remarkably low gas superficial velocity range when compared to the upflow system.

2.4.1.4 Interfacial Area

In cocurrent downflow bubble columns a state of near-suspension of gas bubbles can be observed by controlling the liquid flowrate within the column. As the result, the mean residence time of the gas can be increased and higher interfacial areas for mass transfer can be achieved. Several workers (Fujie et al, 1980; Herbrechtsmeier et al, 1980; Kulkarni et al, 1983) observed a large value of interfacial area per unit volume. Kulkarni et al (1983) reported at least two-fold increase in interfacial area per unit volume in downflow bubble columns compared to the data obtained in upflow bubble columns under similar operating conditions and a gas flowrate up to $0.1 m.s^{-1}$. On the other hand, in downflow bubble columns a high interfacial area can be obtained easily at a low gas superficial velocity ($0.015 m.s^{-1}$) whereas in upflow bubble columns such a value can be achieved only at extremely high gas velocity ($> 0.1 m.s^{-1}$) and with a very efficient gas distributor. Kulkarni et al (1983) explained that such a big difference can be attributed to the quite different characteristics of gas-liquid dispersion between the downflow and upflow systems and is related directly to the flow pattern and dispersion stability. A very stable bubble flow regime prevails even at a high gas flowrate in a downflow bubble column, but in upflow bubble columns the bubble flow regime shifts readily into the unstable churn-turbulent regime due to the formation of large bubbles by coalescence if the gas velocity approaches $0.05 m.s^{-1}$.

The effects of various operating parameters on the interfacial areas in downflow bubble columns vary significantly depending on the type of the contactor. In downflow bubble columns sparged with porous plate, sintered disc or ring-type distributors the interfacial area increased with increase in the gas superficial velocities, but there is no direct relationship between the interfacial area and the liquid superficial velocity (Herbrechtsmeier et al, 1981; Kulkarni et al, 1983). Ohkawa et al (1987) observed an increase in interfacial area with an increase in the liquid velocity in downflow bubble columns with gas entrainment by a liquid jet. Since the amount of gas entrained in the system is a direct function of the jet length and velocity, increasing the liquid velocity would increase the gas holdup and interfacial area. However, the general dependence of interfacial area on the liquid velocity in such a contactor is not always similar to that observed for gas holdup, because there is only a negligible effect of the nozzle diameter, which accounts indirectly for the effect of the liquid velocity on interfacial area. Bando et al (1988) reported that the effects of the liquid superficial velocity on both interfacial area and gas holdup were opposite in downflow bubble columns with simultaneous gas-liquid injections. The interfacial area in both the spouting zone and the calm zone in the column increased with an increase in the liquid superficial velocity.

Bando et al (1988) compared the data obtained in a downflow bubble column with simultaneous gas-liquid injector nozzles and in a downflow bubble column of similar dimension with a gas perforated plate sparger and concluded that for a given column diameter the type of distributor affects the value of the interfacial area in the contactor. The interfacial areas in the downflow bubble column sparged with a perforated plate were lower than those for the downflow bubble column with a

simultaneous gas-liquid injector nozzle. Bando et al (1988) also compared their data for the downflow bubble column sparged with a perforated plate with those obtained by Kulkarni et al (1983) from a similarly-dimensioned downflow bubble column sparged with a ring-type distributor, and concluded that a ring-type distributor produced higher interfacial area than did a perforated plate distributor. They attributed this observation to different flow patterns. Uniform bubbly flow prevails in the contactor sparged with a perforated plate (Bando et al, 1988) but bubble flow with backmixing of bubbles predominates in the contactor sparged with a ring-type distributor (Kulkarni et al, 1983). However, the flow pattern developed in a contactor is influenced significantly by the way the phase is introduced into the contactor. Therefore, a general conclusion should not be drawn on this issue.

Downflow bubble columns sparged with perforated plates can be operated more efficiently at low liquid throughputs since large interfacial area per unit volume can be achieved. Kulkarni et al (1983) reported that at identical energy consumption a much higher interfacial area can be achieved in downflow contactors than that in upflow contactors. In addition the values of the interfacial area per unit volume observed for downflow bubble columns except jet reactors are at least similar to, if not greater than, for identical energy input those for upflow bubble columns and stirred batch contactors, and a equation for interfacial area was developed as follows:

$$a = 225 u_G^{0.635} u_L^{-0.205} \sigma^{-0.11} \qquad (2.4.2)$$

where

a = specific interfacial area, $m^{-2}.m^{-3}$

u_G = superficial gas velocity, $m.s^{-1}$

u_L = superficial liquid velocity, $m.s^{-1}$

σ = liquid surface tension, $kg.s^{-2}$

Nagel et al (1976, 1979), using the Kolmogoroff's isotropic turbulent theory, reported that the energy dissipated per unit volume $\left(\frac{E}{V_R}\right)$ to generate the interfacial area can be correlated by the following equation

$$a = K\left(\frac{E}{V_R}\right)^m \varepsilon_g^n \qquad (2.4.3)$$

where E = energy dissipation, W

V_R = reaction volume, m^3

a = specific interfacial area, $m^2.m^{-3}$

ε_g = gas holdup, %

K, m, n = parameters

2.4.2 Mass Transfer Characteristics

Very limited information is available for mass transfer investigations in downflow bubble columns. Herbrechtsmeier and Steiner (1978) and Fujie et al (1980) studied the absorption of oxygen in water and assumed that both the gas phase and liquid phase were plug flow for the assessment of the volumetric and liquid side mass transfer coefficients in downflow bubble columns with gas spargers. They reported that the volumetric mass transfer coefficient k_La is considerably dependent on the gas superficial velocity but only slightly affected by the liquid flowrate in the range $0.175m.s^{-1}$ to $0.27m.s^{-1}$. The dependence of k_La on the gas superficial velocity can be estimated by the equation $k_La = bu_G^n$, developed by Deckwer et al (1974) for upflow bubble columns. Kulkarni et al (1983) also reported that for liquid velocity up to

$0.33m.s^{-1}$ the volumetric mass transfer coefficient in a downflow bubble column with a gas sparger can be evaluated by the above equation proposed for upflow bubble columns, but they reported much higher k_La values than did Herbrechtsmeier and Steiner (1978) and Fujie et al (1980). Kulkarni et al (1983) explained that the difference of k_La value may result from the different diameter columns used. The dependence of mass transfer coefficients on column diameters may contribute to the decrease in gas holdup with increase in the column diameter (Shah et al, 1982), although this observation differs from the results obtained by Hikita et al (1981) for upflow bubble columns for which k_La is independent of the column diameter.

Fujie et al (1980) investigated the liquid side mass transfer coefficient k_L in a downflow bubble column sparged with a sintered plate and found that k_L varies only slightly with bubble size so that average values of k_L and the interfacial area (a) can be used to predict k_La value.

The concentration distribution in downflow bubble columns varies with the type of contactor. Herbrechtsmeier et al (1981) studied the absorption of oxygen in the liquid phase in a downflow bubble column sparged with a porous plate distributor and reported that the dissolved oxygen concentration increased rapidly directly below the gas distributor but was unchanged along the column further than 200mm from the gas distributor. However, they failed to apply a single k_La value in the liquid phase by using the one dimensional two-phase dispersion model for recalculation of the oxygen profiles along the column, since the calculated values deviated significantly from the measured dissolved oxygen concentrations. Therefore, different k_La values need to used for different points. They claimed that in downflow bubble columns the oxygen

concentration distribution and the value of k_La along the column are affected greatly by the gas distributor. Bando et al (1988) confirmed the possible effect of the gas distributor on the longitudinal oxygen profile and volumetric mass transfer coefficients by comparing the longitudinal oxygen profile obtained in downflow bubble columns with perforated plate spargers or with simultaneous gas-liquid injectors. With a simultaneous gas-liquid injector the oxygen concentration was constant throughout the sprouting section but decreased rapidly in the calm zone so that the complete mixing model in the sprouting section and the plug flow model in the calm zone were applied as the flow pattern in such a contactor.

For the flow pattern in bubble columns, the volumetric mass transfer coefficient should be obtained from the axial dispersion model and the longitudinal gas concentration profile instead of from a simplified model such as plug flow or mixing flow (Shah et al, 1982). Kulkarni and Shah (1984) reported that the plug flow model is applicable to the liquid phase due to the high liquid flowrate used in downflow bubble columns with gas spargers. They compared the axial dispersion in the gas phase with data in the available literature and pointed out that the assumptions of complete mixing (Kulkarni et al, 1983) and plug flow (Herbrechtsmeier and Steiner, 1978; Fujie et al, 1980) in the gas phase are incorrect.

2.5 Loop Reactors

A high mixing effect is obtained best with an ideal stirred tank reactor, whereas the demand of high driving concentration difference for gas mass transfer is fulfilled best

with an ideal tube reactor. Loop reactors offer a favourable combination of high mixing effect and high driving concentration (Blenk, 1979). Loop reactors are the modified models of bubble column reactors and are extensively used for chemical processes. The main advantages of loop reactors (Chisti, 1989) over bubble columns are improved mixing, with higher mass transfer coefficients in some instances. Loop reactors also have a better defined liquid flow than do bubble columns.

The operation of loop reactors is based on the principle of (1) "internal circulation" around a draft tube, which is positioned concentrically in a tower reactor and (2) "external circulation". According to the mode of flow drive loop reactors can be classified into the gas-lift loop reactor (GLR), the propeller loop reactor (PLR) and the jet loop reactor (JLR) (Figure 2.4). A gas-lift loop reactor works with hydrostatic flow drive caused by different densities of fluids because of different gas holdup in the communicating spaces. A propeller loop reactor works with hydromechanical propeller (or pump) flow drive. In principle, a propeller loop reactor is a slim stirred tank reactor with a longitudinal driving propeller-agitator. A propeller loop reactor includes a more complicated construction and causes operating problems related to the sealing of the shaft. A jet loop reactor works with hydrodynamic jet drive.

A type of jet loop reactor, the BUSS loop reactor (Figure 2.3), developed by BUSS Ltd has great potential for catalytic hydrogenation processes (Rylander, 1979; Leuteritz, 1985; Greenwood, 1986; Duveen, 1993; Jack, 1996). BUSS loop reactors can be operated in batch or continuous mode. The loop reactor is incorporated into a reactor system, characterised by a downflow bubble column fitted with a Venturi mixing nozzle and an external pump. The catalyst and substrates are circulated

continuously through a nozzle, in which most of the reduction occurs. The bulk of the turbulent mixing and high bubble shear occurs in the nozzle, while the body of the reactor acts as a reservoir for the circulation pump. The nozzle region in BUSS loop reactors resembles the upper section of the CDC, in which gas and slurry first interact at the T-piece through the orifice and 200mm-300mm into the column where most mass transfer takes place (Boyes et al, 1995).

BUSS loop reactors offer many advantages such as high mass transfer, high heat transfer, intensive mixing and high pressure. These advantages lead to rapid heating and cooling for easy temperature control, shorter reaction times for mass transfer controlled reactions, improved selectivity and high yield due to flexible operating conditions, lower catalyst use due to the better mass transfer rate and easier scale-up due to simple scaleup practice based on the similarity of circulation rates, specific power input and liquid velocity. BUSS loop reactors can be used in gas/liquid systems, liquid/solid catalyst systems, gas/liquid/solid systems and biphasic liquid/liquid systems. However, strongly-foaming mixtures and immiscible liquids with large density difference are not suitable in BUSS loop reactors.

2.6 Clean Technology

Clean technology is a general concept which has risen in recent years as part of the search for more sustainable ways to provide for human needs (Clift, 1995, 1996), and is defined in the Clean Technology Research Programme of the Engineering and Physical Sciences Research Council (EPSRC) as follows:

"A Clean Technology is a means of providing a human benefit which, overall, uses less resources and causes less environmental damage than alternative means with which it is economically competitive."

Clean technology includes the discovery and development of cleaner products to substitute for existing polluting ones and the incorporation of new waste-free processes in the manufacture of existing products (Kirkwood, 1994). The cleanliness of a technology must be assessed by including the environmental performance of both upstream and downstream suppliers. The formal procedure is a process to evaluate the environmental burdens associated with a product, process or activity by identifying and quantifying the energy and materials used and the waste materials released into the environment, and to identify and evaluate opportunities to effect environmental improvements. The assessment includes the entire cycle of the product, process or activity, encompassing extraction and processing of the raw materials, manufacturing, transportation and distribution, use, re-use, maintenance, recycling and final disposal.

Clean technology aspires towards a dematerialised economy in which benefits are provided without trading material products or artefacts. One specific example is organic solvents, which can (in effect) be re-used or taken back for reprocessing rather than sold outright. Materials and processes are chosen to minimise the overall environmental impact, rather than solely addressing the problem of managing post-consumer waste. In spite of some industry resistance, the trend of requiring the supplier to retain responsibility for the product can be seen in legislation (notably in the European Union) and in initiatives like the Responsible Care Programme of the chemical industry. These changes in commercial and social practice may represent more of a barrier to take-up of Clean Technology than are developments in technology.

The important aspects of highly-targeted use and highly-selective action suggest that Clean Technology represents a further drive away from bulk chemicals to lower-volume, higher-value products. For highly selective synthesis, the challenges include:

1. Different approaches to separation and purification Traditionally the chemical industry purifies most of its products by their physical properties, such as using distillation or extraction. For low-volume products selected for specific biological activity, separation by physical properties will be replaced by separation by molecular structure or biological function. Affinity and membrane separation techniques are likely, therefore, to become important.

2. Different approaches to synthesis Rather than concentrating on high yields, there will be more emphasis on product selectivity-particularly on selectivity against difficult or toxic by-products. More attention will be paid to using reagents or reaction media which are contained or fully recycled within the process. Techniques like pressure swing reaction which combine synthesis and separation may be attractive.

3. New synthetic routes Developing chemical routes in which halogens and halogenated compounds are used only if the halogen is essential in the products.

Some biological processing routines are:

1. Systematic identification of effective and selective biological catalysis;

2. Design of protein-based catalysts using protein engineering or antibody technology;

3. Generation of cells with truncated metabolism so that production of unwanted compounds is minimised.

Clean processes in fine chemicals industry may be developed by maximising reaction yields, optimising solvent recovery and minimising energy utilization. Clean alternatives to existing bulk synthesis processes can be achieved by (1) optimisation of synthetic reaction conditions involving biocatalysts, (2) identification of new biocatalysts with appropriate environmental properties, (3) identification of alternative renewable feedstocks with balanced functionality, (4) integration of separation processes into reactor design (Suckling et al, 1992).

2.7 Hydrogenation of α,β-Unsaturated Aldehydes

The importance of cinnamic derivatives in the fine chemicals industry has led to the pursuit of reliable clean synthesis. Commercial processes have focused on condensation reactions between benzaldehyde and various active methylene compounds for assembly of the requisite carbon skeleton. The presence of a di-substituted carbon-carbon double bond in the sidechain of these chemicals gives rise to the existence of cis- or (*Z*)- and trans- or (*E*)-isomers. Hydrogenation of unsaturated aldehydes to saturated aldehydes is readily achieved over most metal catalysts under mild conditions in various solvents, in the liquid or the vapour phase. However, the selective conversion of unsaturated carbonyl compounds into unsaturated alcohols is much more difficult to achieve by heterogeneous catalysis.

The α,β-unsaturated alcohols form an important class in the bulk and fine chemicals industries; thus the selective hydrogenation of α,β-unsaturated carbonyl compounds to their corresponding alcohols has considerable industrial relevance. Due to the importance of unsaturated alcohols as intermediates in the preparation of various fine

chemicals, several attempts have been made to develop a suitable catalytic system. Most catalysts first reduce the alkene double bond and then the carbonyl group, leading to poor selectivity and the formation of the saturated alcohols. This problem may be attributed to: (i) the two bond energies (Pauling, 1967), and (ii) the orientation of the molecule adsorbed on the catalyst (Richard, et al, 1988).

It is well established that over supported transition metals the C=C bond is hydrogenated more readily than the C=O bond. The research in this field has been reviewed with special emphasis on the hydrogenation of cinnamaldehyde (Coq et al, 1993; Gallezot et al, 1991). From the literature review it is evident that the selectivity to cinnamyl alcohol, the desired product, is better: (1) over iridium than palladium, platinum, rhodium or ruthenium, (2) on large metal particles, (3) when graphite is used as a support in place of charcoal or silica, (4) on metals supported on zeolites containing alkali cations, (5) on bimetallic catalysts like platinum-iron/charcoal. In several other studies dealing with the hydrogenation of cinnamaldehyde, these results have been discussed in the general frame of the following two points (Giroir-Fendler et al, 1988; Richard et al, 1988; Richard et al, 1989; Gallezot et al, 1990; Potarzewski et al, 1986), namely: (1) The electronic or ligand effect of the support or the doped metal, wherein there is a transfer of electrons from the support or the doped metal to the active metal, which results in an increase in the electron density; (2) Formation of new catalytic sites involving promoter cations, which are able to co-ordinate the oxygen atom in the carbonyl group and activate it. However, the generality of the above conclusions has been questioned due to the lack of an exhaustive study on several α,β-unsaturated aldehydes over the same family of catalysts, and due to the contradictory results obtained by changing the metal precursor. In particular, the role

of residual chloride ions on the selectivity is still not clear. Nitta et al (1989) have reported an increase in the selectivity to unsaturated alcohol over cobalt catalysts containing chloride ions, whereas the reverse effect has been observed over platinum and ruthenium catalysts (Vannice and Sen, 1989; Wiemeijer et al, 1986).

2.7.1 Difference between the Hydrogenation of Cinnamaldehyde and Crotonaldehyde

Rylander and Himelstein (1963) compared the difference between the hydrogenation of cinnamaldehyde (3-phenyl-2-propanal) and crotonaldehyde (2-butenal). Although crotonaldehyde is similar to cinnamaldehyde their behaviour on hydrogenation is not comparable. In many experiments with palladium on various supports and in various solvents crotonaldehyde was reduced only to butyraldehyde (butanal) with one exception. This difference in behaviour becomes explicable with the knowledge that whereas palladium is a very poor catalyst for the hydrogenation of an aliphatic aldehyde, it is excellent for the hydrogenation of aromatic aldehydes. Cinnamaldehyde is a vinylog of benzaldehyde, but crotonaldehyde is a vinylog of acetaldehyde. The aldehyde function of cinnamaldehyde would therefore be expected to be reduced much more readily than that in crotonaldehyde. Remarkably, for the hydrogenation of crotonaldehyde more than one mole of hydrogen was consumed only if palladium-iron catalysts were used, but with the same catalysts the hydrogenation of cinnamaldehyde stops spontaneously after the uptake of one mole of hydrogen and 100% selectivity to hydrocinnamaldehyde was achieved.

2.7.2 Catalyst Effect

The product distribution and selectivity for the hydrogenation of α,β-unsaturated aldehydes are affected significantly by the catalysts used. Saturated aldehydes can be obtained at high yields and at high rates using a palladium catalyst. The reaction stops almost completely after the hydrogenation of the C=C bond, making palladium a perfect catalyst for hydrogenation to a saturated aldehyde (Poltarzewski et al, 1986; Rylander and Hilmestein, 1963). The reduction of α,β-unsaturated aldehydes to saturated aldehydes is also readily achieved by most platinum metal catalysts under mild conditions, in various solvents, in batch or continuous processing and in liquid phase or vapour phase (Rylander et al, 1963). The preferential formation of saturated aldehydes is related to thermodynamic and kinetic factors. Poltarzewski et al (1986) stated that over a platinum catalyst there is preferential formation of saturated aldehydes due to the lower energy of the C=C bond with respect to the C=O bond. From a thermodynamic point of view it should be considered that the energy of the C=C bond ($615kJ.mol^{-1}$) is smaller than that of the C=O bond ($715kJ.mol^{-1}$). Hydrogenation of C=C bonds occurs at a very rapid rate over platinum catalysts even at low temperature. This preferential formation of saturated aldehydes on platinum/charcoal catalysts is confirmed by the fact that during the hydrogenation of cinnamaldehyde at 333K and atmospheric pressure over 10% platinum/charcoal in ethanol, large amounts of hydrocinnamaldehyde were formed (Poltarzewski et al, 1986). Similar results were obtained in the hydrogenation of acrolein (propenal).

Either a nickel or a copper catalyst should be used for the complete hydrogenation of cinnamaldehyde to the saturated alcohol. With these catalysts the reaction proceeds

by hydrogenation of the alkene bond to the saturated aldehyde and then further by hydrogenation of the carbonyl group to yield the saturated alcohol.

No equally good catalyst is known for the selective hydrogenation of the carbonyl group to yield to unsaturated alcohols. However, relatively high yields of unsaturated alcohol can be obtained using platinum catalysts promoted with iron salts (Tuley and Adams, 1925; Rylander, 1979; Richard et al, 1989; Beccat et al, 1990; Galvagno et al, 1989). Iron increased the reaction rate for forming the unsaturated alcohol. The activity and selectivity to an unsaturated alcohol can also be improved by using promoters such as tin, germanium, (Richard et al, 1989) and cobalt (Rylander, 1979), or by supporting platinum on titania (Vannice and Sen, 1989) or niobium pentoxide (Yoshitake and Iwasawa, 1990). In addition, the catalytic behaviour of platinum is drastically altered by dispersing platinum on a polyamide matrix (Poltarzewski et al, 1986; Galvagno, et al, 1983). During the hydrogenation of acrolein (propenal) this different behaviour resulted in the appearance in the reaction products of a consistent amount of propenol. The higher selectivity toward propenol could be related to the observed lower tendency of platinum/nylon to hydrogenate alkenes. Formation of unsaturated alcohol was, however, not observed in the hydrogenation of cinnamaldehyde. This could result from different reactivities of the carbonyl group in aliphatic or in aromatic aldehydes. A similar difference in the behaviour between the hydrogenation of cinnamaldehyde and crotonaldehyde was observed by Rylander and Hilmestein (1963).

A disadvantage in using platinum for hydrogenation of aldehydes is very low activity. Platinum catalysts are excellent for the hydrogenation of alkenes, but they deactivate

very rapidly when used for the hydrogenation of aldehydes. This is probably due to carbon monoxide produced by decomposition of aldehyde in a side reaction (R-C=O→ R-H + CO). The deactivation can be prevented, however, by the presence of small amounts of oxygen. This leads to the production of carbon dioxide instead of carbon monoxide (Schröder and Andersson 1991).

Coq et al (1993) used ruthenium-based catalysts for hydrogenation of a series of α,β-unsaturated aldehydes to arrive at general guidelines for designing selective catalysts. To avoid the effect arising from residual chloride ions, the catalysts were prepared from organometallic precursors. It was found that the selectivity to cinnamyl alcohol increased until 50-70% of cinnamaldehyde was converted.

Satagopan and Chandalia (1994) reported that when palladium catalysts modified by sodium or potassium hydroxide were used the main reaction is the hydrogenation of the alkene bond whereas when similar platinum catalysts were used the main reaction is the hydrogenation of the carbonyl group.

2.7.3 Metal Precursor Effect

The catalyst precursor also plays a great role in the selectivity to unsaturated alcohols. Platinum or ruthenium catalysts prepared from their chloride salts have been shown to be less selective to unsaturated alcohols than those made from other metal salts (Coq et al, 1993; Wismeijer et al, 1986; Vannice and Sen, 1989). The selectivity in such cases is enhanced on elimination of the residual chloride ions by reduction of the catalyst at high temperature but with a lower activity. However, the opposite behaviour is reported for the hydrogenation of cinnamaldehyde and crotonaldehyde

over supported cobalt catalysts (Nitta et al, 1990). The samples prepared from chlorides showed the highest selectivity to the unsaturated alcohols regardless of the support used. The promoter effect of chloride was due to a favourable crystallite size distribution, which hampers attack by hydrogen on the alkene bond.

2.7.4 Metal Particle Size Effect

The possible influence of the metal particle size on the selective hydrogenation of α,β-unsaturated aldehydes is interesting. Such an effect of metal particle size was investigated for the hydrogenation of cinnamaldehyde over ruthenium/carbon (Galvagno et al, 1991) and platinum or rhodium supported on graphite (Gallezot et al, 1990). In both studies the selectivity to cinnamyl alcohol increased with increasing metal particle size. That behaviour could be due to a steric effect caused by the presence of the phenyl group, which imposes a tilt on the cinnamaldehyde molecule, favouring its adsorption through the carbonyl group on the metal surface of large particles (Gallezot et al, 1990).

Coq et al (1993) reported the effect of ruthenium particle size that some trends are discernible with respect to the selectivity to propenol. For the hydrogenation of cinnamaldehyde over ruthenium/carbon (Galvagno et al, 1991) and platinum or rhodium on graphite (Gallezot et al, 1990) catalysts, a higher selectivity to cinnamyl alcohol was also obtained for the large particles. The behaviour was attributed in part to a steric effect of the phenyl group, which hinders the approach of the carbonyl group to the flat metal surface of large particles. Nitta et al (1989), who reported the same results for the hydrogenation of cinnamaldehyde and crotonaldehyde over cobalt/silica catalysts, proposed that a lower adsorption strength of the

α,β-unsaturated alcohol on large particles was responsible for this effect. Any steric hindrance against the adsorption of the alkene bond can be ruled out, and hence a modification of the relative adsorption strength of that bond on the metal surface between small and large particles can explain the effect (Coq et al, 1993).

In spite of the large amount of work in this area, no clear picture emerges. The majority of existing work is on the liquid-phase hydrogenation of cinnamaldehyde (Giroir-Fendler et al, 1988; Nitta et al, 1989; Nitta et al, 1990; Richard et al, 1989; Galvagno et al, 1991; Gallezot et al, 1990; Fouilloux et al, 1988; Poltarzewski et al, 1986; Troncani et al, 1990), crotonaldehyde (Nitta et al, 1989; Nitta et al, 1990; Vannice and Ben, 1989; Beccat et al, 1990; Noller and Lin, 1984) and citral (Wismeijer et al, 1986) where the effect of the solvent cannot be ignored.

2.7.5 Support Effect

The selectivity to unsaturated alcohols can be much improved by changing the supports. This is why the electronic and geometrical properties of the support are subjects of extensive investigations (Isaeva et al, 1996; Blackmond et al, 1991, Gallezot et al, 1992; Giroir-Fendler et al, 1992).

The selective hydrogenation of an α,β-unsaturated carbonyl compound dates back to 1925. Tuley and Adams (1925) used an unsupported platinum-zinc-iron catalyst for the hydrogenation of cinnamaldehyde to cinnamyl alcohol. A similar system was used by Rylander (1985) to study the selective hydrogenation of crotonaldehyde to crotyl alcohol. Various monometallic catalysts have been used to study the selective hydrogenation of such species (Giroir-Fendler et al, 1988; Nitta et al, 1989, 1990; Wismeijer et al, 1986; Blackmond et al, 1990; Richard et al, 1989; Beccat et al, 1990;

Galvagno et al, 1991), and it was found that iridium, ruthenium and cobalt demonstrated good intrinsic selectivity for the α,β-unsaturated alcohols (Giroir-Fendler et al, 1988; Nitta et al, 1989, 1990). The role of the support for such reactions is examined (Giroir-Fendler et al, 1988; Wismeijer et al, 1986; Vannice and Sen, 1989). Vannice and Sen (1989) studied the hydrogenation of crotonaldehyde in the gas phase and found that, while platinum/silica and platinum/alumina have negligible selectivity to crotyl alcohol, platinum/titania reduced at high temperature shows 37% selectivity to crotyl alcohol. Wismeijer et al (1986) observed similar results on ruthenium/titania for the hydrogenation of citronellal in the liquid phase. Giroir-Fendler et al (1988) observed that selectivity to cinnamyl alcohol during the hydrogenation of cinnamaldehyde on platinum/graphite was better than on platinum/charcoal.

Vennice and Sen (1989) attributed the enhanced selectivity observed on platinum/titania to the strong metal-support interaction (SMSI) effect wherein some titanium suboxide species migrate to the interphase at the high temperature of the reduction. These species then react with the oxygen atoms of the carbonyl groups, thus polarizing the carbonyl bond and facilitating its attack by the adsorbed hydrogen atom. Wismeijer et al (1989) speculated that hydrogen spillover was responsible for the enhanced selectivity to the alcohol. For platinum/graphite, it was proposed that an electron transfer occurs from the graphite to the metal, leading to a lower degree of interaction between the alkene bond and the platinum (Giroir-Fendler, 1988).

Coq et al (1993) reviewed the catalytic properties of the supported metals for the hydrogenation of propenal. Hydrogenation of propenal to propenol was claimed to

occur with good selectivity on rhenium/glass and mixed silver-cadmium-zinc catalysts. Coq et al (1993) focused on gaining insight into the nature of the metal, crystallite size and type of support that led to enhancement of the selectivity to unsaturated alcohols. The role of the support in the selective hydrogenation of propenal is clearly evident. The main point deals with the effect of the nature of the support. In addition, most of the catalysts demonstrate high initial selectivity to propenol. The ruthenium/titania catalysts show very high activity for propenal hydrogenation, but the high-temperature-reduced ruthenium/titania is more selective to propenol than is the low-temperature-reduced ruthenium/titania which gives high selectivity to shortchain compounds. When ruthenium/titania is reduced at temperatures higher than 773K the phenomenon of strong metal-support interaction occurs. Under these conditions, titanium suboxides (TiOx, $x < 2$) species migrate onto the metal particles and inhibit hydrogen chemisorption without any change in the mean size of the ruthenium particles. In order to explain the enhanced reactivity for α,β-unsaturated carbonyl hydrogenation, Vannie and Sen (1989) for platinum/titania, and Yoshitake and Iwasawa for iridium/niobium pentoxide (1990) and platinum/niobium pentoxide (1989), proposed that the activation of the carbonyl group becomes favoured at the boundary between the metal surface and migrating titanium suboxide or niobium suboxide (NbO_x, $x < 2.5$) species. When comparing ruthenium/titania and platinum/silica catalysts, the results obtained on the latter are a little surprising, since it was not claimed that silica induced good selectivity for α,β-unsaturated alcohols (Wismeijier et al, 1986; Vannice and Sen, 1989). Nevertheless, the opposite behaviour was reported for the hydrogenation of butenal over cobalt supported on silica, aluminia, titania and zirconia (Nitta et al, 1990): the cobalt/silica

catalyst was the most selective for butenol among the chloride-free samples. The authors claimed that a specific size distribution of the cobalt particles was responsible for this behaviour. Coq et al (1993) stated that it was difficult to identify the determining factor for the selectivity gained on ruthenium/silica catalysts. Owing to the discrepancy between the dispersion estimated by hydrogen chemisorption and transmission microscopy, promotion of selectivity by some impurities cannot be ruled out.

Rylander and Himelstein (1963) studied the catalyst support effect on selectivity and rate of hydrogenation. The nature of support is an important factor in determining the selectivity of reduction of cinnamaldehyde. There is no evident correlation between the type of support, rate of reduction, and selectivity. Since the selectivity depends also on the solvent, the possibility of a general correlation becomes even less likely. The data establish that the course of reduction can be changed sharply, even though the criteria for selection are purely empirical. A comparison of the rate data for these catalysts in methanol and in ethanol shows an interesting anomaly. In general, the rate in ethanol is only a quarter to half of that in methanol, except when the support is charcoal; with charcoal the rate is slightly faster in ethanol.

Blackmond et al (1991) studied the hydrogenation of cinnamaldehyde in propan-2-ol under a pressure of 4MPa and at 373K with ruthenium and rhodium catalysts or at 343K with platinum catalysts. They compared product yields as a function of conversion up to about 40% for carbon, sodium-yttrium zeolite, and potassium-yttrium zeolite supported ruthenium catalysts. Selectivity to cinnamyl alcohol was greatly enhanced when zeolites were used as supports instead of carbon. The rate of

conversion of cinnamaldehyde, however, was faster for the carbon-supported ruthenium compared to both zeolite-supported ruthenium catalysts. The results for platinum and rhodium supported on the two zeolites were similar to those for ruthenium. There was little difference between the two types of yttrium zeolite for cinnamyl alcohol selectivity, suggesting that the zeolite pore structure, and not any electronic properties caused by the cation, was the important factor for achieving high cinnamyl alcohol selectivity from cinnamaldehyde as the organic substrate. Isomerization from unsaturated alcohol to saturated aldehyde has been observed. While the alkene bond energy is lower than that of carbonyl, the actual product selectivity achieved depends significantly on parameters including the type of metal and the nature of the support, the structure of the reactant and the concomitant steric and electronic factors involved in adsorption of the reactant onto the catalyst surface.

Blackmond et al (1991) pointed out that the structural effects of zeolite catalysts have been well-documented. Gallezot et al (1990) stated that selectivity to cinnamyl alcohol could be enhanced from metals in zeolite micropores, both for platinum, which exhibits moderate selectivity to cinnamyl alcohol, and for rhodium, which is usually quite unselective to cinnamyl alcohol. They compared the zeolite-supported ruthenium catalyst to ruthenium supported on an amorphous carbon substrate. Cinnamaldehyde can enter the 0.74nm zeolite pore opening only end-on, and its mobility once inside the 1.33nm diameter supercages is constrained because of the rigidity of the side chain, the bulk of the phenyl group, and the fact that a significant portion of any supercage where hydrogenation can occur is occupied by a metal particle. The cinnamaldehyde molecule can easily adsorb onto the metal particle only through the carbonyl group at the end of the side chain because an approach to the

metal surface near the alkene bond is sterically hindered by the phenyl group. In contrast, on ruthenium/carbon the absence of the steric constraints of the zeolite pores means that other modes of adsorption are available to cinnamaldehyde. Hence, in the case of ruthenium/carbon, the intrinsic catalytic properties of ruthenium dominate over any steric constraints imposed by the support. For zeolite-supported ruthenium, the molecular constraints of cinnamaldehyde in the zeolite pores predominate over other potential effects such as the electronic environment of the ruthenium in the zeolite pores, and any changes that occur when potassium ions replaced sodium ions in the zeolite framework. This work shows that for platinum and rhodium catalysts, also, the geometric effect of the zeolite pores predominates over electronic considerations in cinnamaldehyde hydrogenation. The acid strength of the protons in yttrium zeolite decreases as the cation is changed from lithium through sodium, potassium, rubidium, to caesium. This decrease in acidity results in greater electron density on the small metal particles within the zeolite pores. An increase in charge density on the metal may cause a suppression in the alkene hydrogenation rate by enhancing the delocalization of electrons in the reactants absorbed onto the substrate. Selectivity to unsaturated alcohol would thus be increased.

2.7.6 Solvent Effect

Solvents can influence considerably reaction rate and selectivity. Rylander and Himelstein (1963) studied the solvent effect on the rate and the product composition obtained when the reaction stopped spontaneously. For the C_1 to C_4 alcohols used as solvents the effect on rate is much greater than on selectivity. The rate with propanol and butanol is less than half that with methanol or ethanol, yet the selectivity obtained

in these experiments falls in a narrow range (54-59%) and shows no correlation with the rate. Apparently nothing is gained by using the long-chain alcohols. Acetic acid affords a relatively high yield of hydrocinnamaldehyde and a very rapid rate of hydrogenation. The yield of hydrocinnamaldehyde is probably 5-10% higher than reported. Triethylamine, benzene, and ethyl acetate give low rates of hydrogenation. A low rate might be expected from the first two solvents, but it is surprising for ethyl acetate, as this solvent gave a fast rate for the hydrogenation of the alkene bond using palladium/charcoal catalyst.

2.7.7 Additive Effect

Much work has been carried out on this subject. Many kinds of promoters and poisons have been examined. The product distribution and selectivity can be altered significantly by incorporating additives into the reaction system.

2.7.7.1 Effect of Oxygen

Schröder and Verdier (1993) studied the influence of oxygen in the liquid-phase hydrogenation of α,β-unsaturated aldehydes. The addition of small amounts of oxygen greatly increases the activity of pure platinum catalyst as well as iron (II) chloride-promoted platinum catalyst. The explanation for this is probably that carbon dioxide is produced instead of carbon monoxide when the aldehyde is decarbonylated (Schröder and Andersson, 1991). It is interesting to note that the selectivity for the hydrogenation of cinnamaldehyde is changed by the addition of oxygen, and is shifted towards the hydrogenation of the alkene bond to yield more of the saturated

aldehyde. One explanation for this is that oxygen restores sites that are more active for alkene bond hydrogenation. These sites are probably the edge sites, which are also the most active ones for the decarbonylation reaction (R-CH=O → R-H + CO). It is possible that these edge sites are poisoned by carbon monoxide to a high degree when no oxygen is present. The addition of oxygen would restore these sites by the oxidative removal of carbon monoxide. The electronic properties of the platinum catalyst may also be changed by the presence of oxygen, and this might influence the selectivity.

Galvagno et al (1989) reported that oxygen and transition metal chlorides act differently. They suggested that the addition of promoters modifies the course of the reaction through two main effects, one on the reactant and the other on the noble metal catalyst. The effect of the aldehyde is to activate the carbonyl group by increasing polarisation and thus making it more nucleophilic. The effect on platinum is of blocking the active sites, thus decreasing hydrogenation activity. The activation of the substrate prevails with lower additive contents, but the poisoning effect would prevail at higher additive contents. This hypothesis is supported by the finding that the maximum reaction rate was found at intermediate concentration of the additive. The promoting action is not related to the presence of chloride. The addition of tin has similar effects.

Oxygen, which has been reported to improve the catalytic activity of platinum, probably acts by removing catalyst poisons, possibly carbon monoxide, formed by decarbonylation of the aldehyde (Rylander, 1967; Hoffman et al, 1962). Higher selectivities were found generally on the more active systems, with the exception of

selenium (IV) chloride. The catalytic activity and selectivity to cinnamyl alcohol tend to increase with the electron density of the metal cation.

2.7.7.2 Effect of Iron

The addition of iron (II) chloride to the platinum catalyst increased the selectivity towards the hydrogenation of the carbonyl group to yield the unsaturated alcohol. The activity also increased for the hydrogenation of cinnamaldehyde in the absence of oxygen at moderate iron concentrations. However, addition of iron (II) chloride did not prevent the deactivation. Measurement of the iron concentration in the solution before the aldehyde was added showed that the adsorption rate was somewhat higher in the presence of hydrogen. This suggests that some of the added iron (II) chloride is reduced on the platinum.

Different explanations for the effect of iron have been proposed. Hotta and Kubomatsu (1969) examined the effect of iron on a cobalt catalyst. They suggested that the effect is due to a smaller amount of strongly adsorbed hydrogen. This hydrogen is believed to react easily with the alkene bond. Another explanation has been proposed by Beccat et al (1990), who examined the hydrogenation of unsaturated aldehydes on platinum/iron alloy catalysts. They suggested that the effect was caused by a change in the structural and electronic properties of some platinum atoms. The common explanation is that iron deposited on the catalyst surface acts as an adsorption site for the carbonyl group (Richard et al, 1989).

Richard et al (1989) studied the effect of iron on the hydrogenation of cinnamaldehyde. Iron atoms associated with platinum in the same particle promote

the hydrogenation of the carbonyl group and thus the overall rate of cinnamaldehyde hydrogenation and selectivity to cinnamyl alcohol. They suggested that the iron atoms absorbed onto the surface of the platinum particles are positively charged either because they are incompletely reduced or because there is some electron transfer from iron atoms to platinum atoms as iron is more electropositive than platinum. In the case of the platinum-iron/charcoal catalysts, an increase in the electron density of platinum was detected.

As more iron is deposited on the catalyst, the area of the platinum surface free for hydrogen adsorption decreases. This could explain why the activity decreases at higher iron concentrations. At high iron (II) chloride concentrations two kinds of acetals were produced. Separate experiments without any platinum catalyst showed that the acetals were products of a reaction between aldehydes and ethanol catalysed by iron (II) chloride. The acetals disappear after reaction of the aldehydes. The explanation for this is that the acetal reaction is reversible.

The palladium/alumina catalyst was very active for hydrogenation of the alkene bond to the saturated aldehyde. Further hydrogenation of the carbonyl bond to the saturated alcohol was very slow, but the rate was somewhat increased by the presence of iron (II) chloride.

Rylander and Himelstein (1963) studied the effect of iron over palladium catalysts. They found that using iron (II) chloride as a promoter only hydrocinnamaldehyde was obtained and at a very rapid rate. These selectivities are easily reproduced, but they are specific for each palladium catalyst and vary with the activity of the catalyst. The

1:1 ratio of iron (II) chloride to palladium at 100% hydrocinnamaldehyde is fortuitous; with other catalysts maximum selectivity occurs at other ratios, usually between 1:0.9 and 1:1.3. Iron (II) sulphate or iron (III) chloride additives would not produce 100% of hydrocinnamaldehyde. These results may be contrasted with those obtained by Tuley an Adams (1925) using platinum catalysts. They claimed that iron additives gave cinnamyl alcohol on adsorption of one mole of hydrogen. Skita (1915) found that colloidal platinum without additive gave predominantly hydrocinnamaldehyde after adsorption of one mole of hydrogen.

2.7.7.3 Effect of Acid

The effect of acids on the hydrogenation of α,β-unsaturated aldehydes is reported in many papers. Nagase et al (1983) reported that addition of small amounts of iron (III) ions (a Lewis acid) to Raney silver-zinc catalysts increases the selectivity to propenol. An increase in the selectivity to unsaturated alcohols by addition of iron (III) ions has been reported also by Tuley and Adams (1925). The effect of an acidic modifier, such as acetic acid, molybdenum chloride and cobalt (II) chloride, to Raney cobalt catalysts has been reported by Hotta and Kubomasu (1973) for the hydrogenation of 2-methyl-2-pentenal and addition of the acidic modifiers increases the selectivity to the unsaturated 2-methyl-2-pentenol.

Additives are known to affect both rate and selectivity for several reductions (Tuley and Adams, 1925; Maxted 1933; Innes, 1954). The reduction of cinnamaldehyde is such a case. Rylander and Himelstein (1963) studied the additive effect by using palladium catalysts. Both hydrofluoric and hydrochloric acids are effective promoters

for the reduction, while hydrobromic and hydriodic acids are definitely poisons. The product composition has no apparent correlation with rate.

2.7.7.4 Effect of Tin

Addition of tin to supported platinum catalysts modifies substantially their behaviour in the liquid-phase hydrogenation of α,β-unsaturated aldehydes (Poltarzewski et al , 1986; Galvagno et al, 1986; Galvagno et al, 1989). The rate of hydrogenation was found to increase with increasing tin:platinum ratio up to a maximum value, and then to decrease. The selectivity was also affected. While the preferential formation of saturated aldehydes was observed over platinum, the carbonyl bond was selectively hydrogenated over platinum-tin catalysts, resulting in α,β-unsaturated alcohols.

Poltarzewski et al (1986) reported that two types of interaction between platinum and tin supported on nylon would result in any case in a decrease in the rate of hydrogenation of the alkene bond. The occurrence of a platinum-tin solid solution would decrease the rate of hydrogenation by decreasing the number of empty d-orbitals. A similar effect would result from the interaction between tin ions and platinum which would decrease the electron density on platinum causing a lower degree of back-donation to the chemisorbed molecule and therefore a weaker sorption bond. This interpretation, however, does not explain the increase in the rate of hydrogenation of α,β-unsaturated aldehydes observed at low tin content.

Poltarzewski et al (1986) suggested that the effect of tin is related to the acidic properties of the tin ions (Lewis acidity) which activate the carbonyl group by

increasing the positive charge on the carbon atom in the carbonyl group. Another effect could result from the formation of the platinum-tin solid solution which, as in the case of nickel-copper reported by Noller (1982, 1984), would increase the electron density on the platinum sites leading to a stronger negative charge on the absorbed hydrogen. Over platinum-tin/nylon catalysts the addition of tin has a double effect on the hydrogenation of α,β-unsaturated aldehydes over platinum catalysts. First, the acidic properties of tin ions activate the carbonyl group which becomes more reactive than does the alkene bond. A second effect of tin is related to electronic interaction with platinum, which poisons the active metal sites responsible for hydrogenation activation.

2.7.7.5 Effect of Copper

Poltarzewski et al (1986) and Noller and Lin (1982, 1984) reported that addition of small amounts of copper to Raney nickel increases its activity for the hydrogenation of crotonaldehyde and its selectivity for carbonyl hydrogenation. The effect of copper could be due to the increased electron donor properties of the adsorbed hydrogen on the nickel-copper catalyst. It has been suggested that in the rate determining step, an electron donor species (probably H$^-$) attacks the carbon atom in the carbonyl group. The higher the electron donor strength the stronger is its attack.

2.7.7.6 Other Component Effect

Chen et al (1993) studied the hydrogenation of cinnamaldehyde over cobalt borides and concluded that additions of either molybdenum or thorium effectively promoted

the yield of unsaturated alcohol. Molybdenum promoted the hydrogenation rate only. Thorium promoted the rate as well as the selectivity. For monofuctional groups molybdenum effectively promoted the hydrogenation of the alkene and the carbonyl groups, but thorium promoted only the hydrogenation of the carbonyl group. A lower reactant concentration, a higher pressure, a higher temperature (in the range of 373-403K) and a protic solvent such as ethanol or propan-2-ol favoured the formation of cinnamyl alcohol over cobalt borides. The addition of an appropriate amount of water to ethanol (70-90% by mass) was preferable to pure ethanol as solvent for the hydrogenation of cinnamaldehyde.

Galvagno et al (1989) studied the influence of added metal chlorides over supported platinum catalysts for the hydrogenation of cinnamaldehyde in the liquid phase. Iron (III) chloride, tin (IV) chloride and germanium (IV) chloride were found to be the most effective promoters for the selective formation of cinnamyl alcohol. The rate of reaction was increased by the addition of small amounts of metal chlorides and then decreased with larger amounts. Selectivity to cinnamyl alcohol was slightly dependent on the concentration of the additives and on the level of conversion.

Galvagno et al (1989) systematically studied the effect of metal chlorides and found the product distribution to be strongly dependent on the type of catalyst and on the additives used. On supported platinum (in the absence of additive), the main products were hydrocinnamaldehyde and the corresponding diethylacetal. The concentration of the other products was below 5-7%. On platinum/nylon the reaction proceeds similarly to that on platinum/carbon but at a slower rate, due to the lower platinum content and to the polymeric structure of the support. Nylon is able to adsorb the platinum salt within the granules used for catalyst preparation, leading to a lower

amount of platinum available on the surface. The lower activity of platinum/nylon can be ascribed to the larger size of the platinum particles obtained after reduction on nylon compared with those on carbon (Cocco et al, 1985). The rate constant on platinum/carbon is fourteen times that on platinum/nylon. However, the effect of the additive was similar on both the supports used. Addition of metal chlorides was found to modify strongly the reaction pathway. The reaction kinetics were first order with respect to cinnamaldehyde, and the rate constant and the product distribution changed with the amount and chemical nature of the metal chlorides. The additives tested can be classified into three groups. The first group, sodium chloride, calcium chloride and aluminium chloride, did not modify significantly the catalytic activity and selectivity of platinum. The second group, cobalt (II) chloride and selenium (IV) chloride, led to an increase in selectivity towards the formation of unsaturated alcohol but the catalytic activity remained low. The third group, tin (IV) chloride, germanium (IV) chloride and iron (III) chloride, increased both the activity and selectivity. A major effect of the presence of tin (IV) chloride, germanium (IV) chloride or iron (III) chloride was observed in the product distribution; a decrease was observed in the relative amount of hydrocinnamaldehyde formed, with a corresponding increase in the cinnamyl alcohol concentration. Selectivity to cinnamyl alcohol was almost independent of the concentration of the additive and the level of conversion. Addition of tin (II) chloride or iron (II) chloride gave results similar to those observed in the presence of tin (IV) chloride or iron (III) chloride. It is likely that under the operating conditions tin (IV) and iron (III), in particular, are reduced by the catalytic effect of platinum.

The catalytic behaviour of platinum towards the hydrogenation of cinnamaldehyde can be modified significantly by addition of metal chlorides. Catalytic activity and selectivity were found to change with the amount and the nature of the additive used. The largest effect was observed on the addition of tin (IV) chloride, germanium (IV) chloride or iron (III) chloride. Small amounts of these additives raise the catalytic activity of the noble metal, while higher concentrations were found to deactivate the catalyst. Such behaviour has been reported for the hydrogenation of unsaturated aldehydes using alloy catalysts (Galvagno et al, 1986; Poltarzewki et al, 1986; Goupil et al, 1987) and for the hydrogenation of saturated aldehydes (Carothes and Adames, 1923; Maxted and Akhtar, 1959; Rylander and Kaplan, 1961; Galvagno et al, 1986; Cocco et al 1986). In the earlier literature, it was suggested that the presence of the additive inhibits the reduction of the active platinum oxide to inactive reduced platinum catalysts. This hypothesis was supported by the fact that platinum oxide is readily deactivated during aldehyde hydrogenation and its activity can be readily restored by shaking the reaction mixture with oxygen, and after pretreating the catalyst in hydrogen platinum is reduced to the metal state and its oxidation level does not change after reaction (Cocco et al, 1985; Galvagno et al, 1986).

Addition to platinum of iron (III), zinc (II), titanium (IV), and germanium (IV) ions effects the catalysts (Tuley and Adams, 1925; Galvagno et al, 1986; Goupil et al, 1987; Giroir-Fendler et al, 1988; Galvagno et al, 1989; Vannice and Sen, 1989). An enhanced rate of carbonyl group hydrogenation has also been reported for the addition of copper to nickel-based catalysts (Noller and Lin, 1984) and tin and boron to ruthenium (Narasimhan et al, 1988). Such effects appear to be associated with the formation of new catalytic sites, possibly involving promoter cations, which are able

to co-ordinate the oxygen atom in the carbonyl group and to activate it. Accordingly, in the case of platinum-tin catalysts the above results can be interpreted on the basis of a 'two site' mechanism, where platinum metal provides active sites for the hydrogenation of unsaturated substrates, but electrophillic tin ions are preferential sites for the adsorption and activation of carbonyl groups which are easily reduced by hydrogen adsorbed onto the neighbouring platinum sites.

Dunkel et al (1970) studied the effect of potassium acetate on palladium catalysts. It is found that potassium acetate could significantly increase the selectivity to hydrocinnamaldehyde. Arrigo et al (1970) claimed a continuous process for the selective hydrogenation of cinnamaldehyde to hydrocinnamaldehyde using a catalyst composite of palladium and alkali metal.

2.7.8 Reaction Schemes

Galvagno et al (1989) reported that in many respects such a reaction scheme is similar to that proposed by Rylander and Hilmestein (1963) for the hydrogenation of cinnamaldehyde over palladium catalysts. Hydrocinnamaldehyde and cinnamyl alcohol are formed through two parallel reactions (see cinnamaldehyde hydrogenation scheme) whose rates depend on the promoter used. On unpromoted platinum, k_2 (to hydrocinnamaldehyde) is much larger than k_1 (to cinnamyl alcohol). Addition of metal chlorides increases both k_1 and k_2, and in the presence of germanium (IV) chloride, tin (II) chloride or iron (III) chloride leads to a value of $k_1 > k_2$. 3-Phenylpropanol, which is negligible at low conversions of cinnamaldehyde, is formed by consecutive hydrogenation of both hydrocinnamaldehyde and cinnamyl alcohol. 3-Phenylpropanol is stable under the operating conditions and is not transformed

further. β-methylstyrene (phenyl-prop-1-ene) is formed through consecutive reactions from cinnamyl alcohol. The above proposed reaction scheme has been confirmed by measuring separately the rates of hydrogenation of the individual products. In contrast to the reaction scheme reported by Rylander and Hilmestein (1967), hydrocinnamaldehyde is readily converted to 3-phenylpropanol. This indicates that the effect of the promoter on the carbonyl group occurs regardless of the presence of a conjugated system. This agrees with previous results reported for the hydrogenation of saturated aldehydes (Galvagno et al, 1986).

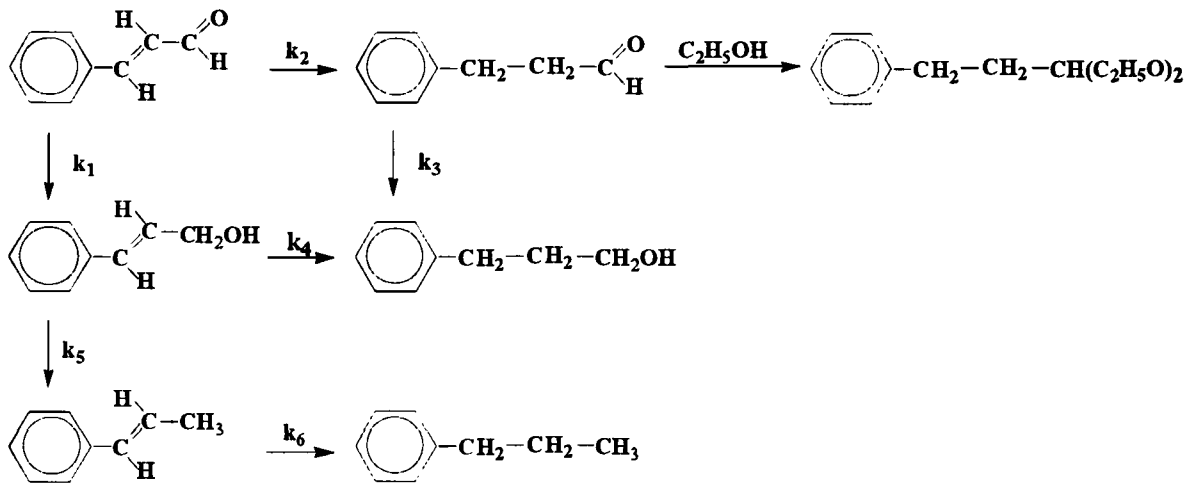

Cinnamaldehyde Hydrogenation Scheme in Ethanol

2.7.9 Formation of Acetals

Poltarzewski et al (1986) reported that at 333K and atmospheric pressure using ethanol as the solvent over platinum/nylon and platinum-tin/nylon catalysts for the hydrogenation of cinnamaldehyde the diethylacetal of hydrocinnamaldehyde was formed while no diethylacetal of cinnamaldehyde was found. Millman and Smith (1977) reported that over supported palladium catalysts, using methanol as solvent, the predominant initial product from the hydrogenation of cinnamaldehyde is cinnamaldehyde dimethylacetal which undergoes subsequent hydrogenation. As

pointed out by Millman and Smith (1977), the presence of hydrogen and the nature of the catalyst play important roles in the acetal formation.

2.7.11 Kinetic Studies

Very limited kinetic studies have been published about the hydrogenation of unsaturated aldehydes. Satagopan and Chandalia (1994) reported that the hydrogenation of cinnamaldehyde is first order with respect to hydrogen and zero order to cinnamaldehyde over both palladium and platinum catalysts. Galvagno et al (1993) reported that over ruthenium-tin catalysts using ethanol as solvent the reaction is first order with respect to the organic reactant.

The kinetics of liquid-phase hydrogenation of 2-methyl-2-pentenal in hexane over several modified Raney cobalt catalysts were investigated by Hotta and Kubomatsu (1971, 1972). It was found that two distinct Langmuir-type rate equations were required to describe the hydrogenation of the α,β-unsaturated aldehyde to 2-methylpentanol and 2-methylpentanal, or to 2-methyl-2-pentenol. This was interpreted as an indication that two different types of adsorbed 2-methyl-2-pentenal were involved in the hydrogenation reaction. Hotta and Kubomatsu's analysis, however, was confined to initial rate data. Niklasson and Smedler (1987) investigated the kinetics of the vapour-phase hydrogenation of 2-ethyl-2-hexenal on a nickel/copper catalyst. The best fit was provided by a mechanistic Langmuir-Hinshelwood model involving two distinct sites: one for alkene hydrogenation and one for hydrogenation of the carbonyl group.

Tronconi et al (1990) conducted an independent adsorption study and showed that much of the catalyst surface was saturated with almost irreversibly-adsorbed aldehydes. A kinetic model for the liquid-phase hydrogenation of cinnamaldehyde over tin-platinum/nylon catalysts was developed by a 'two-site' approach, and was applied to the analysis of the experimental rate data. Given the complexity of the reacting system, consisting of both parallel and consecutive reactions, the hydrogenation kinetics of cinnamyl alcohol over platinum and over platinum/tin catalysts have been studied also in order to obtain preliminary information on the reaction scheme.

Poltarzewski et al (1986) studied the hydrogenation of cinnamaldehyde in ethanol over platinum/nylon and platinum-tin/nylon catalysts, and reported that the experimental data fit first-order kinetics with respect to the organic reactant.

Phillips et al (1993) studied the kinetics over iron-rhodium catalysts in propan-2-ol and reported that at low concentrations of cinnamaldehyde the mechanism can be written as first order to cinnamaldehyde with constant concentrations of catalyst sites and hydrogen. Langmuir-Hinshelwood kinetics predict a first-order dependence if either the cinnamaldehyde adsorption is weak, or hydrogen, propan-2-ol or any other species is much more strongly adsorbed such that the fractional coverage of the surfaces by cinnamaldehyde is low.

A model (Winterbottom, 1998) which might be applicable for the initial hydrogenation of cinnamaldehyde to hydrocinnamaldehyde is a Rideal-Eley version of Langmuir-Hinshelwood model as follows:

$$CAL + * \underset{k_{-1}}{\overset{k_1}{\rightleftharpoons}} CAL^* \qquad (2.7.1)$$

$$CAL^* + H_2 \underset{k_{-2}}{\overset{k_2}{\rightleftharpoons}} HC^* \qquad (2.7.2)$$

$$HC^* \underset{k_3}{\overset{k_{-3}}{\rightleftharpoons}} HC + * \qquad (2.7.3)$$

Suppose that reactions 2.7.1 and 2.7.3 are at equilibrium and reaction 2.7.2 is the rate-controlling step so that

$$\theta_{CAL} = \frac{k_1 C_{CAL} \theta_v}{k_{-1}} = K_{CAL} C_{CAL} \theta_v \qquad (2.7.4)$$

$$\theta_{HC} = \frac{k_3 C_{HC} \theta_v}{k_{-3}} = K_{HC} C_{HC} \theta_v \qquad (2.7.5)$$

If ignore the reverse step of the reaction 2.7.2 the reaction rate of this step can expressed as

$$r_2 = k_2 \theta_{CAL} C_{H2} \qquad (2.7.6)$$

Since $$\theta_v + \theta_{CAL} + \theta_{HC} = 1 \qquad (2.7.7)$$

hence $$\theta_v = \frac{1}{1 + K_{CAL} C_{CAL} + K_{HC} C_{HC}} \qquad (2.7.8)$$

$$r_2 = \frac{k_2 K_{CAL} C_{CAL} C_{H2}}{1 + K_{CAL} C_{CAL} + K_{HC} C_{HC}} \qquad (2.7.9)$$

Under the initial reaction conditions the hydrocinnamaldehyde concentration is very small so that $K_{HC}C_{HC}$ is negligible leading to the following expression

$$r_o = \frac{k_2' C_{CAL_0} C_{H2}}{1 + K_{CAL} C_{CAL_o}} \qquad (2.7.10)$$

where $k_2' = k_2 K_{CAL}$

Under the initial conditions, cinnamaldehyde concentration can be considered as constant compared with the sparingly soluble hydrogen. Rearranging equation 2.7.10 a equation similar to equation 3.9 can be obtained as follow:

$$\frac{C_{H2}}{r_o} = \frac{1}{k_2' C_{CAL_o}} + \frac{1}{k_2} \qquad (2.7.11)$$

Chapter 3 The Cocurrent Downflow Contactor (CDC)

The cocurrent downflow contactor (CDC), a novel gas-liquid and gas-liquid-solid contactor, was conceived originally by Boyes and Ellis (1976). It has been proved to offer a high degree of mass transfer efficiently by the application of a continuously flowing turbulent liquid inlet stream with the simultaneous entrainment of gas into a body of liquid (Boyes and Ellis, 1976; Lu, 1988; Sulidis, 1995).

Figure 3.1 shows the features of the CDC. The basic outline of the CDC reactor is a column with a gas-liquid contacting entry zone at the top of the column. The entry zone has a gas inlet line connected by a T-piece to a high velocity liquid inlet stream. The end of the liquid inlet stream is constricted, allowing the formation of a high velocity fully submerged gas-liquid jet in the column. The constriction is effected simply by a hydrodynamically-designed orifice. The versatility of the CDC reactor allows the gas stream to be introduced at any position in the column, but the usual method is to introduce the gas and the liquid concurrently through the entry zone at the top of the column. The high velocity liquid jet enters the continuous liquid phase and the dispersed gas phase enters the column at the top through a T-piece and passes cocurrently through an orifice into the fully-flooded column. The kinetic energy of the stream entering the column produces intense turbulence and mixing. The balance between the gas bubble rise velocity and the liquid downflow velocity produces a constant rapidly renewed bubble matrix and high efficiency mass transfer between the gas phase and the liquid phase in the body of the column. Rapid surface renewal and frequent bubble coalescence and break-up make the CDC a highly efficient mass

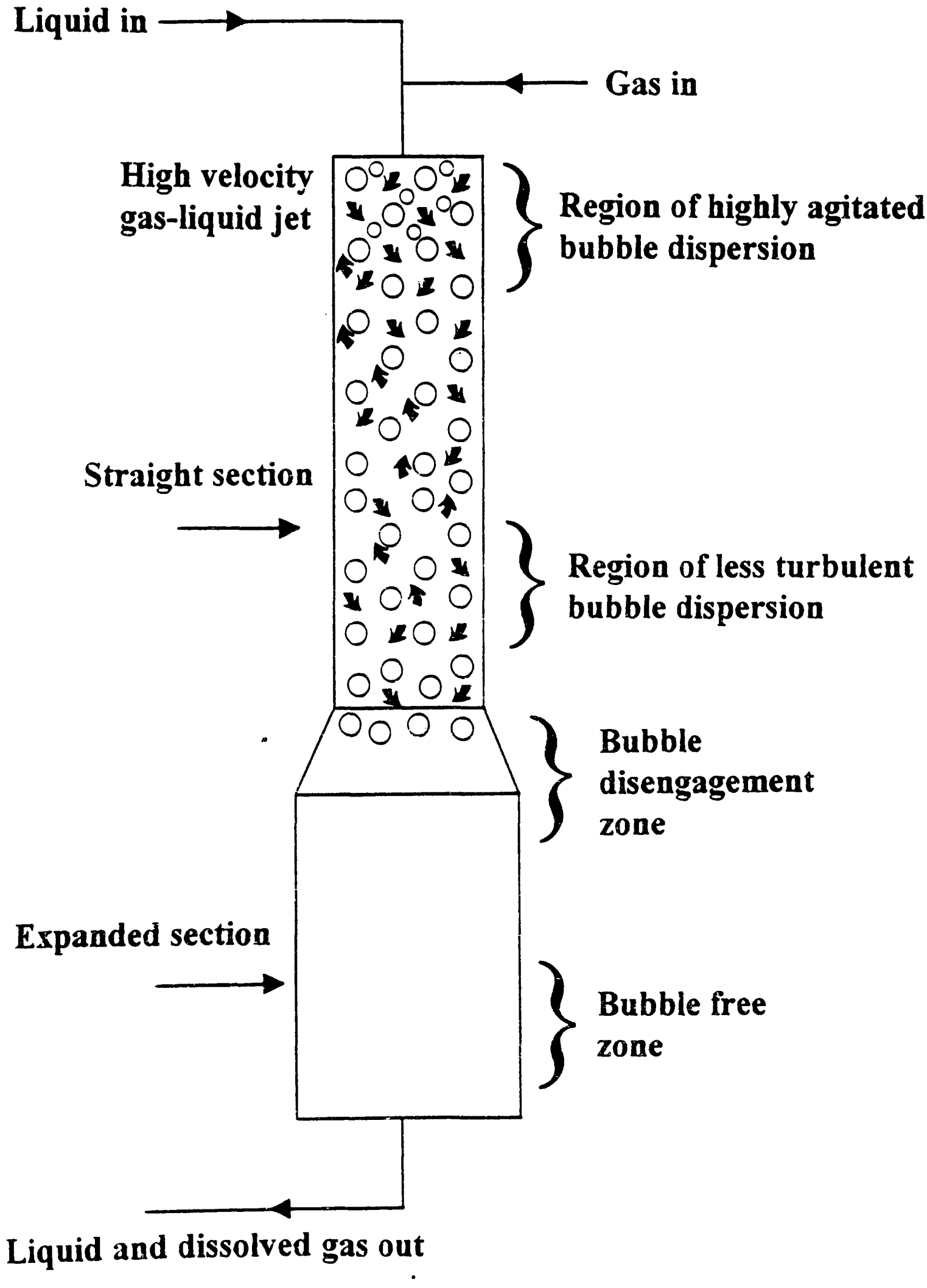

Figure 3.1 The Figures of the Cocurrent Downflow Contactor

transfer device. Some other advantages over conventional gas liquid contactors (stirred reactors) are as follows:

a. Simple design and operation;

b. Efficient gas utilisation (100%);

c. High mass transfer coefficient (k_L=0.8-2.6×10^{-4}m.s^{-1}) and very close approach to equilibrium (97%) in short contact times (< 10s);

d. High gas liquid interfacial area (2000-6000 $m^2.m^{-3}$) and gas holdup (50-65%);

e. Lower power consumption and small operating volume;

f. No internal moving parts and easy maintenance.

Previous Studies of the CDC

Several intensive studies have been carried out on the CDC in the University of Birmingham:

(1) Evinc (1982) studied the mass transfer characteristics of different gas-liquid systems;

(2) Lu (1988) studied the hydrodynamics and mass transfer characteristics of the CDC as well as the hydrogenation of itaconic acid;

(3) Raymahasay (1989) studied the CDC as a chemical reactor for the partial hydrogenation of rapeseed oil, a commercial reaction used in the edible oil industry;

(4) Tilston (1990) studied the mass transfer characteristics for the development of a swirlflow CDC;

(5) Sarmento (1991) studied the hydrodynamics and mass transfer characteristics of a fixed bed CDC;

(6) Chughtai (1995) studied the CDC as a slurry and fixed-bed chemical reactor;

(7) Khan (1995) studied the CDC as a slurry and fixed-bed chemical reactor with and without swirl flow;

(8) Sulidis (1995) studied the hydrodynamics and mass transfer characteristics in a slurry CDC and packed CDC, and the photocatalytic degradation of phenols in slurry CDC reactors.

Different aspects of the CDC have been studied as Final Year or Erasmus projects by various students: Claxon (1982), Turtle (1982), Hay (1982), Jones (1983), Lane (1983), Wheeler (1983), Harding (1984), Marsden (1985), Humphrey (1986), Sarmidi (1986), Smith (1987), Chen (1994), Perriera (1994), Evans (1995), Monteiro (1995).

The main objectives of these previous studies were to investigate the various aspects of the hydrodynamics and mass transfer characteristics of the CDC using different reactor configurations.

3.1 Hydrodynamic Characteristics

3.1.1 Flow Regions

The gas-liquid dispersion presents regions of different flow regimes with very distinct mixing characteristics and bubble sizes along the column length. The number of those zones in the CDC differed for different researchers possibly due to the observation method used and to the configuration of the column. Two distinctive flow regions were reported by Evinc (1982) using a column of internal diameter 100mm. and height 1000mm with nitrogen/water, air/water, oxygen/water, and carbon dioxide/water systems.

1. Upper turbulent region: small bubbles (d_b < 1.5mm) and lower gas holdup (30-40%) were observed in the 350mm top section;

2. Lower region: a uniform larger bubbly two-phase flow (d_b = 3mm for carbon dioxide/water and d_b = 5mm for oxygen/water) and 50% gas holdup were observed in the lower 650mm section.

Jones (1983), Claxton (1982) and Turtle (1982) used the same column in an oxygen/water system as that used by Evinc (1982), but three distinctive regions were reported:

1. Top section: highly turbulent region with loosely packed bubbles due to a high velocity liquid inlet stream;

2. Middle section: less turbulent region with a high packing bubble density;

3. Bottom section: clearly defined bubbles with gentle fluctuations.

A fourth region was reported by Harding (1984) and Humphrey (1986) in a column of internal diameter 76mm. and height 760mm with oxygen/water and air/water system. The first and the second regions corresponded to those described by Evinc (1982). The third region is the liquid-carried-down small bubble region (d_b <1mm) and the fourth region is the small bubble (d_b < 1mm) area located at the junction between the cylindrical and conical sections.

Lu (1988) studied systematically the flow regimes in a column of internal diameter 76mm and height 760mm using oxygen/aqueous sodium alginate, oxygen/aqueous glycerol, oxygen/aqueous propanol and oxygen/water systems, and reported four distinct regions. He concluded that the features of the CDC dispersion were determined by many factors including the liquid phase properties, gas and liquid flowrates, column geometry and liquid inlet velocity.

1. Entrance region: a highly turbulent region characterised by the constant dispersion and re-dispersion of the gas as small bubbles into the liquid phase;

2. Middle region: less turbulent region with a uniform big bubble size (d_b = 3-5mm) and higher gas holdup;

3. Junction region: tiny bubble swarm area with swarms intermittently moving up and down;

4. Conical Region: small bubbles (d_b <1mm) coalescing there and moving upwards.

3.1.2 Residence Time Distribution

Tilston (1989) and Sulidis (1995) studied the residence time distribution in a 100mm CDC. Tilston (1989) reported that the upper cylindrical section of the CDC behaved as a well-mixed vessel or continuously stirred tank reactor (CSTR), while the lower section operated as a plug flow reactor (PFR). Sulidis (1995) found that the degree of backmixing depended on the dispersion height. Sulidis (1995) reported that the CDC appeared to resemble plug flow behaviour from 300mm to 700mm of dispersion height corresponding to gas feedrates of 200-700$mm^3.min^{-1}$. When the dispersion height exceeded 700mm, a large degree of mixing prevailed in the dispersion, corresponding to higher gas feedrate of 700-1000$mm^3.minute^{-1}$. Under these conditions of high gas flowrate, the concentration of gas bubbles in the dispersion is very large, suggesting that the gas bubbles are enhancing the mixing characteristics within this dispersion. Accordingly, the mixing behaviour of the bubbles increases the axial dispersion coefficient of the liquid phase and reduces the Peclet Number.

3.1.3 Formation of Bubble Dispersion

The bubble dispersion is produced by the shearing force of the liquid inlet stream and very small bubbles are produced by the turbulent jet and then coalesce to form larger bubbles. With a continuous gas supply, the dispersion remains as a well-defined bubble matrix, and near-uniform-size bubbles expand downwards in the column due to coalescence and breakup. Previous researchers discovered that a minimum liquid inlet velocity was required to maintain the gas-liquid dispersion in the CDC (Boyes and Ellis, 1976; Harding, 1984; Tilston, 1986; Lu, 1988). Lu (1988) pointed out that the liquid inlet velocity had to be greater that the dispersion initiating velocity to prevent the formation of a gas pocket at the top of the column and to allow the formation of a bubble dispersion. He stated that a minimum energy was required to initiate and maintain the bubble dispersion and a minimum jet velocity equation was developed:

$$u_{o,\min} = K\left(\frac{D_c}{d_{orifice}}\right) \qquad (3.1)$$

where K=0.876 for coalescing systems and 0.37-0.50 for non-coalescing systems.

Tilston (1990) developed a minimum jet momentum M_{min} to produce a stable bubble dispersion with the following relationship:

$$M_{\min} = 260 - 4.1\times10^{3} u_L + 1.2\times10^{3} H_{dead} \qquad (3.2)$$

where H_{dead} = the gas height in the deadleg, m.

M_{min} = minimum jet momentum per unit area, $kg.m^{-1}.s^{-1}$

u_L = liquid superficial velocity, $m.s^{-1}$

Boyes (1987) used a general 'rule of thumb' that states that the liquid inlet jet velocity must be greater than $2m.s^{-1}$. Tilston (1989) claimed that Boyes' rule of thumb may be sufficient for design purposes but in most cases knowledge of the exact criteria of stability would be advantageous.

3.1.4 Bubble Size

Photography was used to investigate bubble sizes in the CDC. As described in Section 3.1.1, bubble size changes in different flow regions. However, two distinct and predominant bubble sizes prevail in the CDC. For example, there is a top turbulent jet region forming tiny bubbles and a lower less turbulent region with relatively uniform larger bubbles forming a stable bubble matrix, although some workers claim that three or four regions exist.

Lu (1988) and Tilston (1990) examined the effect of physical properties on bubble size and showed that the coalescence property of the solvent significantly affected the bubble size. For the oxygen/water system the bubble mean size is 4.5mm. Coalescing systems formed uniform bubble sizes of range 4-5mm while non-coalescing systems formed bubble sizes of 0.5mm. Lu (1988) investigated the effect of surface tension and viscosity, and observed that traces of propanol and glycerol dramatically decreased the bubble size from 4.5mm to 0.5mm. Tilston (1990) demonstrated a change in bubble size from 4.5mm to 0.5mm at a critical concentration of $0.3kmol.m^{-3}$ of electrolyte.

The existence of surfactants causes a decrease in bubble size. Jones (1983) showed that $d_b <$ 1mm bubbles predominated with the addition of surfactant in an oxygen/water system. Similarly, Harding (1984) observed tiny bubbles ($d_b <$ 1mm) in an oxygen/wort system.

Several studies have been made of catalytic reactions. Lu (1988) observed a 20% increase in bubble size for a hydrogen/itaconic acid system using palladium/charcoal catalyst. Raymahasay (1989) reported that bubble size ranged from 2.5-3mm in the middle section and 4-5mm in the bottom section of the column for the hydrogen/rapeseed oil system.

3.1.5 Gas Holdup and Interfacial Area

All the above-mentioned CDC workers assumed that the bubbles in every individual region are the same size and spherical shape and are perfectly packed; and used the following relationship between gas holdup (ε_g), bubble size (d_{vs}) and gas-liquid interfacial area (a) to determine the gas-liquid interfacial area:

$$a = \frac{6\varepsilon_g}{d_{vs}} \qquad (3.3)$$

A static shutdown method, a volume expansion method and a dead-leg method were used to measure the mean gas holdup in the CDC. The first two methods give an accurate value of the gas holdup in the CDC; but the static shut-down method requires stopping of the operation, and the second method can be used only in a recirculation mode. The third method is an on-line method. Lu (1988) studied the effects of various factors on gas holdup and developed the following equation:

$$\varepsilon_g = 0.0572\left(\frac{d_{orifice}}{D_c}\right)^{0.016}\left(\frac{H_d}{D_c}\right)^{0.680} Fr^{-0.290} \qquad (3.4)$$

Lu (1988) observed that gas holdup increases with an increase in the gas flowrate and the dispersion height but decreases with an increase in the liquid column flowrate. The effect of

liquid inlet velocity is negligible. The typical value of the gas holdup ranged from 20% to 64% for coalescent oxygen/water systems and was 47% for the poorly- coalescent aqueous glycerol/oxygen system. Tilston (1990) used a two-point conductivity probe for the accurate measurement of liquid depth in the deadleg, and controlled the gas dispersion level in the CDC by using the outlet oxygen concentration in order to measure the gas holdup. Sarmento (1995) measured the gas holdup up to a value of 50% in a packed CDC using various types of packings.

Some typical values of interfacial area are listed in Table 3.1.

Table 3.1 Interfacial Area Values for Oxygen/Water and Oxygen/Wort Systems

System	ε_g, %	d_b, mm	a, $m^2.m^{-3}$
Oxygen/Water	25	4.5	300
	50	4.5	600
	65	4.5	867
Oxygen/Wort	50	1.0	3000
	50	0.5	6000

Boyes et al (1992) using a sulphite oxidation method, confirmed that a higher interfacial area (600-3000$m^2.m^{-3}$) was observed. This is in accordance with values obtained by photography.

3.2 Mass Transfer Characteristics

The mass transfer characteristics of the CDC were studied by Evinc (1982), Jones (1983), Harding (1984), Marsden (1985), Humphrey (1986), Smith (1987), Lu (1988), Tilston (1990), Sarmento (1995) and Sulidis (1995). In order to improve the performance of the ordinary CDC Claxton (1982), Turtle (1982), Lane (1983), Jones (1984), Tilston (1990), and Khan (1995) developed the swirl CDC contactor. The performance of a packed CDC column

was studied by Sarmento (1991), Sulidis (1995) and Khan (1995). They used the steady state absorption of a gas into a liquid to investigate the volumetric mass transfer coefficient (k_La) based on the assumption that the liquid phase shows either plug flow or perfect mixing. The liquid-side mass transfer coefficient (k_L) is calculated from the interfacial area a. The data before 1988 were based on the plug flow pattern and the data from 1990 were based on the perfect mixing flow pattern. The values of k_La and k_L reported by various workers are shown in Table 3.2.

Table 3.2 The Values of k_La and k_L Obtained in the CDC

System	k_La, s^{-1}	$k_L \times 10^4$, $m.s^{-1}$	Reference
Nitrogen/Water	0.08-0.14	0.8-1.3	Evinc (1982)
Air/Water	0.12-0.18	1.1-1.7	Evinc (1982)
Oxygen/Water	0.14-0.20	1.3-2.3	Evinc (1982)
Carbon dioxide/Water	0.21-0.25	1.8-2.6	Evinc (1982)
Oxygen /Water	-	1.0	Jones (1983)
Oxygen /Water	-	0.6-1.0	Harding (1984)
Oxygen /Wort	-	0.10	Harding (1984)
Oxygen /Wort	-	0.05-0.11	Marsden (1985)
Oxygen /Water	0.05-0.22	0.04-0.29	Lu (1988)
Oxygen/Water	0.07-1.53	-	Tilston (1990)
Oxygen/Water	0.04-0.15	-	Sarmento (1995)
Oxygen/Water	0.053-6.18	-	Sulidis (1995)

The volumetric mass transfer coefficient k_La is a function of the gas and liquid flowrate as well as of the height of the gas-liquid dispersion. Evinc (1982) reported that k_La increased with increasing gas flowrate in the upper section of the column but became independent of gas flowrate in the lower section, because in the upper section very small bubbles dominated

leading to high interfacial area while in the lower section uniform larger bubbles occupied the column leading to a decrease in interfacial area.

Lu (1988) also showed that k_La decreases with an increase in dispersion height and claimed that a high degree of turbulence and a large interfacial area generated in the upper section resulted in high k_La values. Lu (1988) developed a dimensionless correlation between k_La and process conditions:

$$k_L a = \alpha \left(\frac{D_c}{d_{orifice}} \right)^m \left(\frac{H_d}{D_c} \right)^n Fr^p \qquad (3.5)$$

Lu (1988) observed that the k_La value increased with the increase of liquid superficial velocity, whereas Jones (1982) and Evinc (1982) reported a negligible and slightly negative effect of the liquid superficial velocity on k_La. Lu (1988) claimed that k_La increased with the liquid inlet velocity u_{jet} and that it was proportional to $u_{jet}^{0.25}$. Tilston (1990) developed a theoretical model to predict the k_La value with higher accuracy.

Jones (1983) reported that the liquid side mass transfer coefficient k_L decreased with an increase in liquid flowrate, and that column pressure was independent of gas flowrate at high liquid flowrate but proportional to the gas flowrate at low liquid flowrate. However, Enivc (1990) and Harding (1984) claimed that k_L is independent of the operating conditions (gas flowrate, liquid flowrate, column diameter and column pressure) but dependent on the physical properties of the system (such as liquid density, liquid viscosity and surface tension).

Tilston (1990) reported a five-fold increase in k_La for an oxygen/water system with the addition of swirlflow to the ordinary CDC due to intensified and better recirculation of the gas and to a restriction of the dispersion caused by a region of high coalescence acting as a barrier to the downward expanding dispersion. Sarmento (1995) noted a slight increase of k_La when high voidage packings (Pall Rings) were in use and a slight decrease in k_La values when using low voidage packings (Raschig Rings). Sarmento (1995) suggested that the shape of Intalox Rings offered less disturbance to the balance between coalescence and the break-up of bubbles in the column, so that higher k_La values for Intalox Rings (voidage = 0.78) were observed than for Pall Rings (voidage = 0.87).

3.3 Catalytic Reaction Studies

After the successful demonstration of the CDC as an efficient gas-liquid contactor, the CDC was developed further as a three phase reactor for studies in chemical reaction processes and biochemical processes. Lu (1988) and Tilston (1990) used the hydrogenation of itaconic acid as a model reaction for the CDC as a slurry reactor at 273-343K and 0.1-0.3MPa with palladium/charcoal catalysts. Tilston (1990) further modified the CDC with a swirlflow for the hydrogenation of itaconic acid. This work was continued by Khan (1995). Raymahasay (1989) studied the partial hydrogenation of rapeseed oil using both nickel and palladium catalysts operating at 0.2-0.6MPa and 398-508K. Chughtai (1993) studied the model and commercial reaction in a slurry CDC reactor using palladium/charcoal catalysts and in a packed bed CDC reactor using palladium re-treated packing catalysts operated at 0.1-0.3MPa and 298-323K. Sulidis (1995) and Khan (1996) studied the photo-catalysed degradation of phenols using titania catalysts with oxygen and with ozone. Khan (1995) investigated the hydrogenation of butynediol and butenediol. Chen (1994), Evans (1995), and Monteiro

(1995) studied the organic waste digestion by naturally-present micro-organisms operating at 0.1MPa and 273-350K.

3.3.1 Model Hydrogenation Reactions

When a first-order catalytic reaction process (see appendix 8.2) occurred in three-phase slurry reactors, the gas liquid volumetric mass transfer coefficient k_La, the liquid-solid mass transfer coefficient k_L and the surface reaction rate constant k_r were evaluated by the first order model:

$$\frac{C_A^*}{R_a} = \frac{1}{k_L a} + \frac{\rho_p d_p}{6W}\left(\frac{1}{k_s} + \frac{1}{k_r}\right) \qquad (3.6)$$

and the Frössling equation by previous workers:

$$Sh = \frac{k_s d_p}{D_A} = 2.0 \qquad (3.7)$$

The relative importance of liquid-solid mass transfer resistance and surface reaction resistance was calculated by the following equation:

$$X_{L\text{-}S} = \frac{\frac{1}{k_s}}{\frac{1}{k_s} + \frac{1}{k_r}} \qquad (3.8)$$

Itaconic acid hydrogenation was studied by several workers. Table 3.3 summarizes the transport parameters for itaconic acid hydrogenation in the CDC at 293K.

Table 3.3 Transport Parameters for Itaconic Acid Hydrogenation in the CDC for 293K

Catalyst	Solvent	k_La, s^{-1}	$k_s \times 10^3$, $m.s^{-1}$	$k_r \times 10^3$, $m.s^{-1}$	X_{L-S}, %	Reference
5% Pd/C	Water	5.7	3.2	2.36	42.6	Lu (1988)
10% Pd/C	Water	3.6	3.2	4.56	58.6	Lu (1988)
5% Pd/C	Propanol	1.1	1.5	0.31	16.9	Lu (1988)
5% Pd/C	Water	10.7	3.2	12.40	79.5	Tilston (1990)
5% Pd/C	Water	2.1	21.5	8.70	32.0	Chughtai (1993)
5% Pd/C	Propanol	1.2	17.7	6.05	22.1	Chughtai (1993)

Lu (1988) concluded that the hydrogenation of itaconic acid is first order for hydrogen and zero order for itaconic acid concentration. A minimum catalyst loading of $0.4kg.m^{-3}$ occurred, indicating the presence of impurities in the reaction system when the classic first order model equation (3.6) was applied. Lu (1988) confirmed that the volumetric mass transfer coefficient k_La is much higher for chemical absorption than that for physical absorption due to the enhancement of gas absorption by the fine catalyst particles and the enhancement of the chemical reaction.

A significant increase in reaction rates and k_La values resulted because the gas holdup, turbulence and bubble shear were increased by the addition of a swirlflow in the ordinary CDC, as described in the previous sections. Tilston (1990) and Chughtai (1993) found that the reaction rates increased 3.5 times and k_La values doubled for the hydrogenation of itaconic acid. A similar situation was reported by Khan (1995) for the hydrogenation of butenediol.

Chughtai (1993) prepared packing catalysts for use in a packed bed CDC by the direct impregnation of palladium catalysts onto low surface area alumina Raschig Rings. Although

the activity of the in-house-prepared packing catalyst was lower than that of commercial catalysts, the higher reaction activation energies indicated that the reaction in the packed bed CDC was surface reaction rate controlled as in the ordinary CDC.

Khan (1995) studied the hydrogenation of itaconic acid and nitrobenzoic acid using 5% palladium/charcoal catalyst in a slurry CDC, and reported that the reactions were first order with respect to hydrogen and zero order to the reactant. Large values of k_La and higher activation energies indicated that the reactions were surface reaction rate controlled. When swirl flow was applied to the slurry CDC reactor the reaction rates and k_La values increased up to ten times. When a 3% (w/w) palladium/alumina (Pd/Al_2O_3) catalyst was used in a packed bed CDC the degree of gas-liquid mass transfer was less compared with that in the slurry reactor.

3.3.2 Commercial Hydrogenation Reactions

Raymahasay (1989) hydrogenated rapeseed oil in a slurry CDC using both nickel and palladium catalysts and observed that the reaction order with respect to hydrogen is 1.8 instead of 1. He found that the hydrogenation process can be operated to achieve high selectivity under surface reaction rate control. For instance, only one of the three double bonds of linolenic acid is hydrogenated. The activity of the palladium catalyst is much higher than that of a nickel catalyst in this case, and therefore much less palladium catalyst is required than nickel catalyst for the same reaction rate. The calculated transport parameters using the classic first order model are summarized in the Table 3.4.

Table 3.4 Transport Parameters for Rapeseed Oil Hydrogenation

Catalyst	Pressure, Pa	k_La, s^{-1}	X_{L-S}, %	E_A, $kJ.mol^{-1}$	Trans acid, %
Nickel	375	1.39-2.38	10-20	58±12	23
Nickel	500	-	20-42	-	15
Palladium	375	0.63-0.85	18-29	58±12	29
Palladium	500	-	-	-	29

Chughtai (1993) and Khan (1995) studied the hydrogenation of soybean oil in both packed bed and slurry CDC reactors and observed a reaction order greater than one (1.2-1.4) with respect to hydrogen. This is related to a surface reaction-rate-controlled process corresponding to higher activation energy. The packed bed CDC was more efficient than the slurry CDC for the hydrogenation of linolenate with less conversion of the formed linoleate to oleate and stearate, even though the slurry CDC showed higher reaction rates. Some typical results obtained by Chughtai (1990) are given in the following Table 3.5.

Table 3.5 Selectivity for Soybean Oil Hydrogenation

CDC Reactor	S_{ln}, %	S_{lo}, %	Trans Isomers, %	Iodine Value
Slurry	2.5-4.6	5-84	25-29	73-110
Packed bed	2.3-5.6	2-77	27-32	73-110

Chughtai (1993) hydrogenated glucose to sorbitol using a ruthenium catalyst in a slurry CDC operated at 900-1600Pa. He found that the reaction was first order with respect to hydrogen, and that a higher operating pressure tended to improve the activity of the ruthenium catalyst.

Khan (1995) investigated the hydrogenation of butynediol using 5% palladium/charcoal catalyst in a slurry CDC and concluded that the reaction was first order with respect to

hydrogen and zero order with respect to butynediol. The low apparent activation energy suggested that the reaction was diffusion controlled.

3.3.3 Photocatalytic Degradation of Organic Pollutants

Sulidis (1995) and Khan (1996) studied the degradation of phenols using titanium dioxide as a photocatalyst in aqueous dispersion with the presence of ultra-violet (UV) irradiation at 0.2MPa and 313-323K. They reported that the phenol degradation was pseudo first order and that a Langmuir-Hinshelwood rate expression was applicable to the reaction:

$$\frac{1}{r_o} = \frac{1}{kK}\frac{1}{C_o} + \frac{1}{k} \qquad (3.9)$$

where r_o is the initial reaction rate, C_o is the initial phenol concentration, k is the rate constant and K is the adsorption equilibrium constant of the organic species. The addition of hydrogen peroxide could enhance oxidation rates for phenol oxidation in the presence of UV irradiation and supports the theory that $HO^{\bullet}$ radicals are the main oxidation species.

3.3.4 Biodegradation of Organic Wastes

After the successful application of the CDC reactors in some chemical reaction processes further investigation needs to be done in biochemical processes in order to extend the application of the CDC as an efficient mass transfer device. Chen (1994), Evans (1995) and Monteiro (1995) studied the biodegradation of organic wastes to produce single cell proteins. The yeasts naturally present in the produce were used for digestion without addition of any other micro-organisms. The results showed that the CDC is a very effective fermentor.

Chapter 4 Experimental Apparatus and Materials

4.1 Experimental Apparatus

4.1.1 Stirred Pyrex Glass Tank Reactor (the 250ml Pyrex Glass Reactor)

An overall view of the experimental apparatus is shown in Figure 4.1 and Plate 4.1.

The stirred glass batch reactor consisted of two sections: a reactor base made of a cylindrical vessel fitted with four standard baffles, and a reactor head consisting of a gas dispersion stirrer and accommodating gas and purge lines. The reactor head also accommodated a side tube for slurry addition and a side tube for sampling. A single stage type of stirrer was used, which had an impeller with six radial blades. The impeller was positioned directly beneath the liquid/slurry surface in order to maximise the gas dispersion. The reactor head was provided with a removable mercury seal and was joined to the reactor base by a conical ground Pyrex glass adapter. A centreless ground Pyrex glass rod and a length of precision bore tubing were used for the stirrer bearing. High vacuum grease was used to seal the ground Pyrex glass surfaces. The temperature of the reactor was maintained and controlled by immersing the reactor base in a thermostated water bath. The hydrogen gas supply to the reactor was regulated and measured by a hydrogenation control unit (Section 4.1.8).

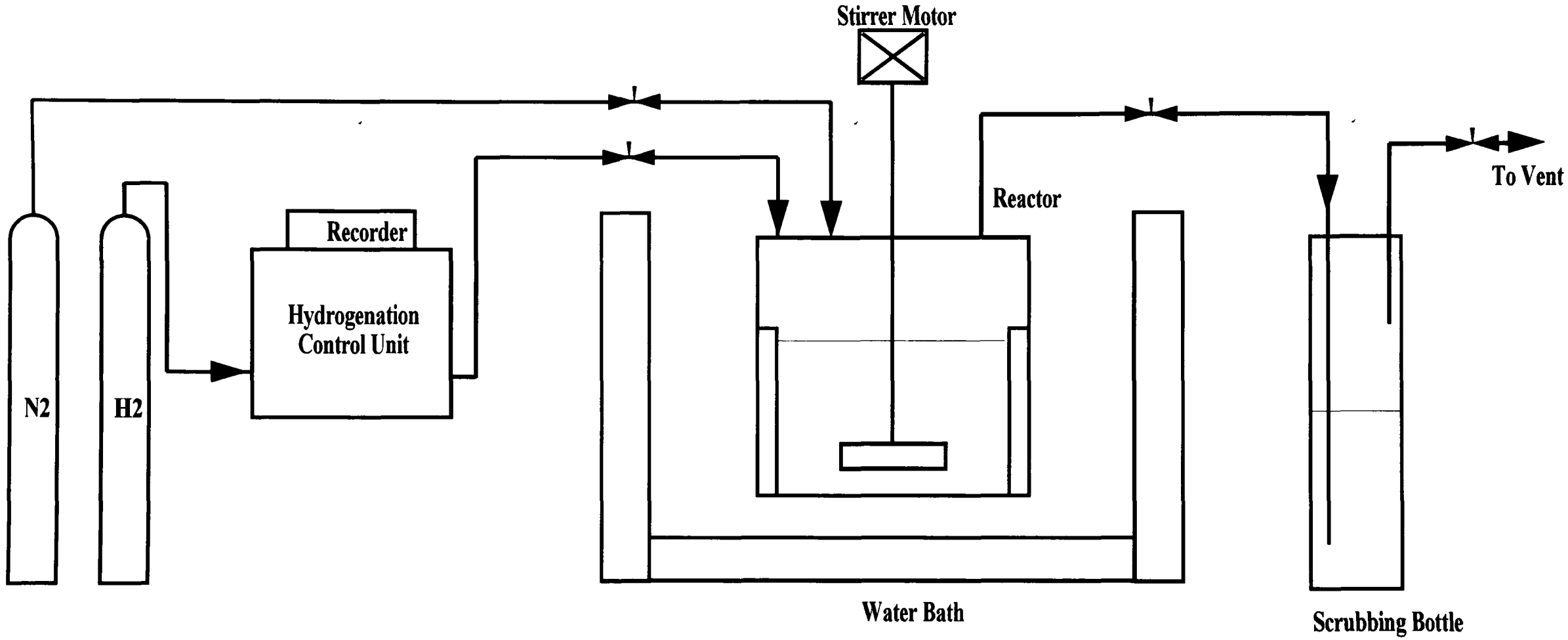

Figure 4.1 Schematic Diagram of the Stirred Batch Reactor System

Plate 4.1

Stirred Tank Pyrex Glass Reactor

Stirred Tank Pyrex Class Reactor

Plate 4.1

The stirred reactor had the following dimensions:

Parameter	Dimension
Tank diameter	70mm
Tank height	65mm
Impeller diameter	65mm
Stirrer shaft height	400mm
Stirrer shaft diameter	10mm
Stirrer guide tube height	100mm
Stirrer guide tube diameter	10mm
Width of the baffles	10mm
Baffle height	30mm
Height of impeller blades	10mm
Diameter of impeller blades	43mm

4.1.2 Stirred Stainless Steel Tank Reactor (the 500ml Autoclave)

The overall view of the experimental apparatus is shown in Figure 4.2 and Plate 4.2.

The stirred stainless steel batch reactor was a Baskerville Autoclave (Model 7678; maximum pressure 3.0MPa, maximum temperature 673K, maximum stirring speed 2000rpm, Baskeville & Lindsay Ltd). It consisted of two sections: a reactor base made of a cylindrical vessel fitted with four standard baffles, and a reactor head consisting of a gas dispersion stirrer and incorporating gas and purge lines with a pressure gauge. The reactor head also accommodated a thermocouple and a pressure relief valve (bursting disc type). The stirrer

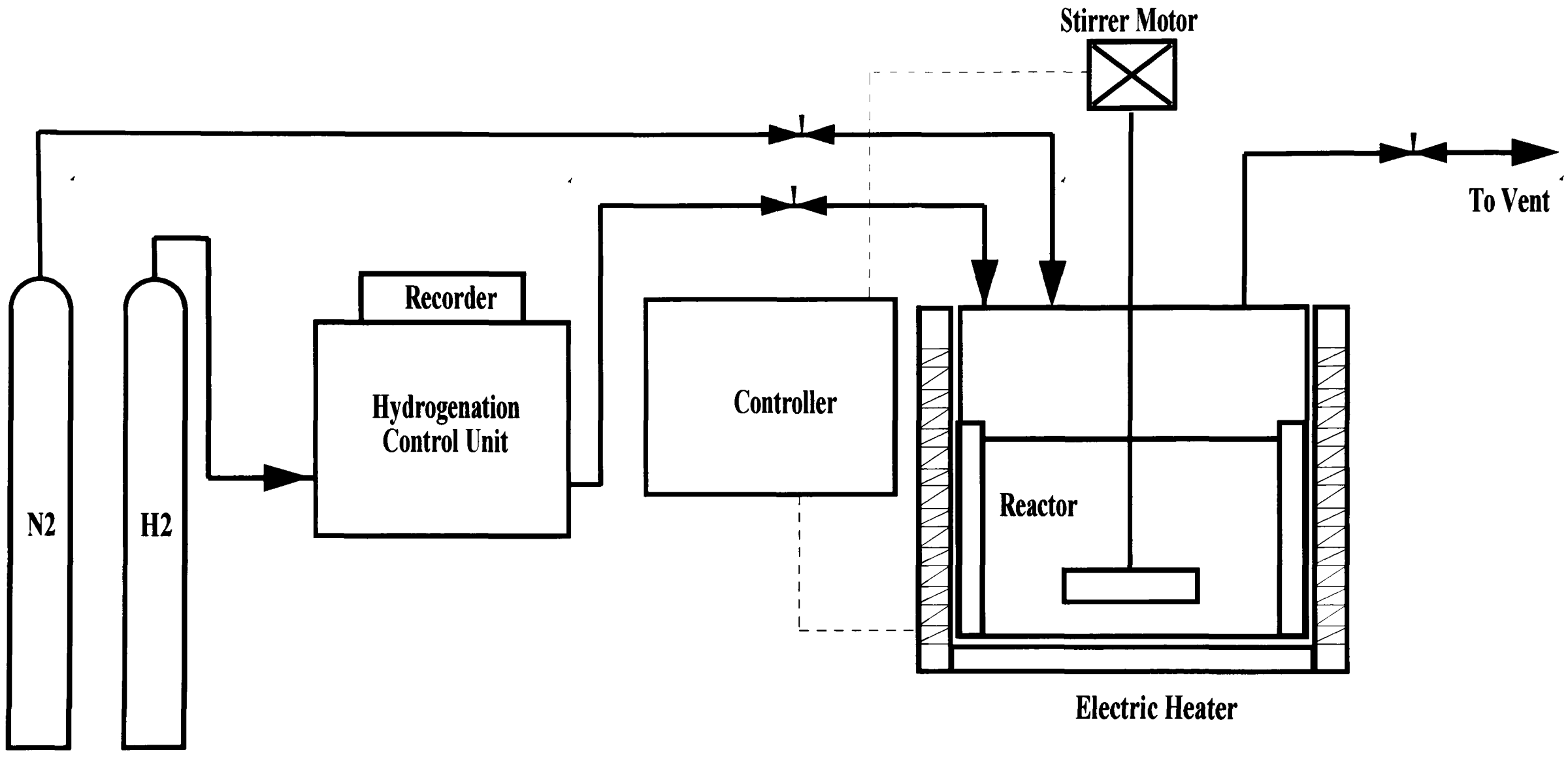

Figure 4.2 Schematic Diagram of the Stirred Stainless Steel Batch Reactor

Plate 4.2

Stirred Tank Reactor (Autoclave)

Stirred Tank Reactor (Autoclave)

Plate 4.5

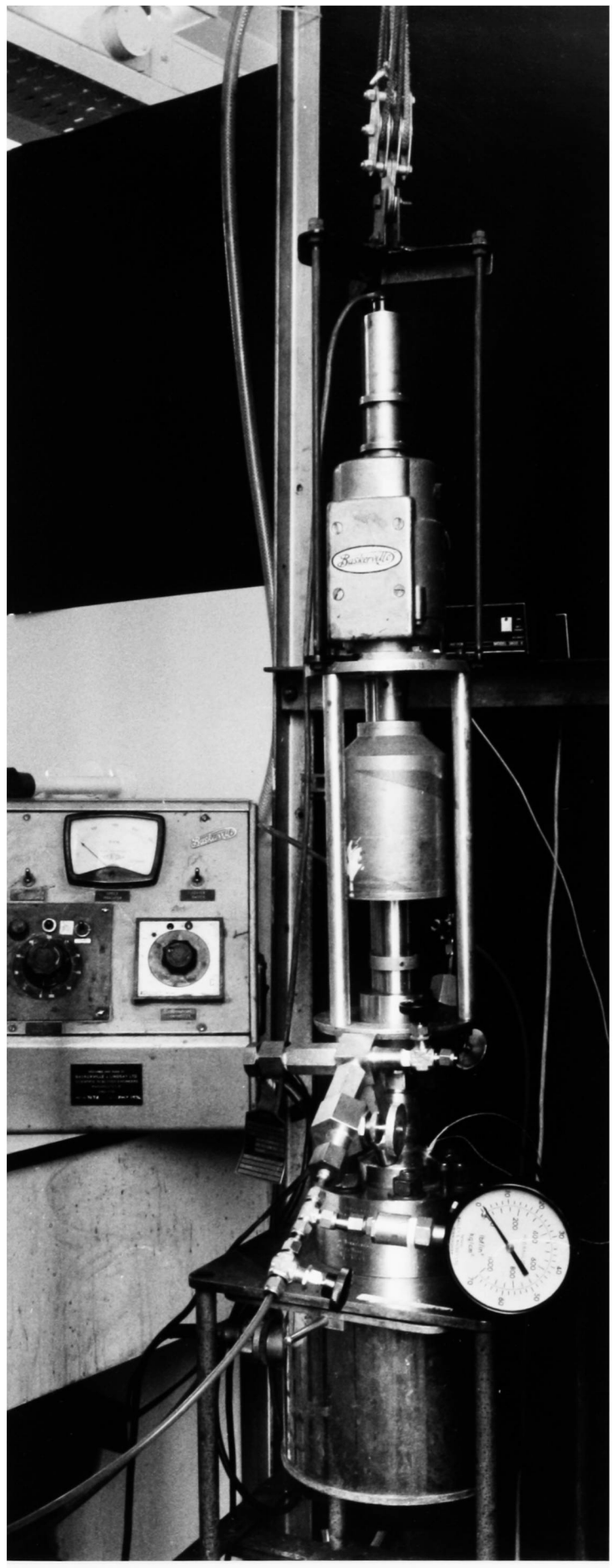

was single stage with four turbine blades on the shaft. The impeller was positioned directly beneath the liquid/slurry surface to maximise the dispersion of the gas. The temperature was maintained by surrounding the reactor base with an electrical heater. The temperature and the stirrer speed could be varied and controlled in the range of 273-673K and 0-2000rpm respectively by the Baskerville control unit (Model 7678). The gas supply to the reactor was regulated and measured by the hydrogen control unit (Section 4.1.8) and monitored on a chart recorder. A dip leg was added at a late stage, allowing liquid samples to be taken during the course of the reaction.

The stirred stainless steel reactor had the following design details:

Parameter	Dimensions
Tank diameter	75mm
Tank height	135mm
Stirrer shaft height (in the reactor)	125mm
Stirrer shaft diameter	5mm
Width of the baffles	10mm
Baffle height	100mm
Height of impeller blades	25mm
Diameter of impeller blades	57mm

4.1.3 Cocurrent Downflow Contactor (CDC)

Used for Mass Transfer Studies (the 100mm Pyrex Glass Column)

An overall view of the experimental apparatus is shown in Figure 4.3 and Plate 4.3.

The CDC reactor consisted essentially of three standard pieces of QVF™ glassware, assemble into two sections (Figure 3.1). The top straight section was 1300mm in length and 100mm in internal diameter. The lower section consisted of two 200mm/100mm standard reducers joined to make the enlarged base of the column. The lower section was designed specifically to prevent bubble entrainment in the out-going fluid at the flowrate used. The two sections were joined together with standard QVF™ coupling flanges and standard fibre gaskets. At the top end of the column the stainless steel plate was fitted with a centrally-positioned 25mm entrance pipe and a vent line. An orifice plate was screwed onto the flange from the inside surface and was aligned with the entrance pipeline, with gasket sealing between the flange surface and the orifice plate at the top. The incorporation of the orifice plate on the top flange allowed various orifice sizes to be used by changing the orifice plate. Orifice plates with orifice diameters ranging from 8mm to 20mm were fabricated to give a wide range of column diameter to orifice diameter ratios. The use of the vent at the top facilitated start-up, when the column had to be filled up with liquid, and shut-down, when the system had to be drained. Both gas and liquid streams entered the column at the top through T-pieces. The gas entered the system through a non-return valve (6.4mm) to prevent liquid slurry flowing back into the gas flowrate meter and the hydrogenation control unit. A dead-leg was fitted to the column in order to measure gas holdup in the conjunction with the volume expansion method and the static shutdown method (Section 5.1.4). Both ends of the deadleg were fitted to the stainless steel plates at the top and bottom of the reactor. The base flange was fitted with a

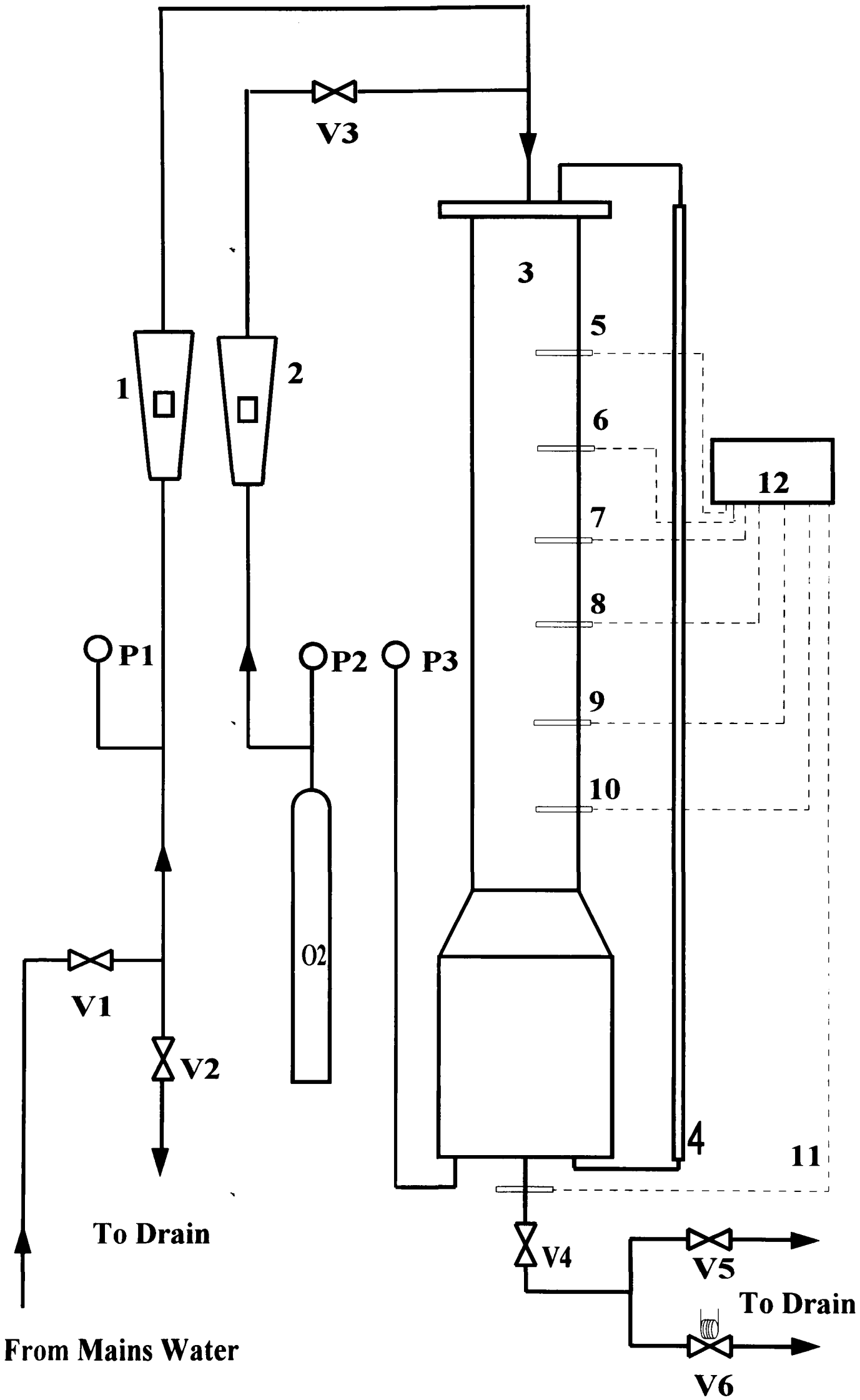

Figure 4.3 Schematic Diagram of Mass Transfer Studies in 100mm CDC

1: Liquid flowmeter; 2: Gas flowmeter; 3: CDC; 4: Deadleg;
5-11: Sample points; 12: DO meter;
P1-P3: Pressure gauges; V1-V6: Vavles;

Plate 4.3

100mm Pyrex Glass CDC Used for Mass Transfer and Residence Time Distribution Studies

Plate 4.3

100mm Pyrex Glass CDC Used for Mass Transfer and Residence Time Distribution Studies

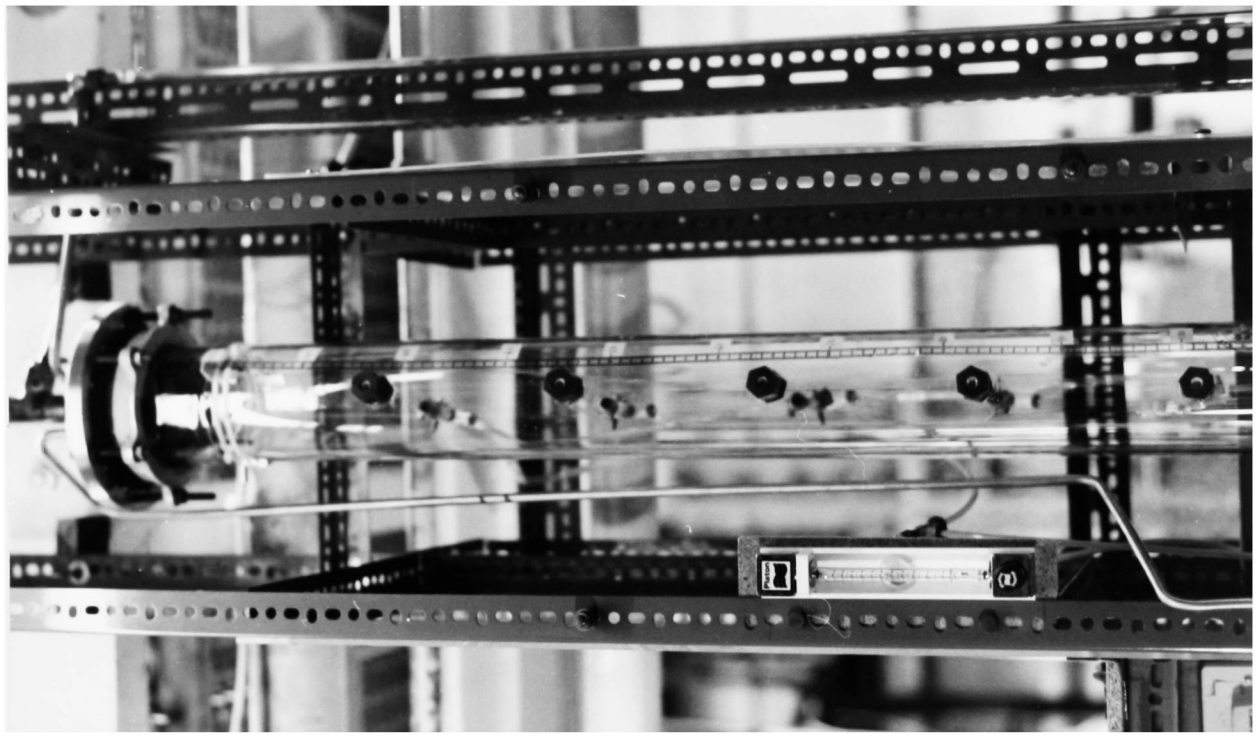

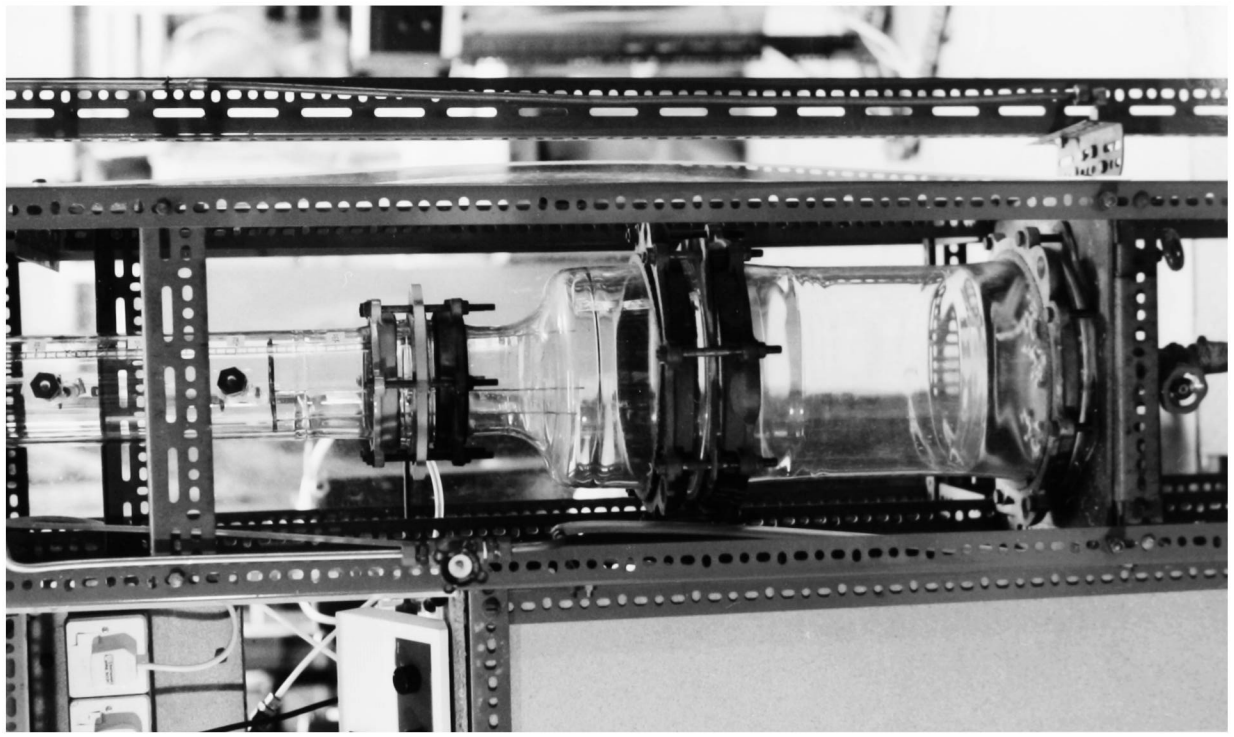

centrally positioned 25mm exit pipe and a pressure gauge. A ball valve was fitted to the exit line to regulate the column pressure. A solenoid valve was fitted to the exit pipe to measure the gas holdup by the static shutdown method.

Six sample ports were positioned at fixed intervals along the straight section at the back of the column and were used to measure the dissolved oxygen (DO) concentration (Section 5.2) for determining mass transfer characteristics. A Pyrex glass stopcock was connected to the outlet of each sample port. The first port was located 280mm from the top of the column and thereafter the ports were spaced at 190mm intervals. Table 4.1.3.1 shows the distances of the sample ports from the top of the column. On sampling, each individual stream passed through the stopcock and the sampling device (Section 5.2.2) and over a dissolved oxygen probe connected to a Dissolved Oxygen Analyzer (Model 27274, from Orbisphere Laboratories, Switzerland). The DO probe was mounted within a hollow stainless steel chamber which allowed the liquid stream to pass freely over the probe.

Table 4.1.3.1 Sample Port Position

Port Number	1	2	3	4	5	6
Distance from top, mm	280	470	660	850	1040	1230

4.1.4 Cocurrent Downflow Contactor (CDC) Used for Residence Time Distribution Measurements (the 100mm Pyrex Glass Column)

An overall view of the experimental apparatus is shown in Figure 4.4 and Plate 4.3.

The reactor system was as the same as discussed in Section 4.1.3 but fitted with conductivity probe ports instead of the sample ports.

Residence time distribution measurements were undertaken to determine the mixing characteristics within the CDC for the gas liquid system and the reactor flow pattern.

Six Pyrex glass conductivity probe ports were positioned opposite to the sample points of the reactors. The first port was positioned 280mm from the top of the reactor and the remaining ports were at 190mm intervals (the port positions were as the same as in Table 4.1.3.1). The conductivity probes were made of nichrome wire by the School of Chemical Engineering, The University of Birmingham. The probes were calibrated (see Appendix 8.7) with different concentrations of standard sodium chloride solutions and were connected to a conductivity meter and in turn to a chart recorder. 70kg.m^{-3} aqueous sodium chloride solution was employed as a tracer. This tracer was injected from the top flange or other port in the CDC, using a pulse method with compressed nitrogen through a solenoid valve controlled by a pre-set time trigger, when the CDC was operating in a stable condition (normally 30 minutes are needed after start-up or operation alteration), as indicated by a dissolved oxygen meter with constant DO reading and the stable dispersion height in the column.

In addition the flow pattern was monitored visually by photography and video recording.

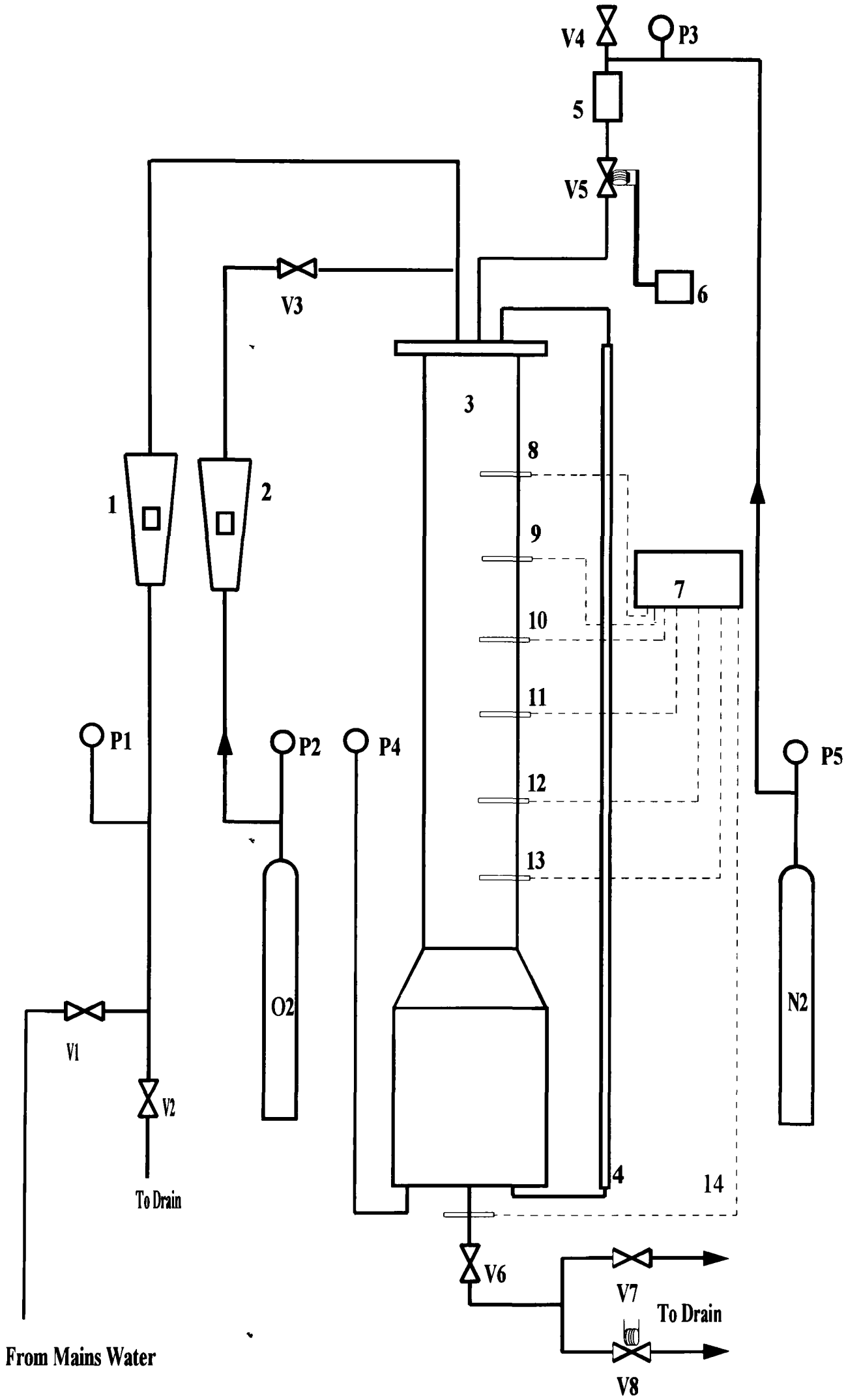

Figure 4.4 Schematic Diagram of RTD Studies in 100mm CDC

1: Liquid flowmeter; 2: Gas flowmeter; 3: CDC; 4: Deadleg;
5: NaCl reservior; 6: Trigger; 7: Conductivity meter;
8-14: Conductivity probes; P1-P5: Pressure gauges; V1-V8: Valves

4.1.5 Cocurrent Downflow Contactor Reactor for Low Pressure Hydrogenation (the 50mm Pyrex Glass Column)

An overall view of the experimental apparatus is shown in Figure 4.5 and Plate 4.4.

The CDC reactor consists essentially of two pieces of QVF™ glassware, separated into two distinct sections. The top section is a 1200mm long Pyrex glass column of 50mm fitted with a Pyrex glass jacket for maintaining the column temperature of the reactor. The lower section was a 150/50mm standard reducer to make an enlarged base for the column. The lower section was designed to prevent bubble entrainment for the gas and liquid flow rates used. QVF™ couplings and standard O-ring fibre gaskets were used to join and seal the Pyrex glass sections. A stainless steel plate was fitted at each end of the reactor, sealed with QVF™ couplings and standard O-ring fibre gaskets. The top stainless steel plate was fitted with a centrally positioned 12mm pipe, the inside of which was threaded to accept different sizes of orifices. A deadleg was fitted to the reactor from the top and bottom flanges to measure the gas holdup of the reactor and two pressure gauges were connected to the inlet and the outlet of the reactor. A vent pipe was fitted to the top flange to facilitate start-up, when the column had to be filled with liquid, and the shut-down, when the system had to be drained. The solvent, substrate, catalyst and additive were added into a 10 litre cylindrical feed vessel, heated by an immersed coil heater and stirred.

The outlet of the feed vessel was connected to a centrifugal pump, which was connected to the CDC reactor by 12mm outlet pipe. The liquid was supplied from a reservoir, and the flowrate was adjusted by a ball valve. Two thermocouples were fitted into the reactor and the reservoir from the top flanges. Hydrogen gas was introduced to the reactor inlet line from a hydrogenation control unit and the flowrate was adjusted by a needle valve in the gas

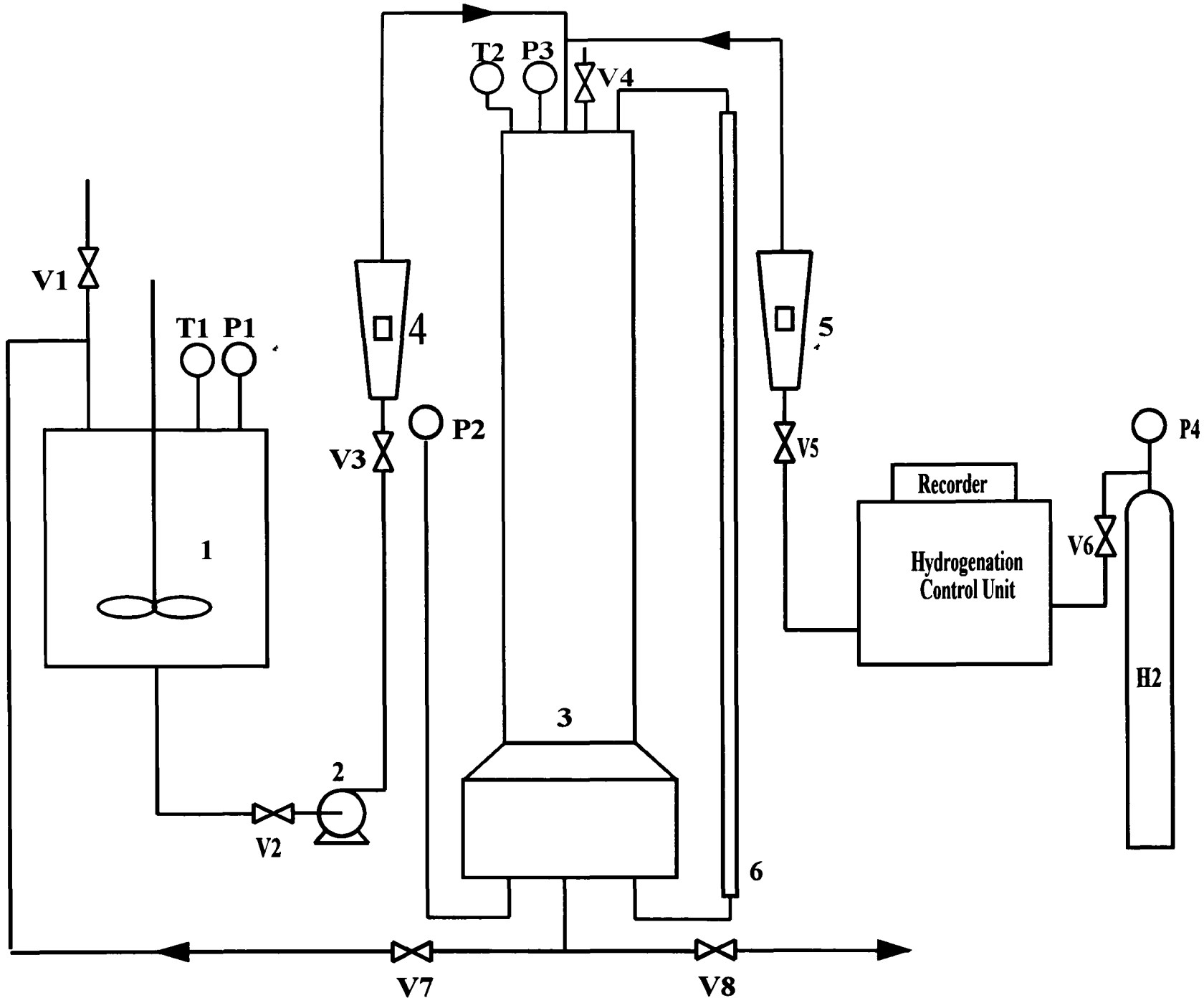

Figurre 4.5 Schematic Diagram of Hydrogenation in Low Pressure CDC

1:Mixing vessel; 2 :Pump; 3: CDC; 4: Slurry rotameter; 5: Gas rotameter;
6: Deadleg; P1-P4: Pressure gauges; T1-T2: Temperature indicators; V1-V8: Valves;

Plate 4.4

The 50mm Pyrex Glass CDC Used for Hydrogenation Study

The 20mm Pyrex Glass CDC Used for Hydrogenation Study

Plate 4.4

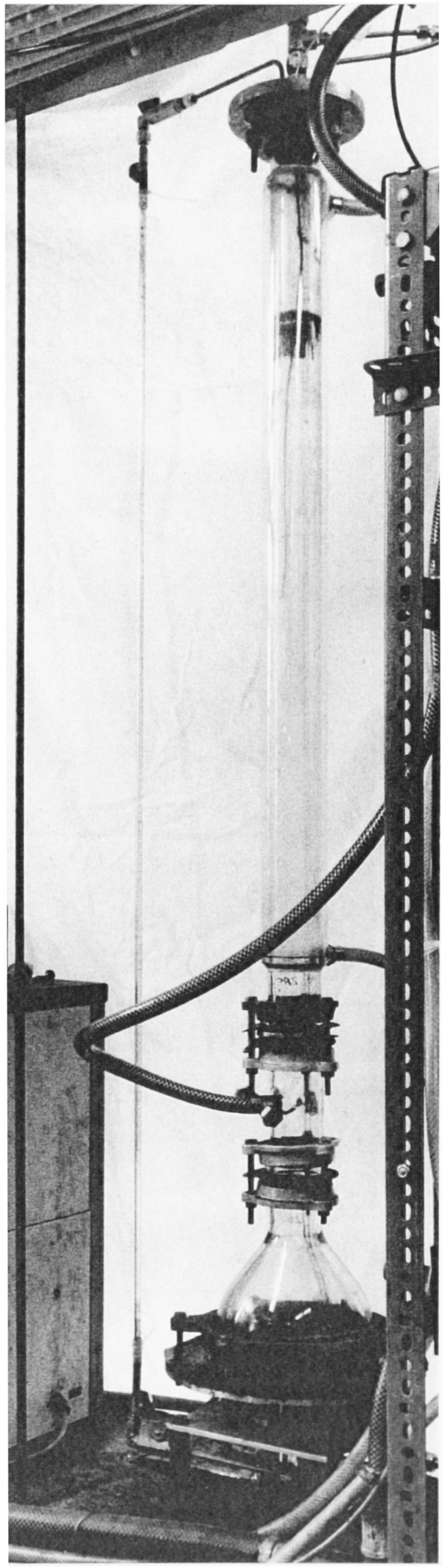

rotameter. A non-return valve was fitted to the gas line to prevent the entry of liquid into the gas flowmeter and the hydrogenation control unit. The outlet of the reactor was fitted with a ball valve to regulate the column pressure and was connected to the feed reservoir for recirculation of the liquid.

4.1.6 Cocurrent Downflow Contactor Reactor for High Pressure Hydrogenation (the 100 mm Stainless Steel Reactor)

An overall view of the experimental apparatus is shown in Figure 4.6 and Plate 4.5.

The reactor system consists mainly of a hydrogenation control unit, a main (pressure and electrical) control unit, a CDC reactor, a receiver, a feeding vessel and a gear pump with essential ancillary facilities and fittings.

The CDC reactor consisted essentially of two 100mm diameter columns with a top section 500mm in length and a bottom section 1000mm in length constructed from 100mm stainless steel pipes. The reactor columns were connected and sealed by standard flanges and gaskets. For slurry hydrogenation reactions the required amounts of reactants and catalysts were added to the feed vessel and mixed with a stirrer. The cylindrical feed vessel of 200mm diameter and 350mm in length was incorporated within the reaction system. A receiver of 250mm in diameter and 1000mm in length is an essential part for the batch/recycle operation. External calibrated pressure gauges (differential pressure cells) were used to measure the individual liquid levels in the CDC reactor and in the receiver based on the hydrostatic pressure difference between a reference level and their individual levels. The outside of the

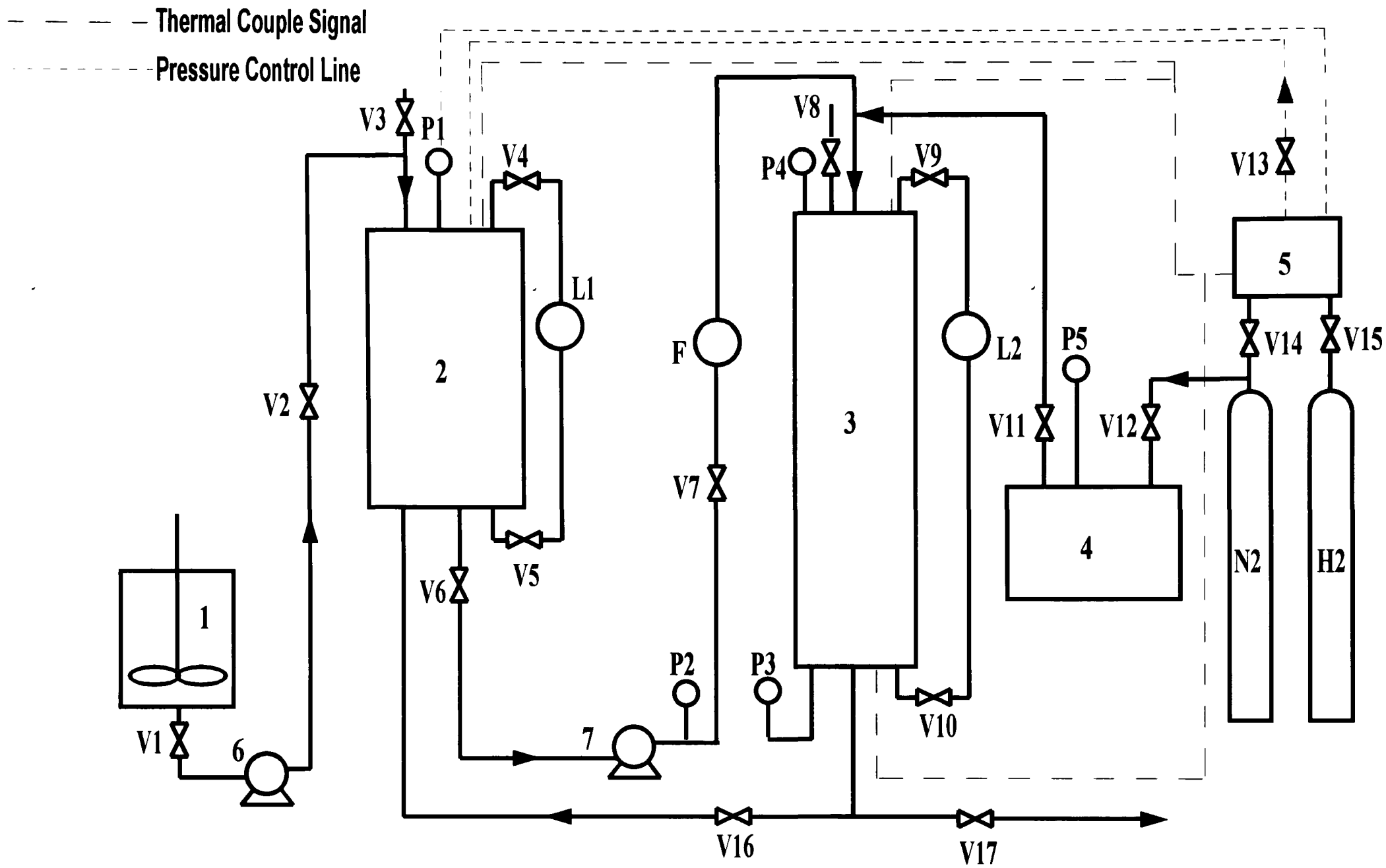

Figure 4.6 Schematic Diagram of Hydrogenation in High Pressure CDC

1:Mixing vessel; 2: Break vessel; 3: CDC; 4: Hydrogenation control unit; 5: Main control unit;
6: Feed pump; 7: Recirculation pump; V1-V17: Valves; P1-P5: Pressure gauges

Plate 4.5

The 100mm Stainless Steel CDC Used for Hydrogenation Study

The 100mm Stainless Steel CDC Used for Hydrogenation Study

Plate 4.2

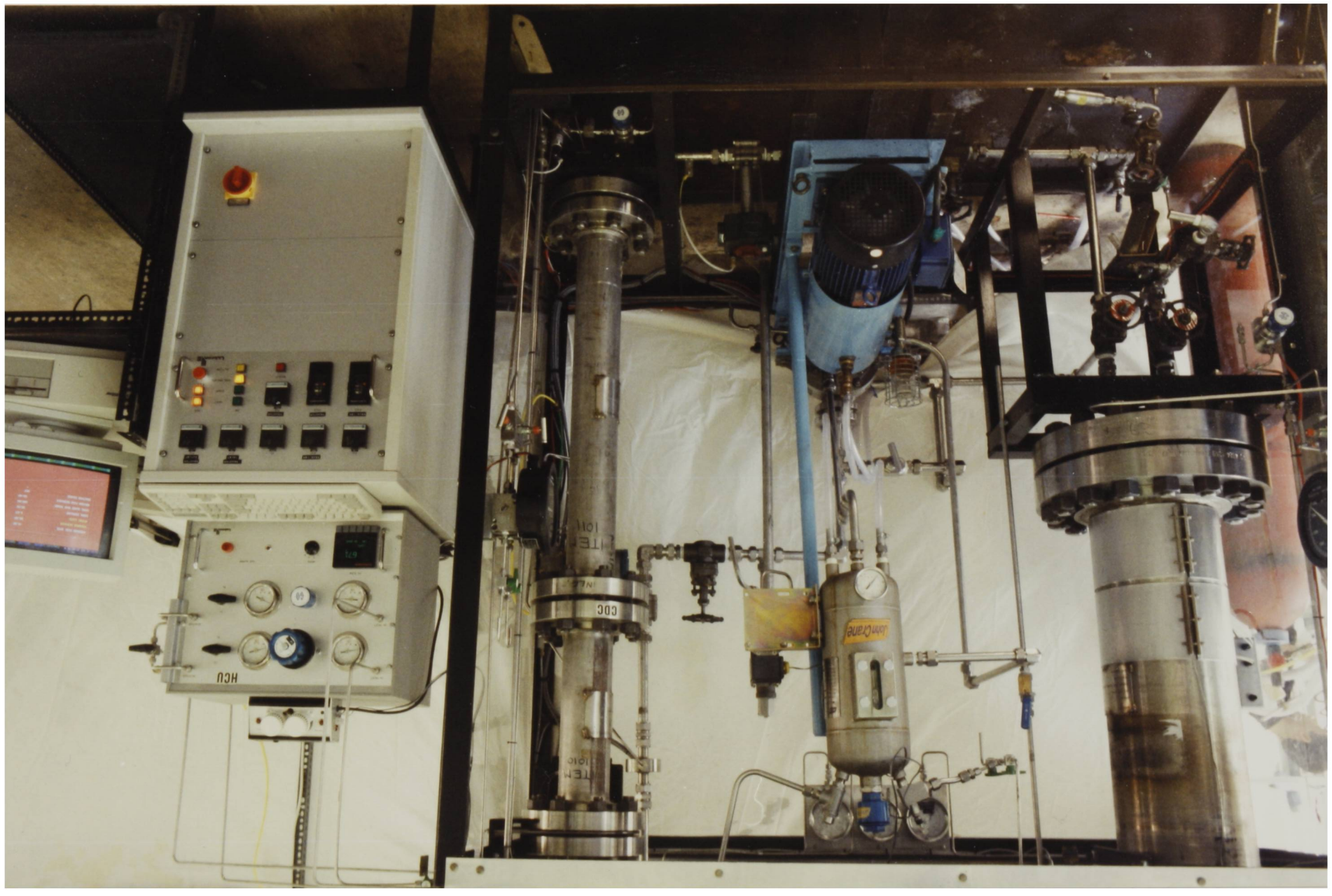
HCU
CDC

receiver was fitted with band heaters for heating the reactant medium. The outlet of the receiver was connected to a Avon centrifugal pump fitted with a cooling jacket. For flow regulation and smooth operation, the pump was connected to the CDC reactor by a 25mm outlet, and the flowrate was measured using the principle of pressure difference over an orifice and regulated by the main control unit. At the top flanges of the reactor and the receiver individual thermocouples and pressure measurement lines were fitted. The top flange in the reactor incorporated a centrally-positioned 16mm screwed inlet allowing orifice units of different sizes to be used. The pressure in the reactor was regulated by an outlet valve in order for the reaction to take place at a constant pressure. Gas was introduced above the top flange from the hydrogenation control unit through T configuration and the flowrate was regulated and measured by a needle valve and flowmeter. Non-return valves were fitted in the gas lines to prevent back-flow of liquid into the gas line and the hydrogenation control unit. A sample point was connected to the outlet of the reactor and pressure relief valves were fitted in case of over-pressure. Pressure reducing valves were fitted in the sample line and the draining lines to reduce the pressure to atmospheric pressure when sampling and draining.

4.1.7 Catalyst Characterization Equipment

A general view of the experimental apparatus is shown in Figure 4.7 and Plate 4.6.

In-house prepared catalysts and modified commercial catalysts were characterised by temperature programmed reduction. The equipment (PYE Chromatograph 104) comprised an oven, a thermal conductivity detector, an amplifier, a U-shaped reactor and a controller (Model 9999, Gow-MAC Instrument Co., Madison, New Jersey). The reduction took place at

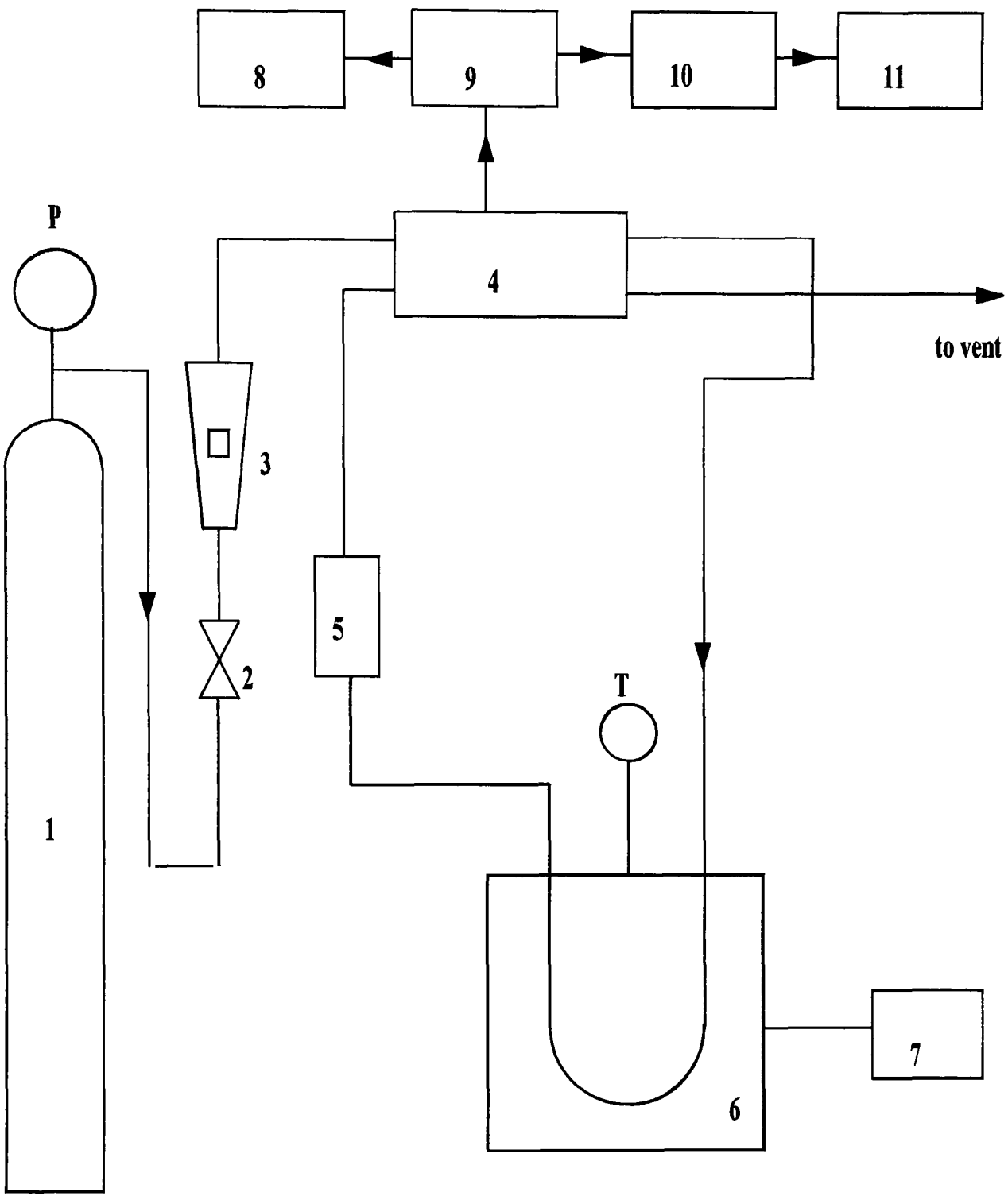

Figure 4.7 Schematic Diagram of TPR Apparatus

1: 5%H2 in Ar Cylinder; 2: Valve; 3: Gas rotameter; 4: Thermal conductivity cell;
5: Molecular sieve; 6: Oven and sample tube; 7: Controller; 8: Chart recorder;
9: Bridge circuit; 10: Integrator; 11: Recorder; T: Thermometer; P: Pressure gauge

Plate 4.6

Temperature-Programmed Reduction Rig

Temperature-Programmed Reduction Rig

Plate 4.9

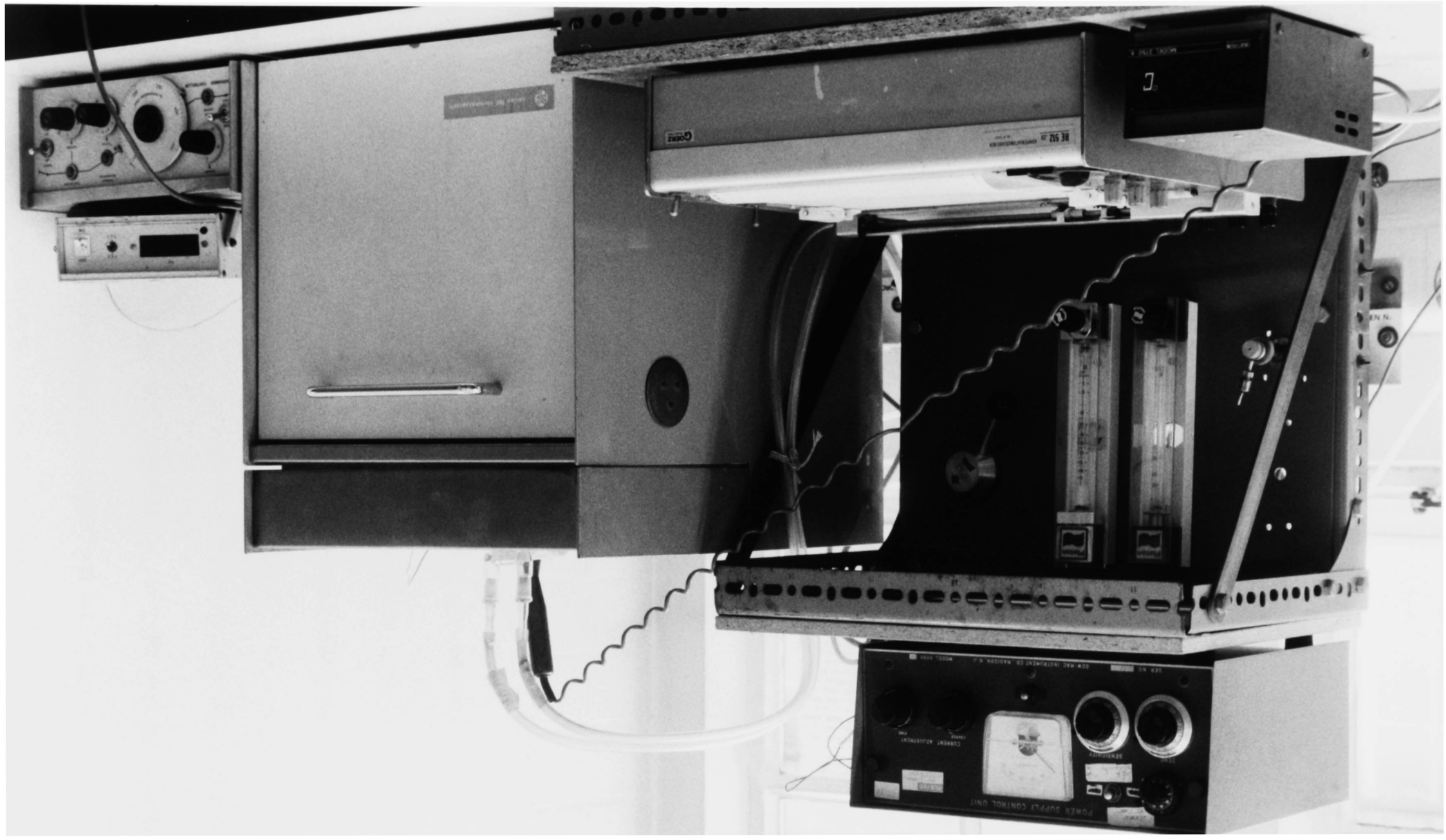
POWER SUPPLY CONTROL UNIT

constant pressure. The thermal conductivity detector measured the variation in gas composition within the system, and the output was fed to an integrator and then to a chart recorder. The oven was connected to a temperature-programmed controller. A 5% hydrogen in 95% (v/v) argon mixture was used as the reduction gas. The reduction peak was recorded on the chart recorder with the corresponding temperature.

The total surface area measurement was carried out in a liquid nitrogen bath instead of in a temperature programmed oven by using a continuous flow (BET) method (Appendix 8.5) and nitrogen adsorption. The gas used was a special mixture of 30% nitrogen and 70% helium by volume supplied by BOC Ltd. An integrator (C1-C10B Milton Roy) was connected to the thermal conductivity detector and used to calculate the peak areas which were recorded on a chart recorder.

The operation details of the catalyst characterization equipment:

Reducing gas flow rate: 40-60$cm^3.min^{-1}$

Bridge Current: 100mA

Bridge Sensitivity: 100%

Ramp Rate: 8-24$K.min^{-1}$

Temperature Range: 288-723K

Chart recorder sensitivity: 100mV

Chart recorder speed: 10-40$mm.min^{-1}$

4.1.8 Hydrogenation Control Unit

4.1.8.1-Hydrogenation Control Unit (Model: Mk 1, Engelhard)

The hydrogenation control unit (Plate 4.7, Top) equipped with two different sizes of reservoir was used to supply hydrogen for all the hydrogenation reactions. A description of the principles of its operation will suffice. The unit was linked to a 5mv recorder, so, to obtain maximum sensitivity, a hydrogen reservoir of appropriate size had to be selected according to the likely hydrogen consumption of the reaction system. The outlet hydrogen pressure could be selected in two ranges: (1) low pressure (8×10^{-5}MPa) and (2) high pressure (0.05-1.0MPa). The pressure was selected and then maintained at the desired level. When the unit was connected to the stirred Pyrex glass reactor and the autoclave, reservoir No. 4 (model 4B, 1.05 litre) was fitted and hydrogen was supplied through the low or high pressure outlet of the unit, depending on the reaction pressure. A low pressure purge valve was opened while purging the low pressure system. When the unit was connected to the CDC for low pressure hydrogenation, reservoir No 1 (model 1B, 15.31 litre) was used. A pressure transducer monitored the pressure decrease in the reservoir. The unit was maintained at 303K. The volume of the reservoir had been determined by the manufacturer, so the pressure drop could be related to the volume of hydrogen consumed. The volume of hydrogen delivered to the reactor was recorded as a decrease in the hydrogen pressure in the reservoir and displayed on the chart recorder. The rate of hydrogen takeup and the amount of hydrogen consumed were calculated from the slope of the volume-time trace on the chart recorder.

Plate 4.7

Hydrogenation Control Units

Hydrogenation Control Units

Plate 4.7

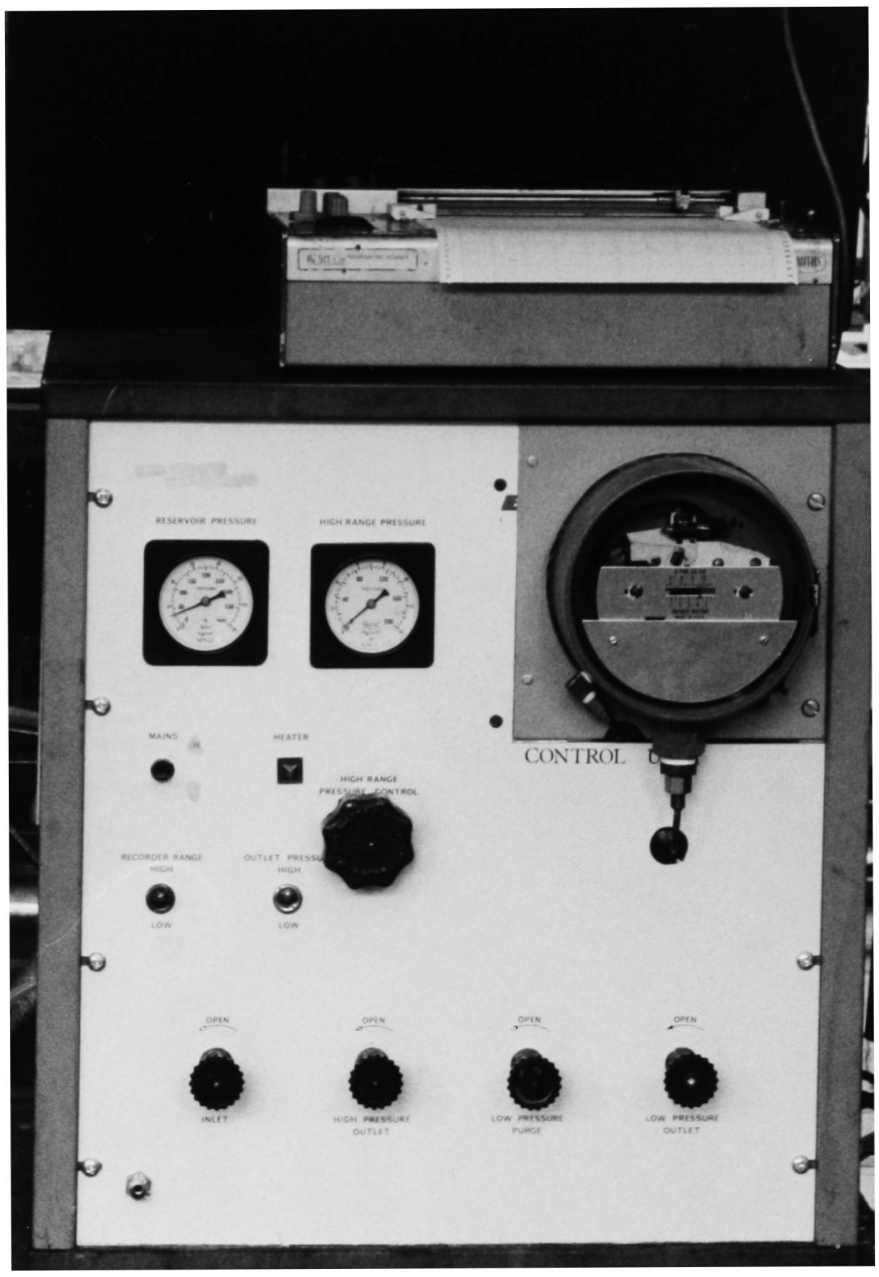
RESERVOIR PRESSURE
HIGH RANGE PRESSURE
MAINS
HEATER
HIGH RANGE
PRESSURE CONTROL
RECORDER RANGE
HIGH
LOW
LOW
OPEN
OPEN
OPEN
OPEN
INLET
HIGH PRESSURE
OUTLET
LOW PRESSURE
PURGE
LOW PRESSURE
OUTLET

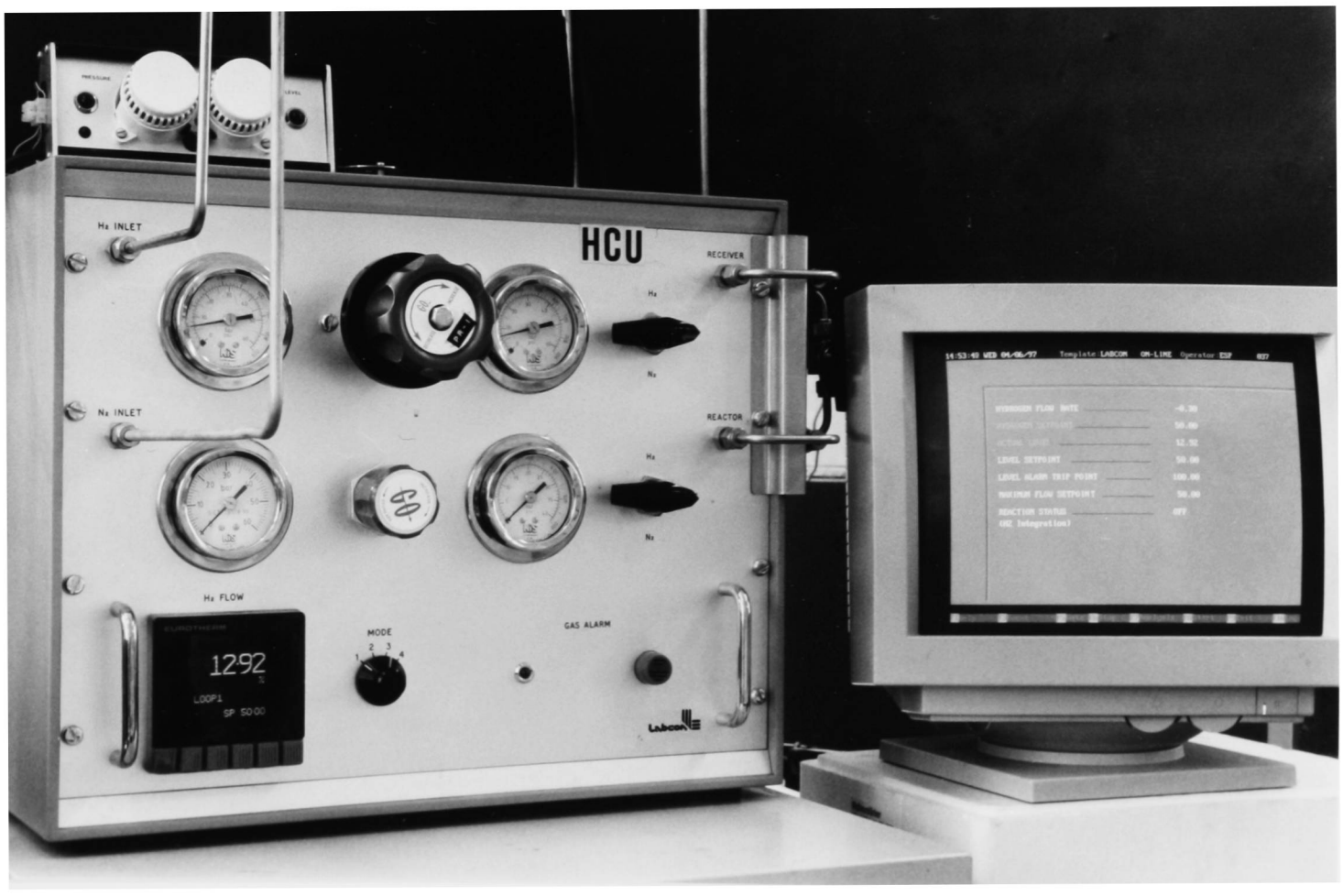
HCU
H₂ INLET
N₂ INLET
RECEIVER
REACTOR
H₂ FLOW
1292
LOOP1
SP 5000
MODE
GAS ALARM
Template LABCOM
ON-LINE
Operator ESP
HYDROGEN FLOW RATE
-0.38
50.00
12.52
LEVEL SETPOINT
50.00
LEVEL ALARM TRIP POINT
100.00
MAXIMUM FLOW SETPOINT
50.00
REACTION STATUS
OFF

The conditions under which the hydrogenation control unit was operated were as follows:

Table 4.1.8.1 Operation Conditions for the Hydrogenation Control Unit

Hydrogen Unit	Stirred Reactor (Pyrex glass)	Stirred Reactor (Autoclave)	CDC Reactor
Reservoir	Model 4B	Model 4B	Model 1B
Outlet Pressure	L.P.	H.P	H.P.
Outlet Pressure Range	Low	High	High
Reservoir Pressure, MPa	0.7	*	*
Outlet Hydrogen Pressure, MPa	8×10^{-5}	*	*
Recorder Range	Low	Low	Low
Reservoir Volume at STP, litre	1.05	1.05	15.31
Temperature, K	303	303	303

* Differs from run to run depending on the inlet liquid pressure

4.1.8.2 Hydrogenation Control Unit (Labcon)

The unit (Plate 4.7, Bottom) is for the measurement and control of hydrogen flow and the regulation of downstream pressure, and hence the hydrogen flowrate. When using the 'pressure control' mode, the hydrogen flow set point must be high enough to ensure correct operation of the pressure regulator under the particular conditions of hydrogen consumption. While in the 'hydrogen flow' mode, the pressure regulator must be set at the correct value to ensure that correct operation of the flow controller will shut off all flow when the downstream pressure rises to its set pressure.

The hydrogenation control unit (Labcon) connected to nitrogen and hydrogen cylinders was used to supply nitrogen for purging the reactor system and to supply hydrogen for the hydrogenation reactions. A description of the principles of its operation will suffice. Since the unit was linked to a data logging system, a hydrogen flow mode had to be selected

according to the likely hydrogen consumption of the reaction system to obtain maximum sensitivity. The outlet hydrogen pressure could be selected within the range of 0.1MPa to 3.1MPa. Once selected the pressure was maintained at the desired level. The unit was maintained at 303K. The hydrogen flowrate had been calibrated by the manufacturer, so the pressure drop could be related to the volume of hydrogen consumed. The volume of hydrogen delivered to the reactor as hydrogen flowrate, and the amount of hydrogen consumed with time, were recorded and displayed on the data logging system. The rate of hydrogen takeup was calculated from the slope of the volume-time trace.

The condition under which the hydrogenation control unit was operated were as follows:

Table 4.1.8.2 Operation Conditions in Hydrogenation Control Unit

Hydrogen Unit	Stirred Reactor (Autoclave)	CDC Reactor (High Pressure)
Outlet Pressure	H.P	H.P.
Outlet Pressure Range	High	High
Reservoir Pressure	*	*
Outlet Hydrogen Pressure	*	*
Temperature, K	303	303

* Differs from run to run depending on the inlet liquid pressure

4.1.9 Analytical Instrumental Methods

For this study two gas chromatographs, nuclear magnetic resonance and gas chromatography/mass spectra were used to identify and analyse the products from the hydrogenation of cinnamaldehyde.

4.1.9.1 Gas Chromatography (Model GC 94)

The first gas chromatograph (Model GC 94, from Analytical Instruments Limited, Cambridge, UK) was used with a capillary column and a flame ionization detector using helium as the carrier gas. The column used was supplied by J & M Scientific and was 0.25mm diameter and 60m long with a 0.25μm DB-1 coating.

The GC was operated under the following conditions:

Column Temperature: 393K-523KK

Carrier Helium Flowrate: 1.5ml.min^{-1} at 393K

Make-up Helium Flowrate: 30ml.min^{-1}

Split Helium Flowrate: 30ml.min^{-1}

Air Flowrate: 300ml.min^{-1}

Hydrogen Flowrate: 30ml.min^{-1}

Detector Scale: 1/10

Chart Speed: 10mm.min^{-1}

4.1.9.2 Gas Chromatography (Model PYE UNICAM 304)

This gas chromatograph (PYE UNICAM 304, Philips) consisted of an oven, a temperature controller, a packed column and a flame ionization detector using nitrogen as the carrier gas. The Pyrex glass column was 3m in length 6mm in diameter, packed with 10% SP-210 on 80-100 BS-mesh Supelcoport supplied by Supelco Inc., USA.

The GC was operated under the following conditions:

Column Temperature: 353-523K

Carrier Gas Flowrate: 1.5 $ml.min^{-1}$ at 393K

Air Flowrate: $300ml.min^{-1}$

Hydrogen Flowrate: $30ml.min^{-1}$

Detector Scale: 1/10

Chart Speed: $10mm.min^{-1}$

Attenuation: 1/8

4.1.9.3 Nuclear Magnetic Resonance

A high resolution nuclear magnetic resonance (NMR) spectrometer consists mainly of a radio-frequency source and a magnetic field, both of which have to be stable and homogenous to a very high degree. The sample is placed in a probe positioned between the poles of the magnet. The radiation is transmitted by a coil on the probe and detected by another coil. When the magnetic field or radio-frequency radiation changes slowly and the resonance condition is satisfied for the nuclei under observation, the sample absorbs enough energy from the radio-frequency radiation and the resulting signal is detected on the receiver coil, amplified and recorded. The instrument used is Bruker AC300 at $300MH_Z$ and chloroform-d (^1H) was used as the solvent in order to detect hydrogen atoms in the compounds. NMR analysis was carried out in School of Chemistry.

4.1.9.4 Gas Chromatography/Mass Spectroscopy

Mass spectrometers are used to determine relative atomic masses. The sample is ionised, and the positive ions produced are accelerated into a high-vacuum region by electrical and magnetic fields, which separate the ions according to their mass-to-charge ratios to produce a mass spectrum. SGE BPX5 capillary GC column was used with the temperature varied from 333K to 553K at 10K/minute and VG ProSpec magenetic sector mass spectrometer (UK) was used at 70ev based on electron impact ionization. GC/MS analysis was carried out in the School of Chemistry at the University of Birmingham.

4.1.10 Sampling Rig for Dissolved Oxygen Measurement in the CDC

The sample rig was designed after much trial and error in order to obtain reproducible data. It consisted mainly of a gas-liquid separator, gas pocket and pipelines (Figure 4.8). When the rig was fitted to the sample points its position had to be adjusted carefully to match the pressure difference between the sample point and gas return point, otherwise gas-liquid separation would be difficult and erroneous readings would be obtained.

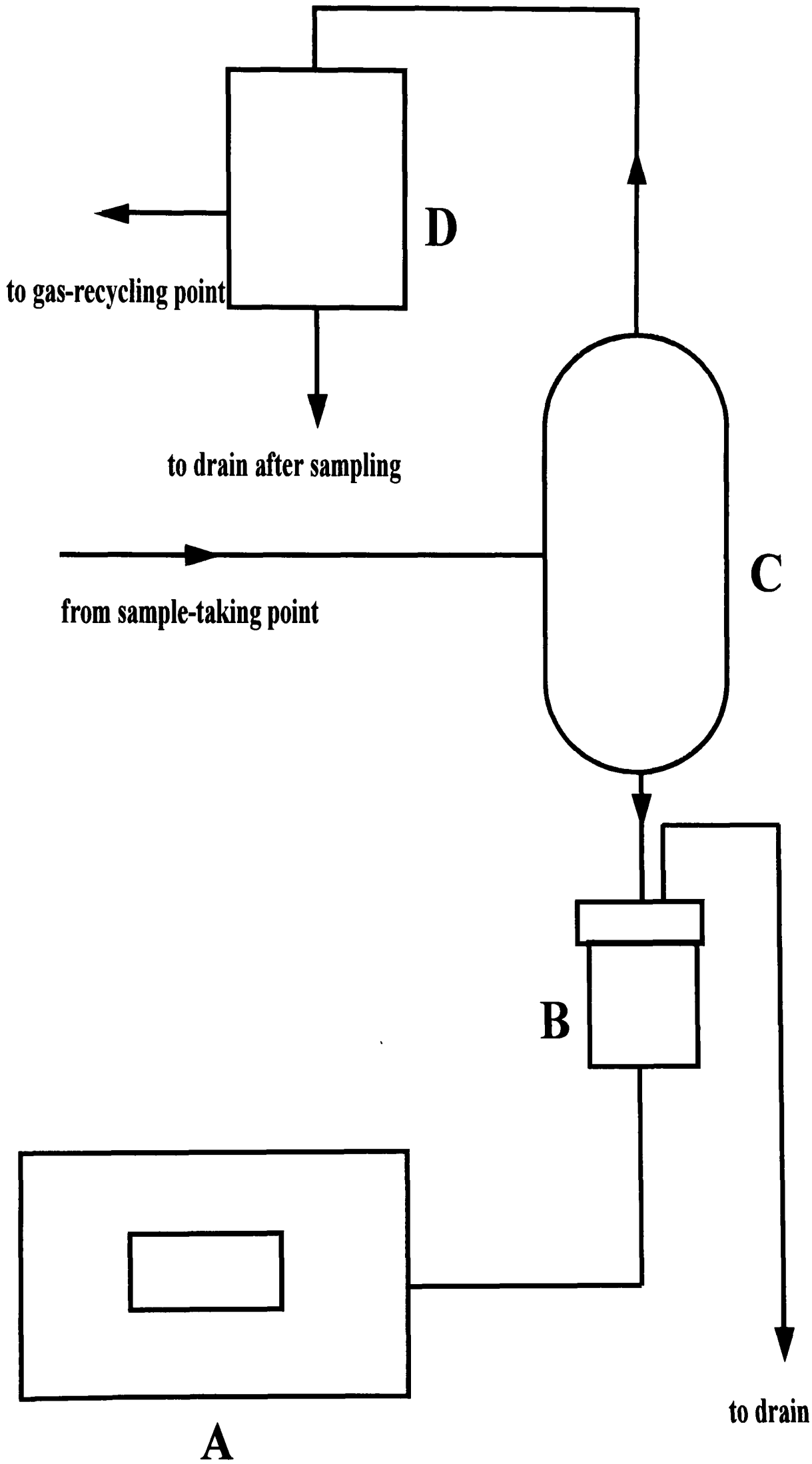

Figure 4.8 Schematic Diagram of Dissolved Oxygen Rig

A:DO meter; B:DO probe; C:Separation tube; D:Gas vessel

4.2 Materials Used

The physical properties of some of the materials used are given in Appendix 8.1.

4.2.1 Catalysts

The catalysts used were 5% palladium/charcoal (type 37, reduced) and 5% platinum/graphite (Type 286, reduced) and 5% ruthenium/charcoal (Type 97 PWD), all supplied by Johnson Matthey & Co. Ltd. Palladium, platinum, and ruthenium catalysts were prepared in-house by the impregnation method (Section 5.4.1). Some details of the catalysts are given as follows.

Table 4.2.1.1 Catalyst Properties*

catalyst	% Metal	Metal Surface Area ($m^2.g^{-1}$)	Support	Particle diameter (m)	Particle density ($kg.m^{-3}$)
Palladium (Type 37)	5.1	13.9	Charcoal	2×10^{-6}	2150
Platinum (Type 286)	4.95	0.29	Graphite	-	2360
Ruthenium (Type 97 PWD)	5	13.0	Charcoal	18×10^{-6}-	2150

* The data supplied by Johnson Matthey

Precursors used for preparing for Catalysts

Precursors	Supplier
Sodium hexachloroplatinate (IV)	Johnson Matthey
Sodium tetrachloropalladate (II)	Johnson Matthey
Ruthenium (II) Chloride	Johnson Matthey
Cobalt (II) Nitrate	Fisons

4.2.2 Gases

Gas	Purity	Supplier
Air	99.5%	BOC
Hydrogen	99.5%	BOC
Nitrogen	99.5%	BOC
Oxygen	99.5%	BOC
Helium	99.5%	BOC
5 % hydrogen/95% argon		BOC

4.2.3 Solvents

Material	Purity	Grade	Supplier
Water	Potable	-	Severn Trent
Methanol	99.5%	SLR	Fisons
Ethanol	99%	SLR	Fisons
Propan-1-ol	99%	SLR	Fisons
Propan-2-ol	99.5%	SLR	Fisons
Butan-1-ol	99.5%	SLR	Aldrich
Butan-2-ol	99%	SLR	Fisons
Heptane	99%	AR	Fisons
Toluene	99%	SLR	Fisons
Decane	99%	Pure	Koch-Light
Decalin (Decahydronaphthalene)	98%	Pure	Aldrich
Methylcyclohexane	99%	SLR	BDH
Diethyl ether	99%	Pure	Aldrich

4.2.4 Reagents

Material	Purity	Grade	Supplier
Cinnamaldehyde	98%	SLR	Fisons
Cinnamaldehyde	99%	Pure	Aldrich
Hydrocinnamaldehyde	90%	TECH	Aldrich
β-Methylstyrene	99%	GC	Aldrich
Propyl benzene	98%	GC	Aldrich
Phenyl propanol	98%	GC	Aldrich
Cinnamyl alcohol	98%	GC	Aldrich

4.2.5 Additives

The following chemicals were incorporated into the catalysts.

Material	Purity	Grade	Supplier
Aluminium chloride	99%	SLR	Fisons
Iron (II) chloride	98%	SLR	Fisons
Iron (II) sulphate	98%	SLR	Fisons
Potassium acetate	99%	SLR	Fisons
Potassium bromide	99%	SLR	Fisons
Potassium chloride	99%	SLR	Fisons
Potassium hydroxide	85%	SLR	Fisons
Silver nitrate	95%	SLR	Fisons
Sodium acetate	99%	SLR	Fisons
Sodium chloride	99.5%	SLR	Fisons
Sodium hydroxide	97%	SLR	Fisons
Tin (II) chloride	96%	SLR	Fisons
Thiophene	95%	SLR	BDH

Chapter 5 Experimental Methods

5.1 Hydrodynamic Investigation

5.1.1 Operation of the CDC

5.1.1.1 Start-up Procedure

1. The drainage valve was checked so that if the liquid was to be supplied from the mains water the valve was fully opened, whereas the valve was closed if the liquid was to be supplied from the storage tank.
2. The vent, column outlet valve, and pump by-pass valve were fully opened.
3. With the column inlet valve partially open, the water supply valve was opened to supply water to the column for the mass transfer study and residence time distribution; or the pump was switched on to pump liquid from the feed reservoir to the column for the hydrogenation studies.
4. The column was filled with liquid by adjusting the inlet and outlet valves (and the pump by-pass valve).
5. When the liquid reached the required level in the column, the vent was closed and the liquid flowrate and column pressure were regulated by adjusting the inlet and outlet valves and the pump by-pass valve. Great care was taken to ensure that the outlet valve was not fully shut when the vent was closed.
6. The pressure of the gas supply from the gas cylinder was regulated to match the inlet pressure. Usually a slightly higher gas pressure was maintained.
7. The gas inlet valves were opened and the gas flowrate was controlled by adjusting the needle valve on the gas rotameter.

8. A stable matrix of bubble dispersion in the column was maintained by controlling the gas flowrate.

5.1.1.2 Shutdown Procedures

1. The gas supply to the column was shut off by closing the gas inlet valve and the regulating valve on the cylinder.

2. The liquid supply to the column was shut off by closing the mains water valve or by switching off the pump.

3. The system was drained by opening the vent, column outlet valve, and drainage valve.

5.1.2 Dispersion-Initiating Velocity (u_{oi})

The minimum inlet liquid velocity required to break up a small gas cushion at the top of the column was determined during the start-up operation. When the liquid level in the column was about 30mm from the top of the column, with the liquid flowrate being kept sufficiently low to preserve a small gas cushion at the top of the column, the liquid flowrate was gradually increased until it reached a critical point at which the gas cushion was broken up, dispersing the gas into the liquid as bubbles, and thus indicating the start of the dispersion process.

5.1.3 Entrainment of Bubbles

When very small bubbles were produced in the dispersion, they were observed to be carried away in the outlet liquid stream, thus decreasing the gas utilization efficiency of the system. In order to keep the entrainment of bubbles at an acceptable level, the liquid flowrate in the column base section had to be kept below the maximum level. This maximum base liquid flowrate is a significant parameter in designing a CDC if maximum gas utilization is desirable.

5.1.4 Gas Holdup Measurements

5.1.4.1 Deadleg Method

This on-line method could be used by observing the clear liquid level in a deadleg connected in parallel to the side of the column. The deadleg was fitted to the top and the bottom stainless steel plates of the CDC. In theory, if the dispersion is confined to the cylindrical section of the column, gas holdup is given by the ratio of the liquid level in the deadleg to the dispersion height in the column:

$$\varepsilon_g = \frac{H_d - H_{c_1}}{H_d} \qquad (5.1.1)$$

5.1.4.2 Static Shut-down Method

When the CDC performed stably with a constant dispersion height the gas supply and both inlet and outlet valves were closed simultaneously, allowing the dispersion to collapse while maintaining the static pressure in the column. The dispersion height before shutdown and the clear liquid level upon shutdown were then used to calculate the gas holdup:

$$\varepsilon_g = \frac{H_d - H_{c\,2}}{H_d} \qquad (5.1.2)$$

5.1.4.3 Volume Expansion Method

When hydrogenation was carried out in the 50mm glass reactor and the 100mm stainless steel reactor operated as circulation systems, the gas holdup was measured by observing the changes of the slurry level in the reservoir:

$$\varepsilon_g = \frac{V_d - V_c}{V_d} \qquad (5.1.3)$$

5.1.5 Gas-Liquid Interfacial Areas

The specific gas-liquid interfacial area was calculated from the measured mean bubble diameter and the gas holdup using the following equation:

$$a = \frac{6\varepsilon_g}{d_{vs}} \qquad (5.1.4)$$

5.2 Gas Liquid Mass Transfer Investigations

5.2.1 Mass Balance over the CDC

The oxygen utilization was checked by a mass balance with respect to oxygen for oxygen-water concentration in the 100mm column. The dissolved oxygen concentrations in the inlet liquid and outlet liquid were measured by the dissolved oxygen meter and the oxygen input was calculated from the oxygen input flowrate measured by the oxygen flowmeter. The comparison between the measured and calculated concentrations gave the percentage of oxygen utilization.

$$O_2\% = \frac{(DO_{out} - DO_{in})V_R}{O_{2input}} \qquad (5.2.1)$$

5.2.2 Sampling Techniques for the Measurement of Dissolved Oxygen

The sampling rig for the measurement of dissolved oxygen is shown in Figure 4.7.

Measurement of the dissolved oxygen concentration in the bubble dispersion section requires proper separation of the liquid from the bubbles without changing the pressure. A suitable device (Figure 4.8) was designed following much trial and error. The following procedure was used for the efficient separation of gas and liquid for each individual measurement:

1. The gas-containing liquid sample tube and the gas return tube were connected to the sample points, making sure that the gas-liquid separation device was correctly levelled to ensure complete separation of gas from liquid.

2. The gas-containing liquid sample stopcock was opened to let the pressure in the sampling rig reach the column pressure.

3. The gas return stopcock was opened to allow enough time for the oxygen indicator reading to become stable (at least 10 minutes) and the result was recorded.

4. The gas return stopcock was closed first then the liquid-containing-gas sample stopcock was closed.

5. The two connecting tubes were disconnected from the sampling points.

6. The sample points were changed and the above steps were repeated for measurement at another sample point.

5.2.3. Steady State Gas/Liquid Absorption

The steady state absorption of oxygen into water was carried out in the CDC (Section 5.2.2). The start-up and shutdown procedure were as described previously (Section 5.1.1). To ensure that the absorption process reached a steady state, all the measurements were taken after the dispersion height and the outlet dissolved oxygen concentration were stabilised, as indicated by the concentration-time trace on the chart recorder. An average period of 30 minutes was required for the absorption to reach steady-state after start-up or after the operational conditions were changed.

The following parameters were applied:

1. Orifice Diameter

Single circular orifices of hole diameter 8-20mm were used to investigate the effect of input energy and orifice diameters.

2. Liquid Flowrate

The lower limit of liquid flowrate was the minimum flowrate required to maintain the dispersion, whereas the upper limit was the pressure drop limit, since an excessively high pressure drop through the orifice prevented any increase in the liquid flowrate.

3. Height of Bubble Dispersion

For a given liquid flowrate, the height of dispersion in the column increased with increase of gas flowrate, the upper limit being the maximum dispersion height which the given liquid flowrate could maintain. The system pressure in the column was maintained at 0.07MPa for most of the runs by adjusting the liquid outlet valve.

5.3 Residence Time Distribution Measurements

The residence time distribution measurement was carried out in the 100mm CDC using a pulse injection method (Section 4.1.4). The following procedure was used:

1. The required sodium chloride solution was prepared by dissolving the salt in tap water.

2. The relationship between the conductivity and the salt concentration was determined at the experimental temperature before residence time distribution study.

3. The sodium chloride reservoir was filled with the sodium chloride solution and the feed valve was closed.

4. When the oxygen absorption process reached a steady state, as indicated by the dissolved oxygen meter and a steady dispersion height, the compressed nitrogen valve connected to the sodium chloride reservoir was opened.

5. The conductivity meter and the chart recorder were switched on, and the time noted.

6. The actuator of the solenoid valve controller was pressed, the time was noted and the conductivity change in the CDC was recorded on the chart recorder.

7. When the conductivity signal on the chart recorder returned to the starting position the chart recorder was switched off and the nitrogen supply valve was closed.

5.4 Catalyst Preparation and Catalyst Modification

5.4.1 Catalyst Preparation

Some supported palladium, ruthenium and platinum catalysts were prepared by the incipient wetness method on various supports, using 5% (w/w) metal loading. 10g of catalyst were prepared each time.

The following procedure was used:

1. The required ratio of water or other solvent to the support was worked out empirically so that the support was just totally wetted to give a stiff but mobile paste.

2. The required amount of the catalyst precursor (sodium tetrachloropaladinate, sodium hexachloroplatinate, or ruthenium chloride) was weighed out.

3. The precursor sample was dissolved in the volume of the solvent found previously in step 1 above.

4. 10g of support was dissolved and added to the salt solution and stirred until mixed completely.

6. The paste was dried on a hot plate at 393K.

7. The sample was vacuum-dried at 373K overnight.

8. The catalyst was calcined at 473-773K in a muffle furnace for 4-20 hours depending on the support, precursor and the temperature.

5.4.2 Catalyst Modification

In order to increase the selectivity with respect to the desired products, the commercially-prepared and in-house prepared catalysts were modified by the incorporation of metal salts into the catalysts.

0.25-20 part of additive was used for 1 part of metal. The organic poison was added directly to the reactant solution without pre-treating the catalyst. The catalysts were modified by inorganic salts mostly by the following procedure:

1. The favourable ratio of solvent to catalyst was worked out by the incipient wetness method.

2. The required amount of the additive was weighed out and dissolved into the determined volume of deionized water.

3. The catalyst sample was added into the salt solution, stirred until mixed completely.

4. The modified catalysts were dried on a hot plate at 393K.

5. The modified catalysts were vacuum-dried overnight at 393K.

6. The vacuum-dried and modified catalysts were calcined at different temperatures for varying times depending on the properties of the catalyst, the support and the promoter, and were then ready for the reaction studies.

5.5 Hydrogenation in the Stirred Pyrex Glass Tank Reactor

A diagram of the reaction system is shown in Figure 4.1 and Plate 4.1.

The reactor was operated as a batch system in which hydrogen gas was continuously supplied to the system from the hydrogenation control unit (HCU) according to the hydrogen take-up rate demanded by the liquid slurry in the reactor. Rapid stirring was used to disperse the gas in the slurry.

When hydrogenation was carried out in the stirred reactor the following operation procedure was used:

1. The reactor base was charged with a weighed amount of the catalyst sample and 70ml of the solvent.

2. The reactor base was fitted with the head, the stirrer unit, the inlet and outlet tubes, the sample tube and the reactant charging funnel, and sealed with high vacuum grease and a mercury seal.

3. The reactor base was submerged in a constant-temperature water bath fitted circulation pump. Hydrogen from the low purge outlet of the HCU was passed through the reactor headspace and in turn to the vent, thus purging the reactor system. Meanwhile, the slurry was heated to the reaction temperature.

4. While purging the reactor, a solution containing the reactant was prepared by dissolving cinnamaldehyde in the chosen solvent. Four purges were carried out in order completely to replace all the air in the reactor (one purge was defined as purging one reservoir volume of hydrogen through the reactor).

5. After purging was completed, the lower pressure purge outlet valve on the HCU and the reactor inlet valve were closed. The reactant solution was charged into the reactor through the separation funnel and the reactor outlet was shut off. The liquid slurry was stirred for five minutes without hydrogen supply, then an initial sample was taken by a syringe through the sample tube.

6. After mixing the slurry, the reservoir was refilled with hydrogen. The low pressure outlet valve on the HCU and the inlet valve of the reactor were opened and the reaction started by switching on the stirrer motor. Stirring speed was increased gradually until the required stirring speed was reached. By doing so, the possibility that the reactor would be damaged due to sudden shock was minimised.

7. The progress of the reaction was monitored by observing the pressure/volume-time trace on the chart recorder. When the hydrogen in the reservoir had decreased to about 0.3MPa, the reservoir was refilled with hydrogen by quickly opening and closing the hydrogen inlet valve on the HCU. During the course of the hydrogenation, samples were taken regularly for GC, GC/MS, or NMR analysis to obtain the product composition and selectivity data with time.

8. When hydrogenation was approaching completion, as indicated by the levelling-off of the volume-time trace on the chart recorder, the reaction was stopped by switching off the stirrer and closing the hydrogen outlet valve on the HCU and the inlet valve of the reactor.

5.6 Hydrogenation in Stirred Stainless Steel Tank Reactor (Autoclave)

A diagram of the reaction system is shown in Figure 4.2 and Plate 4.2. The reactor was operated as a batch system in which hydrogen was supplied continuously to the

reactor from the HCU. The slurry was stirred vigorously to disperse the gas. The following procedure was used:

1. The reactor base was charged with weighed amounts of the catalyst sample and cinnamaldehyde, and with the promoter and the solvent.

2. The reactor base was fitted with the reactor head and sealed.

3. The reactor base was surrounded by an electrical heater with a temperature controller. Hydrogen from the high pressure outlet on the HCU was passed through the reactor headspace and in turn to the vent to purge the reactor system. Four purges were carried out in order to replace all the air in the reactor.

4. When the purging was finished the high pressure outlet valve on the HCU and the reactor inlet valve and outlet valve were closed. The slurry was stirred and heated to the reaction temperature. (If the reactor contents were heated first and then purged by hydrogen, especially at high temperatures, significant reactant losses would result.)

5. After mixing the slurry, the stirrer was switched off and the reservoir was refilled with hydrogen. The high pressure outlet valve on the HCU and the inlet valve of the reactor were opened and the reaction started by switching on the stirrer motor. Stirring speed was increased gradually to the required level.

6. The progress of the reaction was monitored by observing the pressure-time trace on the chart recorder. When the pressure in the reservoir was about 0.1MPa higher than the reaction pressure the reservoir was refilled with hydrogen by quickly opening and closing the hydrogen inlet valve on the HCU.

7. When the hydrogenation was approaching completion, indicated by the levelling-off of the volume-time trace on the chart recorder, the reaction was stopped by

switching off the stirrer and closing the hydrogen outlet valve on the HCU and the inlet valve of the reactor.

8. The reactor was cooled to the ambient temperature by submerging the reactor in a cold water bath in order to prevent the loss of solvent to the environment by evaporation when discharging, then the reactor was vented and a final sample was taken for analysis and then the reactor was discharged.

5.7 Hydrogenation in the 50mm Pyrex Glass CDC Reactor

The hydrogenation of cinnamaldehyde dissolved in various solvents was carried out as a model reaction system to study the mass transfer and reaction characteristics of the CDC (Section 6.4) and the kinetics and selectivity for the reaction. A diagram of the reactor assembly is shown in Figure 4.5 and Plate 4.5.

Efficient contacting between the continuous phase and the dispersed phase in a reaction system is essential. A large amount of research has been carried out and various types of equipment have been developed to meet these needs. Among them the Cocurrent Downflow Contactor (CDC) has evolved from a novel concept of contacting a liquid continuous phase and a dispersed phase. It has been proved to offer a high degree of mass transfer by the application of a continuous turbulent liquid inlet stream with simultaneous entrainment of gas into a body of liquid. Rapid surface renewal and frequent bubble coalescence and rupture make the CDC a highly efficient mass transfer device. Some other advantages over conventional gas liquid contactors are simple design and operation, efficient gas utilization (100%), high mass transfer coefficient, a very close approach to equilibrium (97%) in short contact

time, high gas liquid interfacial area and gas holdup, lower power consumption, small operating volume, no internal moving parts and easy maintenance.

The reactor was operated in the batch mode, whereby a certain volume of slurry was fed into the reactor and circulated by the pump. Hydrogen was supplied continuously to the reactor from the HCU according to the consumption rate.

The following operating procedure was followed:

1. The required amounts of catalysts and cinnamaldehyde were weighed out.

2. 8 litres of slurry were prepared by dissolving the catalyst in a measured volume of the reactant solution.

3 The slurry was mixed by stirring and heated to the required reaction temperature with circulating hot water from the submerged coil heat exchanger.

4. The stirrer was taken out and the break vessel was sealed.

5. The vent and column inlet valves in the CDC were opened, the gas inlet valve was closed in case the slurry entered the gas line, and the drain valve was closed.

6. The slurry was pumped from the feed/break vessel to the CDC column inlet using the circulation pump, and when the CDC was nearly full the vent valve in the CDC was closed. The column pressure was adjusted by the column outlet valve; The volume of the feed was calculated from the difference between the initial and remaining slurry volumes in the container.

7. Water was circulated through the jacket of the glass vessel and the coil heat exchanger in the reservoir.

8 The gas inlet valve of the column was opened so that the free headspace in the column and vessel was pressurised.

9. The gas inlet valves were shut and the vent valves were opened to release the gas in the head space, thus purging the system with the gas.

10. Steps 9 and 10 were repeated several times.

11. The gas supply to the system was switched from nitrogen to hydrogen from the HCU and the outlet hydrogen pressure of which was set to about 0.2MPa.

12. Steps 9 and 10 were repeated until the hydrogenation reservoir was emptied.

13. The hydrogenation reservoir was refilled and steps 9 and 10 were repeated. Usually three or four reservoir volumes of hydrogen were used to purge the system.

14. The gas inlet and the two vent valves were closed, the column inlet and outlet valves were opened and the circulation pump was switched on.

15. The slurry circulation rate was adjusted by use of the column inlet and pump bypass valves. The system pressure in the column was obtained by carefully opening the gas inlet valve leading to the glass vessel to pressurise the system.

16. The hydrogen outlet pressure of the HCU was adjusted to match the pressure of slurry entering the column. Usually a slightly higher pressure was maintained.

17. The gas inlet valve leading to the column was opened and a three-phase dispersion was produced in the column.

18. The vent valve on the glass vessel was opened carefully and then closed to release the pressure build-up due to the volume expansion in the system.

19. Once the process was stabilised, the progress of the reaction was followed by observing the volume-time trace on the chart recorder. The gas holdup in the CDC was measured by the deadleg method and the liquid level difference between the operation and gas shut down levels. The reservoir was refilled when the pressure in the reservoir decreased and approached the hydrogen outlet pressure.

20. When complete hydrogenation was approached, as indicated by the levelling-off of the volume-time trace, the reaction was ended by closing the gas inlet valves and switching off the circulation pump.

21. The system was discharged to a waste collection drum by opening the drainage and vent valves.

22. The reactor was cleaned, if required, by running mains water through the system.

5.8 Hydrogenation in the 100mm Stainless Steel CDC Reactor

The following procedure was used for the hydrogenation of cinnamaldehyde:

1. The reactor system was flushed several times with water to remove all contaminants. GC analysis was used to check that the reactor was clean.

2. The required amounts of the 5% platinum/graphite catalyst, cinnamaldehyde, potassium hydroxide and toluene were prepared separately. The potassium hydroxide was dissolved in 1 litre of water.

3. The reactor system was purged with nitrogen to eliminate air and any residual gases. After completion of the purge, the nitrogen purge valve was switched off .

4. The mains water supply valve was opened to fill the receiver and water then flowed under gravity into the reactor. While filling the receiver the vent line was opened to discharge any trapped gas and the reactor was filled by gravity flow. When the reactor was filled with water the vent lines were closed.

5. The recirculating pump was switched on to transfer water from the receiver into the reactor then water passed through the reactor and returned to the receiver.

6. The feed vessel was filled with toluene, cinnamaldehyde, catalyst and the concentrated potassium hydroxide solution and was stirred. The contents in the feed

vessel were pumped into the receiver and then the receiver was filled to the desired level with water. The final slurry was recirculated for some time to obtain thorough mixing.

7. The reactor system was purged with hydrogen from the control unit and the system pressure was increased gradually to the desired level.

8. The pressure and the liquid flowrate were adjusted to the desired operating levels.

9. When the correct system pressure was reached, the slurry was heated by band heaters and was circulated continuously.

10. When the pre-set temperature and pressure in the reactor were obtained, the reactor was fed with hydrogen set at a slightly higher pressure from the hydrogenation control unit. The hydrogen was introduced into the liquid inlet line through a T-piece and the gas and liquid mixture flowed through the orifice of the reactor and produced a turbulent bubble dispersion in the reactor. The dispersion height was determined by the gas inlet rate, the reaction rate and the absorption rate. In all the experiments the dispersion was set to 35%.

11. During the course of the reaction, samples were taken regularly for chemical analysis to determine the product distribution and the selectivity, and the hydrogen input rate was monitored by the hydrogenation control unit and collected by a data logging system to obtain the reaction rate and hydrogen consumption.

12. When hydrogenation was complete, the hydrogen flow from the hydrogenation control unit was stopped and the heating was switched off. The recirculation of the liquid was continued to cool the hot liquid.

13. When the temperature was reduced to ambient, the system was depressurised.

14. When the system pressure was reduced to atmospheric pressure, the pump was switched off and the drain valves of the reactor and the receiver were opened to discharge the contents into a waste container.

5.9 Temperature-Programmed Reduction

The in-house-prepared catalysts were characterized by temperature-programmed reduction in order to determine the reduction temperature of a given catalyst prior to use in a reaction. The following procedure was used:

1. The reduction unit, the amplifier, the oven, the integrator and the chart recorder were switched on for half an hour before the measurement in order to stabilise the equipment.

2. 0.2-1g catalyst was charged into the sample tube.

3. The hydrogen/argon gas mixture was switched on, and its flowrate was adjusted to the desired level.

4. The programmed-temperature controller was switched on to start the reduction.

5. The progress of the reduction was recorded on the chart recorder and the temperature corresponding to the reduction was noted. The reduction temperature was used to activate the catalyst for reaction studies.

6. When the reduction course was finished the oven heater was switched off and the oven door was opened. The rapid change of temperature and subsequent adsorption of hydrogen produced a adsorption peak. This procedure was repeated three or four times to ensure reproducibility.

7. The system was calibrated by injecting 2ml of pure hydrogen gas into the system. Proportionality was assumed between the volume of calibration gas injected and the

integrated peak area. Accordingly, the volume of hydrogen adsorbed could be determined assuming monolayer adsorption by the catalyst.

5.10 Total Surface Area Measurement

Total surface areas of catalysts were measured by physical adsorption. The following steps were used.

1. A pre-weighed amount of catalyst sample was charged into the U-tube.

2. The gas flowrate through the system and over the sample tube was adjusted to 40ml.min^{-1}.

3. After the system had stabilized, as shown by a straight line on the chart recorder, the U-tube was immersed in liquid nitrogen. This caused a disturbance to be detected by the katharometer producing a peak corresponding to the amount of nitrogen adsorbed by the catalyst. After about 5 minutes, the tube was removed from the liquid nitrogen.

4. The rapid change of temperature and subsequent adsorption of nitrogen produced a adsorption peak. This procedure was repeated three to four times to ensure reproducibility.

5. The system was calibrated by injecting 2ml of pure nitrogen into the system. Proportionality was assumed between the volume of calibration gas injected and the integrated peak area. Accordingly the volume of nitrogen subsequently adsorbed could be determined assuming monolayer adsorption by the catalyst. A one-point Brunauer-Emmett-Teller (BET) method (Smith, 1981) was used to calculate the specific surface area. The relevant equations and method have been described by Smith (1981).

5.11 Product Analysis of Hydrogenation

The product composition in various solvents was measured by analysing the samples of the reaction using gas chromatography, nuclear magnetic spectrometry, and mass spectroscopy.

5.11.1. Separation of Samples

The reaction samples was taken by syringe through a sampling port in the reactor tube. After sampling the slurry was separated from the catalyst by filtration. The filtrate was used for analysis.

5.11.2 Calibration of GC Results

The two gas chromatographs were calibrated for product response by injecting various dissolved standards. 0.2μl aliquots of dilute solutions (0.4M) of the standards were injected individually by syringe onto the column to obtain the corresponding retention times. A dilute standard mixture (0.4M) prepared by dissolving known amounts of different standards in the solvent. The areas of the standard peaks responding to the injected samples were measured by a Milton-Roy integrator.

Reagents and products were identified by comparison with authentic standards. Unknown products were identified by nuclear magnetic resonance and GC/MS. Qualitative analysis was carried out by calculating the area, and corrected by the corresponding factor of the chromatographic peaks.

Chapter 6 Results and Discussion

6.1 Hydrodynamic Investigations in the CDC

6.1.1 Introduction

The objective of this study was to investigate various aspects of the hydrodynamics of multi-phase systems in the CDC. Water, propan-2-ol and toluene were used as the liquid phases, and hydrogen and oxygen were used as the gas phases. The hydrodynamic characteristics investigation promotes understanding of the operation and design of the CDC and to assess the possible applications and limitations of the CDC for such processes. The following aspects of hydrodynamics were investigated in the three gas/liquid systems:

1. Flow regimes.
2. Minimum inlet liquid velocities
3. Entrainment of bubbles.
4. Bubble sizes.
5. Gas holdup.
6. Bubble dispersion and coalescence
7. Gas-liquid interfacial area.

(1) Oxygen/Water System

The oxygen/water system was studied by previous workers (Boyes and Ellis, 1976; Evinc, 1982; Jones, 1983, Sulidis, 1995) and is used here as the basis for comparison.

(2) Hydrogen/Organic Liquid Systems

Basic information was obtained about the hydrodynamics and general operating conditions of the CDC for the hydrogenation of cinnamaldehyde. Two systems were used: (1) Hydrogen/propan-2-ol with palladium catalysts, (2) Hydrogen/toluene with palladium or platinum catalysts.

6.1.2 Liquid Flowmeter Calibration

When hydrodynamics and mass transfer studies were carried out in the 100mm CDC a liquid flowmeter was used to measure the flowrate. A calibration graph of the actual flowrate against the flowmeter reading using water as the liquid phase is included (Table 8.6.1.1 and Figure 8.7.1.1).

6.1.3 General Observations

Studies of the hydrodynamics of the oxygen/water system were carried out in the 100mm column (see Section 4.1.3). Studies with hydrogen/propan-2-ol and hydrogen/toluene were carried out in the 50mm column (see Section 4.1.5). A qualitative description is given in the following sections.

6.1.3.1 Flow Regimes

(1) Oxygen/Water System

With the oxygen/water system, small bubbles produced in the turbulent jet coalesced rapidly to form large bubbles, leading to a well defined bubble matrix with seemingly uniform bubble size, thus preventing any bubbles from being carried away. Water was introduced on a single pass basis into the column from the mains. Oxygen was

introduced into the column through a T-piece in the top of the column after the column was filled with liquid. When the oxygen feed rate was greater than the oxygen dissolution rate tiny bubbles were produced in the liquid jet in the top section of the column and these tiny bubbles did not coalesce. On increasing the gas feed rate the inlet liquid velocity had to be greater than the dispersion-initiating flowrate in order to prevent the formation of gas pocket at the top of the column. A further increase in the gas flowrate would result in the coalescence of tiny bubbles to form large bubbles and an increase in the local gas holdup in the upper part of the column causing the formation of a well-defined flow regime.

The flow regimes depended on many factors, such as orifice diameter, liquid column velocity and the physical properties of the system, because the bubble matrix in the column was determined by the balance between the gas bubble rise velocity and the liquid downflow velocity while the bubble rise velocity was affected by the bubble size and system properties such as, density, surface tension, and the effect of additives such as electrolytes or surfactants. For the oxygen/water system, as the gas flowrate was increased different regions could be observed.

Condition A

When the bubble dispersion height in the column is small, two distinct regions were observed:

(A) The Entrance Region

This region was characterized by an intense turbulent liquid inlet stream containing small dispersed gas bubbles. In the first 10cm of the top section of the column there

was an end-effect section with a relatively low gas holdup and a relatively low volumetric mass transfer coefficient because of the existence of stagnant zones, and although k_L was high, the interfacial area was low. In the second section of this region, below the first 10cm, the gas dispersed as small bubbles (1-3mm in diameter) until the bubbles coalesced to form large bubbles. The overall height of this entrance region was 30-40cm.

(B) The Middle Region

Beyond the entrance region the bubbles coalesced to form larger bubbles (about 4.5mm in diameter). The turbulence was reduced and the bubble matrix consisted of close-packed bubbles occupying the whole cross-sectional area of the column. The gas holdup in this region appeared to be at its highest (Lu, 1988). This region extended almost to the top of the bottom flange in the straight section of the column.

Below the lower end of the bubble dispersion the liquid was largely clear with the exception of a few small bubbles (less than 0.5mm in diameter). The oxygen concentration was almost the same as that in the lower end of the middle region.

Condition B

(C) Small Bubble Cloud Region

With further increase of gas flowrate the lower end of the bubble dispersion extended nearly to the flange which connected the column to the enlarged section (see Figure 3.1). In addition a third region appeared with the formation of small (0.5mm

in diameter) bubbles which were quite densely packed. The height of this bubble region varied from 3cm to 10cm. Beyond this point in the expanded section the liquid was clear.

Condition C

If the gas flowrate was increased further, the dispersion extended and the whole of the liquid became very turbulent with a decrease in the height of the lower density entrance region. Finally a critical condition was reached when the gas supply exceeded the liquid absorption capacity, and a gas pocket was formed at the top of the column resulting in an unstable collapse of the dispersion. The operating gas flowrate should not exceed this critical level in the practice.

(2) Hydrogen/Organic Systems

In hydrogen/organic liquid systems very small bubbles were produced by the highly intensively turbulent jet stream at the entry zone. Two flow regimes were observed along the column.

(A) Entrance Section

In this region, very small bubbles (1-2mm) were dispersed throughout. The agitation and turbulence were very intensive. The gas holdup was relatively low. The overall length was about 25-30cm.

(B) Middle Section

Beyond the entrance section some bubbles began to coalesce to form large bubbles but due to poor coalescence in these systems some small bubbles did not coalesce and remained unchanged. A bubble size distribution (d_b = 1-3mm) existed in this region unlike the situation in the oxygen/water system. The turbulence was reduced and the bubble matrix consisted of close-packed bubbles occupying the whole cross-sectional area of the column. The gas holdup in this region appeared to be higher. This region extended almost to the top of the bottom flange of the column in the straight section. Below the middle section there is a clear disengagement area in the expanded section.

6.1.3.2 Minimum Inlet Liquid Flowrate

The performance of the cocurrent downflow contactor is determined by the balance between the bubble rise velocity and the liquid downflow velocity, so if the bubble rise velocity was larger than the liquid downflow velocity the bubbles rose to the top of the column owing to their buoyancy and accumulated there to form a gas pocket. A minimum inlet liquid velocity was required to initiate the dispersion of the gas into the liquid. Once the gas had been dispersed into the liquid to produce a bubble matrix in the column, a sufficiently high inlet liquid velocity was required to maintain the dispersion. An insufficient liquid velocity would result in the collapse of the dispersion, hence for a given column with a particular orifice there was a minimum inlet liquid flowrate for a given system to initiate the operation of the CDC. For this experiment the five orifice diameters ($D_{orifice}$ = 7.6, 10, 12, 16, 18, 20mm) were

examined. It was found that for $D_{orifice}$= 10mm and 12mm the minimum inlet liquid flowrate was 650$cm^3.s^{-1}$ (u_{jet} = 8.3$m.s^{-1}$ and 5.8$m.s^{-1}$), for $D_{orifice}$=16mm and 18mm the minimum inlet liquid flowrate was 950$cm^3.s^{-1}$ (u_{jet} = 4.7$m.s^{-1}$ and 3.7$m.s^{-1}$) and for $D_{orifice}$ = 20mm the minimum inlet liquid flowrate was 1230$cm^3.s^{-1}$ (u_{jet} = 3.9$m.s^{-1}$). When the 7.6mm orifice was used oxygen could not be introduced into the column by the liquid inlet stream because of the large pressure drop across the orifice. It can be seen that the jet velocity corresponding to the minimum liquid velocity is greater than 2$m.s^{-1}$ which was suggested by Boyes (1987) as a general rule of thumb for the CDC operation. The minimum inlet liquid velocity is a function of the column-to-orifice diameter ratio. For a given column, the minimum inlet liquid velocity varied with the orifice size. The smaller the orifice size, the lower the inlet liquid flowrate required since the inlet jet velocity increases with the decrease of the orifice diameter. This finding is in accordance with Lu's observation (1988) which claimed that the smaller the orifice size, the higher was the required inlet liquid velocity. The suitable orifice diameter, therefore, ranged from 10mm to 20mm for a given column and given conditions, and the operating liquid flowrate to maintain a certain length of bubble dispersion was generally greater than the minimum inlet liquid flowrate.

6.1.3.3 Entrainment of Bubbles

The CDC can achieve 100% utilization of the gas due to the complete separation of the gas phase from the liquid phase in the lower section of the column. This can be done by the addition of an expanded section with a diameter greater than that of the column to the lower end of the column, causing a reduction in the column liquid velocity. Theoretically, if the downflow liquid velocity is lower than the bubble rise

velocity the bubbles will rise, resulting in the disengagement of the gas from the liquid. However, this behaviour is dependent on the viscosity and coalescence properties of the liquid. Very few bubbles may be observed in the downstream part of the main matrix of the bubble dispersion. In the oxygen/water system, very good disengagement can be achieved without any difficulty. In hydrogen/propan-2-ol or hydrogen/toluene systems with cinnamaldehyde no small bubbles were observed in the outlet stream, but in the hydrogen/toluene-water catalyst slurry system small bubbles were entrained in the outlet stream.

6.1.3.4 Bubble Size

A fairly narrow bubble size distribution was observed in the oxygen/water system. In the entrance region of the column very small bubbles of 1-3mm in diameter are observed. Due to coalescence a uniform size of bubbles with a diameter of about 4.5mm was formed in the middle region. Below the bubble dispersion a few very small bubbles with a diameter of less than 0.5mm were observed. In the hydrogen/water system a uniform bubble size of 5mm predominated in the whole column. In the hydrogen/toluene system with cinnamaldehyde slurry operated at ambient temperature and 0.3MPa in the 50mm column a wider bubble size distribution with a diameter of 2-4mm predominated in the whole dispersion section in the column and a clear disengagement was seen at the junction of the expanded section. When palladium/charcoal catalyst was added to the system the bubble size reduced to 1-2mm. It is suggested that the catalyst particles prevented bubble coalescence. In the hydrogen/propan-2-ol system with cinnamaldehyde the bubble

size distribution varied with the dispersion height. When the dispersion height is within the entrance region 0.5-1mm bubbles prevailed, but when the bubble dispersion occupied the whole column bubbles of 1-3mm in diameter were observed throughout the column. The inlet liquid jet velocity was significant in determining bubble size distribution. Higher jet velocities produced higher turbulence resulting in production of smaller bubbles.

6.1.3.5 Gas Holdup

There was a gas holdup distribution in the column. The gas holdup build-up can be described as follows: from the top of the column gas holdup increased gradually with distance until the bubbles coalesced into large bubbles. At the entrance region, owing to the end effect, a relatively low gas holdup was observed. The middle large-bubble section seemed to have higher gas holdup (40~65%). Although a deadleg was used to measure the gas holdup based on the ratio of the gas space height in the deadleg and the dispersion height in the column, the method was of limited use. The ratio of $D_{orifice}$:D_{column} and the ratio of inlet gas and liquid flowrate affected the height of gas space in the deadleg. When the ratio of inlet gas and liquid flowrate was low with a low dispersion height the deadleg gave inaccurate readings, and sometimes even no gas space height was recorded in the deadleg, so that some other methods of measuring gas holdup need to be used especially when the dispersion height was not high enough to overcome the error of the deadleg method. The total shutdown method, which was to close all the inlet and outlet streams simultaneously and then separate gas and liquid, can be used to overcome this limitation.

The gas holdup data under different operation conditions using the oxygen/water system are given in Table 8.6.2.1. It was observed that in the oxygen/water system the gas holdup appeared to be uniform throughout the dispersion although the gas holdup in the entrance region is slightly lower and the gas holdup in the middle section reached its highest value. It was noted that the gas holdup is a function of orifice diameter, liquid flowrate and gas flowrate. Gas holdup increased with an increase in gas flowrate and a decrease in liquid flowrate. Use of a small orifice could produce a higher gas holdup. For the hydrogen/water system the situation is similar to that of the oxygen/water system. However, in the hydrogen/toluene/cinnamaldehyde and hydrogen/propan-2-ol/cinnamaldehyde systems different-sized small bubbles were dispersed evenly throughout the dispersion as a whole with no clear uniform gas holdup variation along the column due to the poor coalescence properties of the liquid. It was found that the value of gas holdup in the hydrogen/propan-2-ol/ cinnamaldehyde/palladium-on-charcoal system was a function of temperature. The higher the temperature the higher was the gas holdup. A similar observation was reported by Quicker and Decker (1981) and Zhang et al. (1988) in gas-liquid upflow bubble columns.

6.1.3.6 Bubble Dispersion and Coalescence

The primary bubble formation mechanism depends on the method of gas introduction and the specific design of the gas distributor. For the CDC a simple T-piece immediately prior to the liquid entry in conjunction with an orifice at the liquid entry was used for distribution of gas into the liquid. The primary bubbles were formed by the shearing action of the liquid stream at the T-piece. The bubbles were then

entrained in the liquid jet passing through the orifice. Previous studies (Lu, 1988) proved that very small bubbles were generated at the liquid jet entering the column regardless of the liquid properties and operating conditions if a sufficiently high liquid velocity was maintained.

Primary bubbles entrained in the incoming liquid jet were observed to be coalescing rapidly into large bubbles in the oxygen/water and hydrogen/water systems. However, in the hydrogen/organic liquid systems there was no significant coalescence, leading to a wide bubble size distribution. As a result of bubble coalescence and re-dispersion, different dispersions were obtained in the column. Likely factors affecting coalescence and re-dispersion of bubbles include: (1) liquid properties, such as surface tension, viscosity, density and surface properties, (2) the relative gas-to-liquid velocity, (3) the liquid jet velocity, and (4) the primary bubble size. The balance between coalescence and re-dispersion determines the bubble size in the column. It was found that the liquid surface property was the most important factor to determine the coalescence properties. Large bubbles (4-5mm) were formed for strongly coalescing liquids such as water, but for liquid solutions such as cinnamaldehyde solution in propan-2-ol or cinnamaldehyde solution in toluene, or aqueous potassium chloride and aqueous sodium chloride different-sized small bubbles were distributed throughout the column. This was because coalescence inhibition varied due to the nature and amount of additive. These findings agree to those of Lu (1988).

In the oxygen/water and hydrogen/water systems bubble size was determined by the intensity of turbulence in the liquid. In the upper section of the column where the liquid jet caused high turbulence, slightly smaller bubbles were obtained. In the lower

section of the column larger bubbles were formed. The uniformity of bubble sizes both in the upper and lower sections indicates that there are two different zones of turbulence with a fairly constant intensity of turbulence in each zone. Tilston (1990) described the upper section as a well stirred-reactor and the lower section as a plug-flow region, which could explain the relationship between bulk bubble size and turbulence.

In the hydrogen/cinnamaldehyde/propan-2-ol or hydrogen/cinnamaldehyde/toluene systems, the wide bubble size distribution was caused by coalescence inhibition. At low gas flowrates coalescence inhibition was relatively important, resulting in the prevalence of small bubbles, but at high gas flowrates both coalescence and its inhibition became important. Although there is a bubble-size distribution along the column, a complete disengagement of bubbles from the liquid phase was achieved at the expanded section.

6.1.3.7 Gas Liquid Interfacial Area

The specific interfacial area can be calculated from the relationship between mean gas holdup, mean bubble size and interfacial area (Equation 3.3). Although the mean gas holdup can be measured exactly, the difficulty of precise measurement of bubble size distribution using a photographic technique would result in errors especially when the dispersion is not high and wide bubble size distribution exists. In addition the bubble size measured in the bulk dispersion cannot be used to represent the mean bubble size in the column due to the relatively large proportion of mass transfer taking place in the top section of the column. A more accurate measurement of the bubble size is

required in order to evaluate the interfacial area. However, for qualitative comparison the mean bulk size was used here to estimate the interfacial area. For the oxygen/water and hydrogen/water systems a bubble size of 4.5mm and up to 65% of gas holdup were observed so that an interfacial area of up to $870m^2.m^{-3}$ can be expected. For the hydrogen/propan-2-ol/cinnamaldehyde and hydrogen/toluene/ cinnamaldehyde systems bubble sizes of 0.5-3mm and up to 30% of gas holdup were observed, so that an interfacial area of $600\text{-}3600m^2.m^{-3}$ is expected.

6.2 Gas Liquid Mass Transfer

6.2.1 Dissolved Oxygen Profiles

In order to understand the flow pattern in the column it is necessary to know its concentration profile. The axial dissolved oxygen (DO) concentration was measured at six positions along the column. At a fixed position the value of DO depended on the orifice diameter, column diameter, liquid flowrate and gas flowrate. The results are given in Table 8.6.2.1.

Typical relationships for DO concentration, distance, gas flowrate and liquid flowrate are given in Figure 6.2.1 and Figure 6.2.2. The results indicated that the dissolved oxygen concentration increased with an increase in the gas flowrate but decreased with the liquid flowrate. For a given column and orifice diameter the liquid column velocity increased with an increase in the liquid flowrate. When a constant flow of oxygen was introduced into a large amount of water a decrease in the dissolved oxygen concentration was expected. Increasing the gas flowrate would increase the bubble packing density so that the dissolved oxygen concentration increased. Within the bubble dispersion region the dissolved oxygen concentration increased with an increase in the axial distance from the top of the column due to the progress of mass transfer from the gas phase to the liquid phase. Initially, the DO concentration increased more quickly than at the later stage because at the top section agitation was more vigorous and the driving force of oxygen concentration was greater than at the bottom section. After the bubble dispersion region the DO concentration become constant, since the difference between the concentration at equilibrium and that in the bulk was very small

Figure 6.2.1 Dissolved Oxygen vs Distance

$d_{orifice}$ = 12mm; d_c = 100mm; F_L = 1230cm^3.min^{-1}

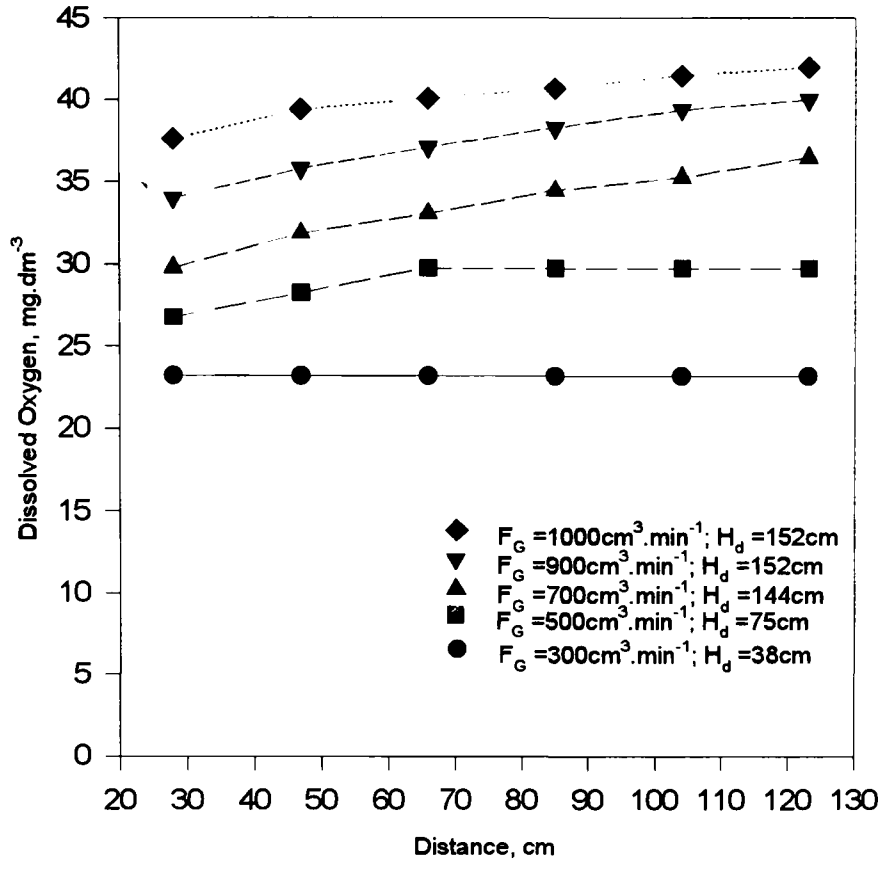

Figure 6.2.2 Dissolved Oxygen vs Distance

$d_{orifice}$ = 18mm; D_c = 100mm; F_G = 1000cm^3.min^{-1}

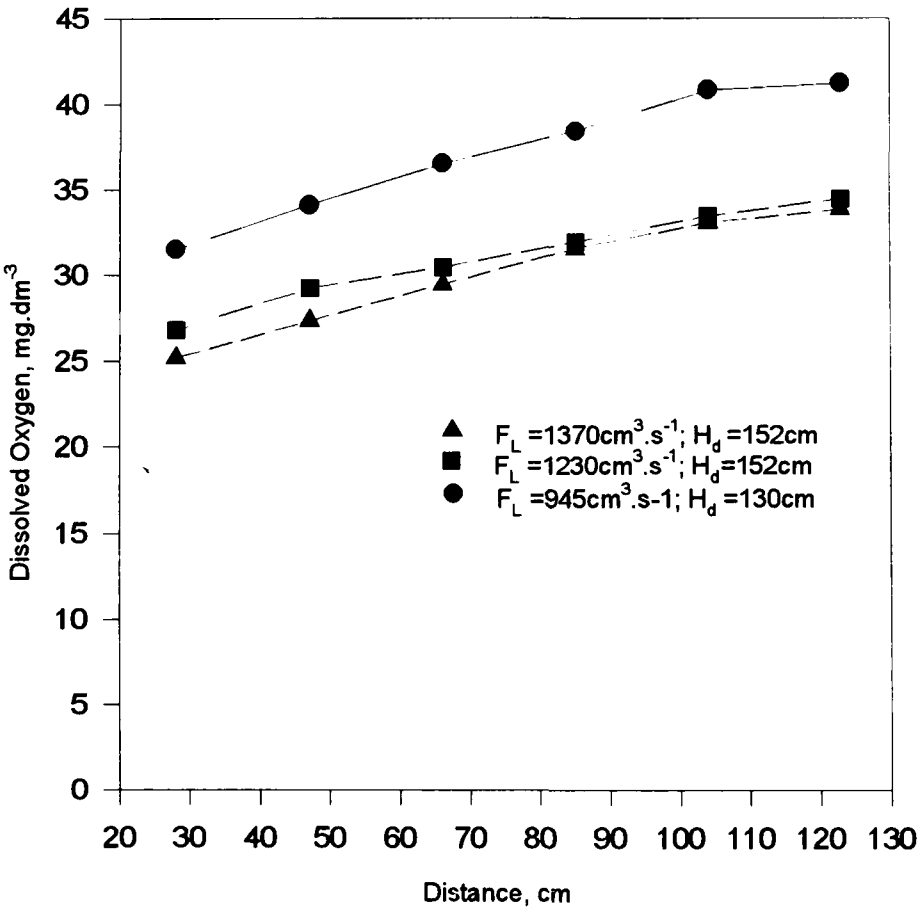

further mass transfer from the gas phase to the liquid phase was negligible. These results were expected, for when oxygen is passed into water it is dissolved until the equilibrium concentration is reached.

The inlet liquid velocity was increased by reducing the orifice diameter with fixed liquid and gas flowrates, since the same amounts of water and oxygen were introduced and in a steady state all the oxygen was dissolved into water. However, with a higher inlet liquid velocity a stèady state can be achieved rapidly with greater agitation, so that at the same position in the column under constant gas and liquid flowrates a higher dissolved oxygen concentration can be obtained.

6.2.3 k_La Measurements by Oxygen/Water Absorption

The assessment of the volumetric gas-liquid mass transfer coefficient (k_La) required knowledge of the liquid flow pattern in the column. Since that was unclear, k_La was evaluated by the two ideal flow patterns: the plug flow model and the complete mixing model (see Appendix 8.4). Based on these relationships and supposing the whole dispersion section to be plug flow or complete mixing, the results were calculated and typical results are shown in Figure 6.2.3.

The column liquid velocity had negative effects. When column liquid velocity was increased, it is possible that the liquid mass transfer coefficient (k_L) value increased as a result of a higher slip velocity between the gas phase and the liquid phase leading to thinner boundary layer. The interfacial area value decreased because the column liquid velocity inhibited the upward movement of bubbles, therefore reducing the bubble packing density. The fact that k_La in these experiments decreased with an increase in

the column liquid velocity suggests that interfacial area values had more effect under these conditions.

Figure 6.2.3 Volumetric Mass Transfer Coeffient vs Gas Flowrate

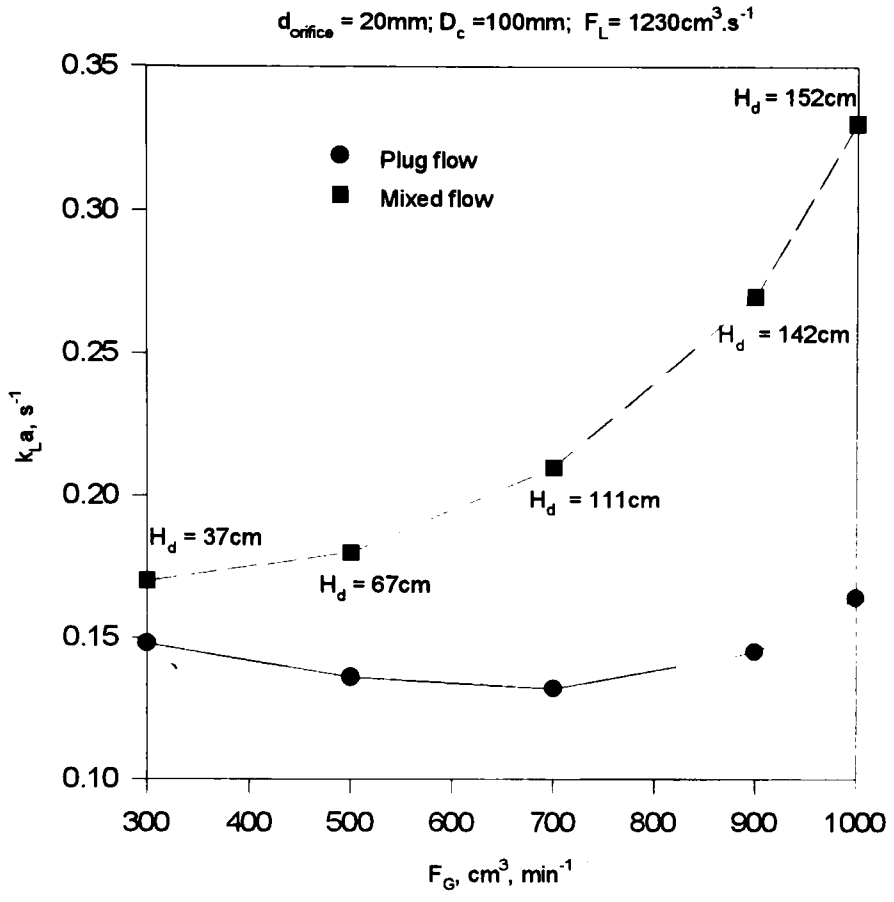

Increase of the gas flowrate led to an increase in the bubble dispersion height and this resulted in the variation of both k_L and the interfacial area value. In the top section there was more intensive agitation and k_L values were nearly constant. Increasing the gas flowrate led to an increase in the bubble packing density, increasing the interfacial area value and consequently the k_La value. The liquid in the second section was less agitated and the k_L value was lower, but the gas holdup was higher and consequently the interfacial area was higher. These two effects caused the variation of the k_La values. Most results showed a tendency to increase k_La with increase in gas flowrate.

Generally speaking the mixed flow model gave higher k_La values than the plug flow model did but both showed similar behaviour. Actual values of k_La are between those calculated by the plug flow model and complete mixing model. The real flow pattern may be described by complete mixing plus plug flow but this will be tested by residence time distribution experiments and the ratio of these two parts depends on the operating conditions of the CDC and the physical properties of the gas phase and the liquid phase.

6.3 Residence Time Distribution

6.3.1 Introduction

It is necessary to know the effect of the mixing characteristics on the conversion of the reactions and the product distribution in a bubble column reactor (Kato and Nishiwaki, 1972). The mixing characteristics within a bubble column may be determined from the residence time distribution (RTD). A bubble column is characterized by backmixing and dispersion in the individual phases. Backmixing in the gas or liquid phase in a bubble column may have significant effects on the reaction rates or product selectivity (Shah et al, 1978). Therefore it is important to study the mixing characteristics in the CDC.

6.3.2 Residence Time Distribution

In order to investigate the flow pattern in the column a pulsation method was used. 100ml of 70kg.m^{-3} aqueous sodium chloride solution were injected into the top of the column and the salt concentration was determined by a conductivity probe. The liquid in the top section of the column seemed to behave as mixed flow (C.S.T.R.), and that in the bottom section behaved as plug flow (P.F.R). The observed height of the C.S.T.R. section was from 25cm to 40cm. After the bubbles were dispersed fully in the column further increase in the gas flowrate increased the bubble packing density, and increasing agitation caused the development of mixed flow. Preliminary experiments showed that the flow pattern in the CDC depended on the operating conditions such as dispersion height, gas flowrate, liquid flowrate and orifice diameter, and on the liquid viscosity, coalescence and surface tension but the results are not consistent because the

length of injection time was too long leading to big errors. Further experimental investigation is required by the improved tracer injection method for the better understanding of the flow pattern in the CDC. However, this work was paused due to the change of the research emphasis into the selective hydrogenation of cinnamaldehyde.

6.4 Catalyst Preparation and Characterization

6.4.1 Introduction

Heterogeneous catalysis deals with the transformation of molecules at the interface between a solid catalyst and the gaseous or liquid phase carrying these molecules. Before using a catalyst it has to be characterized. Catalyst characterization provides information on the chemical composition, structure, mechanical properties, texture and catalyst activity. The chemical composition deals with the elemental content, proportion, structure and composition of various phases. The texture of a catalyst provides information on the particle size, shape, morphology, surface topography and mechanical properties. Catalyst characterization takes place before, during and after the catalytic reaction.

In this project palladium, platinum and ruthenium catalysts were prepared in-house from metal salts by impregnation methods in order to compare these catalysts with commercial catalysts. In addition in-house-prepared and commercial palladium and platinum catalysts were modified by the incorporation of additives in order to improve the selectivity to desired products. Before using the in-house-prepared and modified catalysts temperature-programmed reduction was used to characterize them, and their surface areas were measured by gas adsorption.

6.4.2 Surface Area Measurements

The surface area of a catalyst has a direct effect on its catalytic abilities and on the amount of reactant absorbed. Gas adsorption is the most widely used technique for the measurement of the surface areas of catalysts. There are two methods for the

measurement of surface area, non-selective adsorption involved in measuring total surface area, and selective adsorption (chemisorption) used mainly in the measurement of the specific surface area of the catalyst. The chemisorption of active gases such as hydrogen, carbon monoxide and oxygen is a widely used method to determine the metal surface area (Anderson, 1975). Chemisorption method requires the measurement of gas uptake under conditions where it is reliably and reproducibly defined and where the chemisorption stoichiometry is also well defined. The stoichiometry of hydrogen in monolayer chemisorption corresponds to one adsorbed hydrogen atom per surface metal atom.

The total surface area measurement is usually determined by the adsorption of inert molecules such as the rare gases and nitrogen (Young and Crowell, 1962; Gregg and Sing, 1967). The catalyst for which surface area is to be measured is placed inside a silica tube and the adsorbate gas is passed through it while the tube is placed in a liquid nitrogen bath at a temperature of 77.4K. The gas is adsorbed as a monolayer. For monolayer adsorption and knowing the surface area of a single molecule of the adsorbate gas the total surface area of the catalyst can be calculated from the amount of gas adsorbed by using the method of Brunauer-Emmett-Tayler (BET) (see Appendix 8.5**).** Some results are given in Table 6.4.1.

Table 6.4.1 BET Measured Total Surface Area

Catalyst	Specific Surface Area ($m^2.g^{-1}$)	Catalyst	Specific Surface Area ($m^2.g^{-1}$)
0.5%Pt/TiO_2	40.4	0.5%Pd/TiO_2	26.2
5% Ru/Al_2O_3	100	Al_2O_3	132
TiO_2 (Degussa P25)	63.9	TiO_2 (Fisons)	4.2

6.4.3 Temperature-Programmed Reduction and Desorption

Reduction is an activation step for metal catalyst preparation, and when the dispersion of metallic catalysts is investigated it is an essential pretreatment for chemisorption measurements. Temperature-programmed desorption is used to obtain information on the surface characteristics of porous catalysts, such as surface area, desorption activation energy and desorption mechanism (Cvetanovic and Amenomiya, 1972; Falconer and Schwarz, 1983). Temperature-programmed reduction is used to study the effect of supports (Jacobs et al, 1977), the effect of pretreatment procedure (Issacs and Petersen, 1982; Wagstaff and Prins, 1979) and the effect of promoters on the reducibility of the catalyst surface.

Temperature-programmed reduction was used to determine the most efficient reduction temperature and to perform the pre-reduction routine while temperature-programmed desorption was used to measure the metal surface area. Some reduction temperatures are summarized in Table 6.4.2.

It can be seen that the reduction temperature is related to the precursor and the support used. It is known that unsupported palladium precursors generally have a low reduction temperatures, around room temperature. Charcoal-supported, titania-supported and alumina-supported palladium catalysts had low reduction temperatures. However, silica-supported palladium catalysts had a higher reduction temperatures about 408K. For palladium/titania catalysts, two peaks may be expected since titania is a reducible support. There should be one peak for the reduction of palladium oxide to palladium metal and another for reduction of titania to titanium suboxide (TiO_x, $x < 2$) (Tauster, 1987), but the reduction of titania is likely to occur only if the catalyst is reduced at high temperature. For ruthenium and platinum catalysts a high reduction temperature (above 463K) is expected. When cobalt and platinum were combined to

make a bimetallic catalyst the reduction temperature increased with increase of cobalt content as shown in Table 6.4.2.

Table 6.4.2 Catalyst Reduction Temperature in TPR

Catalyst	Support	T_{max}, K	R_{heat}, K /min
Pd*	Charcoal	293	16
Pd*	Al_2O_3	295	8
Pd*	SiO_2	408	16
Pd*	TiO_2	293	16
Ru**	Charcoal	543	16
Ru**	Graphite	463	16
Ru**	TiO_2	472	16
Ru**	SiO_2	493	16
Ru**	Al_2O_3	476	16
Pt***	Graphite	503	16
Pt***	TiO_2	523	16
Pt***	SiO_2	538	16
95%Pt-5%Co#	Graphite	503	16
90%Pt-10%Co#	Graphite	510	16
80%Pt-20%Co#	Graphite	546	16

* from sodium tetrachloropalladate (II), $Na_2PdCl_4.3H_2O$ (Johnson Matthey)

** from ruthenium (III) chloride, $RuCl_3.3H_2O$, (Johnson Matthey)

*** from sodium hexachloroplatinate (IV), $Na_2PtCl_6.6H_2O$ (Johnson Matthey)

\# from cobalt (II) nitrate, $Co(NO_3)_2.6H_2O$ (Fisons)

Commercial ruthenium catalysts and in-house-prepared ruthenium, platinum, platinum-cobalt catalysts were tested for the hydrogenation of cinnamaldehyde and it was found that these catalysts were not as selective as the commercial platinum/graphite catalyst so that commercial platinum/graphite catalysts were mainly used for studying the hydrogenation of cinnamaldehyde to produce cinnamyl alcohol. Both in-house prepared and commercial palladium catalysts were used to investigate cinnamaldehyde hydrogenation for the production of hydrocinnamaldehyde.

6.5 Hydrogenation over Palladium Catalysts in Stirred Tank Reactors

6.5.1 Introduction

In order to exploit the industrial potential of the CDC, a suitable reaction is needed with the following requirements:

(1) The reaction should involve one reactant in the gas phase and another reactant in the liquid phase, catalysed by a solid catalyst suspended in the liquid.

(2) The products should be highly profitable and the reaction should be commercially important.

(3) The intrinsic kinetics of the reaction should be clearly described.

The hydrogenation of cinnamaldehyde fits these conditions and was chosen for this purpose. The selective hydrogenation of α,β-unsaturated aldehydes is an important step in the preparation of certain fine chemicals and pharmaceuticals due to their wide uses. It is a challenging problem to reduce only the carbonyl group, or the carbon-carbon double bond, in the conjugated system, since almost all metal catalysts readily reduce the carbon-carbon double bond to yield a saturated aldehyde as the main product with low or intermediate selectivity. Some additives can change the properties of transition metal catalysts so that they yield either saturated aldehydes or unsaturated alcohols as the main products when reducing α,β-unsaturated aldehydes. The objective of this study is to seek the optimal combination of catalysts and reaction conditions for the clean synthesis of the desired products, cinnamyl alcohol or hydrocinnamaldehyde from cinnamaldehyde, and to provide the basic information for economic industrial production.

In-house prepared and commercial palladium, ruthenium or platinum catalysts with a variety of supports such as graphite, charcoal, silica, titania, and alumina were used to study the selectivity in both polar solvents (methanol, ethanol, propan-1-ol, propan-2-ol, butan-1-ol, butan-2-ol) and non-polar solvents (toluene, heptane, decalin, decane, cyclohexane) in gas/liquid slurry systems and in gas/liquid/liquid slurry systems. Various metal promoters and organic poisons were used to modify the catalysts. Temperature ranged from 273K to 373K and pressure from 0.1MPa to 1.1MPa. In this section the results obtained in the stirred batch reactors (SBR) are discussed in order to study the kinetic, mass transfer and selectivity conditions.

6.5.2 General Observations

The hydrogenation of cinnamaldehyde over commercial palladium/charcoal catalysts and in-house prepared palladium catalysts was carried out in stirred tank reactors. The palladium metal was deposited on the exterior surface of the support, so that pore diffusion was considered not to be important under the experimental conditions.

(1) The rate observations indicated that no distinct step changes occurred during the course of the hydrogenation of cinnamaldehyde. Although at atmospheric pressure (in a Pyrex glass stirred reactor) the hydrogen take-up rate decreased slightly with time, the hydrogen take-up increased nearly linearly with time except when the reaction approached completion. A typical plot of hydrogen consumption against time during the course of hydrogenation is shown in Figure 6.5.1. The effect of initial cinnamaldehyde concentration on the hydrogen take-up rate indicated that the

hydrogen take-up rate is independent of cinnamaldehyde concentration, so the initial hydrogen take-up rate, based on hydrogen consumption as observed by the recorder of a hydrogenation control unit, was used for the kinetic analysis.

(2) The sample analysis indicated that all the products were present even in the initial samples, indicating that all the products were produced simultaneously, so that the reaction mechanism would be quite complex. In addition, more than one mole of hydrogen is required for complete conversion of one mole of cinnamaldehyde, so the overall conversion of cinnamaldehyde was used to define the extent of the hydrogenation.

Figure 6.5.1 A Typical Plot of Hydrogen Uptake vs Time

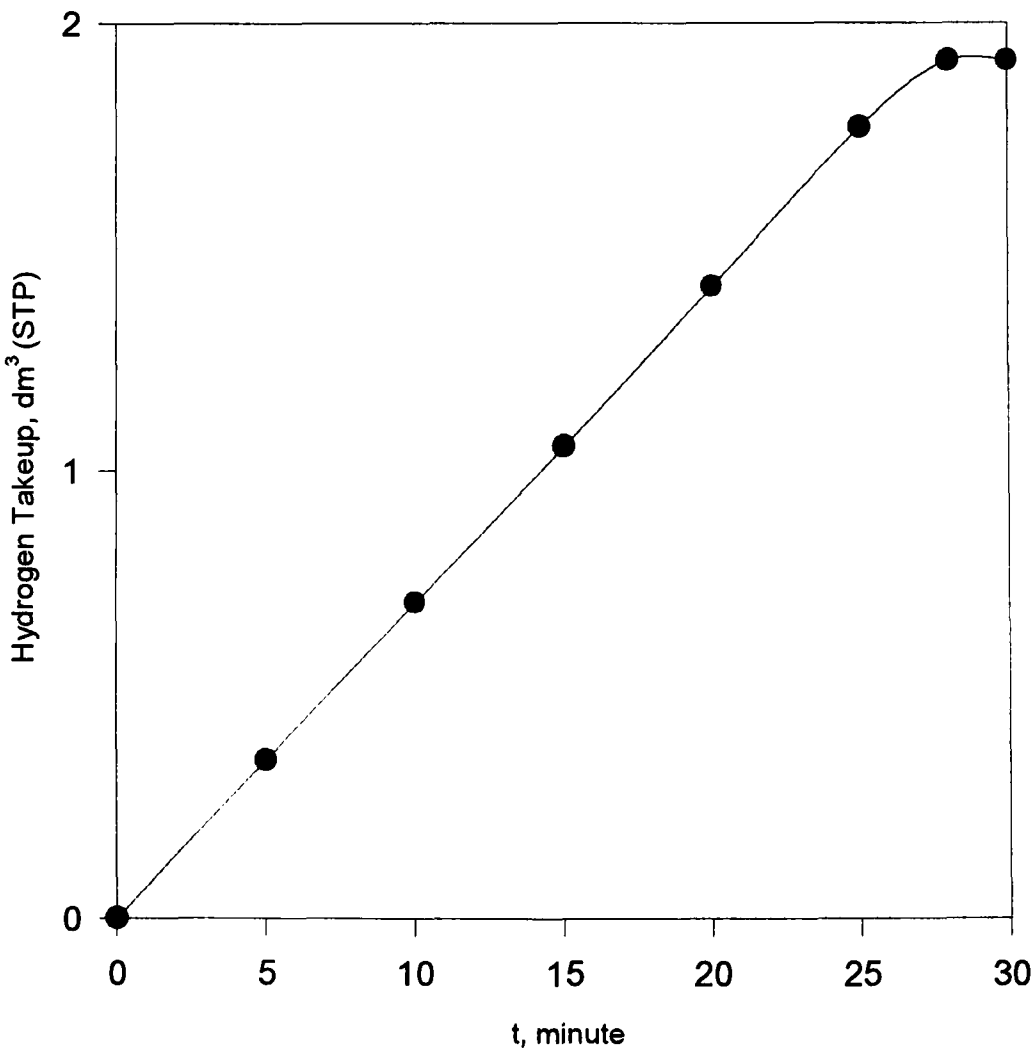

(3) Preliminary studies indicated that when alcohol solvents were used, hemiacetals and diacetals of aldehydes with alcohols were produced and the concentrations of acetals and aldehydes are in equilibrium. When pre-prepared reactant solutions in propan-2-ol were used some homogeneous reactions occurred leading to the formation of products with long-retention-times, presumably with higher molar masses, but when fresh solutions were used, especially in non-polar solvents, no homogeneous reactions were observed. Consequently, it was deduced that under these conditions the contribution of homogeneous reaction to the product spectrum was negligible and the reactions occurred only in the presence of the catalysts used in this work.

6.5.3 Sample Analysis and Reaction Schemes

(1) Product Identification

During the course of the hydrogenation of cinnamaldehyde samples were collected regularly and the catalyst particles were separated by filtration. When organic solvents were used, the catalyst-free samples were analysed using gas chromatography without further sample treatment (Section 5.11). When water or water/organic solvents were used the organic components in the solvents were extracted by toluene from the catalyst-free samples and the toluene-extracted samples were analysed by gas chromatography. Alternatively, the organic phase can be analysed using gas chromatography and the aqueous phase by high performance liquid chromatography. It is found that if the catalyst-free samples were extracted by

toluene at least 24 hours were needed to ensure the complete extraction of the organic components from the aqueous phase. It was advantageous to store the catalyst-free samples in a refrigerator below ambient temperature to prevent reactions between the compounds and the solvent. In order to establish a standard and reliable set of retention times for the reactants and the expected products, when analysed by gas chromatography, a solution was prepared in toluene of equimolar amounts of propyl benzene, β-methylstyrene, hydrocinnamaldehyde, 3-phenyl propanol, cinnamaldehyde and cinnamyl alcohol. The solution was analysed by gas chromatography to obtain the relative concentration of each component. Hydrocinnamaldehyde was chosen as the reference product due to its presence in most samples and the corresponding relative correction factor was assigned as one. The correction factor was calculated based on the GC peak areas of the equimolar standard solution by the following definition:

$$f_i = \frac{A_{i(S)}}{A_{HC(S)}} \qquad (6.5.1)$$

where f_i = the correction factor of component i

$A_{i(S)}$ = the area of component i peak.

$A_{HC(S)}$ = the area of hydrocinnamaldehyde peak

For unknown components (especially when using pre-prepared solutions in propan-2-ol) in the GC the value of one was used as the correction factor when using the DB-1 capillary column (supplied by J & M Scientific) in the gas chromatograph of AI from Analytical Instrument Limited, Cambridge, UK. When a packed column of 10%

SP-210 on 80/100 BS-mesh Supelcoport (supplied by Supelco Inc., USA) was used in the gas chromatography of Pye 304 from Philips, a previously-analysed sample was used to obtain the corresponding correction factor for the unknown components (although cinnamaldehyde diacetal, hydrocinnamaldehyde hemiacetal and hydrocinnamaldehyde diacetal were identified by nuclear magnetic resonance (NMR) spectroscopy and gas chromatography/mass spectrometry (GC/MS) the value of one for the AI and the corresponding calculated values for the Pye 304 were still used due to unavailability of their respective standards. Table 6.5.1 summarizes the correction factors and a gas chromatogram of the standard solution is presented in Figure 8.7.5.1. The peak areas of the experimental samples were modified by the correction factors to yield the product distribution in mole percentage.

Table 6.5.1 The Relative Correction Factors for GC Analysis*

GC Model	AI		304	
Components	Retention Time, min.	Correction Factor	Retention Time, min.	Correction Factor
Propyl benzene	4.76	1	5.38	1.3189
β-Methyl styrene	5.19	1	5.83	1.5469
Hydrocinnamaldehyde	6.38	1	7.58	1
3-Phenyl propanol	7.19	1.0297	8.47	1.1556
Cinnamaldehyde	7.95	1.0316	9.06	1.1526
Cinnamyl alcohol	8.38	1.0188	9.53	1.1163
Cinnamaldehyde diacetal	*	1	*	1
Hydrocinnamaldehyde hemiacetal	*	1	*	0.8731
Hydrocinnamaldehyde diacetal	*	1	*	0.8141

* varied with the solvent used

(2) Determination of Selectivity

The area of each component peak from the GC results was divided by its corresponding relative correction factor to convert to the corrected area A_i. The mole fraction X_i of each individual component was determined by the following definition:

$$X_i\% = \frac{A_i}{\Sigma A_j} \times 100 \qquad (6.5.2)$$

and the corresponding selectivity S_i can be calculated by the definition:

$$S_i\% = \frac{X_i}{100 - X_{CAL}} \times 100 \qquad (6.5.3)$$

The conversion of cinnamaldehyde was determined by the following relationship:

$$X_{conv}\% = 100 - X_{CAL} \qquad (6.5.4)$$

(3) Reaction Schemes

When palladium catalysts were used the desired product was hydrocinnamaldehyde whereas when platinum or ruthenium catalysts were used the desired product was cinnamyl alcohol. When palladium catalysts were used, the sample analysis revealed that besides the desired product, the formation of 3-phenyl propanol in a significant quantity and the existence of propyl benzene indicated a sequential reaction without preferential formation of the desired product. Hydrocinnamaldehyde and cinnamyl

alcohol are respectively formed through two parallel reactions whose rates depend on the solvent and promoter used.

The hydrogenation reaction of cinnamaldehyde may be described as a parallel-consecutive network in which one or both of the unsaturated functional groups can be reduced. Under the experimental conditions, the reaction scheme can vary and depends strongly on the polarities of the solvents used. For non-polar solvents (e.g. toluene and heptane), the main products (Scheme 1) are hydrocinnamaldehyde ($C_6H_5CH_2CH_2CHO$), phenyl propanol ($C_6H_5CH_2CH_2CH_2OH$), propyl benzene ($C_6H_5CH_2CH_2CH_3$), and a trace of β-methyl styrene ($C_6H_5CH{:}CHCH_3$) was detected. 3-Phenyl propanol is formed by consecutive hydrogenation of both hydrocinnamaldehyde and cinnamyl alcohol. 3-Phenyl propanol is stable and is not further transformed under the reaction conditions. β-methyl styrene is formed through consecutive reactions from cinnamyl alcohol. In contrast to the reaction scheme reported by Rylander and Himelstein (1963), it is noted that in this research hydrocinnamaldehyde is readily transformed to 3-phenyl propanol. Although cinnamyl alcohol was not detected while using palladium catalysts, the existence of β-methyl styrene and propyl benzene indicated that cinnamyl alcohol was produced but was further hydrogenated because it is very difficult under the reaction conditions to convert 3-phenyl propanol to propyl benzene. However, when polar solvents are used, the situation is different (Scheme-2). Besides the products produced in non-polar solvents, cinnamaldehyde diacetal and hydrocinnamaldehyde diacetal were formed in alcohol solvents.

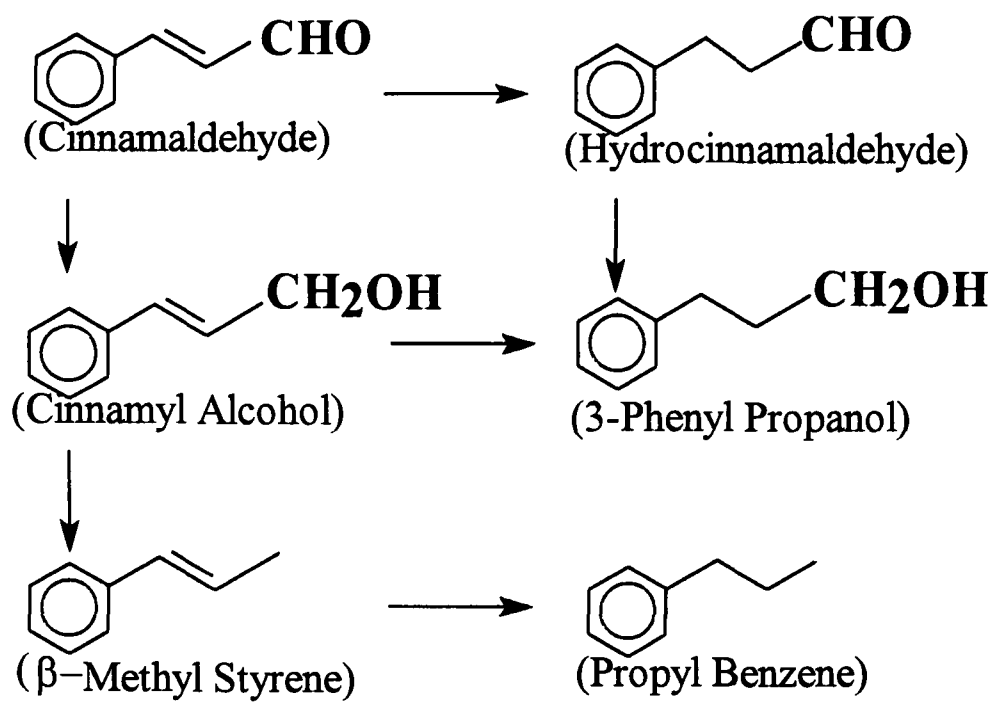

Scheme 1 Product Link in Non-polar Solvents

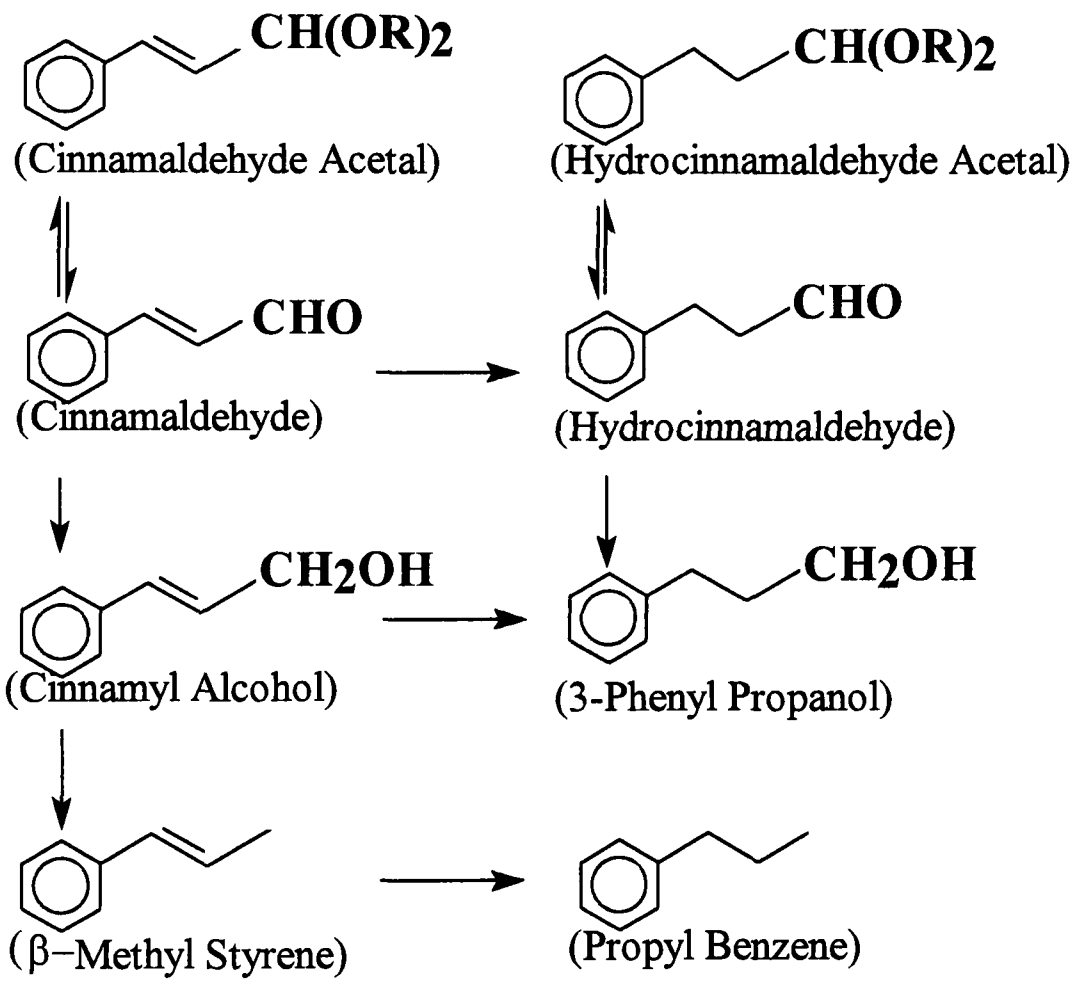

Scheme 2 Product Link in Polar Solvents

The formation of cinnamaldehyde diacetal, hydrocinnamaldehyde hemiacetal and hydrocinnamaldehyde diacetal was confirmed by gas chromatography (GC), nuclear magnetic resonance (NMR) and gas chromatography/mass spectrometry (GC/MS). The nuclear magnetic resonance spectra of the initial and final samples from the hydrogenation of cinnamaldehyde in ethanol at 303K and atmospheric pressure with a catalyst loading of 4kg.m^{-3} and an initial cinnamaldehyde concentration of 50 kg.m^{-3} are presented in Figure 8.7.5.2 and Figure 8.7.5.3 for the determination of diacetal. The former confirmed the formation of cinnamaldehyde diethylacetal and the latter confirmed the production of hydrocinnamaldehyde diethylacetal. The gas chromatography/mass spectrometry of the initial and final samples from the hydrogenation of cinnamaldehyde in propan-1-ol at 303K and atmospheric pressure with a catalyst loading of 4kg.m^{-3} and an initial cinnamaldehyde concentration of 50kg.m^{-3} revealed that in the initial sample cinnamaldehyde hemiisopropylacetal and cinnamaldehyde diisopropylacetal were produced and in the final sample propylbenzene, hydrocinnamaldehyde, 3-phenyl propanol, hydrocinnamaldehyde hemiisopropylacetal and hydrocinnamaldehyde diisopropylacetal existed. The mass spectra of cinnamaldehyde diisopropylacetal, hydrocinnamaldehyde hemiisopropylacetal, and hydrocinnamaldehyde diisopropylacetal are given in Figure 8.7.5.4, Figure 8.7.5.5 and Figure 8.7.5.6, respectively.

6.5.4 Selectivity Investigations

6.5.4.1. Homogeneous Reactions

Preliminary runs were carried out using a pre-prepared reactant solution in propan-2-ol to study the reaction kinetics. GC analysis showed that propyl benzene was formed at a higher selectivity by using the pre-prepared reactant solutions, and the range of by-products was greater than with fresh reactant solutions. Table 6.5.2 presents some results obtained by using a fresh solution and using pre-prepared solutions to compare the effect of homogeneous reactions. When using the pre-prepared solutions stored for 50 days an unknown long-chain product was detected and its concentration ranged from 2% to 8% depending on the temperature and the catalyst loading. The longer the reactant solution was stored in the laboratory at ambient temperatures (well-sealed) the greater was the concentration of by-products. This suggests that cinnamaldehyde reacts easily with the polar solvents before hydrogenation, but with a fresh solution only cinnamaldehyde diacetal was produced and it is suggested that impurities in cinnamaldehyde and the solvent accelerated the formation of by-products. This was further supported by analysis of a pre-prepared cinnamaldehyde solution with different storage times in propan-2-ol. It was found that for 50 days of storage 7% of cinnamaldehyde was converted into its acetals, and for 80 days storage 8% of cinnamaldehyde was converted into its acetals (see Table 6.5.3). This suggests that some kind of equilibrium is established. It appears that several homogeneous reactions of cinnamaldehyde can occur, especially in polar solvents, in addition to or as a result of acetal formation. This situation became more pronounced the longer a

solution remained standing, so it is advisable to prepare fresh solutions for all reactions.

Table 6.5.2 Effect of Homogeneous Reactions

T=283 K; P=0.1MPa; $W_{cat.}$= 4 kg.m^{-3}; W_{CAL} = 50 kg.m^{-3}; N_{stir} = 1200 rpm

Selectivity	S_{PB}, %	S_{HC}, %	S_{PP}, %	S_{other}, %
Pre-prepared	10.6	8.4	42.5	38.6
Fresh Solution	14.6	31.9	43.1	10.4

Table 6.5.3 Analysis of a Pre-prepared Cinnamaldehyde Solution in Propan-2-ol

(in a sealed vessel at ambient temperature)

t_s, day	X_{conv}, %	X_{HC}, %	X_{PP}, %	X_{PB}, %	X_{CAL}, %	X_{MS},%	$X_{acetals.}$, %
0	0	0	0	0	100	0	0
50	7.1	0	0	0	92.9	0	7.1
80	8.5	0	0	0	91.5	0	8.5

To investigate the extent of the effect of homogenous reactions, blank experiments were carried out using propan-2-ol, butan-1-ol and toluene. The results of the blank experiments are given in Table 8.6.5.1 and Figure 6.5.2. When blank experiments were carried out only cinnamaldehyde and a solvent (propan-1-ol, butan-1-ol, or toluene) were added to the reactor. After purging the reactor with hydrogen the solution was stirred for three hours at 303K and 0.1MPa with hydrogen flow through the reactor but without catalyst inside the reactor. It was found that when either propan-2-ol or butan-1-ol was used as the solvent only cinnamaldehyde hemiacetal and cinnamaldehyde diacetals were produced, but when toluene was used as the solvent no conversion of cinnamaldehyde occurred. Although further investigation of

this phenomenon is needed especially to identify the long-retention-time product, after analysis of the products, it was concluded that the problems arose from use of pre-prepared solutions and the emphasis was focused on using fresh solutions in each run in order to promote the research objective of clean synthesis.

It can be seen that when using a fresh solution the effect of homogeneous reactions is not important although the impurities played an important role in the hydrogenation of cinnamaldehyde when using pre-prepared solutions in propan-2-ol. It seems, and it is recommended, that fresh reactant cinnamaldehyde solution should be prepared in situ.

Figure 6.5.2 Conversion vs Time in Blank Experiments

T=303K; P=0.1MPa; W_{CAL}=50kg.m^{-3}; N_{stir}=1200rpm; No Catalyst Present

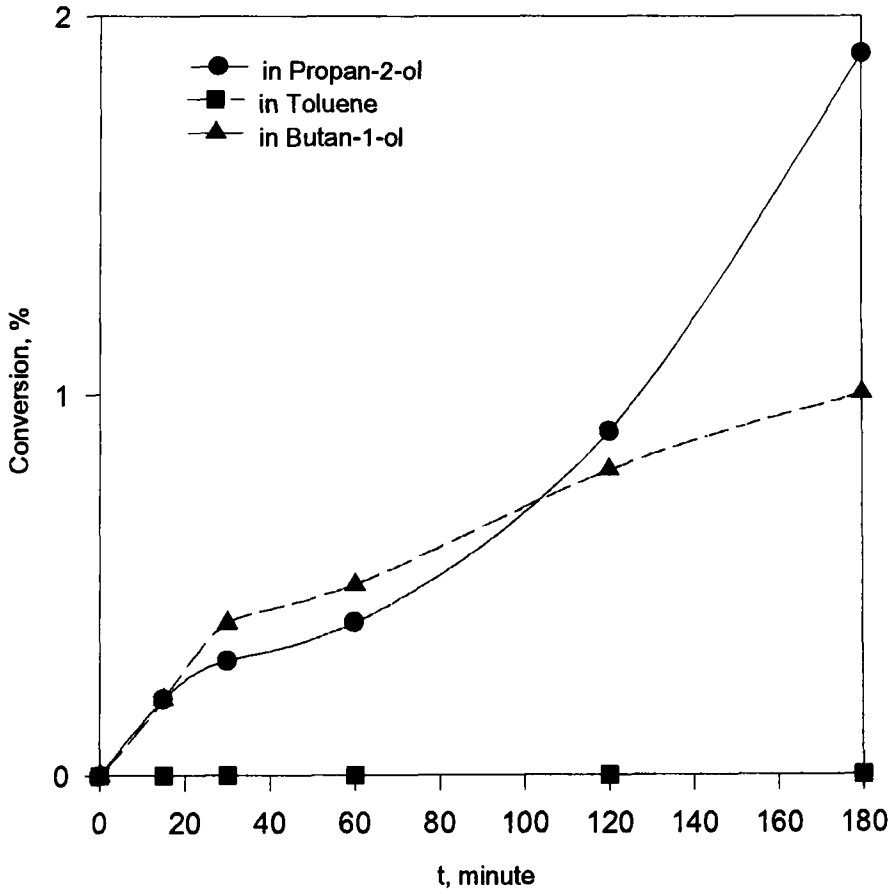

6.5.4.2 Effect of Solvents

As stated in Section 6.5.3 the product distribution and selectivity varied with the conversion of cinnamaldehyde and were affected significantly by the solvents used. In order to select a suitable solvent the solvent effect was compared only from the selectivity data at the end products. When non-polar solvents were used the main products were hydrocinnamaldehyde, 3-phenyl propanol, propyl benzene and a trace of β-methylstyrene. When polar solvents (alcohol solvents) were used cinnamaldehyde diacetal, hydrocinnamaldehyde hemiacetal and hydrocinnamaldehyde diacetal were formed. Table 6.5.4 summarizes some typical results of selectivity data in various solvents. Although comparing the data at different cinnamaldehyde conversion would give more information, the results presented here are mainly obtained at 100% conversion from the view of

Table 6.5.4 Selectivity Data (in fresh solution)

T = 303K; P_{H2} = 0.1MPa; W_{CAL} = 50kg.m^{-3}; $W_{cat.}$ = 4kg.m^{-3}

Solvent	$X_{Conv.}$, %	S_{PB}, %	S_{HC}, %	S_{PP}, %
Methanol	100	4.8	**64.6* (93.6)**	20.9
Ethanol	100	10.8	**46.3*(76.2)**	28.7
Propan-1-ol	100	11.8	**43.5(61.8)**	36.5
Propan-2-ol	100	3.4	**44.4*(27.4)**	49.4
Butan-1-ol	100	7.2	**43.5*(57.0)**	45.0
Butan-2-ol	47	1.0	**38.5*(47.9)**	59.0
Toluene	100	4.4	**36.3**	56.0
Heptane	100	28.6	**18.1**	53.3
Methylcyclohexane	43	9.8	**41.1**	49.1
Decalin	100	14.7	**33.6**	51.7
Decane	100	13.2	**42.9**	44.0
Ether	14	33.4	**22.7**	26.1

*** = HC + HC Diacetal; ( ) = HC Diacetal percent of ***

cinnamaldehyde utilization. The typical product distribution and selectivity profiles in various solvents are presented in Figure 8.7.5.7-Figure 8.7.5.16.

The mechanism for the formation of acetals is proposed as follows:

A molecule of aldehyde adds to a molecule of alcohol to form a moderately stable addition product (hemiacetal) which combines with a second molecule of the alcohol to yield a stable derivative (diacetal). Acetal formation is reversible and the tendency of acetal formation is respectively as follows:

The extent of equilibrium toward acetal formation for various alcohols lies in the order primary > secondary > tertiary, although the reaction rate in forming acetals is in the order tertiary > secondary > primary in the presence of hydrogen chloride (Turner and Harris, 1952; Whitmore, 1952).

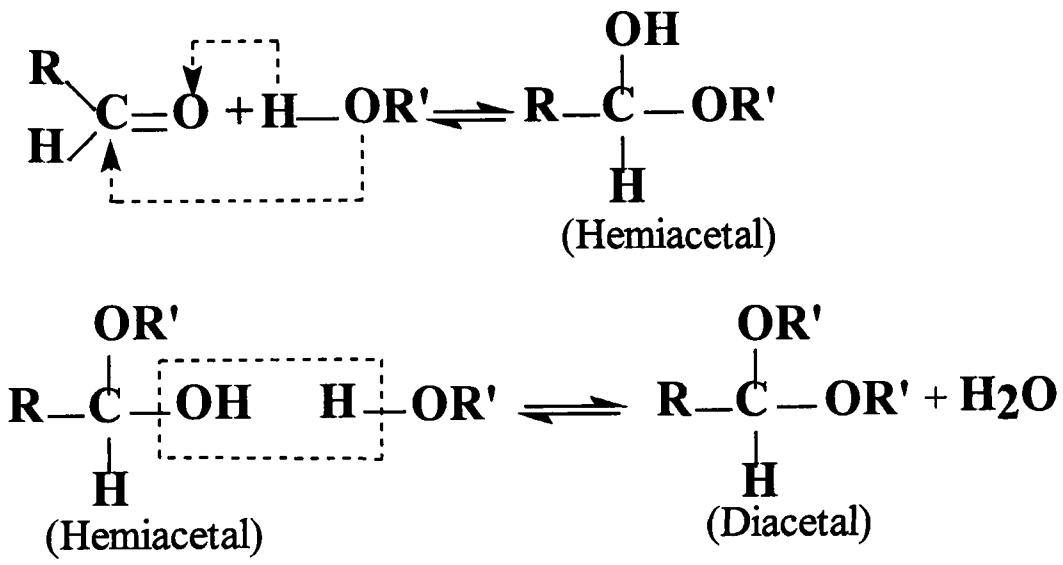

The Mechanism of Formation of Acetals

The formation of hydrocinnamaldehyde diacetal agrees with previous results (Galvagno et al, 1989, 1991, 1993; Coq et al, 1993). The formation of hydrocinnamaldehyde diacetal occurs readily through the reaction between

hydrocinnamaldehyde and the alcohol solvent. As the diacetal is in equilibrium with hydrocinnamaldehyde they are kinetically indistinguishable for the hydrogenation reactions. For simplicity, diacetal was reported together with hydrocinnamaldehyde. Acetals are considerably more stable to bases than to acids, and they are much more stable than free aldehydes to basic reagents and oxidizing agents. It is worth noting that the hydrocinnamaldehyde diacetal can be decomposed under acid conditions to hydrocinnamaldehyde (Fieser and Fieser, 1956). It was surprising that cinnamaldehyde diacetal concentration was large even in the initial sample prior to the hydrogenation in primary alcohol solvents. It is suggested that cinnamaldehyde diacetal was produced due to the high activity of the hydroxyl group in the primary alcohol solvents whereas the activity of the hydroxyl group in the secondary alcohol solvents was relatively low. For comparison the effect of the hydroxyl position in alcohols, such as propan-1-ol (1°) and propan-2-ol (2°), and butan-1-ol (1°) and butan-2-ol (2°) were examined. Cinnamaldehyde diacetal was found in propan-1-ol and butan-1-ol (1^{0}) but not in propan-2-ol (2°) and butan-2-ol (2°). These results were different from those of others (Blackmond et al, 1991; Galvagno et al, 1989 & 1993), who stated that cinnamaldehyde diacetal was not detected. GC analysis shows that cinnamaldehyde diacetal composition decreased with time to zero. It is suggested that before the hydrogenation, cinnamaldehyde diacetal was formed due to the activity of cinnamaldehyde and the alcohol solvents, and that it was in equilibrium with cinnamaldehyde. For the same reason cinnamaldehyde diacetal is reported together with cinnamaldehyde in this work.

The percentages of hydrocinnamaldehyde diacetal were strongly dependent on the polarity of the solvents used. The more polar the solvent the more diacetal could be produced. The order of solvent polarity is as follows:

Methanol > Ethanol > Propan-1-ol > Propan-2-ol > Butan-1-ol > Butan-2-ol

Although a high yield of hydrocinnamaldehyde could be produced in polar solvents it was converted by the solvent into its corresponding diacetal. Toluene produced a higher yield and a higher selectivity to hydrocinnamaldehyde. n-Heptane appeared to promote the further hydrogenation of hydrocinnamaldehyde to phenyl propanol. Toluene, therefore, is the best solvent for the formation of hydrocinnamaldehyde Furthermore, reaction rates were greater in toluene than in other non-polar solvents (see Section 6.5.5).

6.5.4.3 Effect of Catalyst Loading

To investigate the effect of catalyst loading on the selectivity to hydrocinnamaldehyde the reaction was carried out in the range of 2-15 $kg.m^{-3}$ of catalyst loading in toluene at 303K and 0.9MPa, and in the range of 2-8 $kg.m^{-3}$ in propan-2-ol at 303K and atmospheric pressure. Table 8.6.5.2 and Figure 6.5.3 show the effect of catalyst loading in toluene and Table 8.6.5.3 and Figure 6.5.4 show the results in propan-2-ol.

When toluene was used as the solvent, the selectivity to hydrocinnamaldehyde ranged within 28-37%. Although the selectivity to hydrocinnamaldehyde changed with catalyst loading the influence is not important so that from the economical view it is better to use lower catalyst loading provided a reasonable rate is achieved. Therefore, in this project a catalyst loading of 4kg.m^{-3} was used in most runs.

Figure 6.5.3 Selectivity vs Catalyst Loading in Toluene

T=303K; P=0.6MPa; $W_{cat.}$=4 kg.m^{-3}; W_{CAL} =50kg.m^{-3}; Solvent =Toluene

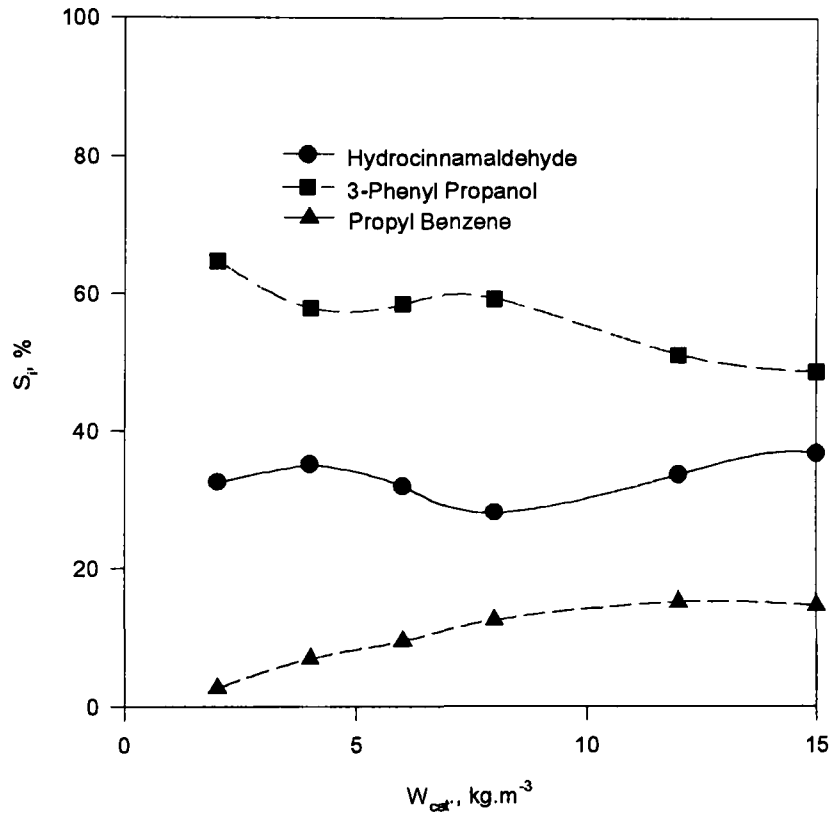

Catalyst loading effect in propan-2-ol at 273-323K and atmospheric pressure has been discussed briefly. When propan-2-ol was used as the solvent, the total selectivity to hydrocinnamaldehyde and its acetals decreased with increase in catalyst loading. As stated previously, hydrocinnamaldehyde diacetal is formed easily from the reaction between hydrocinnamaldehyde and propan-2-ol. The more catalyst was used the quicker was the overall reaction rate and the intermediate product hydrocinnamaldehyde would be converted to its acetal and phenyl propanol so that

the selectivity decreased. Using pre-prepared cinnamaldehyde solutions in propan-2-ol the situation is similar to using freshly prepared cinnamaldehyde solutions.

Figure 6.5.4 Selectivity vs Catalyst Loading in Propan-2-ol

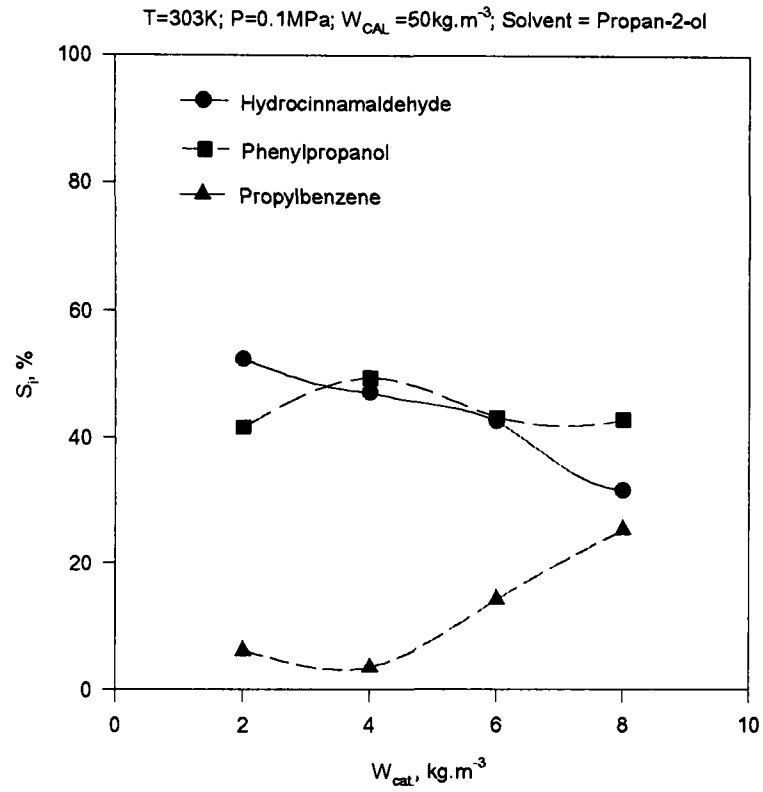

6.5.4.4 Effect of Temperature

To study the effect of temperature on the selectivity to hydrocinnamaldehyde the hydrogenation was carried out from 273K to 343K and 0.1MPa to 0.9MPa at a catalyst loading of 4kg.m^{-3} in toluene and in propan-2-ol. The results in toluene are presented in Table 8.6.5.4 and Figure 6.5.5 and those in propan-1-ol in Table 8.6.5.5 and Figure 6.5.6.

When toluene was used as the solvent the lower the temperature was the higher selectivity can be achieved. It was also noticed incidentally that the pre-heating rate influenced the selectivity. If overheating occurred the selectivity would be significantly lower under otherwise identical conditions although the reaction system was cooled to the required temperature before the start of the hydrogenation.

Figure 6.5.5 Selectivity vs Temperature in Toluene

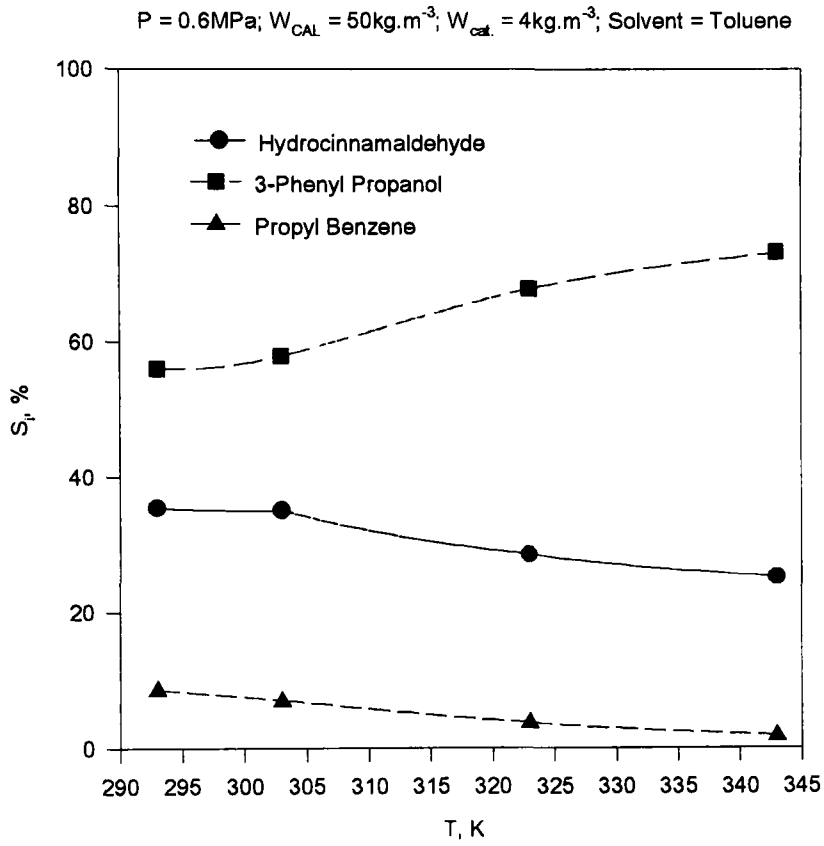

Figure 6.5.6 Selectivity vs Temperature in Propan-2-ol

P = 0.5MPa; W_{CAL} = 50kg.m^{-3}; W_{cal} = 4 kg.m^{-3}; Solvent = Propan-2-ol

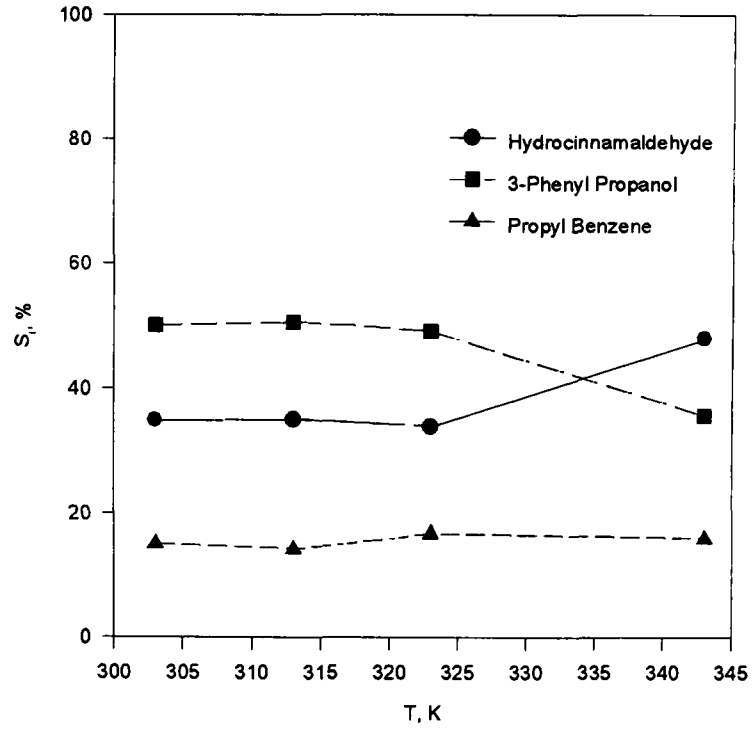

When propan-2-ol was used as the solvent, the total selectivity to hydrocinnamaldehyde and its acetal increased and the percentage of acetal increased with increase in the temperature because higher temperatures favoured acetal formation.

6.5.4.5 Effect of Pressure

To study the effect of pressure on the selectivity to hydrocinnamaldehyde the hydrogenation was carried out from 273K to 343K and 0.1MPa to 0.9MPa at a catalyst loading of 4 kg.m^{-3}. The results in propan-2-ol are given in Table 8.6.5.6 and Figure 6.5.7. The selectivity towards hydrocinnamaldehyde decreased with increase in hydrogen pressure.

Figure 6.5.7 Selectivity vs Pressure in Propan-2-ol

T = 303K; W_{CAL} =50kg.m^{-3}; $W_{cat.}$ = 4kg.m^{-3}; Solvent = Propan-2-ol

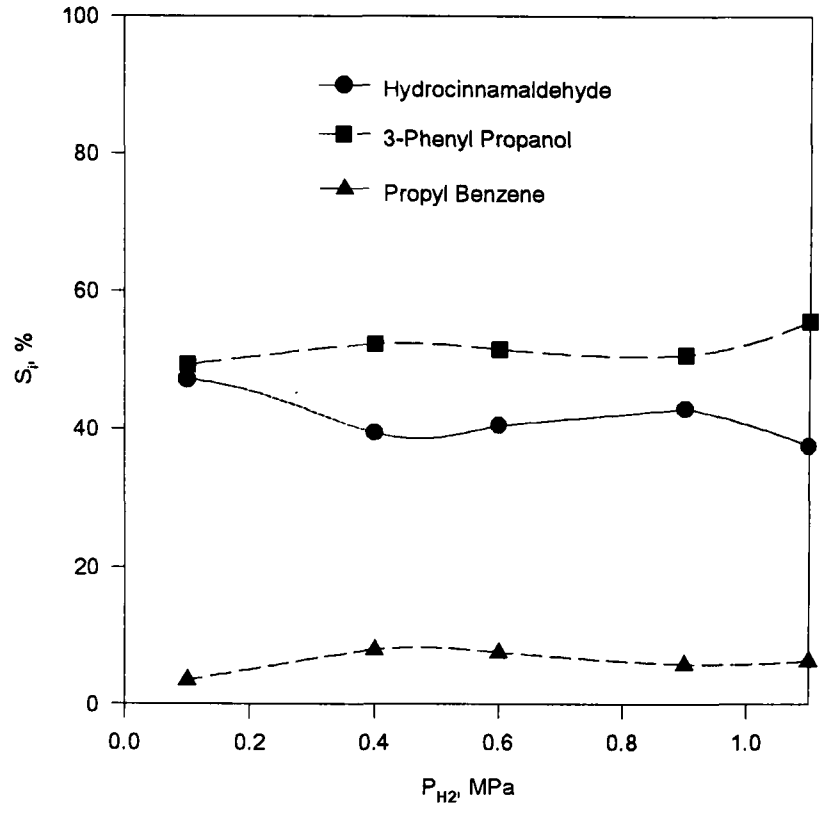

However, when toluene was used as the solvent the selectivity towards hydrocinnamaldehyde increased with increase in hydrogen pressure at 293K, 303K and 343K but at 323K the results showed an opposite tendency (see Table 6.5.5 and Figure 8.7.5.17-8.7.5.20).

Table 6.5.5 Selectivity vs. Pressure in Toluene

$W_{cat.}$ = 4kg.m^{-3}; W_{CAL} = 50kg.m^{-3}

T, K	P, MPa	S_{HC}, %	S_{PP}, %	S_{PB}, %
293	0.4	31.2	62.8	6.0
	0.6	35.4	56.0	8.6
	0.9	35.7	57.0	7.3
303	0.1	20.4	71.0	8.6
	0.4	33.0	61.8	5.2
	0.6	35.1	57.9	7.0
	0.9	35.5	58.9	5.6
323	0.4	30.0	66.2	3.8
	0.6	32.9	62.8	4.3
	0.9	18.5	79.5	2.0
343	0.4	25.0	73.6	1.4
	0.6	32.9	62.8	4.3
	0.9	36.4	62.8	0.8

6.5.4.6 Effect of Substrate Concentration

The effect of initial cinnamaldehyde concentration on the selectivity towards hydrocinnamaldehyde was investigated in the range of 10-100kg.m^{-3} in toluene and the results are given in Table 8.6.5.7 and Figure 6.5.8. It is found that the selectivity towards hydrocinnamaldehyde decreased with increase in the cinnamaldehyde concentration.

Figure 6.5.8 Selectivity vs Substrate Concentration in Toluene

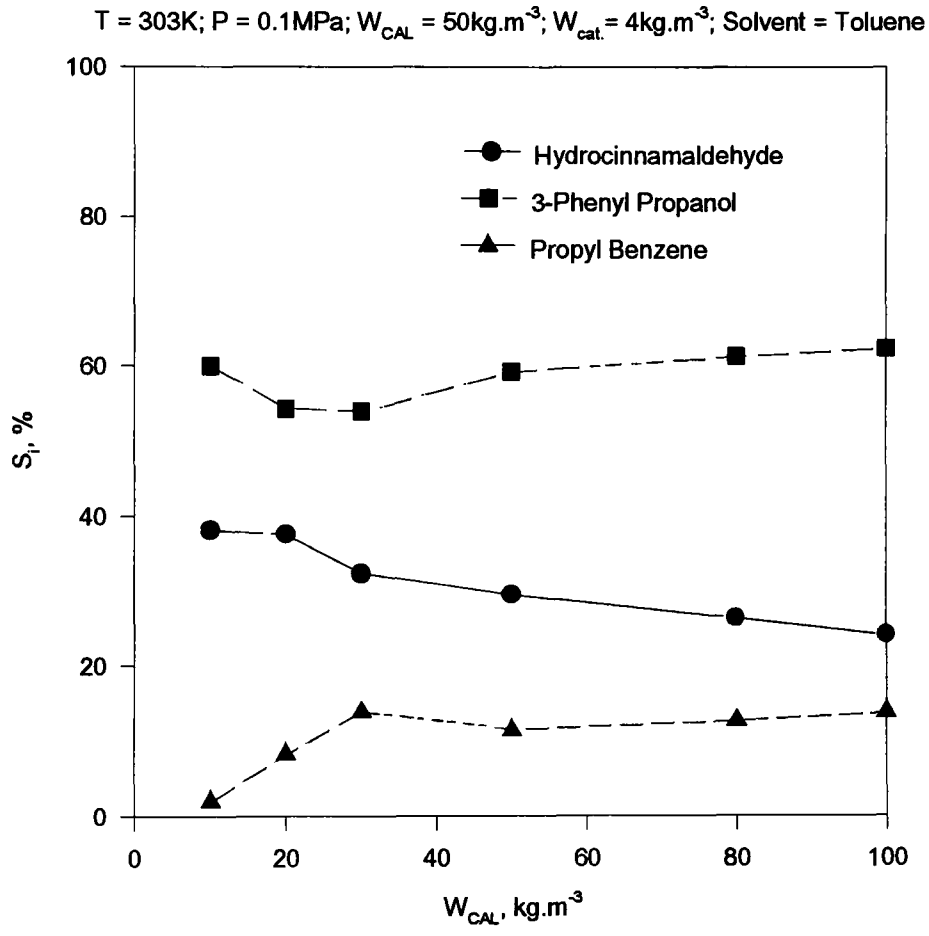

6.5.4.7 Effect of Promoters and Poisons

In order to improve the selectivity to hydrocinnamaldehyde, various promoters such as potassium acetate, iron (II) chloride, iron (II) sulphate, and quinoline were

incorporated individually into the catalyst as modifiers with toluene as the solvent. Table 6.5.6 shows some of these results obtained at 303K and 0.1MPa in a 250ml stirred tank Pyrex glass reactor. It was observed that the additive potassium acetate promoted significantly the formation of hydrocinnamaldehyde and prevented its further hydrogenation. That was in accordance with Rylander's results (1979).

Table 6.5.6 Effect of Additive on Selectivity

T = 303K; P = 0.1MPa; W_{CAL} = 50kg.m^{-3}; $W_{cat.}$ = 4kg.m^{-3}

Additives	X_{CAL}, %	S_{PB}, %	S_{HC}, %	S_{PP}, %
*None	100	4.4	36.3	56.0
*$FeSO_4$	100	18.9	15.9	65.1
*$FeCl_2$	100	3.4	23.0	73.5
*KAc (0.02g)	98	0.6	60.0	39.3
*KAc (0.05g)	85	0.5	53.6	31.0
**None	100	3.4	44.4(27.4)	49.4
**Quinoline(50μg)	100	1.9	35.1(11.0)	63.0
**Quinoline(300μg)	100	0.5	50.9(15.7)	48.6

*in Toluene **in propan-2-ol

Increasing the amount of potassium acetate in the range of 0.02g (K^+/Pd=1:1) to 0.05g (K^+/Pd=2:1) per run at 303K and 0.1 MPa did not improve the selectivity but slowed down the reaction rate. Further investigation of this potassium acetate effect was carried out at 303K and 1 MPa with a K^+/Pd ratio of 0.25 to 20 and the results are presented in Table 8.6.5.8 and Figure 6.5.9. It was found that the selectivity to hydrocinnamaldehyde increased with the K^+/Pd ratio but when the ratio was greater than 10:1 further increase of the ratio did not increase the selectivity. This effect

appears to be associated with blocking of the catalytic sites, possibly involving promoter cations which prevents the further hydrogenation of hydrocinnamaldehyde. For platinum catalysts it has been suggested that a similar effect is caused by electron transfer from the doped metal to the active metals so increasing the electron density at the active metal site and decreasing the probability of C=C bond hydrogenation by lowering the interaction between the π bond of C=C and the metal (Coq et al, 1993; Girior-Fendler et al, 1990; Poltarzewski et al, 1986). Alternatively, new catalyst sites may be formed, able to co-ordinate with the carbonyl oxygen, thus activating it. Again, a detailed study of these effects is required to shed light on these speculations. It is presumed that in the case of palladium catalysts, the effect may be caused largely by poisoning the activity which leads to the further hydrogenation of hydrocinnamaldehyde because normally palladium has a high activity for C=C bond hydrogenation. This is in line with the evidence that palladium is not especially active for carbonyl group hydrogenation. The use of Fe^{2+} ion produced conflicting results as Rylander (1963,1979) reported that iron (II) chloride or iron (II) sulphate produced only hydrocinnamaldehyde whilst our experiments revealed that iron (II) additives did not prevent but promoted the further hydrogenation of hydrocinnmaldehyde and reduced the reaction rate.

Figure 6.5.9 Selectivity vs Ratio of K^+/Pd in Toluene

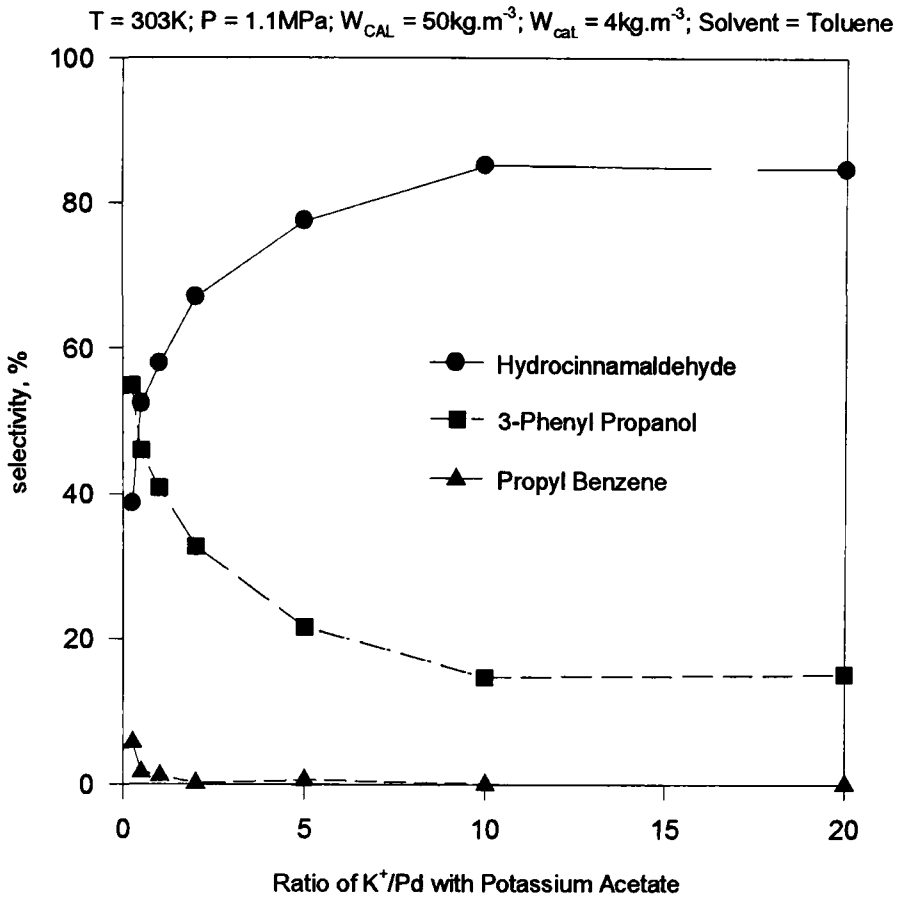

In order to find a better promoter silver nitrate, potassium chloride, potassium bromide, aluminium chloride and potassium hydroxide were incorporated individually into palladium catalysts in ratios of 0.25 to 20. The investigation was carried out at 303K and 1.1MPa and the results are given in Tables 8.6.5.9-8.6.5.12 and Figures 8.7.5.21-8.7.5.24. The results show that potassium chloride had no effect on the selectivity to hydrocinnamaldehyde and aluminium chloride could increase the selectivity to 1.3 fold towards hydrocinnamaldehyde. Potassium bromide, potassium hydroxide and silver nitrate could increase the selectivity to hydrocinnamaldehyde up to two folds.

6.5.4.8 Effect of Cinnamaldehyde Conversion

In order to study the effect of cinnamaldehyde conversion on the selectivity to hydrocinnamaldehyde samples were taken regularly during the course of the hydrogenation. From the selectivity profiles it can be seen that the selectivity with respect to hydrocinnamaldehyde decreased with the reaction time or the conversion. As stated in Section 6.5.3 the hydrogenation of cinnamaldehyde is a parallel-consecutive reaction and over palladium catalysts hydrocinnamaldehyde is the initial product so that the selectivity to hydrocinnamaldehyde reached its highest at the beginning. Afterwards its selectivity gradually decreased with the reaction time until equilibrium had been established and the selectivity remained constant.

6.5.5 Kinetic Investigations

6.5.5.1 Calibration of Stirring Speed

The stirring speed corresponding to each stirrer setting was obtained by the use of a tachometer attached to the free-running stirrer. The data are presented in Table 8.6.5.13 and Figure 8.7.5.25. The actual stirring speeds would be slightly lower than the calibrated speeds due to the higher torque of the stirrer shaft when the stirrer was driving the reactor unit.

6.5.5.2 Reaction Rate against the Stirring Speed

The complete suspension of the catalyst is important for a slurry reaction in stirred reactors, and to maximise the catalyst utilization a minimum degree of agitation is required to ensure that all of the catalyst is properly suspended.

In order to determine the role of mass transfer the catalyst loading was varied from 1kg.m^{-3} to 6kg.m^{-3} and the stirring speed was varied from 600rpm to 1500rpm. The effect of stirring speed on the initial reaction rate was examined by using a palladium/charcoal catalyst loading of 4kg.m^{-3} and 50kg.m^{-3} of cinnamaldehyde solution in propan-2-ol at 303K and 0.1MPa in a 250ml Pyrex glass reactor, and by using a palladium/charcoal catalyst loading of 4kg.m^{-3} and 50kg.m^{-3} cinnamaldehyde solution in toluene at 303K and 0.6MPa. The results are given in Tables 8.6.5.14 and Figure 6.5.10. The results of the cinnamaldehyde hydrogenation showed that when the stirring speed was greater than a certain speed, the resistance due to gas-liquid mass transfer was negligible. In the 250ml Pyrex glass reactor, when the stirring speed was greater than 1000rpm further increase of the stirring speed did not increase the reaction rate. This indicates the absence of a gas liquid absorption effect above a stirring speed of 1000rpm. In the 500ml autoclave the effect of turbulence on gas-liquid mass transfer became negligible above a stirring speed of 800rpm. As mentioned previously the actual stirring speed corresponding to a stirrer setting is slightly lower than the calibrated speed due to the viscosity of the stirred solution. In practice, however, it is not essential to know the exact stirring speed if the identical stirring conditions are maintained and the stirring rate is high enough to ensure the elimination of mass transfer resistance. Stirring speeds of 1200rpm in the 250ml

Pyrex glass reactor and 1000rpm in the 500ml autoclave were chosen for the kinetics, mass transfer and selectivity studies.

Figure 6.5.10 Reaction Rate vs stirring Speed

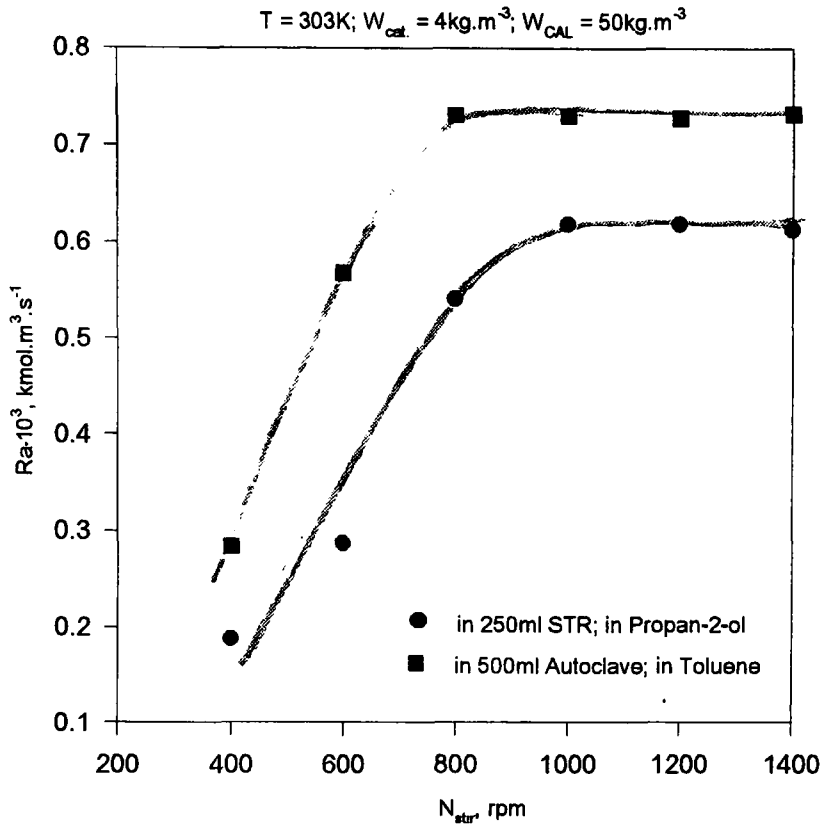

6.5.5.3 Effect of the Gas Introduction Mode

To study the effect of the gas introduction mode on the reaction rate, two modes were compared. In mode A hydrogen was entrained in the liquid phase in the reactor unit (Pyrex glass reactor) from the gas phase by intensive agitation. In mode B hydrogen was introduced into the liquid phase through nozzles. The comparison was made using 4kg.m^{-3} catalyst and 50kg.m^{-3} cinnamaldehyde in propan-2-ol at 303K and 0.1MPa. The results are given in Table 8.6.5.15 and Figure 6.5.11, and show that the reaction rate was independent of the gas-introduction mode. For simplicity, hydrogen gas was introduced into the liquid phase by agitation (Mode A).

Figure 6.5.11 Reaction Rate vs stirring Speed

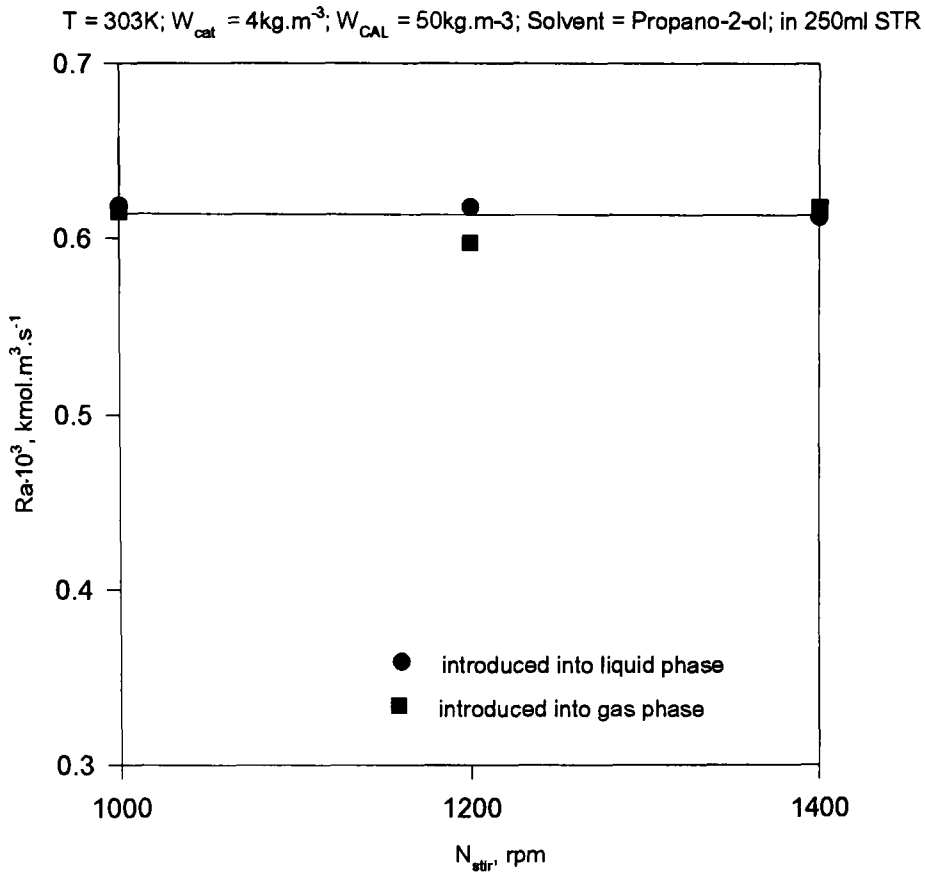

Due to the large gas-liquid interface and the effect of mechanical agitation in Mode A frequent and continuous surface breakage and surface renewal prevail at the gas liquid interface resulting in a large increase in the interfacial area, so accelerating the mass transfer rate. Chaudhari et al (1987) reported that Mode A gave better gas-liquid mass transfer than did Mode B when the hydrogenation of styrene was conducted under mass transfer control, while the hydrogenation of cinnamaldehyde exhibits the surface reaction controlling mechanism, so that the gas introduction mode is not important for the hydrogenation of cinnamaldehyde. The surface-rate-limited mechanism was indicated by a higher apparent activation energy (see Section 6.5.5.8) and low mass transfer resistance (Section 6.5.6).

6.5.5.4 Effect of Initial Concentration of Cinnamaldehyde

The effect of the substrate concentration on the reaction rate was investigated by using cinnamaldehyde solutions in propan-2-ol and in toluene with initial cinnamaldehyde concentrations of 10, 20, 30 50, 80 and 100kg.m^{-3} at 303K and atmospheric pressure in the 250ml Pyrex glass reactor. The results are given in Table 8.6.5.16 and Figure 6.5.12. It can be seen that the reaction rate was independent of the initial cinnamaldehyde concentration in the tested range of 10-100kg.m^{-3}, which indicated that the reaction was zero order with respect to the substrate concentration. This was also confirmed by the finding that during the course of the hydrogenation of cinnamaldehyde there was no distinct rate-step change and the hydrogen consumption increased nearly linearly with time. In some runs, however, when the hydrogenation was approaching completion, the hydrogen takeup-rate decreased slightly. At atmospheric pressure the hydrogen consumption rate decreased slightly with time. The slight deviation of the reaction rate from zero-order in some runs may be explained as follows: The deviation from zero-order kinetics may be caused by a decrease in the solubility of hydrogen with the increase in the concentration of the reaction products and the deactivation of the catalyst by the products either chemically or physically (Ramachandran and Chaudhari, 1983). The slight decrease in reaction rate at the end of the reaction may be due to the decrease in catalyst surface-area available due to poisoning of the active sites or to a change in order towards the end of the reaction. Rajadhyakasha and Karwa (1986) stated that the interaction between the solute and the solvent also may influence the hydrogenation rate. At atmospheric pressure and very low cinnamaldehyde concentration, hydrogen

solubility in the reaction system may become slightly dependent on the cinnamaldehyde concentration.

Figure 6.5.12 Reaction Rate vs Cinnamaldehyde Concentration

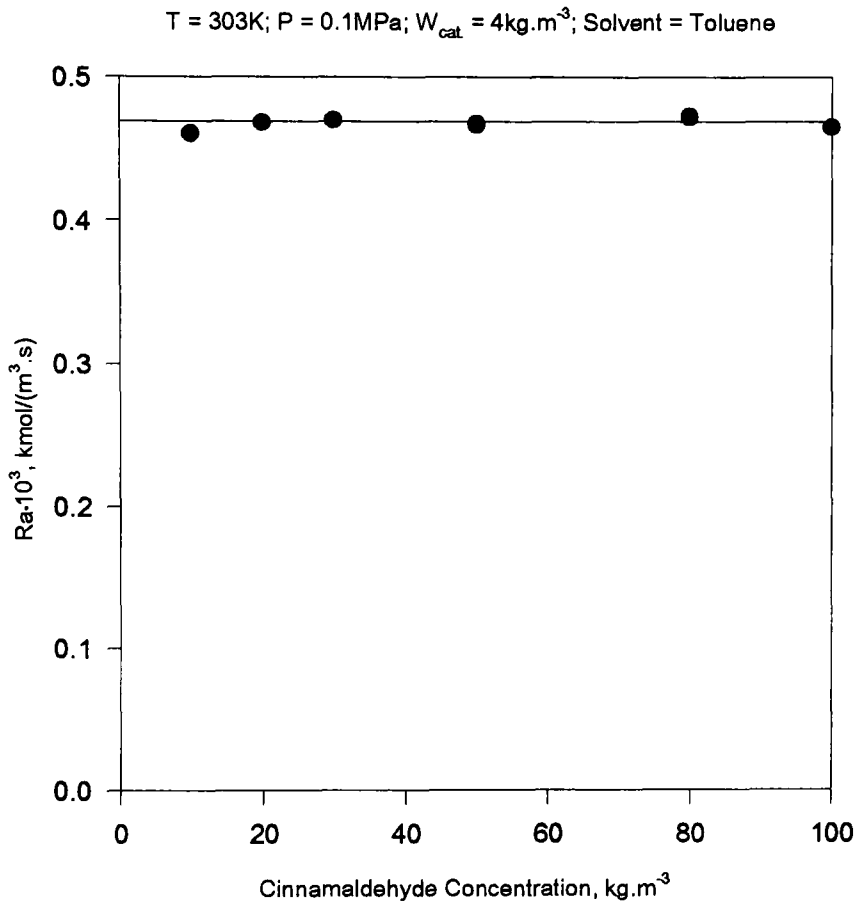

The independence of the reaction rate on the cinnamaldehyde concentration is in accordance with previous studies (Satagopan et al, 1994) over a palladium/charcoal catalyst, although others have reported a first-order rate with respect to cinnamaldehyde concentration over ruthenium/tin catalysts using ethanol as the solvent (Galvagno et al, 1993). If the initial cinnamaldehyde concentration of 50kg.m^{-3} is used, the reaction rate is independent of the cinnamaldehyde concentration, and a substantial amount of the reactant is provided: therefore, a concentration of 50kg.m^{-3} of cinnamaldehyde was used throughout the present work. In this work the effect of cinnamaldehyde concentration on the rate of hydrogenation can be neglected, and the data of hydrogen solubility in propan-2-ol and in toluene were used directly without

counting the effect of other components in the solvent for mass transfer and kinetic studies.

Theoretically, one mole of hydrogen gas is required for the complete conversion of one mole of cinnamaldehyde to hydrocinnamaldehyde. As stated in Section 6.5.3, because the hydrogenation of cinnamaldehyde is a consecutive-parallel reaction and all the reactions occur simultaneously, when one mole of cinnamaldehyde was converted completely more than one mole of hydrogen was used. Therefore, the hydrogen consumption rate was chosen as the overall reaction rate. Product analysis showed that the hydrogenation of cinnamaldehyde over palladium/charcoal catalysts proceeded mainly through hydrocinnamaldehyde.

6.5.5.5 Effect of Homogeneous Reactions

Preliminary experiments were carried out by using a pre-prepared 50kg.m^{-3} cinnamaldehyde solution in propan-2-ol. After the reaction samples were analysed it was realised that by-products other than hydrocinnamaldehyde could be produced by using a pre-prepared cinnamaldehyde solution instead of a freshly prepared solution, so later experiments used fresh solutions. It was found that the reaction rate was greater when pre-prepared reactant solutions in propan-2-ol were used instead of fresh solutions. Table 8.6.5.17 gives some of the results and Figure 6.5.13 shows the effect of homogeneous reactions on the reaction rate. This may be because the impurities present in cinnamaldehyde and in propan-2-ol accelerated the formation of cinnamaldehyde diacetal prior to the hydrogenation due to the reaction between cinnamaldehyde and propan-2-ol, resulting in a transition to partially diffusion

controlled kinetics. As the result of the formation of cinnamaldehyde acetals prior to the hydrogenation as confirmed by analysis of a pre-prepared reactant solution, the reaction mechanism is different from that in non-polar solvents.

Figure 6.5.13 Homogeneous Reaction Effect on Rate

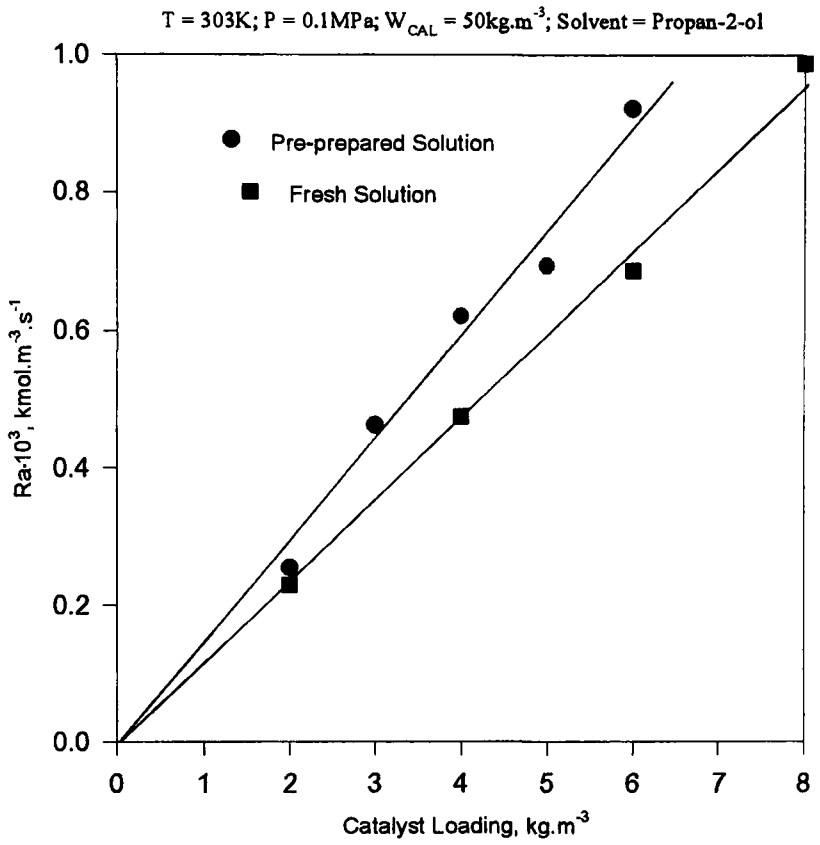

6.5.5.6 Effect of Solvent

In order to select a suitable solvent for the clean production of hydrocinnamaldehyde, experiments were conducted in various solvents using a cinnamaldehyde concentration of 50kg.m^{-3} and palladium/charcoal catalyst loading of 4kg.m^{-3} at 303K and atmospheric pressure. The solvents used can be divided into two groups: polar and non-polar. Table 6.5.7 shows some results.

Table 6.5.7 Reaction Rate in Various Solvents

Solvent	Methanol	Ethanol	Propan-1-ol	Propan-2-ol	Butan-1-ol	Butan-2-ol	Toluene
$Ra \times 10^3$, $kmol.m^{-3}s^{-1}$	0.713	0.577	0.501	0.311	0.482	0.053	0.248

When polar solvents (alcohols) were used the reaction rates were much higher than those in non-polar solvents, and the rates in various solvents were in the order:

methanol > ethanol > propan-1-ol > butan-1-ol > propan-2-ol > butan-2-ol

(Primary > Secondary). This reaction rate acceleration resulted from the formation of the intermediate cinnamaldehyde diacetals and hydrocinnamaldehyde acetals.

When non-polar solvents were used the reaction rate was significantly lower than that in polar solvents under the same operation conditions. This may be due partly to the low solubility of hydrogen in non-polar solvents. In order to maximise the production of hydrocinnamaldehyde only propan-2-ol and toluene were used for the kinetic studies.

6.5.5.7 Effect of Catalyst Loading

The relative importance of the various steps involved in the hydrogenation of cinnamaldehyde was investigated by the use of propan-2-ol and toluene as solvents in the 250ml Pyrex glass reactor and in the 500ml stainless steel autoclave at various temperatures. The data are given in Tables 8.6.5.18-Table 8.6.5.20. The plots of the initial reaction rate against catalyst loading are shown in Figures 6.5.14-Figure 6.5.16.

(1) Using Propan-2-ol as the Solvent for Pre-prepared Cinnamaldehyde Solution

The rate of hydrogenation was proportional to the catalyst concentration in the temperature range 273-343K when a solution of pre-prepared cinnamaldehyde in propan-2-ol was used. The fact that the plot of hydrogenation rate against catalyst loading in propan-2-ol does not pass through the origin suggests that there is some form of poisoning present in the system. It can be seen that a minimum catalyst loading of 0.5kg.m^{-3} is needed to start the hydrogenation of cinnamaldehyde to overcome the poison effect.

Figure 6.5.14 Rate vs. Catalyst Loading

P = 0.1 MPa; W_{CAL} = 50kg.m^{-3}; Solvent = Propan-2-ol

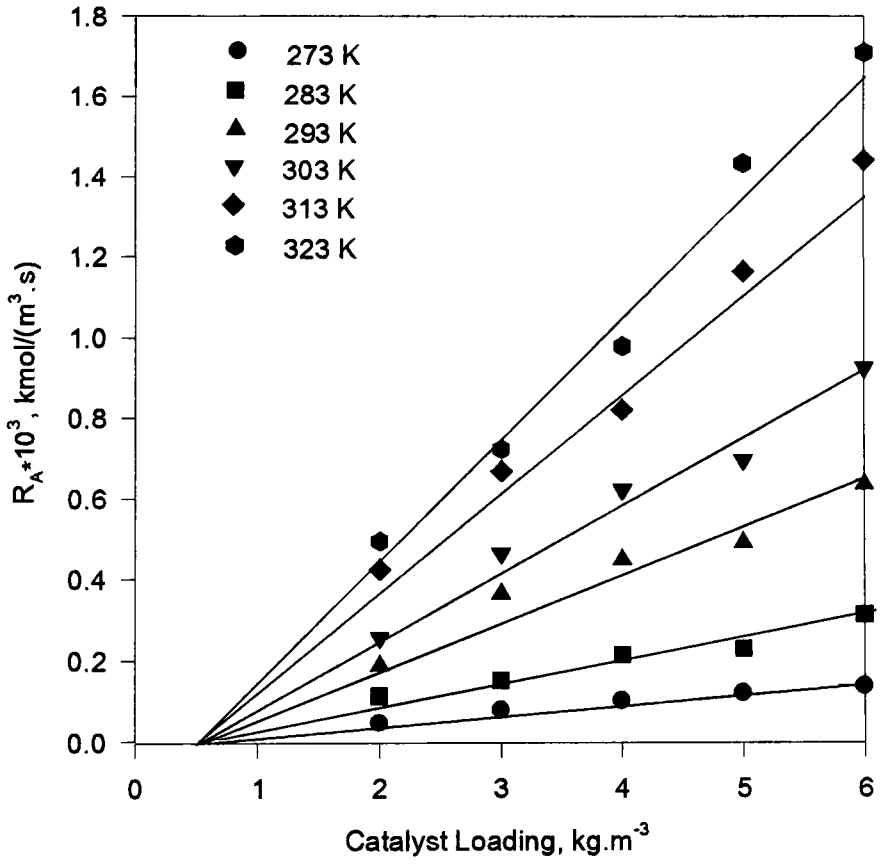

(2) Using Propan-2-ol as the Solvent for Fresh Cinnamaldehyde Solution

Figure 6.5.15 shows the effect of catalyst loading when using a fresh solution of cinnamaldehyde in propan-2-ol. It can be seen that the hydrogenation rate increased with the increase of catalyst loading. When a fresh solution of cinnamaldehyde in propan-2-ol was used there was no minimum catalyst loading for starting the reaction. A comparison of these results with those for propan-2-ol indicated that the impurities present in the pre-prepared solution assisted the homogeneous reactions.

Figure 6.5.15 Rate vs Catalyst Loading in Propan-2-ol (fresh solution)

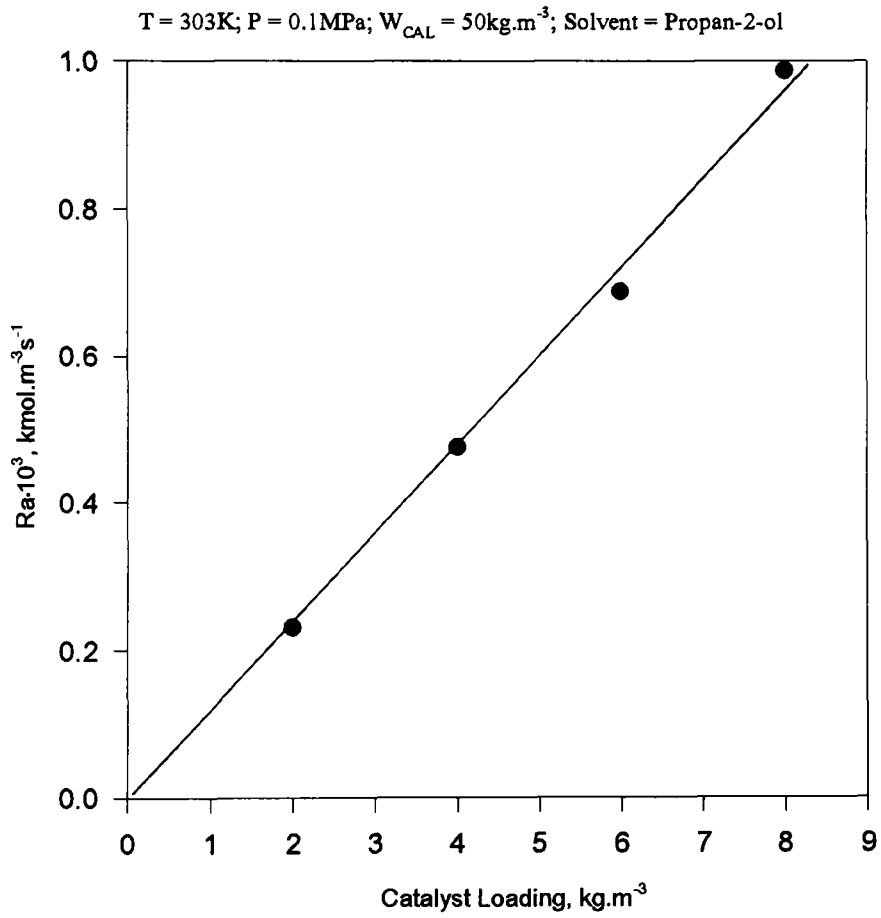

(3) Using Toluene as the Solvent for Fresh Cinnamaldehyde Solution

Figure 6.5.16 shows the effect of catalyst loading when using a fresh solution of cinnamaldehyde in toluene. It was found that the reaction rate varied linearly with the

catalyst loading for a temperature range of 273K to 343K, and the line passed through the original indicating that no minimum catalyst loading was required. This observation suggests that the gas-liquid mass-transfer resistance may not be important under the experimental conditions.

Figure 6.5.16 Rate vs Catalyst Loading in Toluene

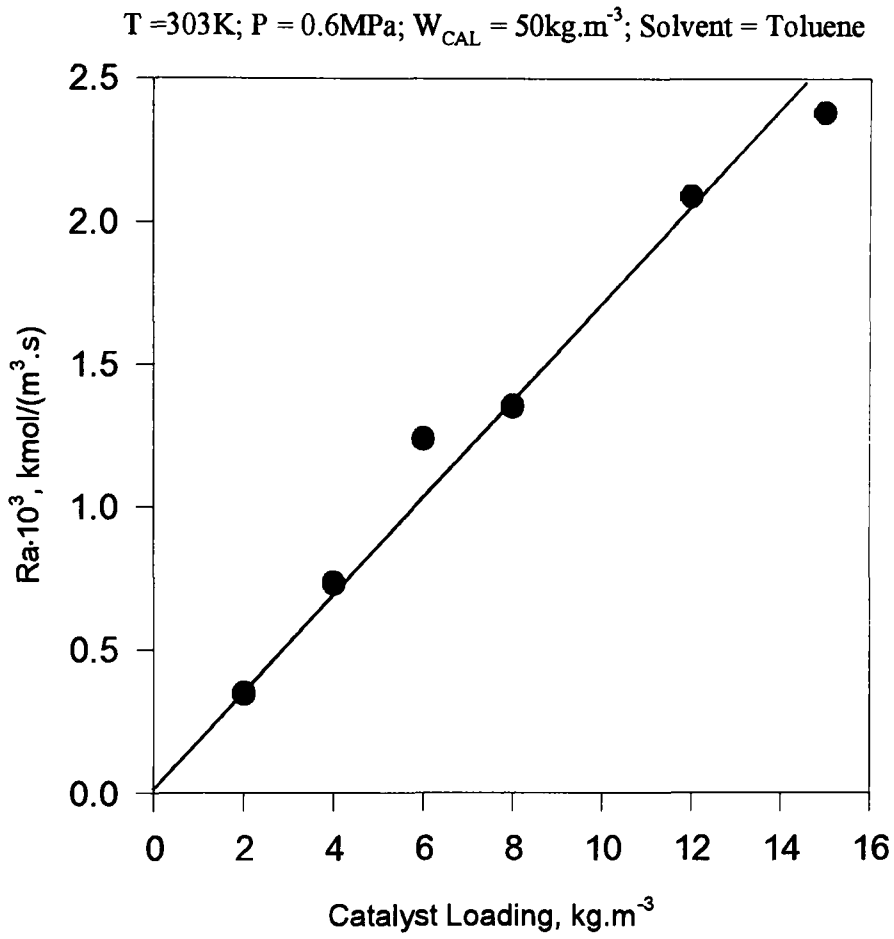

6.5.5.8 Effect of Temperature

The effect of temperature was studied by using both pre-prepared solutions and fresh solutions of cinnamaldehyde in propan-2-ol and in toluene with a catalyst loading of 4kg.m^{-3}, a cinnamaldehyde concentration of 50kg.m^{-3} and a hydrogen pressure range

of 0.1-1.1MPa, in order to clarify the controlling steps and to obtain the apparent activation energy.

Two factors should be taken into account when comparing the reaction data at different temperatures. Firstly, the solubility of hydrogen in a solvent varies with temperature. Secondly, the partial pressure of hydrogen in the gas phase decreases with temperature at a given pressure due to the increase of the solvent vapour pressure with temperature. As a result the equilibrium concentration of hydrogen at the gas-liquid interface varies with temperature. In order to obtain a constant basis for the hydrogen equilibrium concentration at the gas-liquid interface the observed reaction rate should be corrected for temperature. The correction factors of the reaction rate are given in Section 8.2.3.

The relative importance of external mass transfer and surface reaction in three-phase reactions can be evaluated by the temperature dependence of the reaction rate. The usual Arrhenius equation is used to calculate the activation energy as follows:

$$k = A\exp\left(-\frac{E}{RT}\right) \qquad (6.5.5)$$

where k = kinetic constant

A = frequency factor

E = activation energy

R = gas constant, = 8.314 $J.mol^{-1}.K^{-1}$

T = temperature, K

The intrinsic activation energy is determined experimentally by carrying out the reaction at different temperatures. Taking the logarithm of Equation (6.5.5) gaves a linear relationship

$$\ln(k) = \ln(A) - \frac{E}{R}\left(\frac{1}{T}\right) \qquad (6.5.6)$$

The plot of *ln*(k) against (1/T) should give a straight line whose slope is proportional to the activation energy.

However, in three-phase reactions the existence of possible mass transfer resistance may influence the measured reaction rate. In the case of three-phase reactions an apparent activation energy E_{app} is used to reflect this possibility.

$$Ra = A\exp\left(-\frac{E_{app}}{RT}\right) \qquad (6.5.7)$$

E_{app} is the activation energy calculated using experimental data from the slope of the plot of *ln*(Ra) against T^{-1} at a fixed concentration of the substrate. As for the true activation energy the slope is proportional to the apparent activation energy

The following criteria have been proposed to evaluate the contribution of external mass transfer and surface reaction on the reaction rate (Satterfield, 1970; Doraiswamy and Sharma, 1984):

1. $E_{app} < 1$ kcal.mol^{-1} (4kJ.mol^{-1}): gas-liquid mass transfer is important.

2. E_{app} = 1-3 kcal.mol^{-1} (4-12kJ.mol^{-1}): liquid-solid mass transfer is important.

3. $E_{app} \geq 10$ kcal.mol^{-1}(42kJ.mol^{-1}): surface reaction is controlling .

4. E_{app} =5-10 kcal.mol^{-1} (21-42kJ.mol^{-1}): Both liquid-solid mass transfer and surface reaction are important.

The plots of *ln*(Ra) against reciprocal temperature in different solvents are discussed and the activation energy can be calculated as following.

(1) Using Propan-2-ol as the Solvent for Pre-prepared Cinnamaldehyde Solution

Table 8.6.5.21 and Figure 6.5.17 give the temperature effect when pre-prepared cinnamaldehyde solutions in propan-2-ol were used with a catalyst loading of 1-6kg.m^{-3} and a temperature range of 273K to 323K at atmospheric pressure. It was found that the logarithm of the reaction rate varied inversely with temperature, which showed that the effect of temperature on the reaction rate obeyed the Arrhenius equation. From the slope of the graph the activation energy was calculated, and the values of E_A corresponding to the various catalyst loadings are given in Table 6.5.8. It can be seen that there were two slopes in Figure 6.5.17. At lower temperature range (273-293K) the activation energy is 50±5kJ.mol^{-1} and the surface reaction rate is the rate controlling step but at higher temperature range (293-323K) that is 24±5kJ.mol^{-1} indicating that the role of mass transfer became important.

Figure 6.5.17 Rate vs Temperature in Propan-2-ol

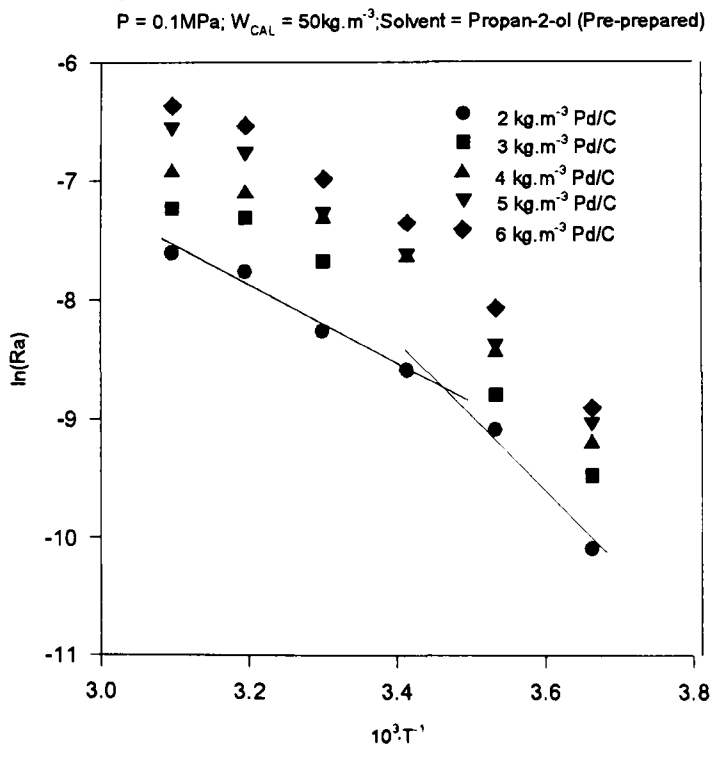

Table 6.5.8 Activation Energy in Propan-2-ol for Pre-prepared Solution

T, K	273-293	293-323
E_A, kJ.mol^{-1}	50±5	24±5

(2) Using Propan-2-ol as the Solvent for Fresh Cinnamaldehyde Solution

Table 8.6.5.22 and Figure 6.5.18 show the temperature effect due to the use of fresh cinnamaldehyde solutions in propan-2-ol with a catalyst loading of 4kg.m^{-3} and a temperature range of 273K to 323K both at atmospheric pressure and at a hydrogen pressure of 0.6MPa. At atmospheric pressure there were two slopes and the activation energy for a fresh solution is much lower than that for a pre-prepared solution indicating that mass transfer under these conditions is more important. The activation energy at 0.6MPa is 57kJ.mol^{-1} indicating that at higher hydrogen pressure the mass transfer effect becomes less important, even negligible.

Figure 6.5.18 Rate vs Temperature in Propan-2-ol (in situ)

$W_{cat.}$ = 4kg.m^{-3}; W_{CAL} = 50kg.m^{-3}; Solvent = Propan-2-ol

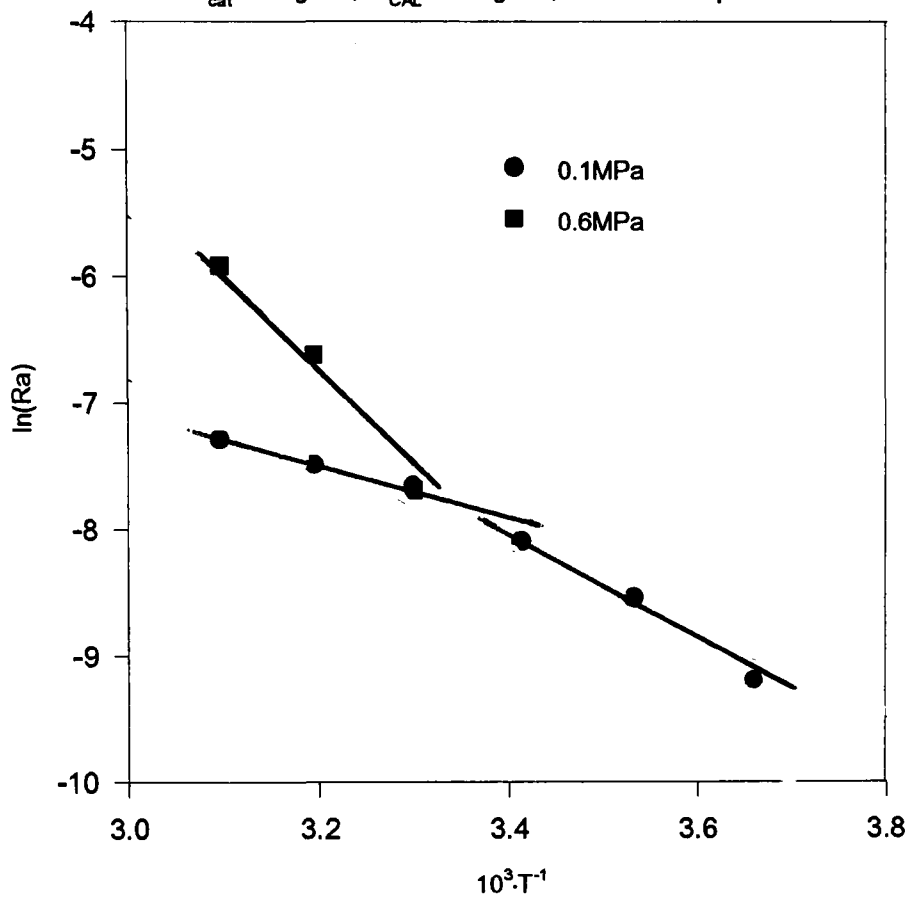

(3) Using Toluene as the Solvent

Table 8.6.5.23 and Figure 6.5.19 show the effect of temperature on the reaction rate with a catalyst loading of 8kg.m^{-3} and a cinnamaldehyde concentration of 50kg.m^{-3}. The plot of the logarithm of the reaction rate against the reciprocal temperature T^{-1} gives a straight line, indicating that the Arrhenius equation can be used to estimate the activation energy. With toluene as the solvent the activation energy was found to be 65 ±5 kJ.mol. The reaction seems to be free of gas-liquid mass-transfer resistance, the important steps being the surface reaction.

Figure 6.5.19 Rate vs Temperature in Toluene

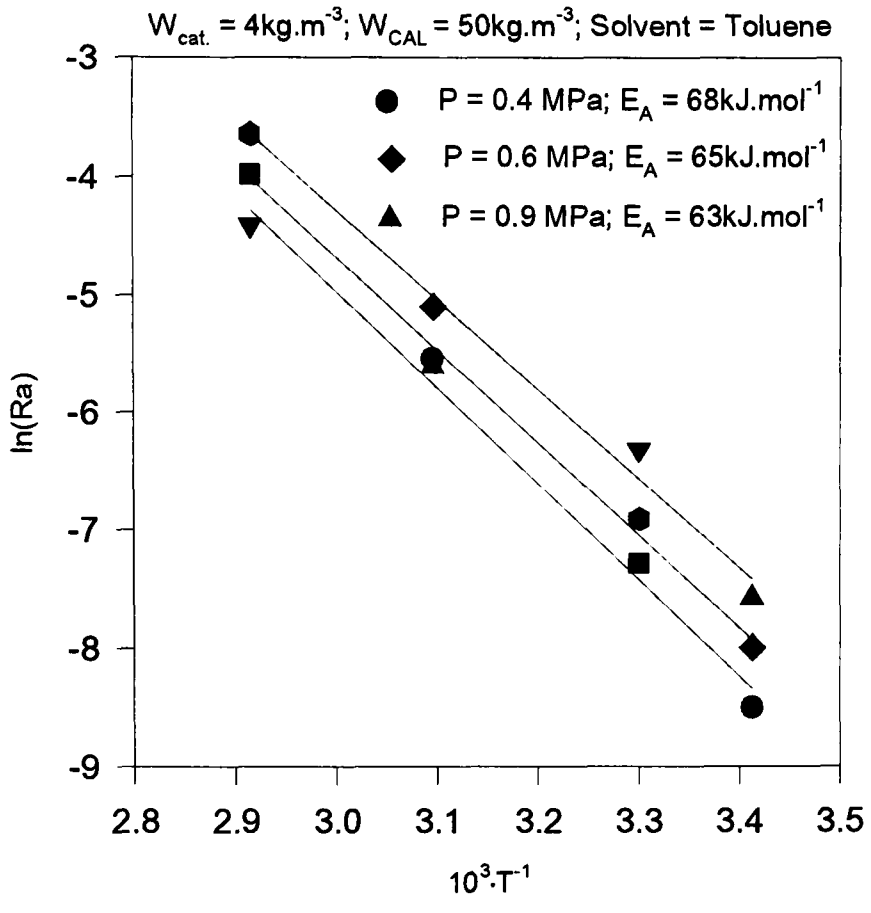

The fact that the activation energy in propan-2-ol is much lower than it is in toluene may be interpreted in the following way. It is possible that the presence of the hydroxyl group in propan-2-ol and the easy formation of acetals in alcohol solvents significantly accelerated the reaction rate, so that the reaction became partly diffusion-controlled in propan-2-ol and the apparent activation energy in propan-2-ol was much lower than it was in toluene.

6.5.5.9 Effect of Pressure

The effect of pressure on the reaction rate was studied in propan-2-ol and in toluene from 0.1MPa to 1.1MPa in the 500ml autoclave. The results are given in Tables

8.6.5.24-8.6.5.25 and Figures 6.5.20-6.5.21. They show that the reaction rate is proportional to hydrogen partial pressure, in agreement with the observation of Satagopan and Chandalia (1994).

Figure 6.5.20 Rate vs Pressure in Propan-2-ol (in situ)

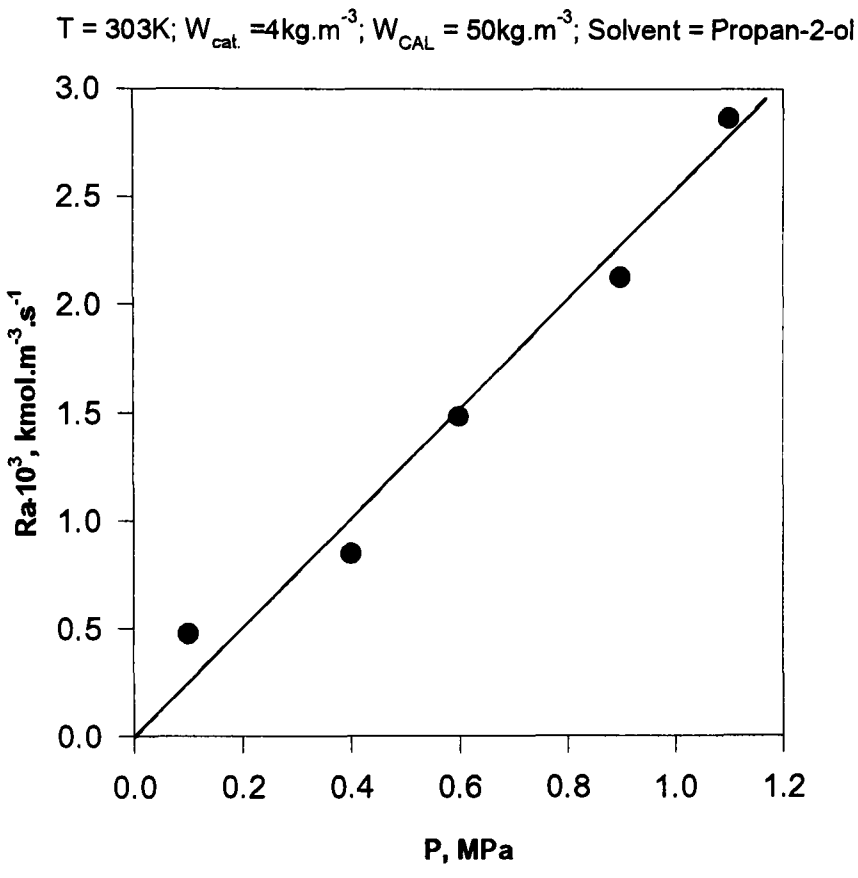

Figure 6.5.21 Rate vs Pressure in Toluene

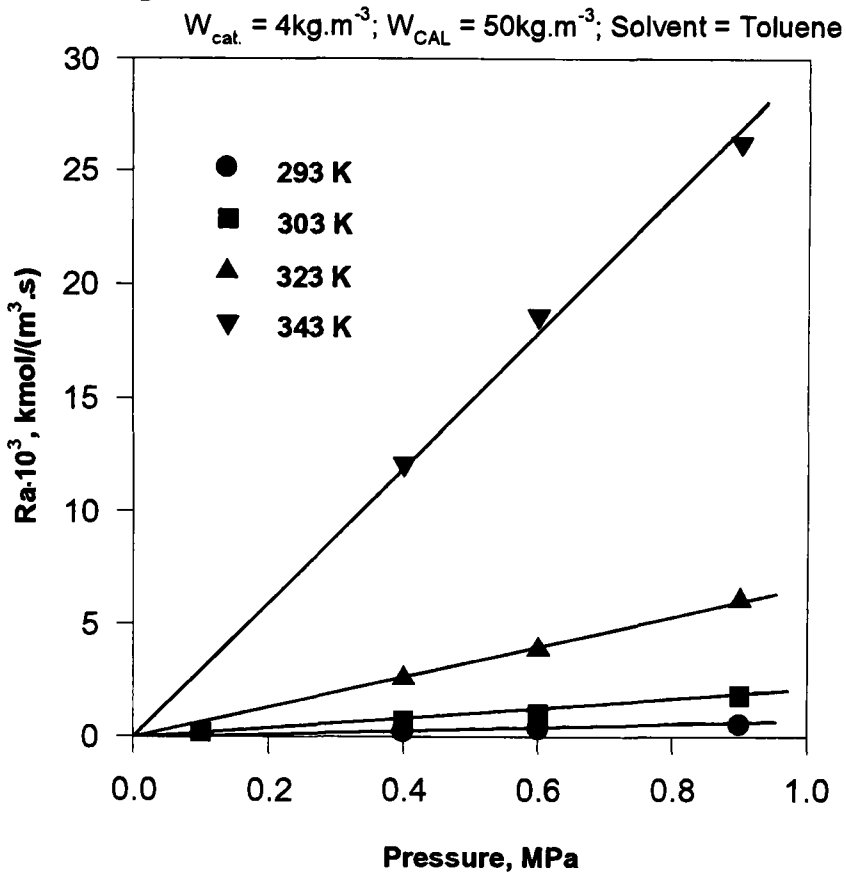

6.5.5.10 Effect of Additives

In order to improve the selectivity to hydrocinnamaldehyde, various metal salts were incorporated in the palladium/charcoal catalysts in the ratio of 0 to 20 of metal to palladium at 303K and 1.1MPa with a catalyst loading of 4kg.m^{-3}. It was found that when potassium acetate was incorporated into the catalysts the reaction rates tended to decrease especially when the factor of metal to palladium exceeded one. Such an effect may be associated with the blocking or poisoning of the catalytic sites, possibly involving cations which prevent the further hydrogenation of hydrocinnamaldehyde. When potassium hydroxide was added to the toluene/water solvents both the selectivity to hydrocinnamaldehyde and the reaction rate were increased. When iron (II) chloride or iron (II) sulphate was incorported into the reaction system some induction time was needed and the reaction rate was significantly reduced. The

addition of iron (II) accelerated the selectivity neither to hydrocinnamaldehyde nor to cinnamyl alcohol but increased the formation of phenyl propanol and propylbenzene. This finding disagrees with the observations of Rylander (1963) and Schröder and Verdier, (1993).

6.5.5.11 Effect of Hydrocinnamaldehyde Concentration

The effect of the initial hydrocinnamaldehyde concentration on the reaction rate was investigated using initial hydrocinnamaldehyde concentrations of 5, 10 and 25kg.m^{-3} and an initial cinnamaldehyde concentration of 50kg.m^{-3} in toluene at 303K and 0.1MPa with a catalyst loading of 8kg.m^{-3} in the 250ml Pyrex glass reactor. The results are given in Table 8.6.5.26 and Figure 6.5.22. It can been seen that the initial reaction rate was not influenced by the presence of hydrocinnamaldehyde. Hydrocinnamaldehyde, either from the reaction product or from feed, behaved almost as an inert component, at least until most of the cinnamaldehyde had reacted. The hydrogen consumption increased almost linearly with time until the end of the reaction. This observation agrees with the findings of Satagopan and Chandalia (1994).

Figure 6.5.22 Reaction Rate vs Hydrocinnamaldehyde Concentration

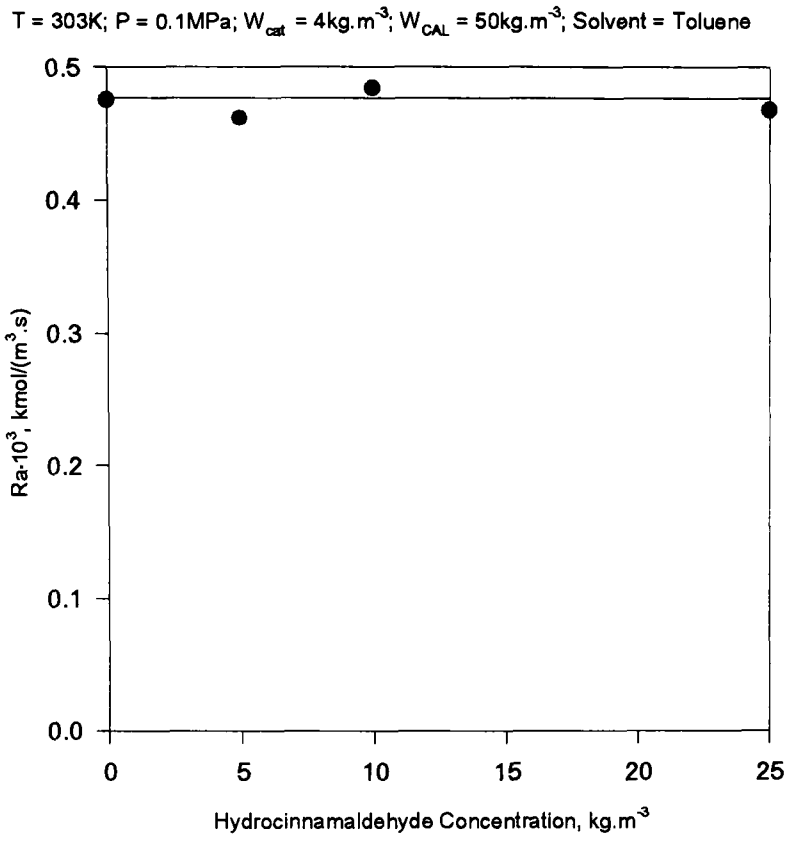

6.5.5.12 Purging the Reactor

In order to remove the air in the headspace of the reactor, it was essential to purge the reactor headspace with hydrogen before starting the reaction. The variation of hydrogenation rate variance with purging duration under otherwise identical conditions would show the extent of volume replacement in the reactor headspace, since the hydrogenation rate was directly affected by the partial pressure of hydrogen in the gas phase. The duration of purging was measured by the number of purges. One purge corresponded to one reservoir of hydrogen of volume about one litre at STP. It was observed that three purges were required to fill the vessel headspace completely with hydrogen. In this work four purges were made before starting the hydrogenation to ensure the complete removal of other gases.

6.5.5.13 Kinetic Expression

As discussed in the previous sections, the linear change of reaction rate with hydrogen pressure proves that the mechanism is first-order with respect to hydrogen concentration. This order is common for hydrogenation reaction.

The reaction rate is independent of the initial cinnamaldehyde concentration, and the reaction seems to be zero-order with respect to cinnamaldehyde concentration. The zero-order mechanism was verified by the fact that at a constant temperature hydrogen takeup during the course of hydrogenation increased linearly with time until the end of the reaction. This finding is in accordance with the observation of Satagopan and Chandalia (1994).

The fact that the reaction rate increased proportionately with catalyst loading in the solvents used indicated a first-order mechanism with respect to catalyst loading. The kinetics can be described by the following equation:

$$R_A = kC_{cat}^{1.0} C_{CAL}^{0} C_{H_2}^{1.0} \qquad (6.5.8)$$

where C_{cat} = catalyst concentration, $kmol.m^{-3}$

C_{CAL} = cinnamaldehyde concentration, $kmol.m^{-3}$

C_{H2} = hydrogen concentration, $kmol.m^{-3}$

Ra = overall hydrogen takeup rate, $kmol.m^{-3}.s^{-1}$

6.5.6 Mass Transfer Studies

To evaluate the mass transfer and kinetic parameters the classical first reaction model (Ramchandran and Chandhari, 1983) and the Frössling equation (Statterfield, 1970) were used. The only parameter estimated using an empirical equation was the liquid-solid mass transfer coefficient $k_{S\text{-}L}$. The choice of the $k_{S\text{-}L}$ correlation is extremely crucial because its value will influence the value of the intrinsic rate coefficients k_r and k_La. Hence, in selecting the appropriate correlation, the calculation results of different correlations for $k_{S\text{-}L}$ have to be correlated by other parameters, in this case, activation energy.

The liquid-solid mass transfer coefficient k_S was calculated using the Frössling equation (Statterfield, 1970)

$$Sh = 2.0 + 0.76 Re^{\frac{1}{2}} Sc^{\frac{1}{3}} \qquad (6.5.9)$$

The calculation of k_S was based on the liquid properties but not on the catalyst particles, since in a highly turbulent system k_S is independent of particle size (Doraiswamy and Sharma, 1984). The k_S calculation for the autoclave was based on the mean value of Re at the tip of the impeller, and at the wall of the reactor where the fluid elements will be relatively stagnant and hence governed by the following equation (Statterfield, 1970)

$$Sh = \frac{k_s d_p}{D_A} = 2 \qquad (6.5.10)$$

The surface reaction constant k_r was evaluated by the following equation based on the classical first order film model (Ramchandran and Chandhari, 1983)

$$\frac{C_A^*}{Ra} = \frac{1}{k_L a} + \frac{\rho_p d_p}{6W}\left(\frac{1}{k_s} + \frac{1}{\eta_c k_r}\right) \qquad (6.5.11)$$

The relative importance for mass transfer and surface reaction rate was evaluated using

$$X_{L-S} = \frac{\frac{1}{k_s}}{\frac{1}{k_r} + \frac{1}{k_s}} \qquad (6.5.12)$$

The value of the gas-liquid mass transfer coefficient $k_L a$ was determined from reciprocal of the plot C_A^*/Ra against W^{-1}. The apparent activation energy was estimated by the plots of $ln(Ra)$ against T^{-1} as described in Section 6.5.5.8. Table 6.5.10 shows the mass transfer data. High values of $k_L a$ and low X_{L-S} indicated surface reaction rate control, in accordance with the higher activation energies stated above.

Figure 6.5.24 C_A^*/Ra vs. 1/W in Toluene

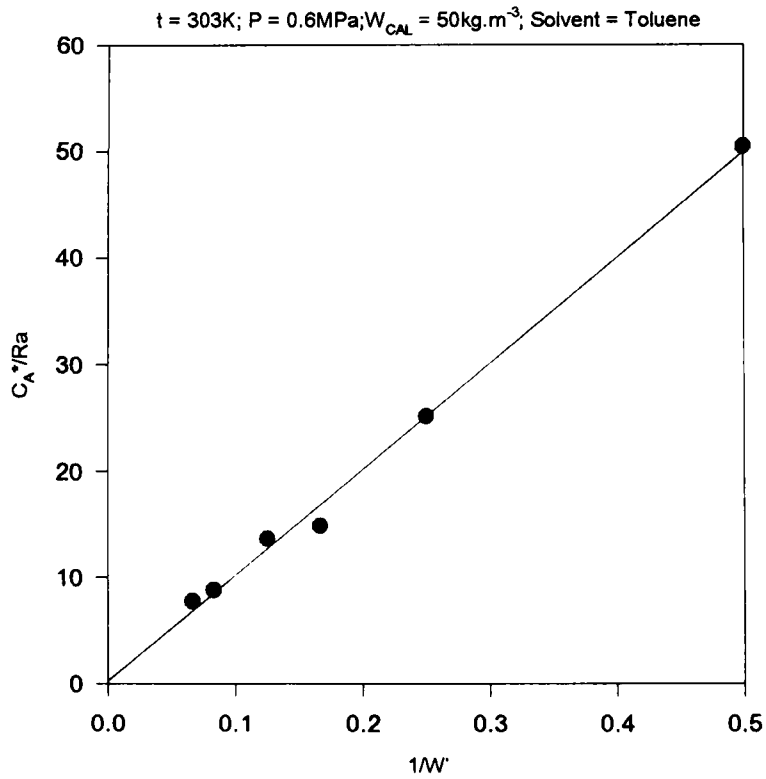

Figure 6.5.23 C_A^*/Ra vs 1/W' in Propan-2-ol (Pre-prepared)

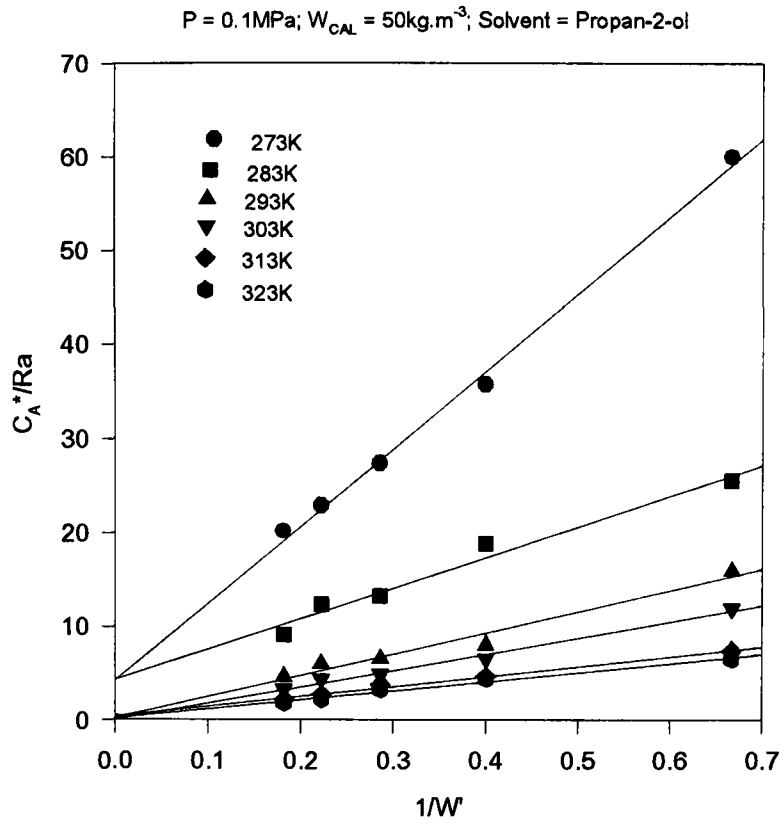

Table 6.5.10 Mass Transfer Results in Propan-2-ol

Solvent	T, K	k_La, s^{-1}	k_r, $m.s^{-1}$	k_S, $m.s^{-1}$	X_{L-s}, %
Propan-2-ol	273-303	0.70-2.3	7.21×10^{-5}-6.48×10^{-4}	0.021-0.64	0.33-1.01
Toluene	303	1.6	7.0×10^{-5}	0.068	0.1

6.6 Hydrogenation over Palladium Catalyst in the 50mm CDC Reactor

6.6.1 Introduction

The preliminary studies using stirred batch reactors have demonstrated that the hydrogenation of cinnamaldehyde in various organic solvents using palladium/charcoal catalysts for the production of hydrocinnamaldehyde can be used as model three-phase reaction systems for studying the CDC. The aims of this investigation were three-fold:

(1) To assess the applicability of the CDC to three-phase systems using various organic solvents as the liquid phases.

(2) To study the relative importance of mass transfer and intrinsic kinetics in the CDC and to evaluate the mass transfer coefficients based on the Frössling Equation.

(3) To investigate the selectivity with respect to hydrocinnamaldehyde in the CDC for academic and industrial interests.

The hydrogenation of cinnamaldehyde over 5% palladium on charcoal (type 37, non-porous, from Johnson Matthey Chemicals, UK) was carried out in a 50mm glass reactor. The previous studies in stirred batch reactors showed that toluene is the best non-polar solvent and propan-2-ol is the best polar solvent. However, due to the insufficiency of ventilation in the vicinity of the reactor and the toxicity of toluene only propan-2-ol was used as a solvent for the hydrogenation of cinnamaldehyde in the CDC reactor. The effect of catalyst loading and the temperature effect were examined. The details of the experiments are given in Section 4.1.5 and Section 5.7.

6.6.2 Calibrations

6.6.2.1 Calibration of the Liquid Flowmeter

The liquid flowmeter was calibrated by using water. While running tap water at room temperature through the CDC column through the flowmeter at a certain reading, the time required to receive a certain amount of water at the column outlet was used to calculate the actual flowrate. The results of the calibration are given in Table 8.6.6.1 and Figure 8.7.6.1. The following correlation was obtained:

$$F_{L,actual} = 0.779F_{L,read} + 0.0148F_{L,read}^2 \qquad (6.6.1)$$

6.6.2.2 Calibration of Reaction Volume

The reactor consists of two sections, an upper straight section and a lower expanded section. The upper section is a 50mm cylindrical glass column, and its reaction volume can be calculated from the height of the gas/liquid/solid dispersion. However, the reaction volume should be determined experimentally when the dispersion extended to the expanded section. Reference scales were attached on to the outer wall of the reactor. The reactor was initially filled with water and calibration was carried out by draining the water from the reactor. The volumes of water received at the outlet corresponding to the liquid levels in the reactor were recorded and the following correlation was obtained from the experimental data:

$$\text{for } h=0\text{-}120\text{cm}, \quad V_R = 2.0258\times10^{-2}\times h \qquad (6.6.2)$$

$$\text{for } h=120\text{-}135\text{cm}, \quad V_R = 2.4310+0.1823\times(h-120) \qquad (6.6.3)$$

where h is the axial distance in cm from the top of the column and V_R is the column volume in litres from the top of the reactor to the position h.

6.6.2.3 Calibration of Break Vessel Volume

In order to calculate the reaction rate per unit volume of liquid-phase and the gas holdup by the volume expansion method during the hydrogenation of cinnamaldehyde, it was essential to know the slurry volume change in the break vessel. Reference scales were attached to the outer wall of the break vessel. Table 8.6.6.2 and Figure 8.7.6.2 shows the liquid levels corresponding to known volumes of water in the break vessel. The following correlation was obtained:

$$V_B = 0.3423 \times h + 0.2368 \qquad (6.6.4)$$

where h is the height in cm from the bottom mark of the break vessel and V_B is the volume in litres contained at the position h.

6.6.3 Selectivity Studies

The results from the hydrogenation of cinnamaldehyde over a palladium/charcoal catalyst in the CDC in propan-2-ol were very similar to those from the stirred tank reactors.

(1) The products were produced simultaneously during the course of hydrogenation and hydrocinnamaldehyde was converted to its acetal due to the reaction between hydrocinnamaldehyde and propan-2-ol. During the whole hydrogenation in every run

in the CDC the percentage of hydrocinnamaldehyde acetal (See Appendix 8.8) remained almost constant, which suggested that the equilibrium was achieved readily in the CDC. This was different from the situation in the stirred batch reactors. The reason for this is that the CDC offers a more efficient mass transfer rate and a high interface area than in the stirred tank reactor (Boyes and Ellis, 1976; Lu, 1988; Khan, 1995). Again, the overall conversion of cinnamaldehyde was used to compare the selectivity.

(2) The hydrogen takeup rate stayed unchanged during the course of the hydrogenation, provided that the operating conditions were unaltered. This result indicated that the reaction rate was independent of both the reactant and the products.

6.6.3.1 Temperature Effect

The effect of temperature was examined by using a 50kg.m^{-3} cinnamaldehyde solution in propan-2-ol with a catalyst loading of 4kg.m^{-3}. The temperature range was 293-343K and the column pressure was kept at 0.2MPa. The results are given at Table 8.6.3 and Figure 6.6.1. It can be seen that the total selectivity with respect to hydrocinnamaldehyde and its acetal increased gradually with the temperature. In addition, when the temperature was greater than 313K the change in selectivity showed that most of hydrocinnamaldehyde was converted to its acetal because the rate of acetal formation at higher temperatures exceeds the rate of formation of hydrocinnamaldehyde. This finding agrees with the results in the stirred batch reactor (Zhang et al., 1995, 1996, 1997, and 1998).

Figure 6.6.1 Selectivity vs Temperature over Pd/C in the CDC

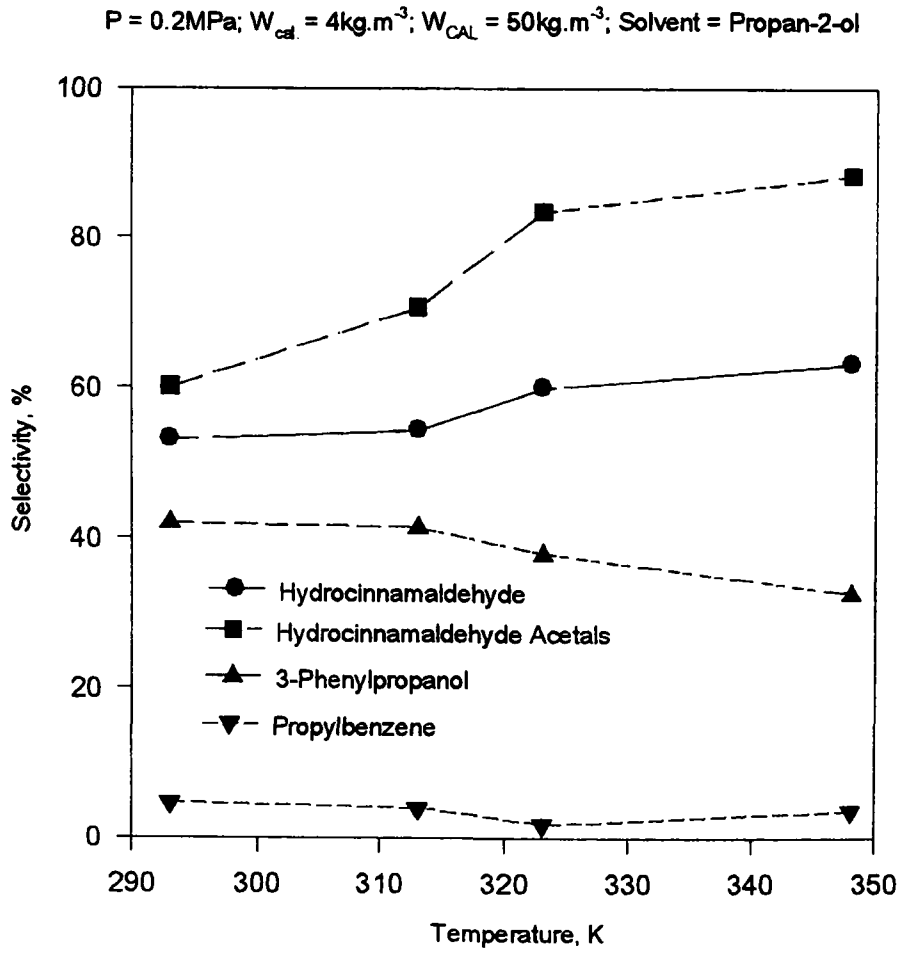

6.6.3.2 Catalyst Loading Effect

The effect of catalyst loading was carried out by using of 50kg.m^{-3} cinnamaldehyde concentration at 293K and 0.2MPa. The catalyst loading was 2, 4, or 8 kg.m^{-3}. The analytical results for the final samples are given at Table 8.6.6.4 and Figure 6.6.2. It can be seen that the catalyst loading has a negative effect on the selectivity with respect of hydrocinnamaldehyde. The amount of hydrocinnamaldehyde converted into its acetal increased with the amount of catalyst used, and the total selectivity was slightly reduced with increase in the catalyst loading. This suggested that the rate of the formation of the acetal is greater than the rate of hydrocinnamaldehyde and difference between both rates increased with increase in reaction temperature.

Figure 6.6.2 Selectivity vs Catalyst Loading over Pd/C in the CDC

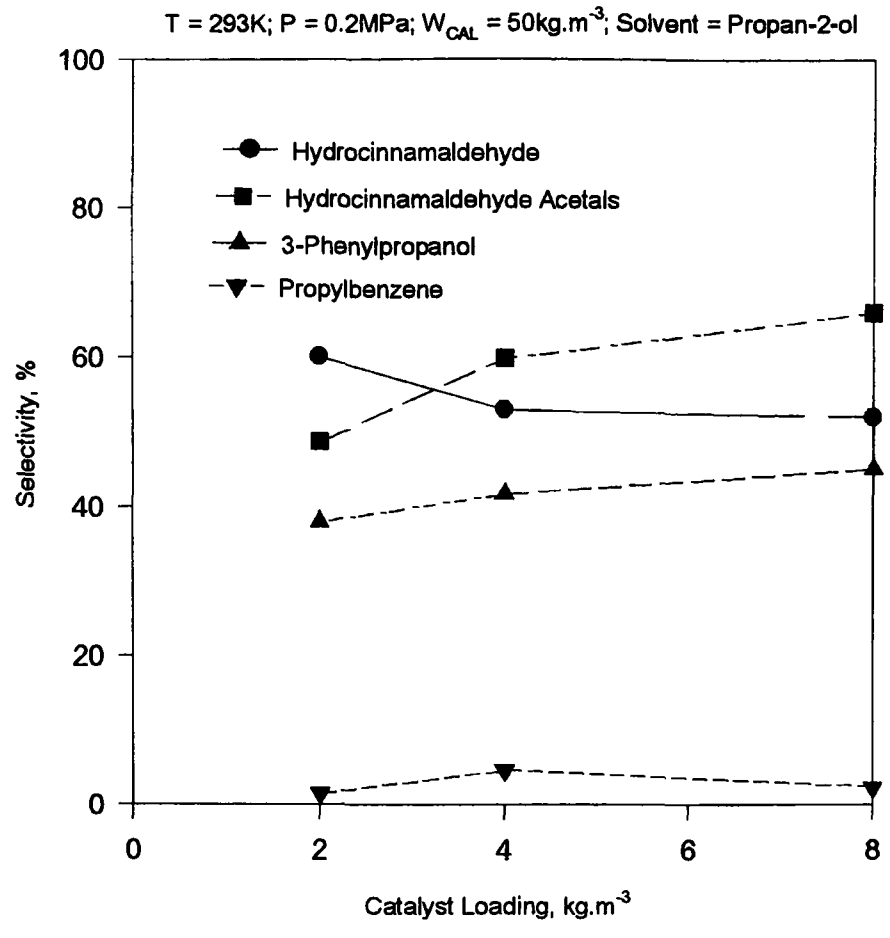

6.6.3.3 Effect of Cinnamaldehyde Conversion

It can be seen from the selectivity profiles in the CDC (see Appendix 8.8) that the selectivity with respect to hydrocinnamaldehyde remained almost constant during the course of the hydrogenation of cinnamaldehyde and a typical result is given in Figure 6.6.3. This suggests that chemical equilibrium was always achieved with palladium catalysts in the CDC. This finding is in contrast with the results from the stirred batch reactors, in which during the course of the reaction, as cinnamaldehyde was converted to hydrocinnamaldehyde, the selectivity to hydrocinnamaldehye decreased, rapidly at first, and then more slowly. This may have been the result of the relatively poor mass transfer characteristics of the stirred batch reactors resulting in a slow rate of establishment of chemical equilibrium, whereas in the CDC the chemical equilibrium can be achieved readily. This is in accordance with the finding that equilibrium in the

CDC for the physical absorption process the equilibrium is easily achieved in less than 10 seconds) (Boyes and Ellis, 1976; Lu, 1988).

Figure 6.6.3 Selectivity vs Conversion over Pd/C in the CDC

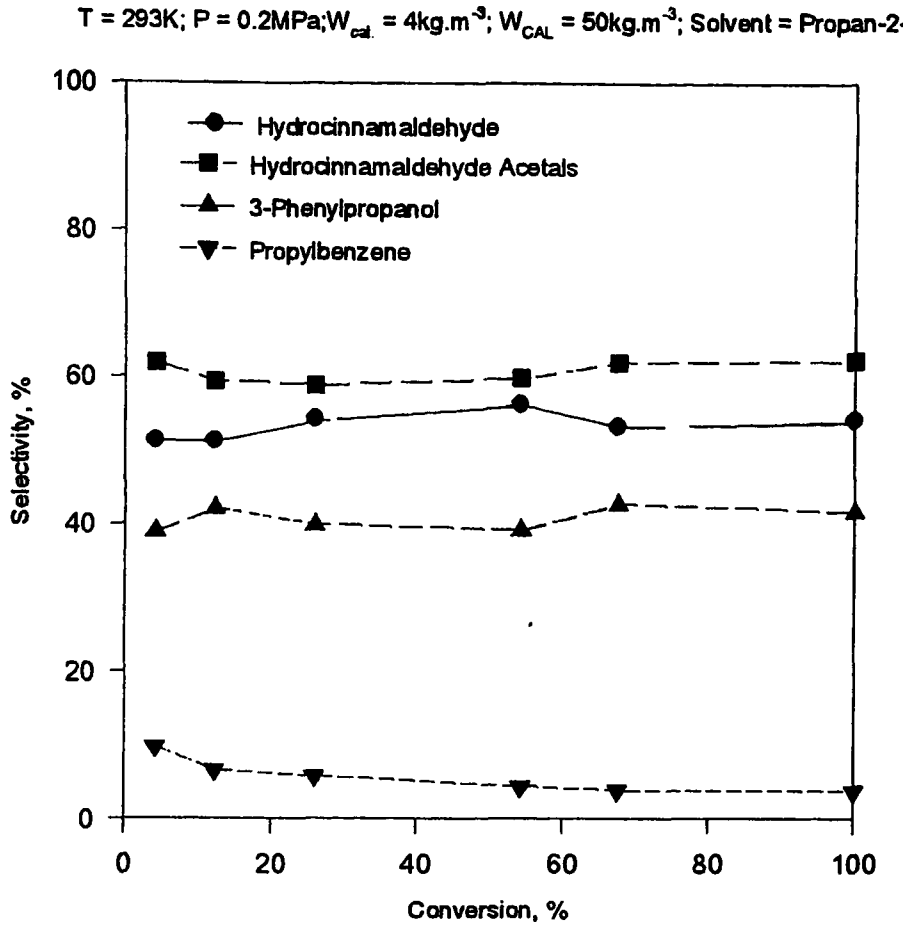

6.6.4 Kinetic Studies

In the CDC only the temperature and catalyst loading effects were examined in respect of their effect on the hydrogen consumption rate. However, the linear relationship between hydrogen takeup and time indicated that the reaction was first order for hydrogen concentration. This confirmed the previous finding in the stirred batch reactors.

6.6.4.1 Temperature Effect

The temperature effect was determined for the temperature range of 293-343K and a pressure of 0.2MPa. The cinnamaldehyde concentration was 50kg.m^{-3} and the catalyst loading was 4kg.m^{-3}. The results are given in Table 8.6.6.5 and Figure 6.6.4. As stated in Section 6.5, the apparent activation energy was calculated from the normal Arrhenius equation and was used to evaluate the relative importance of mass transfer and intrinsic kinetics. When comparing the hydrogenation rate at different temperature the observed rate has to be calibrated with the method used in the stirred tank reactors (see Section 6.5). The apparent activation energy from the experimental data is 45kJ.mol^{-1} so that the reaction is mainly surface reaction controlled.

Figure 6.6.4 Rate vs.Temperature over Pd/C in the CDC

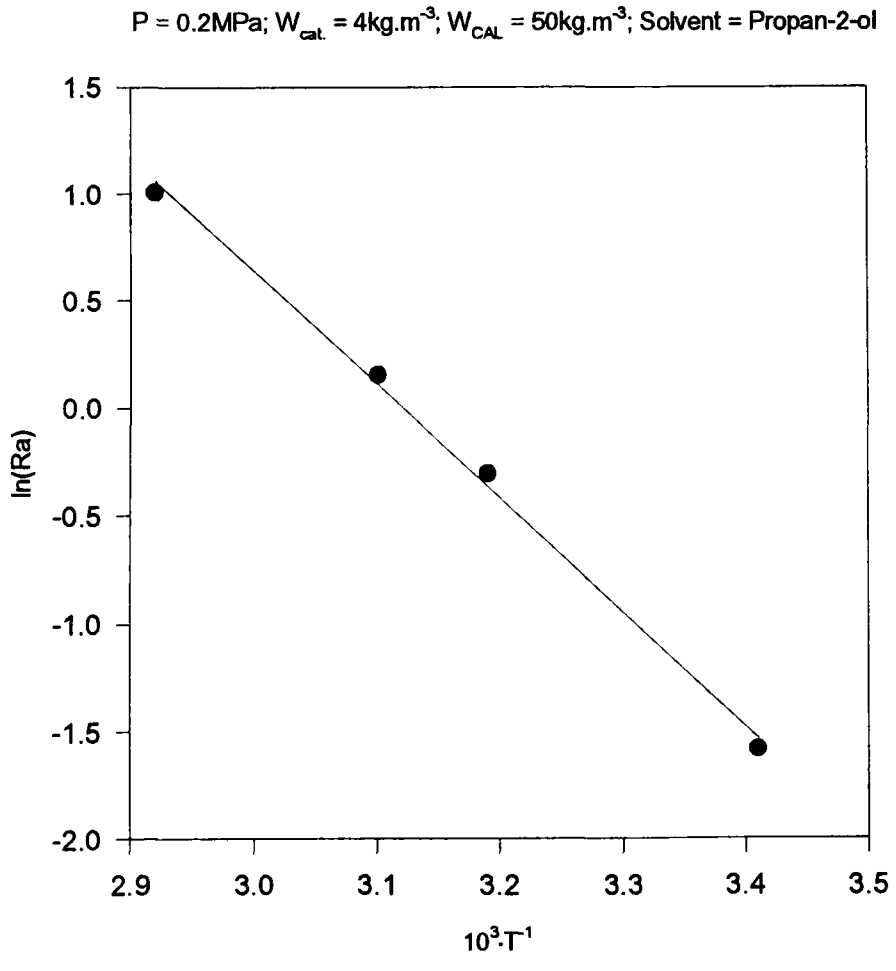

6.6.4.2 Catalyst Loading Effect

The catalyst loading effect was carried out by using propan-2-ol as the solvent at 293K and 0.2MPa with catalyst loadings of 2, 4, 6, and 8kg.m^{-3} and cinnamaldehyde concentration of 50kg.m^{-3}. The experimental data are given in Table 8.6.6.6 and Figure 6.6.5, and show that the reaction rate is proportional to the catalyst loading. This observation suggests that gas-liquid mass transfer resistance may not be important under these conditions and further supported the view that the reaction is first order with respect to hydrogen.

Figure 6.6.5 Rate vs Catalyst Loading over Pd/C in the CDC

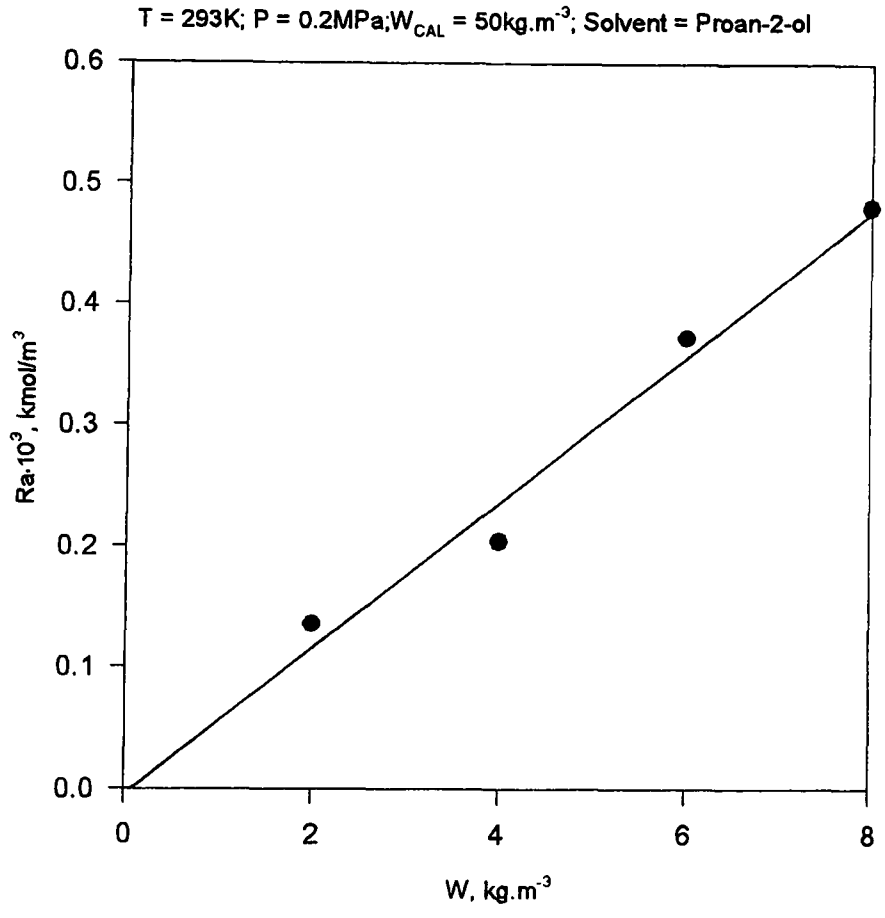

The results of the kinetics of the hydrogenation of cinnamaldehyde over palladium/charcoal catalyst in the CDC can be summarised by the following equation:

$$Ra = kC_{CAL}^{0} C_{cat}^{1.0} C_{H2}^{1} \qquad (6.6.5)$$

6.6.5 Mass Transfer Studies

The mass transfer investigation in the CDC was carried out at 293K and 0.2MPa in propan-2-ol with catalyst loadings of 2, 4, 6, and 8kg.m^{-3} and a cinnamaldehyde concentration of 50kg.m^{-3}. The mass transfer effect was evaluated by the Frössling equation and the first order model. Selecting the suitable liquid velocity is critical in order to assess the mass transfer coefficient. In the CDC, the Frössling equation was applied to the region from the T-piece where the gas and the slurry first interact, through the orifice and 25-30cm into the column. Much mass transfer between the gas and slurry occurred in this region. In this work the liquid velocity used for the calculation of the Reynolds Number (*Re*) was the column velocity giving the lowest value of *Re* and hence the Sherwood Number (*Sh*) and the liquid-solid mass transfer coefficient (k_s). This represents a worst-case calculation of k_s.

The high turbulence in systems with high rates of mass transfer mean that the relationship $Sh = 2.0$ cannot be used as it leads to a negative value for k_r^{-1}, which is clearly wrong. It has been suggested that for systems involving high shear rates and using small catalyst particles a full form of the Frössling equation is permissible (Treybal, 1981) using the liquid properties to calculate *Sh* and hence k_s. In the CDC there are three zones of application of the Frössling equation:

(1) The entry pipe between the gas-liquid mixing T-piece and the inlet orifice

(2) The inlet orifice

(3) The main reaction zone (bubble dispersion).

For this work a mean Reynolds Number for the above three zones was used as defined by

$$Re = \sqrt[3]{Re_1\ Re_2\ Re_3} \qquad (6.6.7)$$

The plot of $\frac{C^*}{Ra}$ against $\frac{1}{W_{cat}}$ is presented in Figure 6.6.6 for which k_La is calculated from the intercept, k_r from the slope and k_s from the Frössling equation. The results are given in Table 6.6.1.

Figure 6.6.6 C*/Ra vs 1/W over Pd/C in the CDC

T = 293K; P = 0.2MPa; W_{CAL} = 50kg.m^{-3}; Solvent = Propan-2-ol

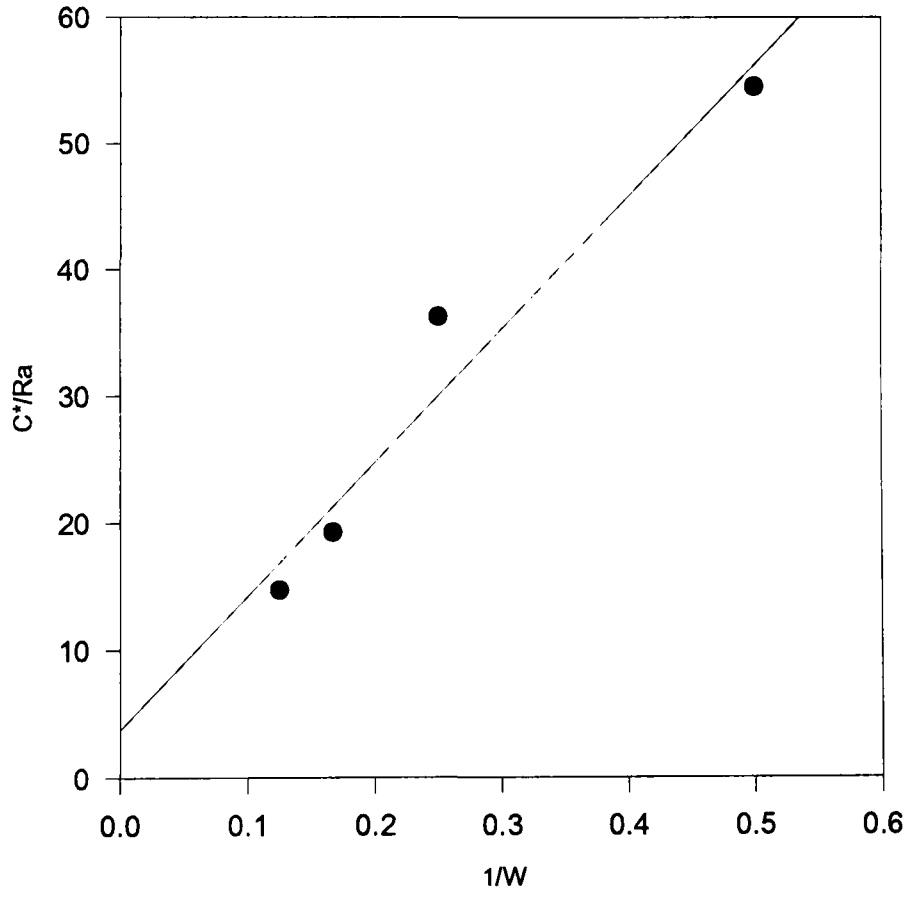

Table 6.6.1 Transport Parameters for Palladium/Charcoal in the CDC

T, K	P, MPa	W_{CAL}, kg.m^{-3}	$W_{cat.}$, kg.m^{-3}	k_La, 1.s^{-1}	k_s, m.s^{-1}	k_r, m.s^{-1}	$X_{L\text{-}S}$, %
293	0.2	50	2-8	0.264	0.0591	6.49×10^{-5}	0.11

That the mass transfer effect is not important for the hydrogenation of cinnamaldehyde in propan-2-ol over a palladium/charcoal catalyst. This proved the previous finding for stirred tank reactors that the reaction is mainly surface reaction controlled so that improving mass transfer would not accelerate the overall rate for this particular case. In fact, the observed reaction rates in the CDC did not increase compared with those obtained in the stirred tank reactors. One reason for this is that the CDC did not behave properly due to the low liquid flowrate supplied by the pump.

6.7 Hydrogenation over Platinum catalyst in Stirred Tank Reactors

6.7.1 Introduction

The preparation of unsaturated alcohols by the hydrogenation of α,β-unsaturated aldehydes on transition metal catalysts is a subject of continuous industrial and academic interest (Gallezot et al, 1991). The selectivity to the unsaturated alcohol is governed by the nature of the metal and by the presence of additives (Rylander, 1979). Palladium is quite unselective, osmium and iridium are intrinsically selective, and the selectivity of platinum can be improved by promoters. Addition of metallic salts to the reaction medium has long been known to increase the selectivity of platinum catalysts (Tuley and Adams, 1925). However, the mode of action of these additives remains obscure; thus it is still not established if they are attached to the base metal, and their oxidation states are uncertain. The selectivity of platinum metal catalysts can be improved also by the addition of Brϕnsted or Lewis bases (Bakhanova et al, 1972; Pascoe and Stenberg, 1979), but the reasons for these promoting effects are not yet known. Other factors, such as the nature and texture of the support or the morphology of the metal particles, might improve selectivity.

The aims of this work are (1) to study the effects of various factors on the selective hydrogenation of cinnamaldehyde towards cinnamyl alcohol over platinum catalysts; (2) to study the kinetics; and (3) to seek the optimal combination of catalyst and reaction conditions for the clean synthesis towards economic industrial production of cinnamyl alcohol. In-house prepared and commercial platinum catalysts supported on graphite were used to study the selectivity in propan-2-ol, toluene, water, propan-2-ol/water and toluene/water in gas/liquid and gas/liquid/liquid systems. A base

promoter (potassium hydroxide or sodium hydroxide) was used to modify the catalysts. The results discussed in this section were obtained at temperatures of 273-373K and pressures of 0.1-1.1MPa in a 500ml stirred batch reactor (SBR).

6.7.2 General Observations

The hydrogenation of cinnamaldehyde over commercial platinum/graphite catalysts (Type 286 from Johnson Matthey Materials, UK) and in-house prepared catalysts was carried out in a stirred tank reactor. The platinum metal was deposited entirely on the exterior surface of the support, so pore diffusion was not considered to be important in the experiments.

(1) No distinct step changes occurred during the course of the hydrogenation of cinnamaldehyde. The effect of initial cinnamaldehyde concentration on the hydrogen take-up rate indicated that the hydrogen take-up rate is independent of the initial cinnamaldehyde concentration, therefore the initial hydrogen take-up rate based on hydrogen consumption measured by the recorder of a hydrogenation control unit was used for the kinetic studies.

(2) Sample analysis (Section 6.5.3) indicated that all the products were observed even in the initial samples showing that all the products were produced rapidly, so the reaction would be complex, and the reaction scheme given in Section 6.5 is applicable to platinum catalysts. In addition, more than one mole of hydrogen was required for the complete conversion of one mole of cinnamaldehyde, so that the overall conversion

of cinnamaldehyde over platinum/graphite catalysts was used to compare the extent of the hydrogenation.

(3) Preliminary studies indicated that when alcohol solvents were used in the presence of a base, aldol condensation would occur to produce orange-coloured products. Blank experiments without catalysts confirmed this.

6.7.3 Selectivity Investigations

6.7.3.1. Solvent Effect

In order to select a suitable solvent for the production of cinnamyl alcohol, propan-2-ol, water, toluene, propan-2-ol/water, and toluene/water were used as the solvents. When liquid/liquid solvent system were used, the component proportions were varied to find the optimal composition for the formation of cinnamyl alcohol.

(1) Water as the Solvent

When water was used as the solvent the platinum catalysts adhered to the reactor walls due to coagulation, and the low aqueous solubility of cinnamaldehyde caused it to become attached to the catalyst so that the catalyst utilization was extremely poor. The dispersion of the catalyst can be improved by the addition of an aqueous-miscible liquid more able to wet the catalyst, such as propan-2-ol.

(2) Toluene as the Solvent

Toluene was the best solvent for the production of hydrocinnamaldehyde with a palladium/charcoal catalyst (see Section 6.5), but when a platinum/graphite catalyst was used the main product was still hydrocinnamaldehyde instead of cinnamyl alcohol regardless of the addition of a base to the catalyst.

(3) Propan-2-ol/Water as the Solvent

Propan-2-ol was the preferred polar solvent for the production of hydrocinnamaldehyde with palladium/charcoal catalysts. The selectivity to cinnamyl alcohol was higher in propan-2-ol/water media with platinum/graphite catalysts and with the presence of a base but a small amount of aldol condensation product was produced.

(4) Toluene/Water as the Solvent System

Catalyst utilisation is inefficient in water (see above) and in toluene the unmodified and modified platinum catalysts showed poor selectivity to cinnamyl alcohol. Platinum catalysts had to be promoted by the addition of inorganic salts or by alloying with metals such tin or iron. Water and toluene used together provided a good environment for both promoter and substrate and may improve the selectivity and catalyst performance. Mixtures containing from 0.1-10 volumes of toluene per volume of water were used at 288K and 0.9MPa with an initial cinnamaldehyde concentration of $50kg.m^{-3}$, a catalyst loading of $10kg.m^{-3}$ and a base loading of $50kg.m^{-3}$. The results are

given in Table 8.6.7.1 and Figure 6.7.1. It can be seen that the selectivity to cinnamyl alcohol was highest when the ratio of toluene to water was from 1:1 to 5:1. Above this range the selectivity to cinnamyl alcohol dropped sharply. . From the view of economics a 1:1 ratio would be best and kinetic studies also showed that the reaction rate was highest (see Section 6.7.4) at a solvent ratio of 1:1. Therefore 1:1 was the best solvent ratio.

As stated previously the platinum/graphite catalyst is very difficult to disperse in the water phase due to coagulation and the solubility of toluene in the water is very low (about 5×10^2ppm). However, it was observed that in the toluene/water solvent system the catalyst dispersed in the water phase instead of in the toluene phase so that it is assumed that the catalyst initially dispersed into toluene but then transferred into the water phase.

For a gas/liquid/liquid slurry phase, the CDC not only gives a high gas-liquid interfacial area, but also a high liquid-liquid interfacial area. The catalyst appeared to preferentially exist in the water phase. However, it is assumed that its reaction occurs at gas-liquid-liquid interface. This would seem to be confirmed by the fact that the optimum toluene/water ratio is about 1:1.

Figure 6.7.1 Selectivity vs Toluene/Water Ratio

T = 288K; P = 0.9MPa; W_{CAL} = 50kg.m^{-3}; W_{Base} = 50kg.m^{-3}; $W_{cat.}$ = 10kg.m^{-3}; Solvent = Toluene/Water

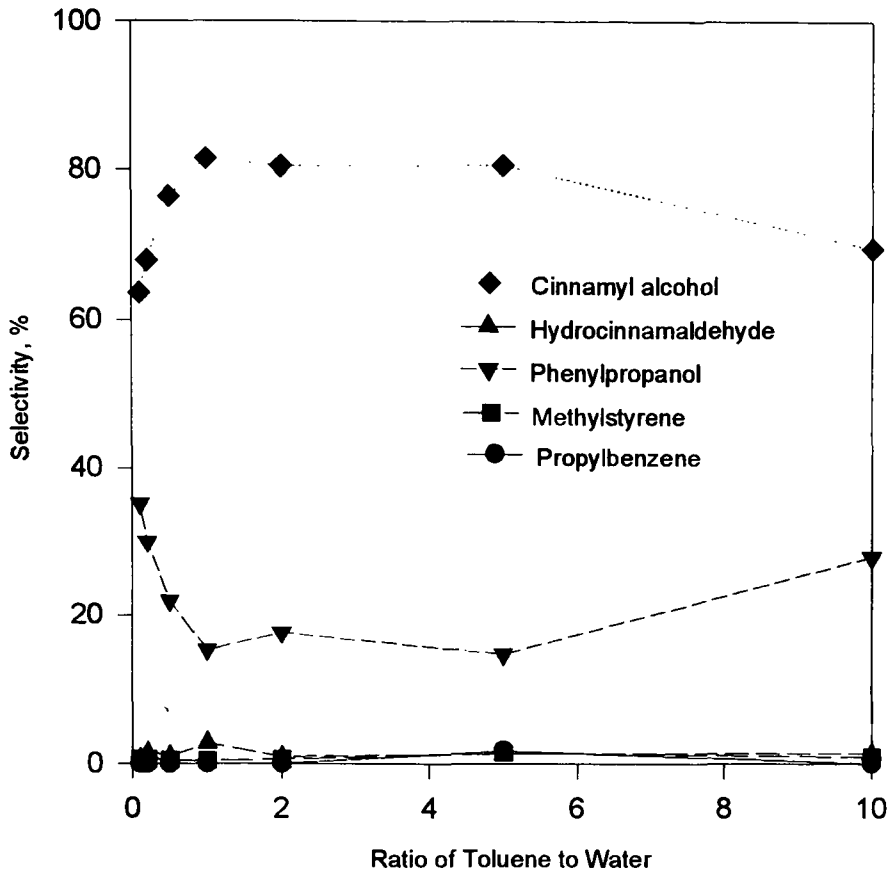

6.7.3.2. Catalyst Loading Effect

The effect of catalyst loading on the selectivity to cinnamyl alcohol was investigated at 303K and 0.9MPa in toluene/water (2:1) with 50kg.m^{-3} of cinnamaldehyde concentration of and 50kg.m^{-3} of base loading. The results are given in Table 8.6.7.2 and Figure 6.7.2. The selectivity to cinnamyl alcohol varied slightly with the catalyst loading. This slight variation in selectivity was possibly due to a real difference of conversion of cinnamaldehyde because the comparison was not at the same extent of cinnamaldehyde conversion, even though at intermediate and high conversion the selectivity to cinnamyl alcohol varied only slightly. This suggests that catalyst concentration had little effect on selectivity.

Figure 6.7.2 Selectivity vs Catalyst Loading

T = 303K; P = 0.9MPa; W_{CAL} = 50kg.m^{-3};

W_{Base} = 50kg.m^{-3}; Solvent = Toluene/Water (2:1)

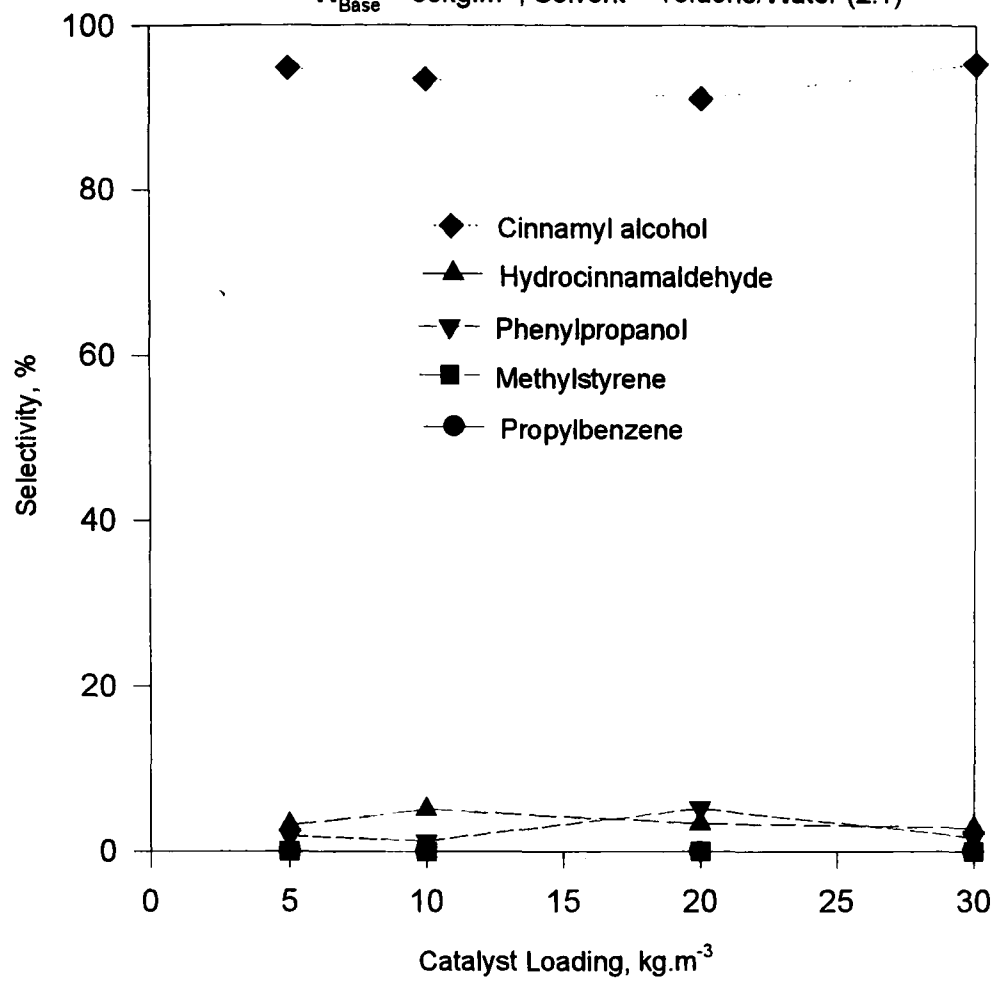

6.7.3 Initial Cinnamaldehyde Concentration Effect

The effect of initial cinnamaldehyde concentration was investigated using initial concentrations of 10, 30, 50, 75 and 100kg.m^{-3} in toluene/water (1:1) at 288K and 0.9MPa with a catalyst loading of 10kg.m^{-3} and a base loading of 50kg.m^{-3}. The results are given in Table 8.6.7.3 and Figure 6.5.3. At 288K the selectivity to cinnamyl alcohol increased rapidly with increase of initial cinnamaldehyde concentration between 10kg.m^{-3} and 75kg.m^{-3} but decreased with further increase of cinnamaldehyde concentration. The selectivity to hydrocinnamaldehyde decreased but that to cinnamyl alcohol increased.

Figure 6.7.3 Selectivity vs Cinnamaldehyde Concentration

T = 288K; P = 0.9MPa; W_{CAL} = 50kg.m^{-3}; W_{Base} = 50kg.m^{-3};
$W_{cat.}$ = 10kg.m^{-3}; Solvent = Toluene/Water (1:1)

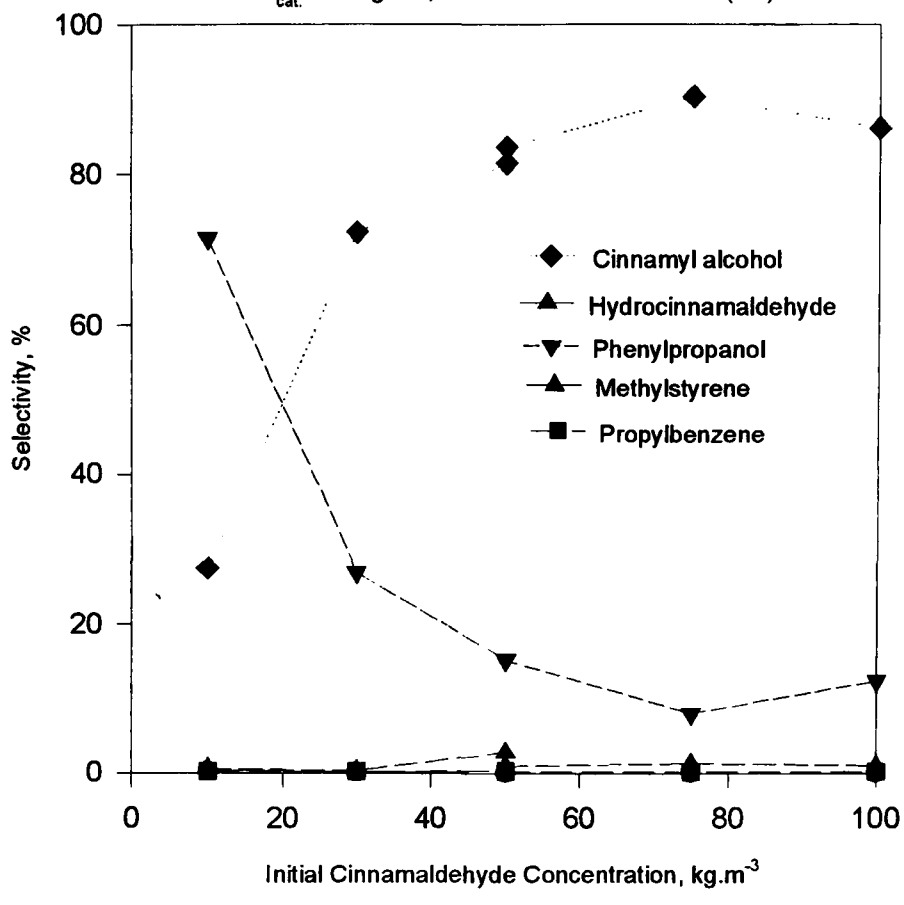

A second comparison was made at 303K under identical conditions, but with the initial cinnamaldehyde concentration at 30, 50 and 100kg.m^{-3}. The results are given in Table 8.6.4 and Figure 6.7.4 and show little change in the selectivity to cinnamyl alcohol over the selected range. The initial cinnamaldehyde concentration was not significant at 303K in respect of cinnamyl alcohol selectivity although the comparison was not made at identical conversions,.

Figure 6.7.4 Selectivity vs Cinnamaldehyde Concentration

T = 303K; P = 0.9MPa; W_{CAL} = 50kg.m^{-3};

W_{Base} = 50kg.m^{-3}; $W_{cat.}$ = 10kg.m^{-3}; Solvent = Toluene/Water (1:1)

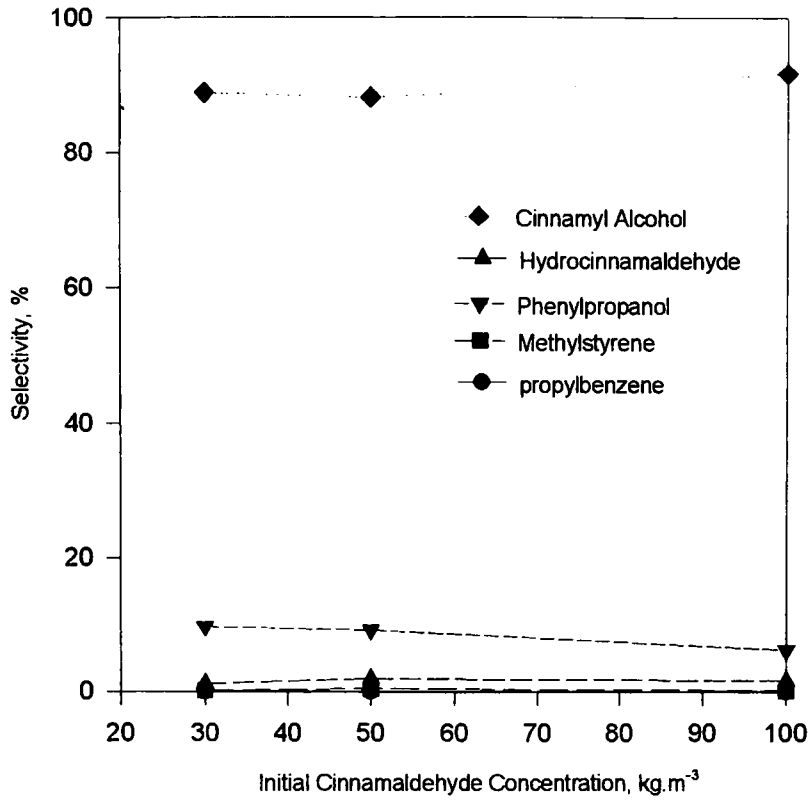

The initial cinnamaldehyde concentration effect except for the range of cinnamaldehyde concentration 75-100kg.m^{-3} at 288K disagrees with results of other workers (Phillips et al, 1993; Coq et al, 1993) that during the course of hydrogenation of cinnamaldehyde the selectivity to cinnamyl alcohol increased with time at the early stage (the higher the cinnamaldehyde concentration the lower the selectivity to cinnamyl alcohol), but in the case of conversion effect the products produced at different stage played an important role (Coq et al, 1993).

In view of the above results at 288K and 303K an initial cinnamaldehyde concentration of 50kg.m^{-3} was used in most experiments.

6.7.4 Base Effect

The effect of base-type on the selectivity was investigated using water, toluene, toluene/water, propan-2-ol and propan-2-ol/water as solvents. Potassium hydroxide was used as the promoter in most experiments and sodium hydroxide was also used in a few runs to compare the influence on the selectivity. The effect of base loading was studied by incorporation of potassium hydroxide in the reaction system. Two ways of adding potassium hydroxide to the reaction system were examined, by pre-treating the platinum catalyst with potassium hydroxide and by using potassium hydroxide in aqueous solution. The base effect varied with the temperature and the solvent used.

(1) Water as Solvent

The base loading effect was examined at 333K and 373K and 1.1MPa with a catalyst loading of 20kg.m^{-3} and an initial cinnamaldehyde concentration of 50kg.m^{-3}. The potassium hydroxide loading ranged from 1-10kg.m^{-3} at 333K and 5-15kg.m^{-3} at 373K. The results at 333k are given in Table 8.6.7.5 and Figure 6.7.5 and those at 373K in Table 8.6.7.6 and Figure 6.7.6.

At 333K the selectivity to cinnamyl alcohol increased and that to hydrocinnamaldehyde decreased with increase in base loading, but at 373K the selectivity to cinnamyl alcohol decreased with increase in base loading. At 373K the reaction was still through cinnamyl alcohol, but the cinnamyl alcohol hydrogenated further to 3-phenylpropanol and β-methylstyrene because high temperature favoured the further hydrogenation of cinnamyl alcohol.

Figure 6.7.5 Selectivity vs Base Loading at 333K in Water

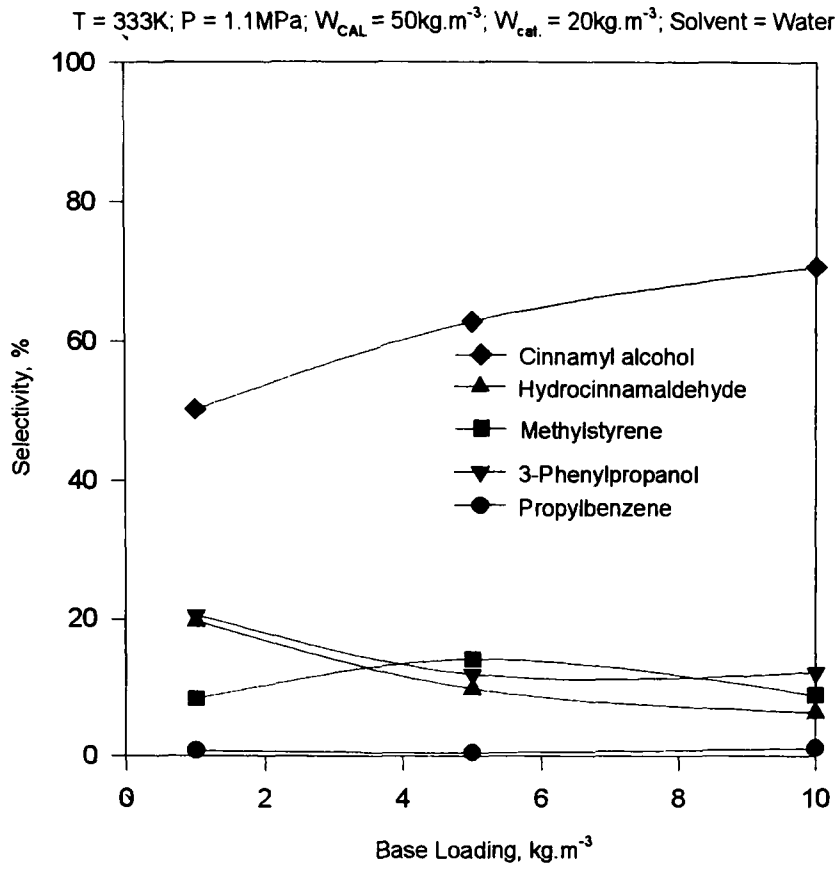

Figure 6.7.6 Selectivity vs Base Loading at 373K in Water

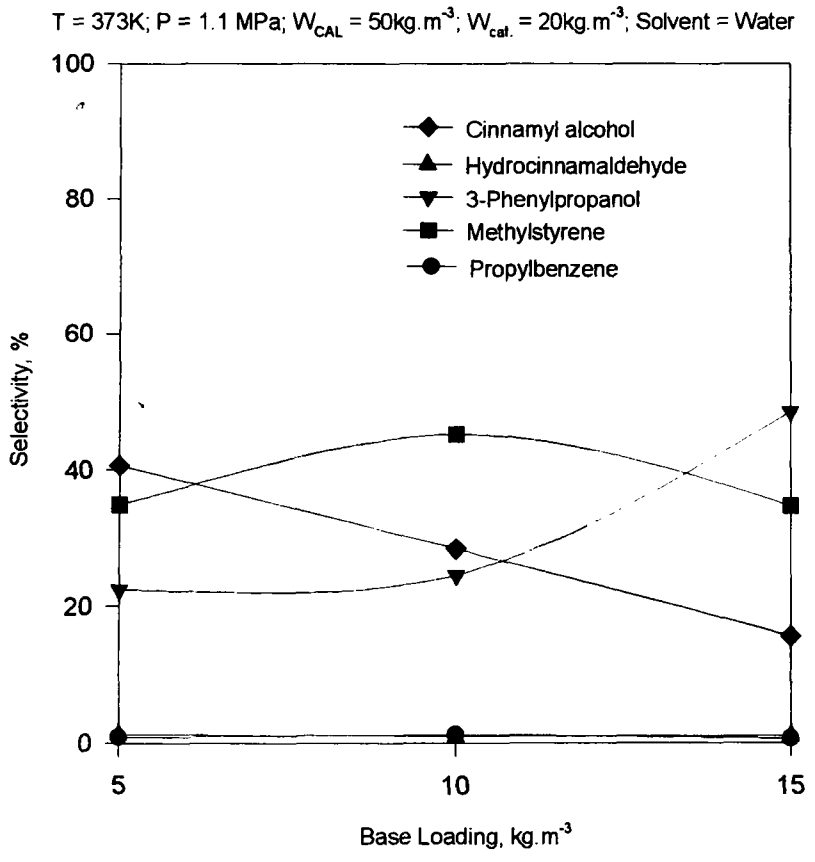

(2) Propan-2-ol/Water as Solvent

In order to determine the best reaction conditions for maximum selectivity to cinnamyl alcohol 15kg.m^{-3} aqueous potassium hydroxide was used as the aqueous phase, so when the base loading was altered the ratio of propan-2-ol to water was changed. The base effect was investigated at 373K and 1.1MPa with an initial cinnamaldehyde concentration of 50kg.m^{-3} and a catalyst loading of 20kg.m^{-3}. The base loading varied from 0.1kg.m^{-3} to 5kg.m^{-3} and the ratio of propan-2-ol to water varied from 2:1 to 150:1. When there was no base present in the system the reaction rate was relatively low and the selectivity with respect to cinnamyl alcohol was poor since substantial amounts of hydrocinnamaldehyde and phenylpropanol were formed. When potassium hydroxide was added, a substantial improvement in the selectivity to cinnamyl alcohol was observed, with a higher reaction rate. When platinum/graphite catalyst pre-treated with potassium hydroxide was used and the solvent was propan-2-ol only the selectivity to cinnamyl alcohol was very poor and the reaction rate was low, suggesting that K^+ or OH^- would be the promoter function group. Some of the results are given in Table 8.6.7.7 and Figure 6.7.7. The highest selectivity to cinnamyl alcohol was obtained with a 5kg.m^{-3} base loading with a propan-2-ol to water ratio of 2:1. Although in these experiments the base loading effect and the propan-2-ol to water ratio effect coexisted, at a lower ratio of propan-2-ol to water the base loading effect prevailed but at a lower base loading the effect of the ratio of propan-2-ol to water predominated. For a base loading of 0.1kg.m^{-3} to 2.5kg.m^{-3} and a resultant propan-2-ol to water ratio change of 150:1 to 5:1 the selectivity to cinnamyl alcohol decreased with base loading, suggesting that a large ratio of propan-2-ol to water would be better for the production of cinnamyl alcohol. However, an experiment conducted at 293K and

1.1MPa using pure propan-2-ol as the solvent yielded a poor selectivity to cinnamyl alcohol. It seemed, therefore, that K^+ or OH^- promoted the catalyst performance and effected the selectivity to cinnamyl alcohol. Chen et al (1993) also reported that aqueous ethanol was better than pure ethanol for the production of cinnamyl alcohol.

The addition of potassium hydroxide to the reaction system with toluene as the solvent did not improve the catalyst performance nor the selectivity, since toluene is aprotic and does not dissolve potassium hydroxide. However, further experimental evidence is needed to support this proposal. The aim of this project is to give clean synthesis of cinnamyl alcohol, so when toluene/water was proved to the best solvent system further experiments with propan-2-ol were ceased. It was noticed also that in propan-2-ol with a base, a small amount (up to 5%) of aldol condensation products was produced and this amount increased with increase in base loading within the range tested.

Figure 6.7.7 Selectivity vs Base Loading at 373K in Propan-2-ol/water

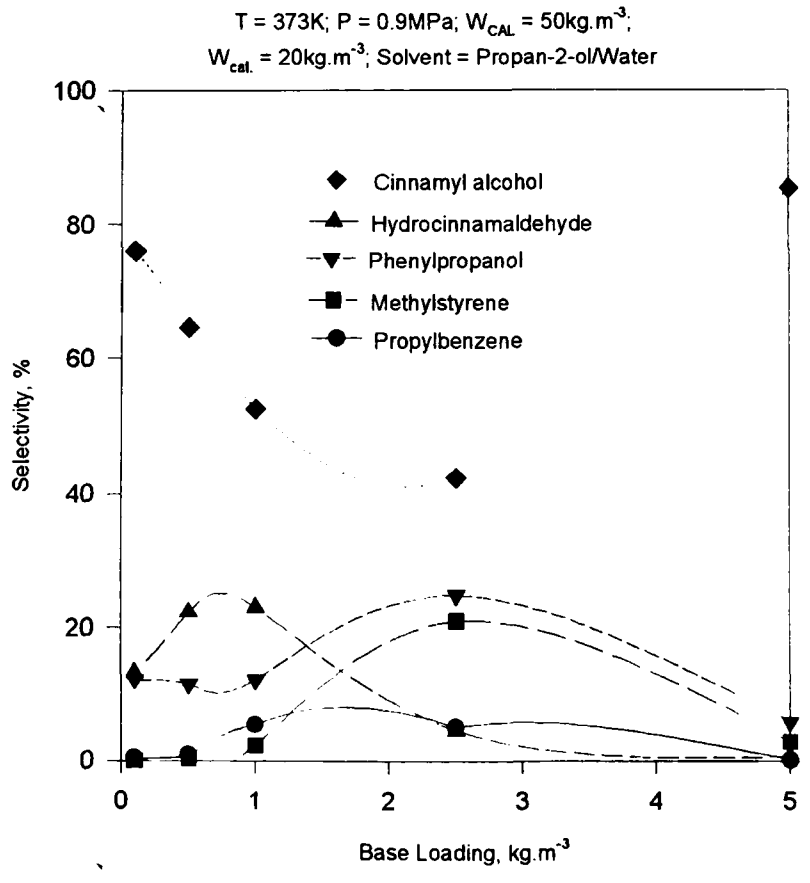

(3) Toluene as Solvent

The base effect on the selectivity in toluene was tested at 323K and 1.1MPa, and 303K and 0.2MPa with an initial cinnamaldehyde concentration of 50kg.m^{-3} and a catalyst loading of 20kg.m^{-3}. The results are given Table 6.7.1. It is clear that in this solvent the main product was hydrocinnamaldehyde and the base effect on the selectivity was very weak. It was noted that when toluene was used as the solvent the platinum/graphite catalyst settled on the bottom of the autoclave. The base had no effect in this system since toluene is aprotic, and cannot hydrolyse the base. Any base effect would be due to a small concentration of water in the toluene.

Table 6.7.1 Selectivity vs Base loading in Toluene

W_{CAL} = 50kg.m^{-3}; $W_{cat.}$ = 20kg.m^{-3}; Solvent = Toluene

W_{Base}, %	T, K	X_{conv}, %	S_{PB}, %	S_{MS}, %	S_{HC}, %	S_{PP}, %	S_{COL}, %
None	323	5.18	5.87	2.17	52.69	0	39.27
50	323	9.71	0	4.71	55.49	0	39.8
None	303	37.93	0.34	0	59.14	33.85	6.67
50	303	17.25	11.66	19.26	51.34	7.52	10.22

(4) Toluene/Water as Solvent

When there is no base in the reaction system the reaction rate is quite slow and the selectivity to cinnamyl alcohol is poor. Addition of a base such as potassium hydroxide into the reaction system could increase the reaction rate significantly and improve the selectivity. The experiments to investigate the base loading effect were carried out with an initial cinnamaldehyde concentration of 50kg.m^{-3} and a catalyst loading of 10kg.m^{-3} at various temperatures and pressures. Table 8.6.7.8 and Figure 6.7.8 summarise the

results obtained at 303K and 0.9MPa with a base loading of 0-50kg.m^{-3} in toluene/water (2:1) at high conversion. Table 8.6.7.9 and Figure 6.7.9 show the results obtained at 303K and 0.2MPa with a base loading of 5-50kg.m^{-3} in toluene/water (1:1) at 28% to 50% of conversion. Table 8.6.7.10 and Figure 6.7.10 show the results obtained at 303K and 0.9MPa with a base loading of 1-10kg.m^{-3} in toluene/water (1:1) at higher conversion. The data show that the selectivity to cinnamyl alcohol increased rapidly at first with increase in the base loading and then more slowly. The more potassium hydroxide was incorporated the higher would be the selectivity with respect to cinnamyl alcohol. Solutions containing more than 100kg.m^{-3} of base loading were not examined since it was found that when higher base loadings were used the base solution should be added last to the system. Over 95% selectivity to cinnamyl alcohol (see Table 8.6.7.2 and Figure 6.7.2) was obtained at 303K and 0.9MPa with a base loading of 50-100kg.m^{-3}. Experiments were conducted at 288K and 0.2MPa with a base loading of 2-50kg.m^{-3} to investigate the base loading effect. The highest selectivity to cinnamyl alcohol was achieved at a 50kg.m^{-3} base loading. It is possible that the general effect of base loading is applicable to these conditions because some of these results were obtained in a very low conversion (less than 6%, within the conversion effect range) due to a very low reaction rate. Further experiments may be required in the future to shed light on these lower temperature studies.

Figure 6.7.8 Selectivity vs Base Loading at 303K in Toluene/Water (2:1)

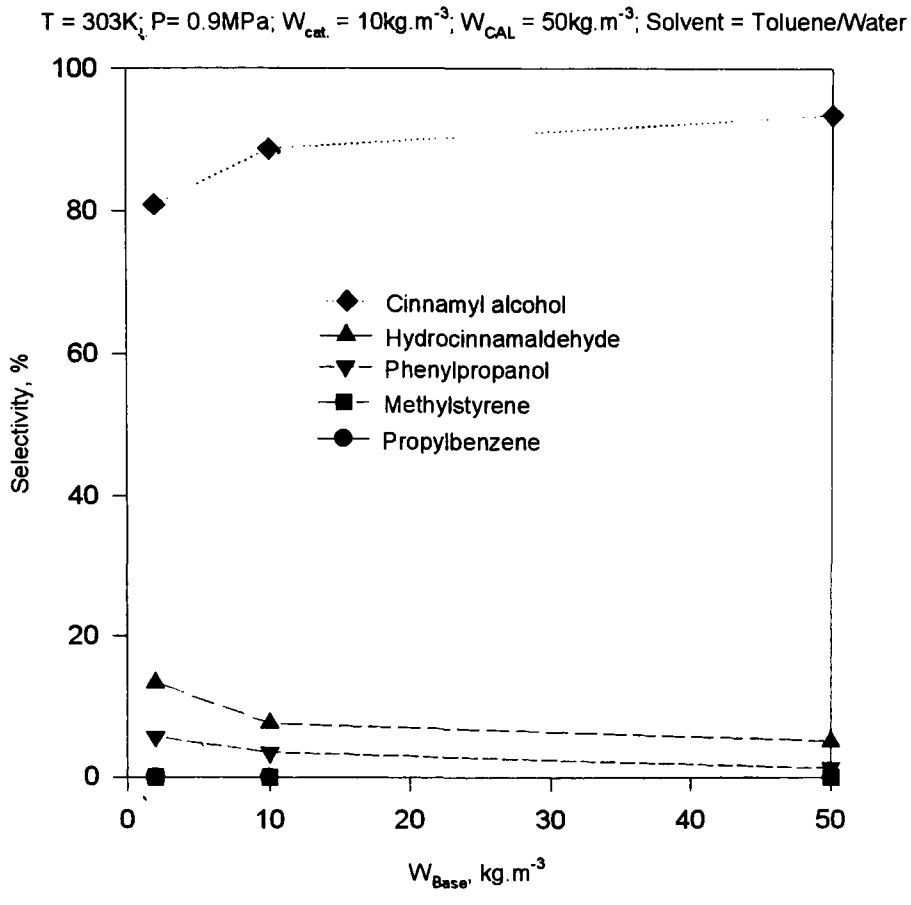

Figure 6.7.9 Selectivity vs Base Loading at 303K in Toluene/Water (1:1)

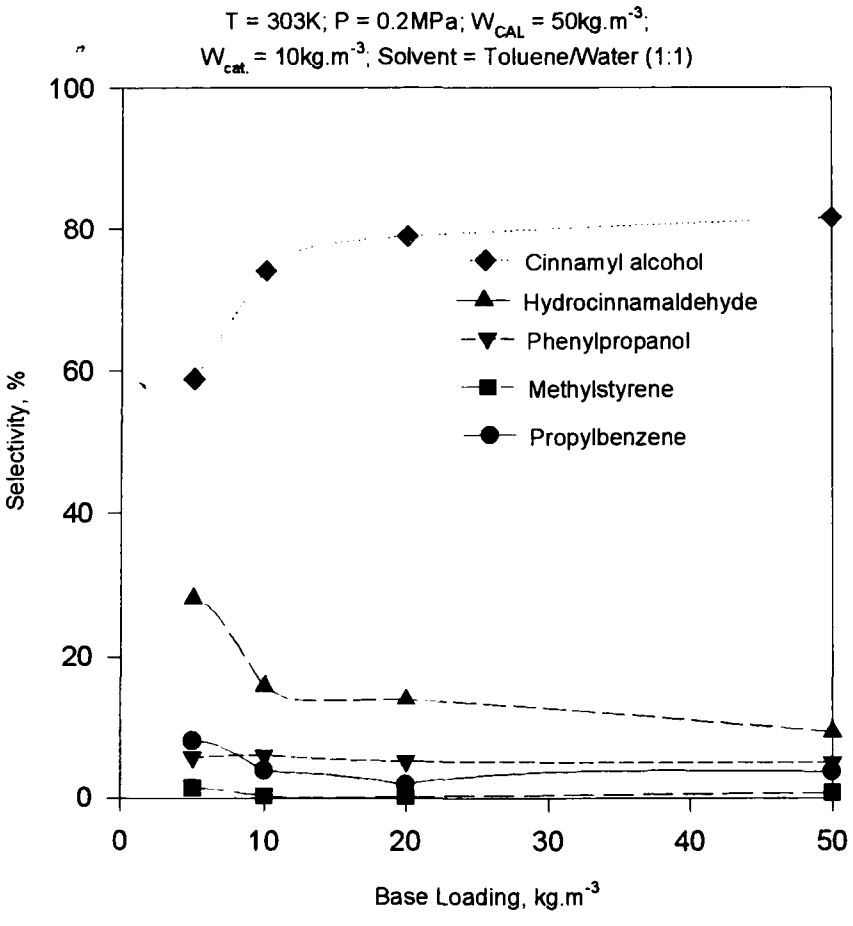

Figure 6.7.10 Selectivity vs Base Loading at 303K in Toluene/Water (1:1)

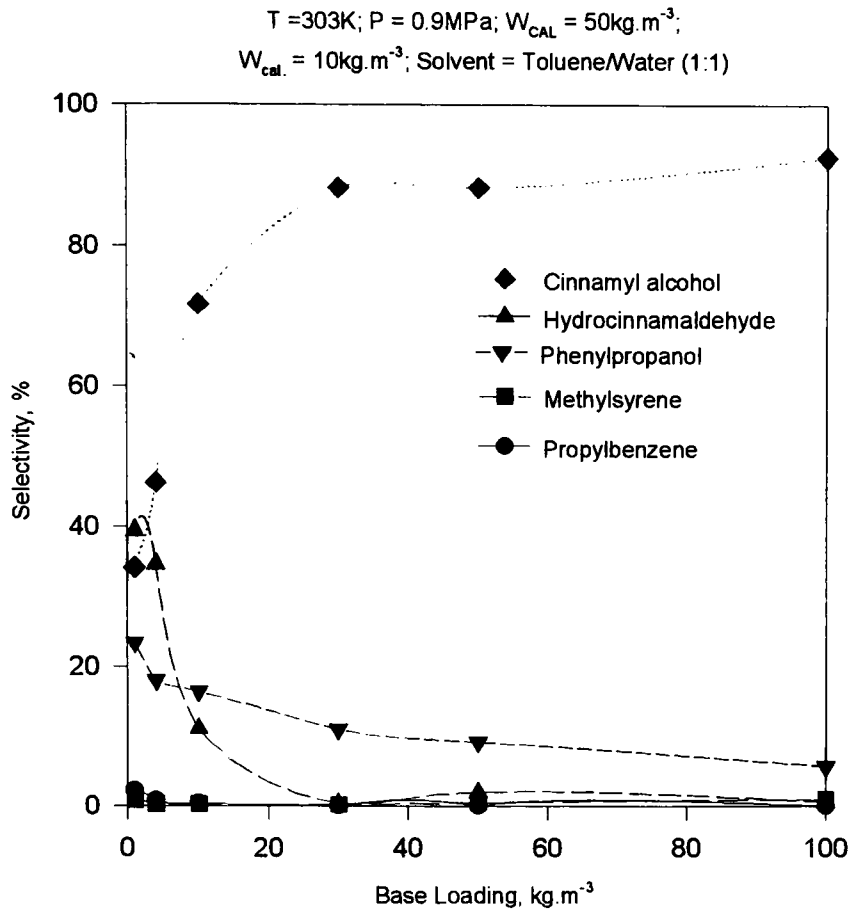

6.7.5 Temperature Effect

The temperature effect on the selectivity was investigated using water, propan-2-ol/water and toluene/water as the solvents with an initial cinnamaldehyde concentration of 50kg.m^{-3}.

(1) Water as the Solvent

The temperature effect on selectivity in water was investigated at 1.1MPa with a catalyst loading of 20kg.m^{-3} and a base loading of 5kg.m^{-3}. The temperature range was 293-373K. The results are given in Table 8.6.7.11 and Figure 6.7.11 and show that temperature had a negative effect on the formation of cinnamyl alcohol: the lower the temperature the higher the selectivity to cinnamyl alcohol can be achieved. This is due

to the fact the further hydrogenation of cinnamyl alcohol occurs readily at higher temperatures so that more β-methylstyrene and phenylpropanol were produced at higher temperatures.

Figure 6.7.11 Selecitivity vs Temperature in Water

P = 1.1MPa; W_{CAL} = 50kg.m^{-3}; W_{cat} = 20kg.m^{-3}; W_{Base} = 5kg.m^{-3}; Solvent = Water

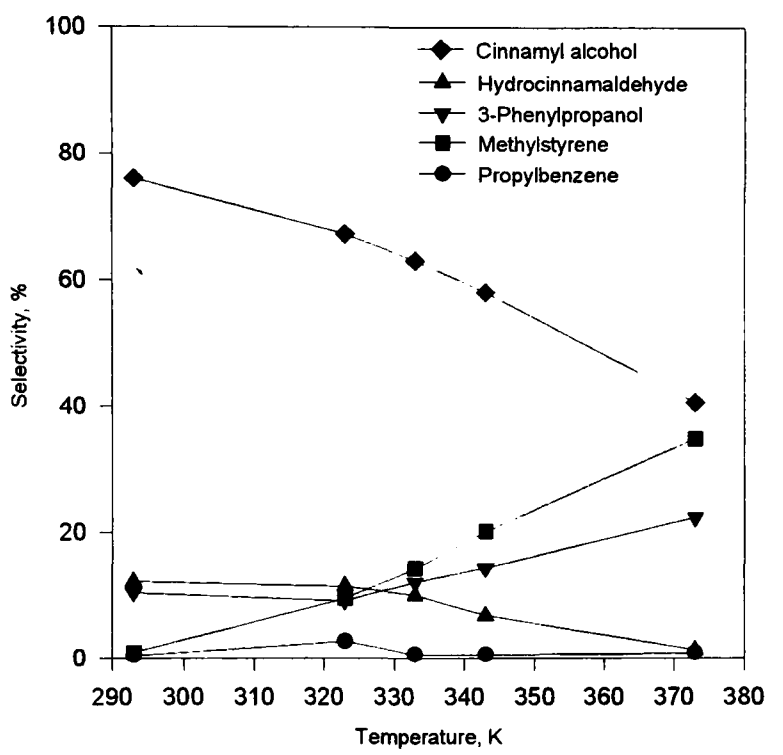

(2) Propan-2-ol/Water as Solvent

The investigation was made at 1.1MPa in propan-2-ol/water (14:1) with a base loading of 0.5kg.m^{-3} and a catalyst loading of 20kg.m^{-3}. The data are given in Table 6.7.2 and show that a higher selectivity to cinnamyl alcohol can be obtained at the higher temperature.

Table 6.7.2 Selectivity vs Temperature in Propan-2-ol/Water

P = 1.1MPa; W_{CAL} = 50kg.m^{-3}; $W_{cat.}$ = 20kg.m^{-3};
W_{Base} = 0.5kg.m^{-3}; Solvent = Propan-2-ol/Water (14:1)

T, K	X_{conv}, %	S_{PB}, %	S_{MS}, %	S_{HC}, %	S_{PP}, %	S_{COL}, %	S_{aldol}, %
343	66.29	0.19	0.09	53.12	12.74	33.25	0.62
373	74.62	0.96	0.31	22.24	11.45	64.46	0.57

(3) Toluene/Water as Solvents

An initial cinnamaldehyde concentration of 50kg.m^{-3} was used under various conditions, as shown in Tables 8.6.7.12-15 and Figure 6.7.12-15. The selectivity decreased to cinnamyl alcohol and increased to hydrocinnamaldehyde with the increase in temperature. When toluene/water was used as the solvent system hydrocinnamaldehyde and cinnamyl alcohol were formed by competitive parallel reactions. At higher temperatures the hydrocinnamaldehyde formation rate-constant was greater than that for cinnamyl alcohol formation, so that it was beneficial to hydrocinnamaldehyde at higher temperature and vice versa. Therefore, lower temperatures should be used for the production of cinnamyl alcohol.

Figure 6.7.12 Selectivity vs Temperature in Toluene/Water (1:1)

P = 0.9MPa; W_{CAL} = 50kg.m^{-3}; W_{Base} = 50kg.m^{-3}

$W_{Cat.}$ = 10kg.m^{-3}; Solvent = Toluene/Water (1:1)

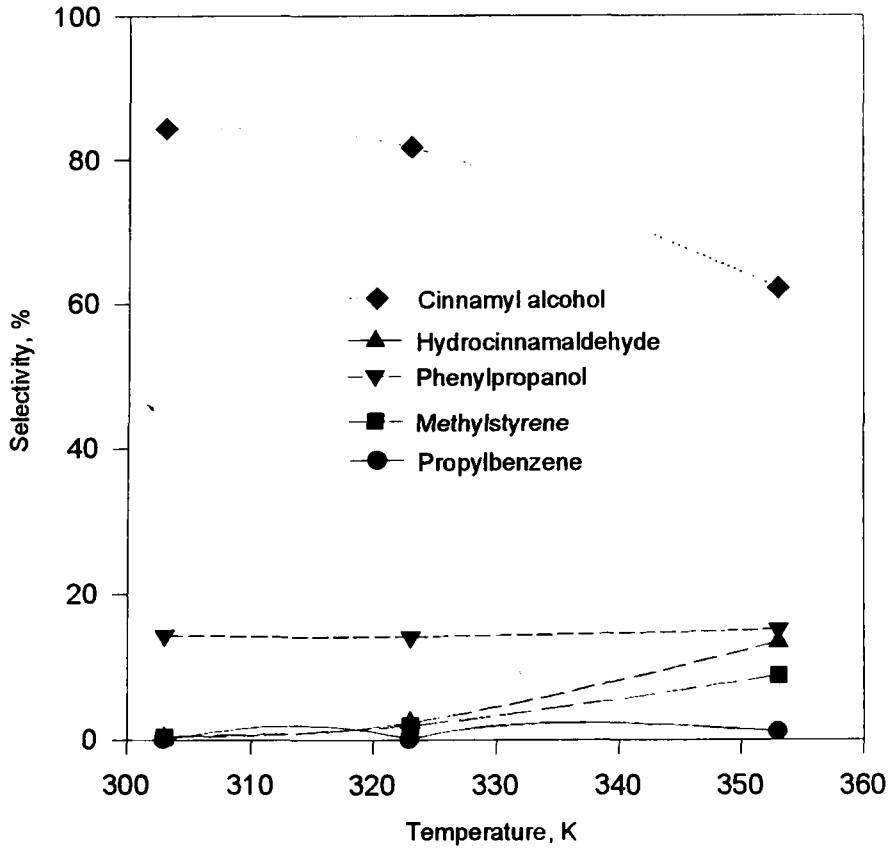

Figure 6.7.13 Selectivity vs Temperature in Toluene/Water (14:1)

P = 1.1MPa; W_{CAL} = 50kg.m^{-3}; W_{Base} = 1kg.m^{-3};

$W_{cat.}$ = 20kg.m^{-3}; Solvent = Toluene/Water (14:1)

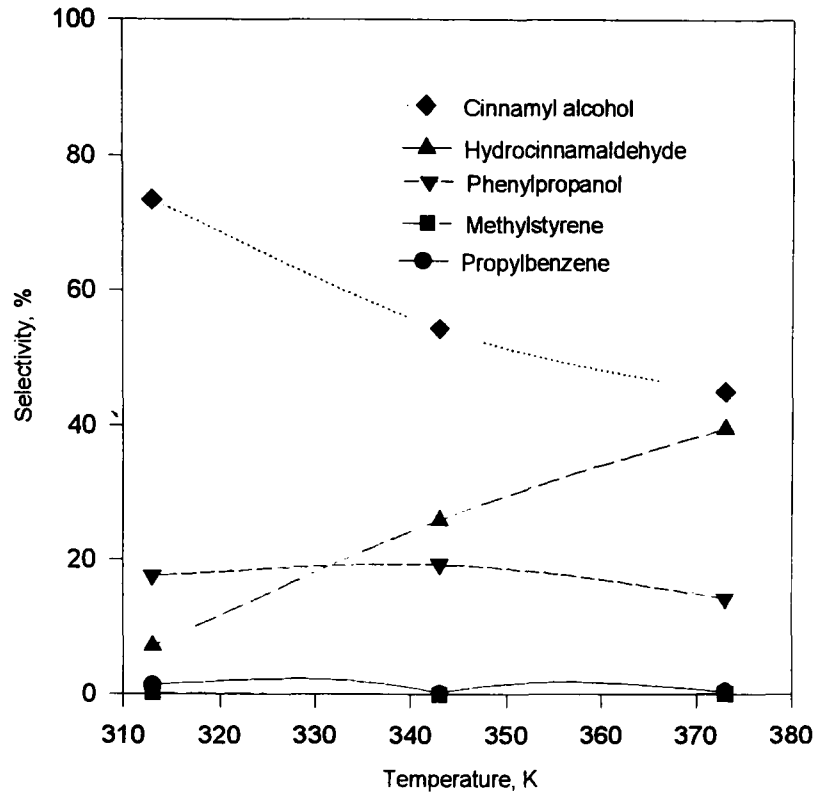

Figure 6.7.14 Selectivity vs Temperature inToluene/Water (5:1)

P = 1.1MPa; W_{CAL} = 50kg.m^{-3}; W_{Base} = 2.5kg.m^{-3};

$W_{cat.}$ = 20kg.m^{-3}; Solvent = Toluene/Water (5:1)

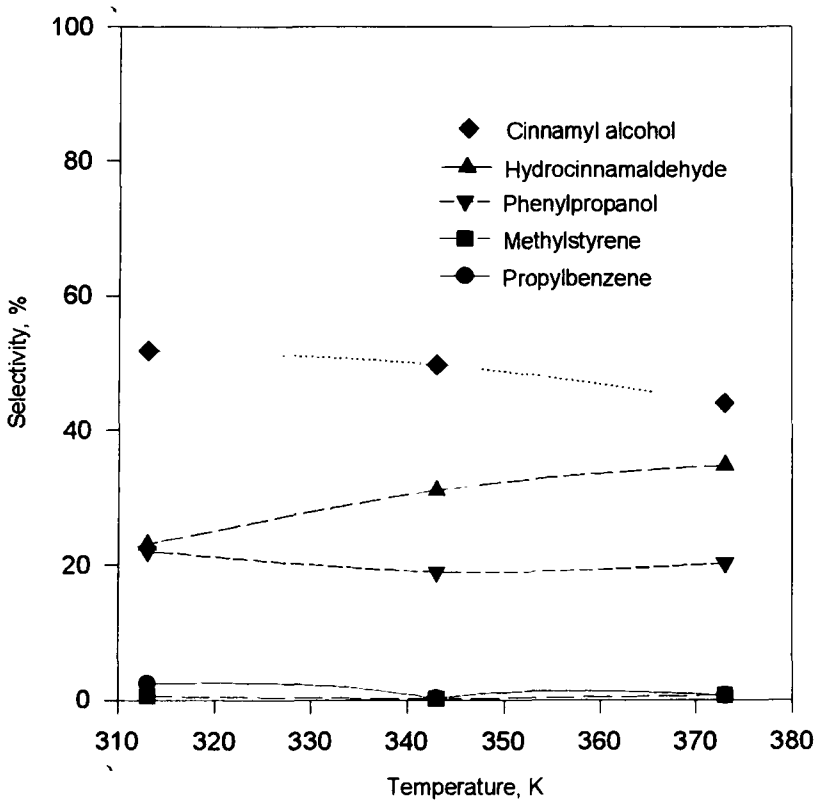

Figure 6.7.15 Selectivity vs Temperature in Toluene/Water (2:1)

P = 1.1MPa; W_{CAL} = 50kg.m^{-3}; W_{Base} = 5kg.m^{-3};
$W_{cat.}$ = 20kg.m^{-3}; Solvent = Toluene/Water (2:1)

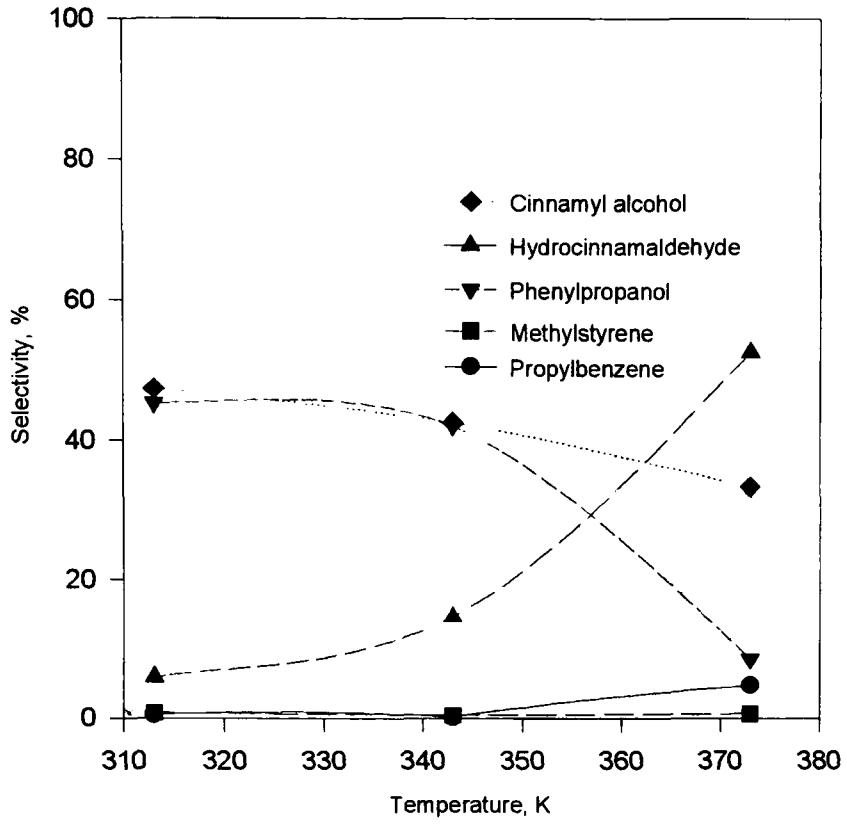

6.7.6 Pressure Effect

This effect was investigated at 303K with a catalyst loading of 10kg.m^{-3} and a cinnamaldehyde concentration of 50kg.m^{-3} in toluene/water (2:1) containing 50kg.m^{-3} of potassium hydroxide. The results are given in Tables 8.6.7.16-17 and Figures 6.7.16-17. It was found that the pressure effect was unimportant. At 288K the results showed that the selectivity to cinnamyl alcohol varied with hydrogen pressure, and that low pressure produced more unsaturated alcohol if higher conversion was achieved. This requires further investigation since a true comparison could not be made under non-identical conversion conditions.

Figure 6.7.16 Selectivity vs Pressure at 288K

T = 288K; W_{CAL} = 50kg.m^{-3}; $W_{cat.}$ = 10kg.m^{-3};

W_{Base} = 50kg.m^{-3}; Solvent = Toluene/Water (1:1)

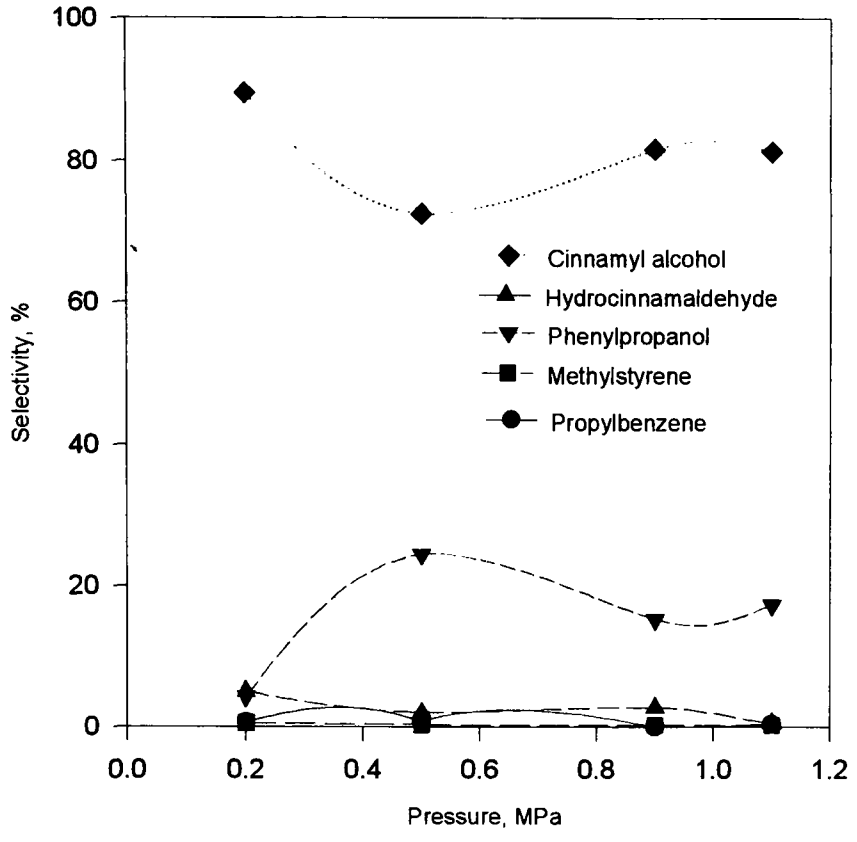

Figure 6.7.17 Selectivity vs Pressure at 303K

T = 303K; W_{CAL} = 50kg.m^{-3}; $W_{cat.}$ = 10kg.m^{-3};

W_{BAse} = 50kg.m^{-3}; Solvent = Toluene/ Water (2:1)

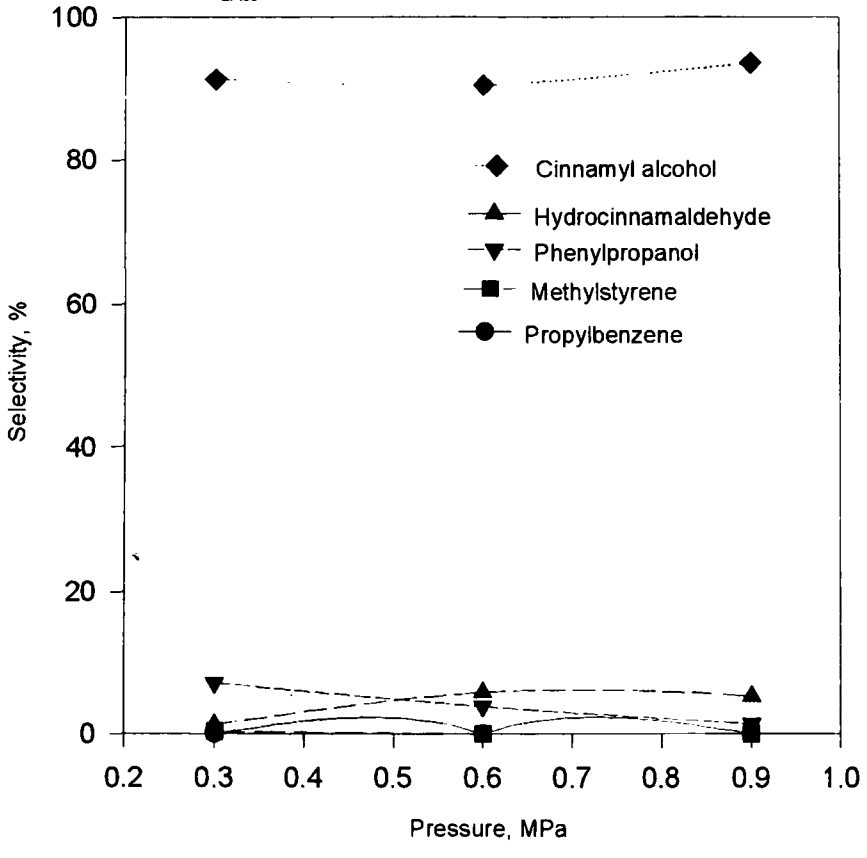

6.7.7 Cinnamaldehyde Conversion Effect

In order to study the relationship between the selectivity with respect to cinnamyl alcohol and the conversion of cinnamaldehyde a sample leg was fitted into the stirred batch reactor (autoclave) at a late stage of this work to enable samples to be taken during the course of the hydrogenation.

The product distribution pattern changed during the course of the reaction. The dependence of the selectivity on the reaction time or on the conversion of cinnamaldehyde can be classified into two groups:

(1) Lower Conversion

An example of this situation was obtained at 288K and 0.2MPa with an initial cinnamaldehyde concentration of 50kg.m^{-3} and a catalyst loading of 10kg.m^{-3} in toluene/water (1:1) with 50kg.m^{-3} of potassium hydroxide as the promoter. The results shown in Figure 6.7.18 indicated that the selectivity to cinnamyl alcohol increased steadily with the conversion of cinnamaldehyde at the early stage of the hydrogenation (up to 26.30% conversion of cinnamaldehyde). The product distribution pattern changed during the course of the reaction. The high initial selectivity for phenylpropanol dropped rapidly with time, while the selectivity to cinnamyl alcohol showed a steady rise. This may be due to the presence of different catalyst sites for the formation of saturated alcohol and unsaturated alcohol.

Figure 6.7.18 Selectivity vs Conversion at Low Conversion

T = 288K; P = 0.2MPa; W_{CAL} = 50kg.m^{-3};

W_{Base} = 50kg.m^{-3}; $W_{cat.}$ = 10kg.m^{-3}; Solvent = Toluene/Water (1:1)

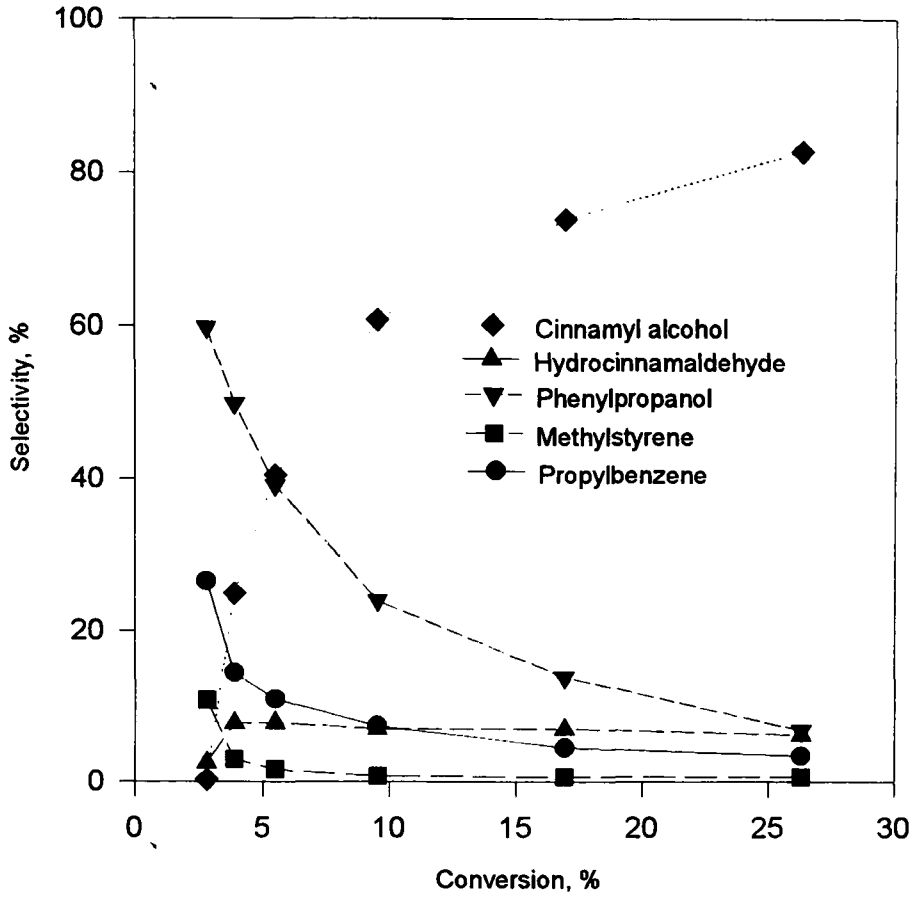

Phillips et al (1993) also observed that the selectivity changed as a function of conversion for a fresh rhodium-iron catalyst. A possible explanation for this shift in selectivity is that the catalyst becomes 'activated' under the reaction conditions, because reduction is not complete before the introduction of the reactant. Another possible explanation is that some sites are preferentially blocked by product or reactant molecules, and that this blocking increases with increasing levels of conversion. A third possible explanation is that the alloy surface promotes the conversion of cinnamyl alcohol to hydrocinnamaldehyde, but there is no experimental evidence for this.

The accumulation of products in the reaction medium during batch reactions may affect the reaction rate and product selectivity if certain products compete with the reactants for catalyst surface sites. Blackmond et al (1991) pointed out that saturated

aldehyde added to the cinnamaldehyde hydrogenation reaction medium acted as an inhibitor for unsaturated aldehyde conversion, and saturated aldehyde produced in the course of the reaction may remain adsorbed on the metal. Unsaturated alcohol selectivity may then be altered by a steric effect, in which the unsaturated aldehyde substrate is forced to adsorb through the carbonyl group, or by an electronic effect in which the adsorbed saturated aldehyde causes an increase in charge density on the metal, lowering the probability for alkene bond activation. This would result in an increase in unsaturated alcohol selectivity.

Coq et al (1993) studied the hydrogenation of cinnamaldehyde over ruthenium catalysts in propan-2-ol at 383K and 4.5MPa and found that the selectivity to cinnamyl alcohol increased until 50-70% of cinnamaldehyde was converted. Two explanations have been proposed for this behaviour: (1) selective poisoning of the sites responsible for carbon-carbon bond hydrogenation, or an electronic modification of the metal sites by adsorbed carbon monoxide formed in the course of the reaction by the decarbonylation of cinnamaldehyde (Galvagno et al, 1991); (2) hydrocinnamaldehyde formed at the beginning of the reaction remains adsorbed in large amounts on the catalyst surface and modifies the properties of the active phase either by a ligand effect which increases the charge density on the metal, resulting in decreased probability for carbon-carbon activation, or by a steric effect which forces an oncoming cinnamaldehyde molecule to adsorb through the carbonyl group (Giroir-Fendler et al, 1988; Galvagno et al, 1991).

Some experimental data showed that the selectivity to cinnamyl alcohol increased with the conversion of cinnamaldehyde under different conditions (Figure 6.7.19).

Figure 6.7.19 Selectivity vs Conversion from Different Runs

T = 313K; P = 1.1MPa; W_{CAL} = 50kg.m^{-3}; W_{Base} = 1-5kg.m^{-3};

$W_{cat.}$ = 20kg.m^{-3}; Solvent = Toluene/Water (2:1-14:1)

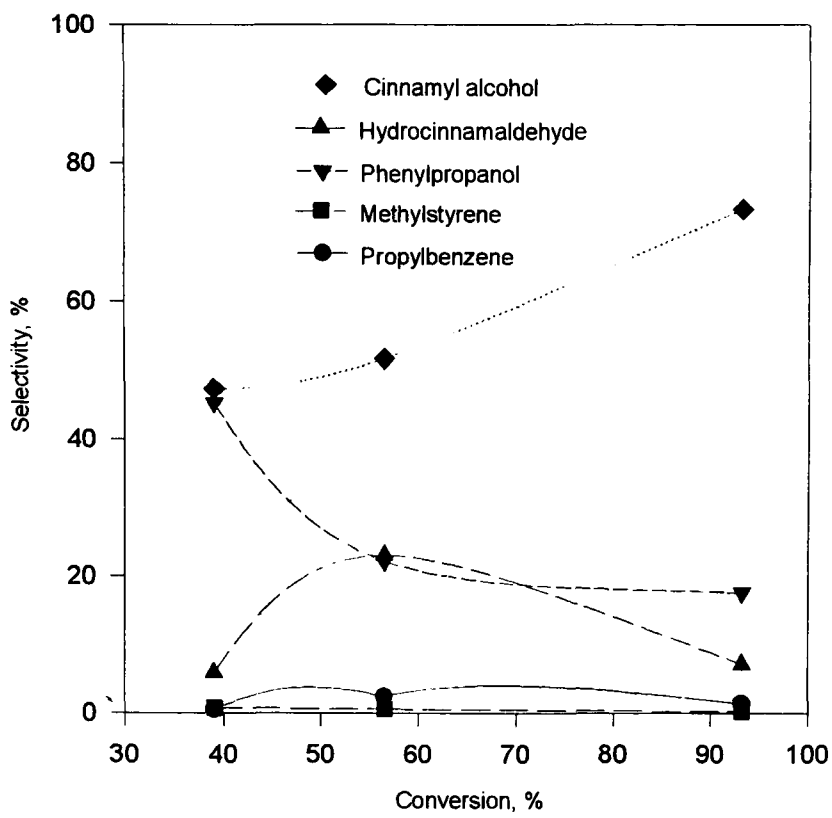

(2) Intermediate to Higher Conversion

A typical case of this was observed at 303K and 0.2MPa with an initial cinnamaldehyde concentration of 50kg.m^{-3}, a catalyst loading of 10kg.m^{-3} and 50kg.m^{-3} of potassium hydroxide as the promoter in toluene/water (1:1). An example is given in Figure 6.7.20. At intermediate to higher levels of conversion of cinnamaldehyde the selectivity to cinnamyl alcohol was almost unchanged.

Figure 6.7.20 Selectivity vs Conversion at High Conversion

T = 303K; P = 0.2MPa; W_{CAL} = 50kg.m^{-3};
W_{Base} = 50kg.m^{-3}; $W_{cat.}$ = 10kg.m^{-3}; Solvent = Toluene/Water (1:1)

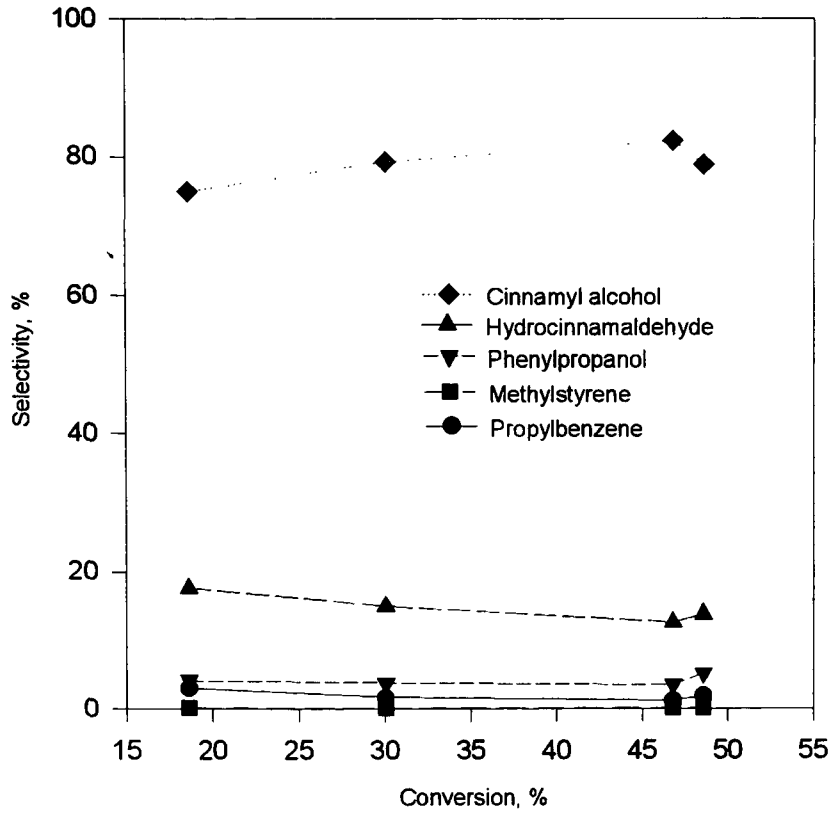

6.7.4 Kinetic Studies

Studying the overall reaction rate may provide some clues about the nature of the predominating effect in a particular reaction. For example, the hydrogenation of cinnamaldehyde proceeds much faster over carbon-supported ruthenium than over zeolite-supported ruthenium. In this case zeolite pore structure would restrict the adsorption of a bulky organic reactant, and hence its selectivity, so the reaction of cinnamaldehyde would proceed much more slowly since the reactant must adopt a particular conformation in order to adsorb onto the catalyst. Steric effects on the catalyst or an organic substrate appear to be first-order effects. When these constraints are related, electronic effects may be involved.

6.7.4.1 Solvent Effect

The solvent effect on the reaction rate was studied by using water, propan-2-ol, toluene, propan-2-ol/water and toluene/water. It was noticed that the nature of the solvent system used was important. Under otherwise identical conditions the reaction rate decreased in the order toluene/water > propan-2-ol > water.

(1) Water as Solvent

The platinum/graphite catalyst was poorly wetted by this solvent, and tended to adhere to the reactor surface and the stirrer, and cinnamaldehyde is only slightly soluble in water.

(2) Propan-2-ol/Water as Solvent

The coagulation phenomena of catalyst in water can be altered by addition of an alcohol solvent. Propan-2-ol and water are miscible and form a single phase able to wet the catalyst and thus to disperse it. The addition of a base, such as potassium hydroxide, increased the catalytic reaction rate.

(3) Toluene/Water as Solvent

Selectivity studies showed that high selectivity could be achieved in toluene/water so the effect of the toluene:water ratio on the reaction rate was investigated at 288K and 0.9MPa with a catalyst loading of 10kg.m^{-3}, an initial cinnamaldehyde concentration of 50kg.m^{-3} and a base loading of 50kg.m^{-3}. The toluene:water ratio was varied from 1:10 to 10:1 and the results are given at Table 8.6.7.18 and Figure 6.7.21. The reaction rate increased rapidly to a maximum value at a toluene:water ratio of 1:1 and then decreased with the increase in the toluene:water ratio. The potassium ions present promoted the selectivity to cinnamyl alcohol and accelerated the catalytic reaction rate. Cinnamaldehyde dissolved completely in toluene but sparingly in water. Similarly the platinum/graphite catalyst was able to disperse completely in toluene but not in water only. However in toluene/water system the platinum catalyst can eventually transferred from toluene to water and dispersed in the water phase. Considerable agitation is needed to maximize the interfacial area between these immiscible liquids, and a 1:1 toluene:water mixture appeared to provide the best opportunity for such optimal interaction so that maximum reaction rates were achieved.

Figure 6.7.21 Rate vs Ratio of Toluene to Water

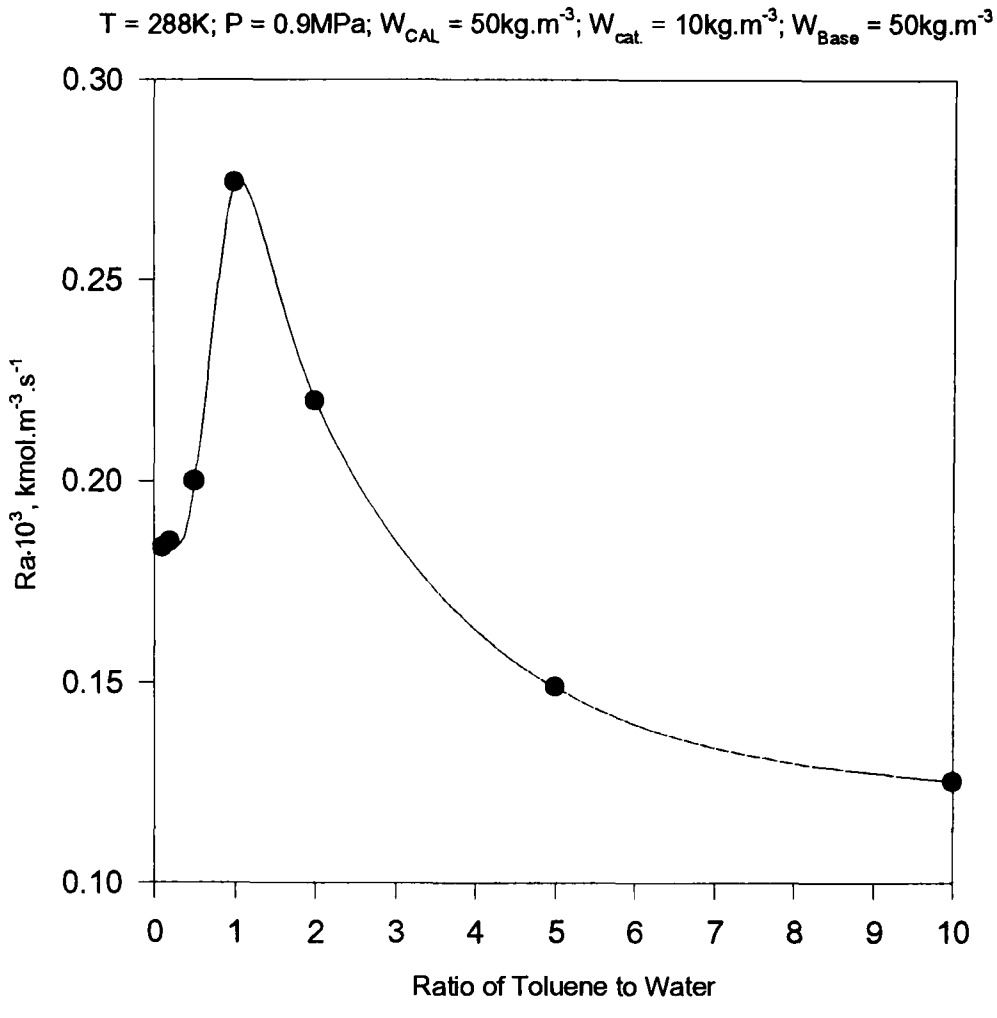

6.7.4.2 Catalyst Loading Effect

The effect of catalyst loading on the reaction rate was studied at 293K and 0.9MPa. The platinum/graphite catalyst loading was varied from 5kg.m^{-3} to 30kg.m^{-3} with an initial cinnamaldehyde concentration of 50kg.m^{-3} and a potassium hydroxide concentration of 50kg.m^{-3} in toluene/water (2:1). The results are given in Table 8.6.7.19 and Figure 6.7.22 The reaction rate increased with increase in the catalyst loading over the range tested indicating that the reaction is first order with respect to the catalyst.

Figure 6.7.22 Rate vs Catalyst Loading

T = 303K; P = 0.9MPa; W_{CAL} = 50kg.m^{-3}; W_{Base} = 50kg.m^{-3}; Solvent = Toluene/Water (2:1)

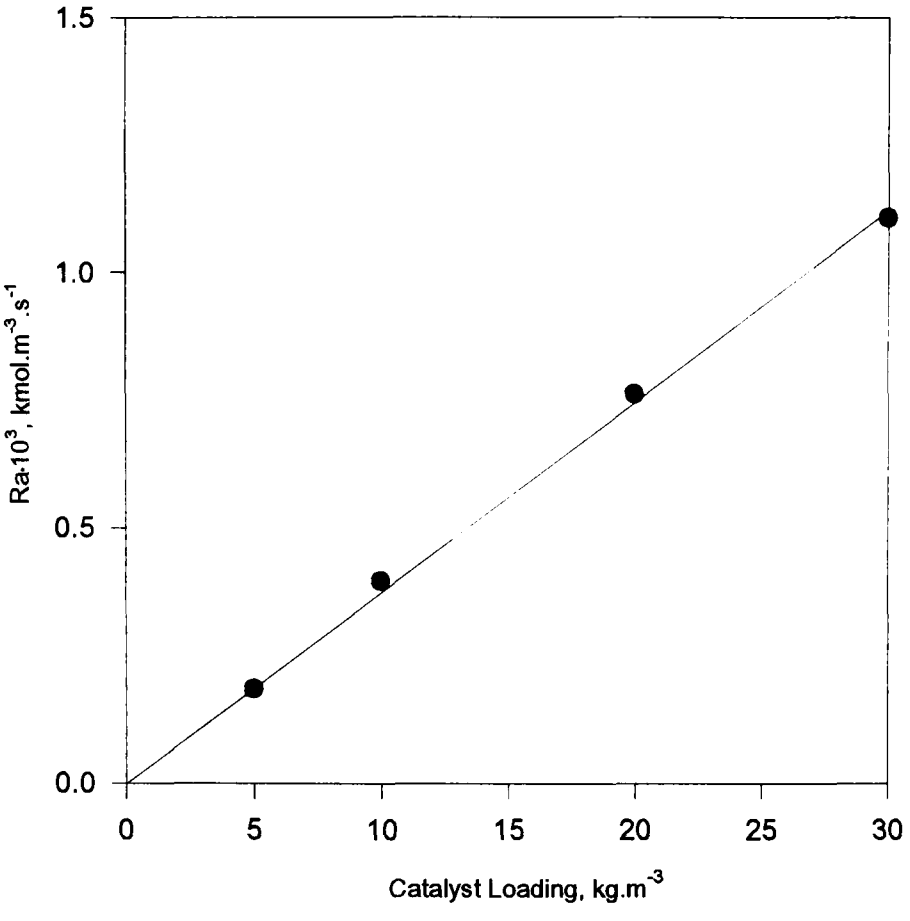

6.7.4.3 Pressure Effect

The effect of hydrogen pressure was investigated over the range of 0.2MPa to 1.1MPa at 288K and 303K with an initial cinnamaldehyde concentration of 50kg.m^{-3}, a base loading of 50kg.m^{-3} and a catalyst loading of 10kg.m^{-3} in toluene/water (1:1). The results are given in Table 8.6.7.20 and Figure 6.7.23. It is evident that the reaction rate is proportional to hydrogen pressure so that first order kinetics apply with respect to hydrogen concentration. This is in accordance with the results that the reaction is first order to hydrogen over 5% platinum/charcoal catalyst (Satagopan et al., 1994).

Figure 6.7.23 Rate vs Pressure in Toluene/Water (1:1)

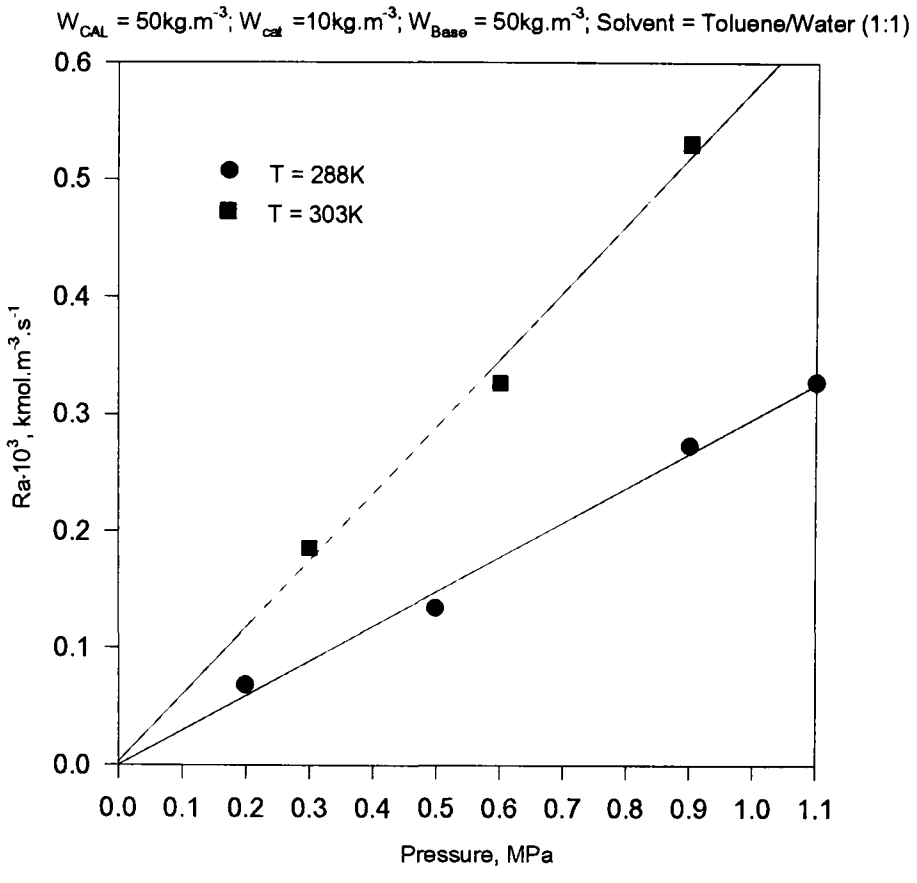

6.7.4.3 Base Concentration Effect

The effect of base loading on the reaction rate was examined using water and toluene/water as solvents. In water the experiments were carried out at 333K and 373K and 1.1MPa with an initial cinnamaldehyde concentration of 50kg.m^{-3} and catalyst loading of 20kg.m^{-3}. The reaction rate increased with increasing base loading at 333K but decreased with increasing base loading at 373K. The reaction rate seemed to depend linearly on the base loading but more experimental evidence may be required to confirm this for a wide range of base loadings and temperatures.

Figure 6.7.24 Rate vs Base Loading in Water

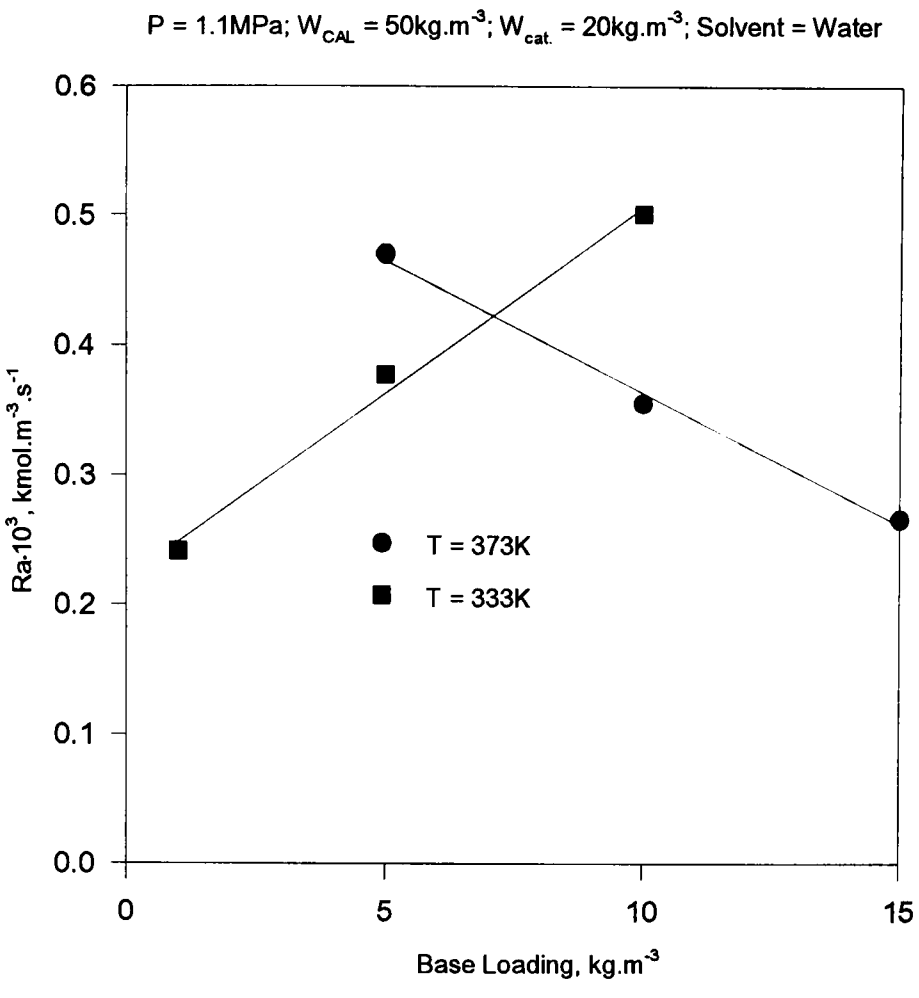

Several sets of experiments were conducted to study the effect of the base concentration on the reaction rate at different conditions in toluene/water. The results are given in Figure 6.7.25. The addition of a base to the reaction system could accelerate the reaction rate significantly. It can be seen that the reaction rate increased linearly with increase in the base loading for the several conditions, although for a small base loading such a tendency might be masked due to experimental error. The easy deactivation of the platinum catalyst during aldehyde hydrogenation may cause the reaction rate data collected at different times or with different batches of catalysts to be inconsistent, so a general conclusion could not be drawn due to very limited data. The base effect on the reaction rate may be because that the hydroxyl ion^{-} reacts with the carbonyl group in the aldehyde and thus deconjugates the molecule so that it

becomes more reactive (this could be similar to the formation of an aldehyde hydrate, McMurry, 1988). However, further investigation is needed to substantiate this theory.

Figure 6.7.25 Rate vs Catalyst Loading in Toluene/Water

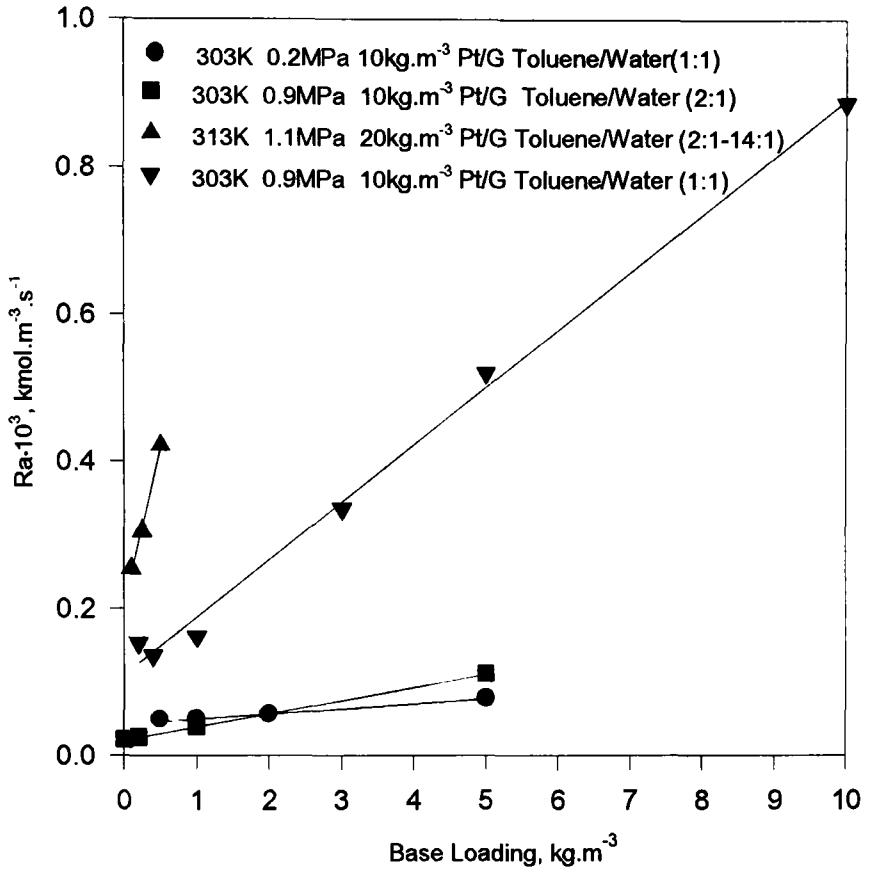

6.7.4.5 Initial Cinnamaldehyde Concentration Effect

The effect of the initial cinnamaldehyde concentration on the reaction rate was studied at 288K and 303K and 0.9MPa with a base loading of 50kg.m^{-3} in toluene/water (1:1). It was found that the reaction rate was independent of the initial cinnamaldehyde concentration (Table 8.6.7.22 and Figure 6.7.26). This was in accordance with the observation of Satagopan et al. (1994) that the reaction was zero order to cinnamaldehyde. However, the reaction rate decreased with the conversion of cinnamaldehyde due to platinum deactivation.

Figure 6.7.26 Rate vs Initial Cinnamaldehyde Concentration

P = 0.9MPa; W_{cat} = 10kg.m^{-3}; W_{Base} = 10kg.m^{-3}; Solvent = Toluene/Water (1:1)

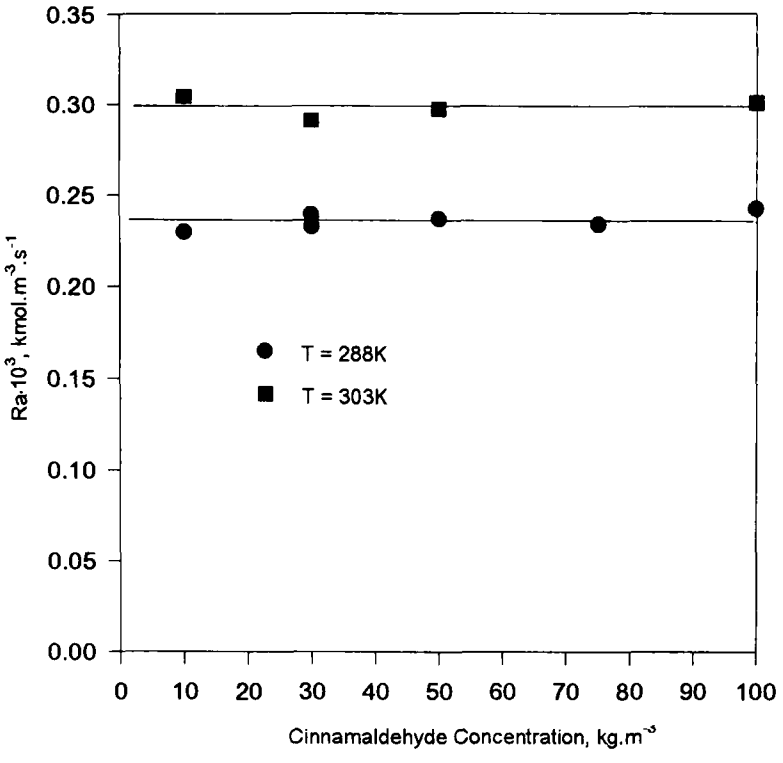

6.7.4.6 Temperature Effect

The effect of temperature on the reaction rate was examined using water and toluene/water as the solvents. With water the temperature range used was 293-373K. The activation energy was calculated using the Arrhenius equation from the plot of *ln*(Ra) against reciprocal temperature as 29kJ.mol^{-1} indicating that both mass transfer and surface reaction rate are important. Using toluene/water (1:1) as the solvents at temperatures of 303K, 323K and 353K and 1.1MPa with a base loading of 5kg.m^{-3} an activation energy of 35kJ.mol^{-1} was obtained. This results should be confirmed using more data points but it would appear that in toluene/water the reaction is more surface reaction rate controlled.

Figure 6.7.27 ln(Ra) vs 1/T

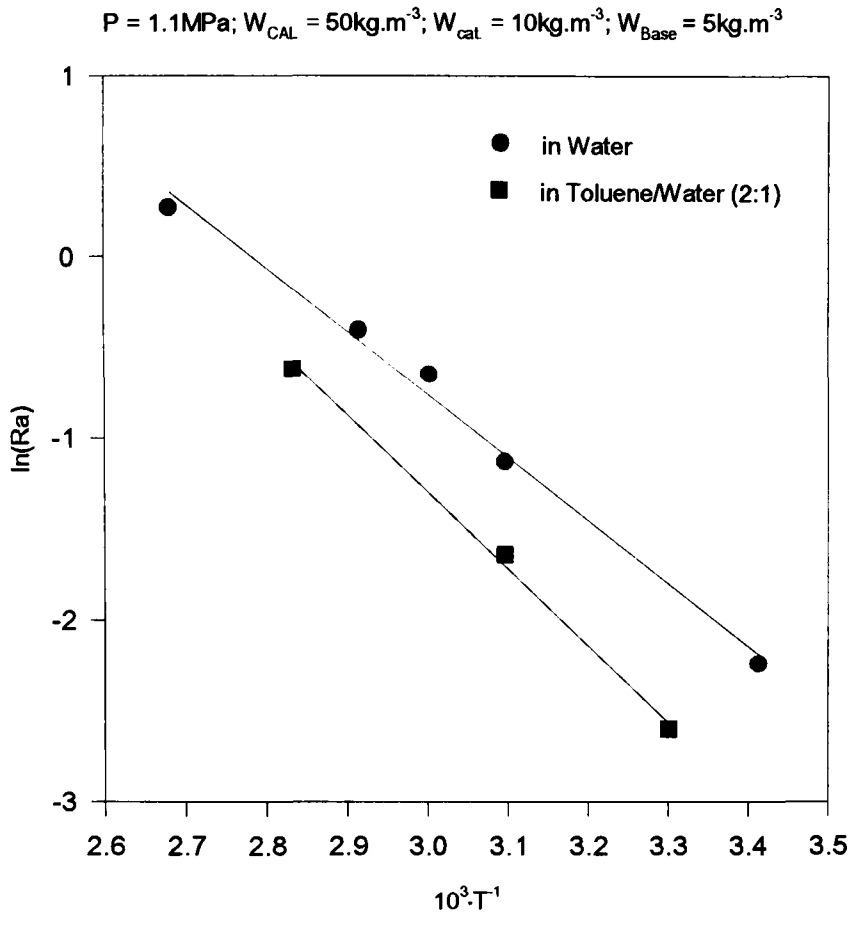

6.8 Hydrogenation over Platinum Catalysts in the 100mm CDC Reactor

6.8.1 Introduction

The selective hydrogenation of α,β-unsaturated aldehydes to unsaturated alcohol is an important step for the preparation of certain fine chemicals and pharmaceuticals. The selective hydrogenation of cinnamaldehyde over platinum/graphite catalysts in the toluene/water media with the addition of a base gave over 95% selectivity towards cinnamyl alcohol in a stirred batch reactor (Zhang et al., 1995 and 1996) and the reaction was dominated both by surface reaction and mass transfer rates. Therefore, the overall reaction rate or selectivity may be improved by efficient contacting between the continuous phase and the dispersed phase for such a reaction system. Bubble columns are widely used in chemical industry because of simplicity of operation, low operating cost and easy adjustment of residence time (see Chapter 2). The cocurrent downflow contactor has evolved from a novel concept of contacting a liquid continuous phase and a dispersed phase, and has been proved to offer a high degree of mass transfer by application of a continuous turbulent liquid inlet stream flowing cocurrently with a gas which is entrained simultaneously into a body of liquid. Rapid surface renewal with frequent bubble coalescence and rupture make the CDC a highly efficient mass transfer device. This study has focused on the selective hydrogenation of cinnamaldehyde towards cinnamyl alcohol in a CDC with a total volume of 55 litres. The objective of this study is to examine the basic information obtained in a stirred batch reactor and to seek the optimal condition for clean industrial synthesis of cinnamyl alcohol.

The experiments carried out in the CDC were based on the previous studies in a 500ml stirred batch reactor (autoclave), as described in Section 4.6. 5% platinum/graphite (Type 286) catalyst from Johnson Matthey Materials Technology (UK) was used in all the experiments. Toluene (Specified Laboratory Reagent, 99%) from Fisons and tap water were used as the solvents. Cinnamaldehyde (98%) from Aldrich was used as the main reactant. Potassium hydroxide (Specified Laboratory Reagent, 85%) from Fisons was used as the catalyst modifier to improve the selectivity and the catalyst activity towards cinnamyl alcohol. The temperature range used was 308K-363K and hydrogen was used at pressures from 0.6MPa to 1.1MPa.

6.8.2 General Observations

The following general aspects of the hydrogenation of cinnamaldehyde over the platinum/graphite catalyst in toluene were noted:

(1) The desired product was cinnamyl alcohol and the byproducts were hydrocinnamaldehyde, 3-phenyl propanol, propyl benzene and β-methylstyrene. The hydrogenation of cinnamaldehyde over a platinum catalyst in the CDC obeys the parallel-consecutive reaction scheme in non-polar solvents (Scheme 1) described in Section 6.5.

(2) In the CDC toluene and water formed an emulsion in which the catalyst was suspended due to vigorous agitation. This allows high mass transfer rates to be achieved in the CDC, leading to higher overall reaction rates.

(3) In the CDC 100% of hydrogen utilization can be achieved if the dispersion height is less than the column height. In this study 35% of dispersion height was used so that the

hydrogen supplied was completely used and the reaction rate was controlled by the hydrogen control unit and was equal to the hydrogen feed rate.

6.8.3 Selectivity Studies

Since large amounts of chemicals are required in each run only a few runs were carried out in the CDC reactor. Based on the results obtained in the stirred batch reactor the minimum amounts of chemicals and catalyst were used in the CDC reactor.

The effect of temperature on the selectivity was investigated at 308K and 363K, and was found be strong. At 363K low selectivity to cinnamyl alcohol (5%-31%) was obtained even at the beginning of the reaction, and the selectivity decreased with increase in the conversion of cinnamaldehyde. The proportion of β-methylstyrene and 3-phenylpropanol in the product increased with increasing cinnamaldehyde conversion (see Figure 6.8.1). These facts suggest that rate of the further hydrogenation of cinnamyl alcohol was greater than the rate of the formation of cinnamyl alcohol with increase in cinnamaldehyde conversion. However, at 308K (Figure 6.8.2) high selectivity (87.8%) to cinnamyl alcohol was achieved, and during the course of the hydrogenation the selectivity increased slightly with the conversion of cinnamaldehyde. At 323K with a catalyst loading of 0.1kg.m^{-3} 74.6% selectivity to cinnamyl alcohol was obtained at 27% conversion (Figure 6.8.3). The temperature effect on the selectivity in the CDC agreed with the results using the stirred batch reactor and showed that lower temperatures favoured the production of cinnamyl alcohol and a high temperature would accelerate the further hydrogenation of cinnamyl alcohol.

Figure 6.8.1 Selectivity vs Conversion at 363K

T = 363K; P = 1.1MPa; W_{CAL} = 250g; W_{cat} = 0.2kg.m^{-3};
W_{Base} = 1kg.m^{-3}; Solvent = Toluene/Water (1:6); Dispersion = 35%

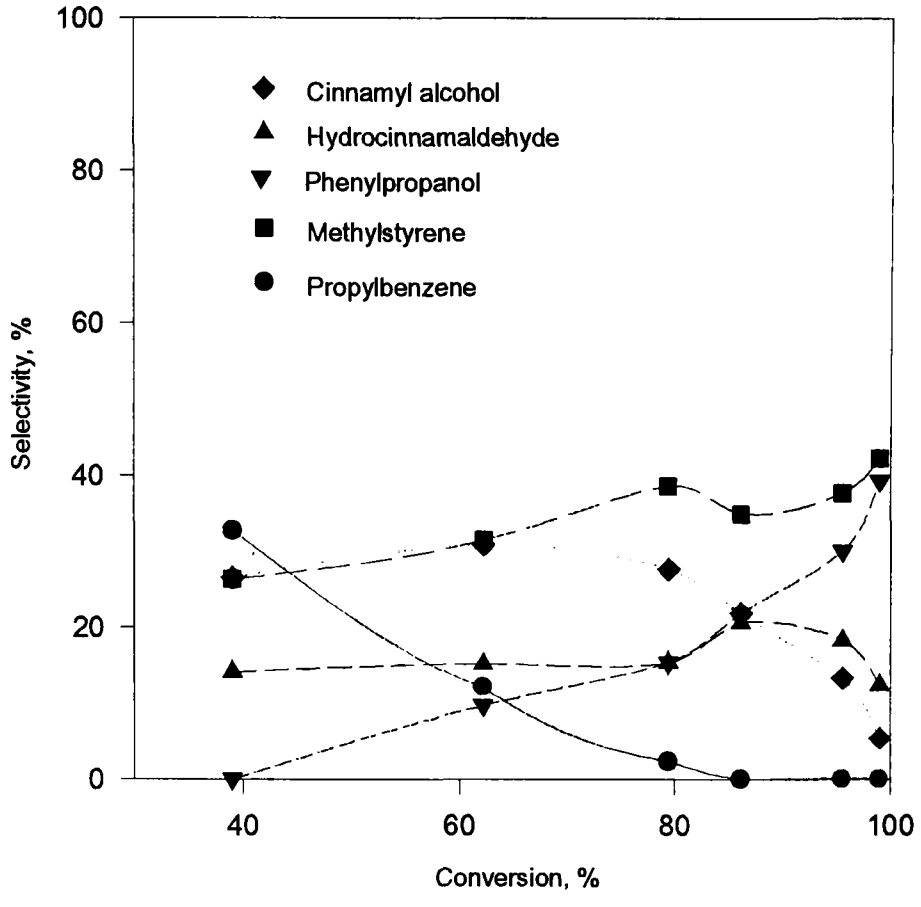

Figure 6.8.2 Selectivity vs Conversion at 308K

T =308K; P = 1.1MPa; W_{CAL} = 250g; W_{cat} = 0.2kg.m^{-3};
W_{Base} = 1kg.m^{-3}; Solvent = Toluene/Water (1:6); Dispersion = 35%

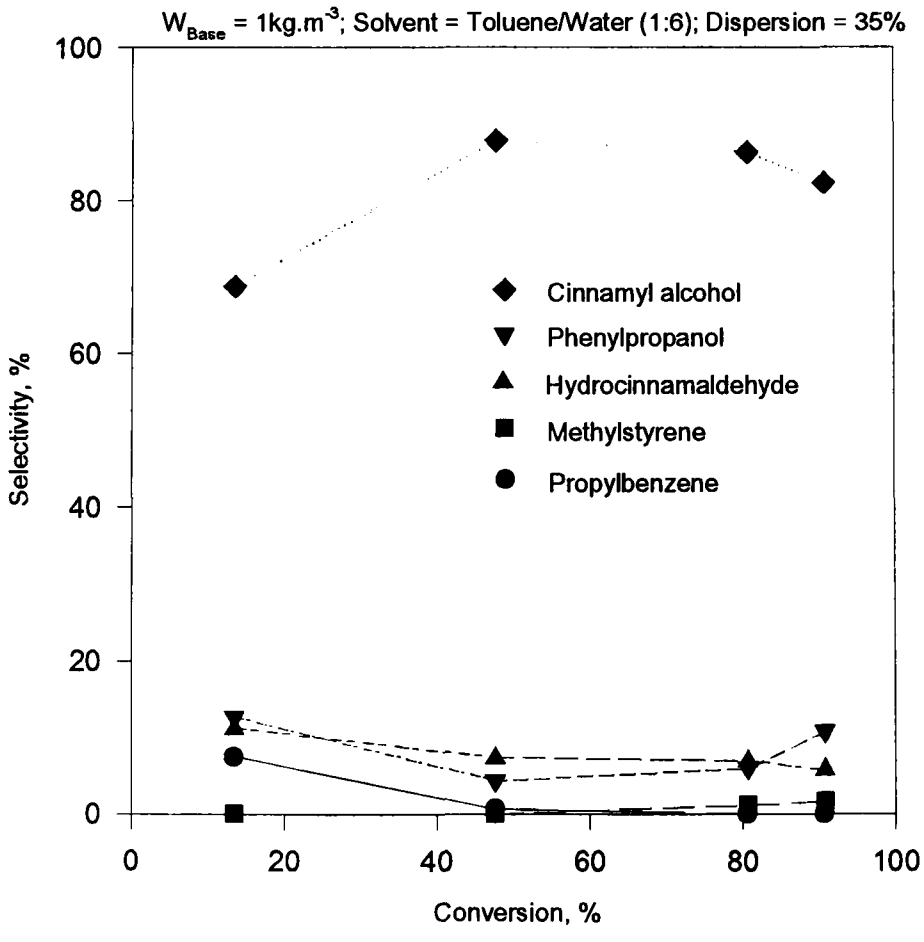

Previous studies in the stirred batch reactor showed that the selectivity to cinnamyl alcohol was a strong function of the base loading and the toluene-to-water ratio. However, in the CDC a high selectivity to cinnamyl alcohol was achieved (Figure 6.8.1 and Figure 6.8.4) although a much lower base loading of $1kg.m^{-3}$ or $2kg.m^{-3}$ and a lower ratio of toluene to water were used.

Figure 6.8.3 Selectivity vs Conversion at 323K
T = 323K; P = 0.5MPa; W_{CAL} = 500g; $W_{cat.}$ = $0.1kg.m^{-3}$;
W_{Base} = $1kg.m^{-3}$; Solvent = Toluene/Water (1:6); Dispersion = 35%

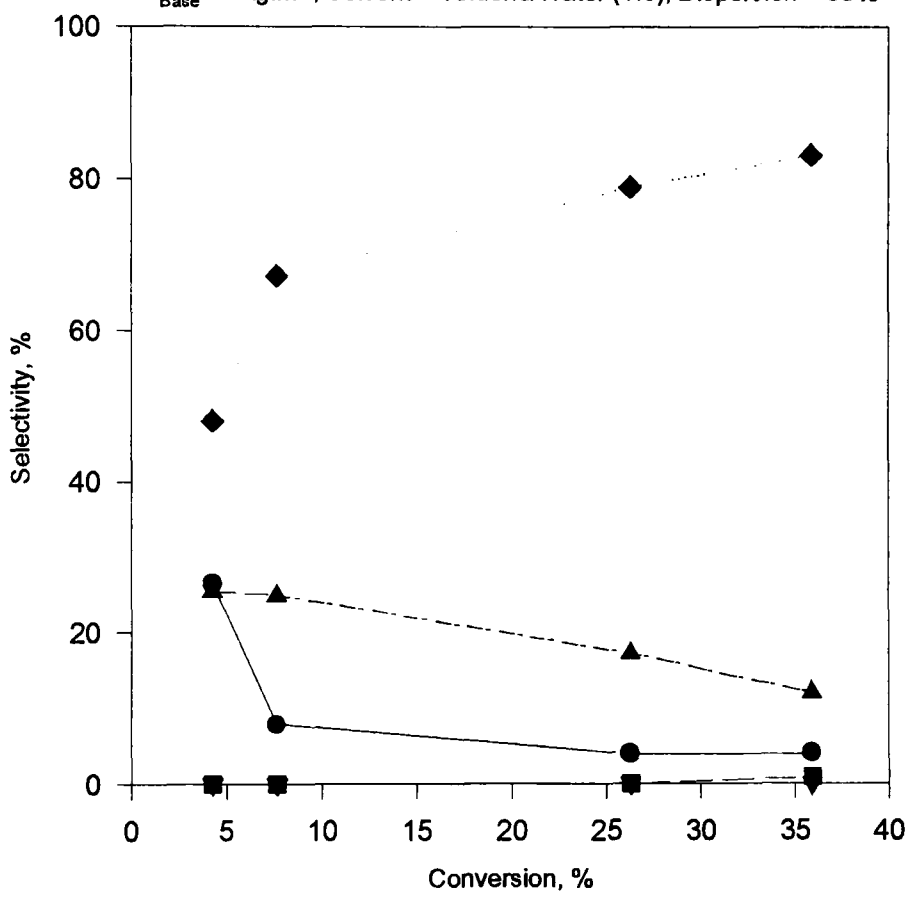

Previous hydrodynamic studies showed that the CDC operated in slurry-mode might behave as a combination of mixed and plug-flow reactors and that vigorous agitation reinforced mass transfer between different phases. This combination may contribute to improved selectivity towards the intermediate formed in the consecutive reaction in the CDC especially with gas/liquid/liquid slurry media. This was also observed in the hydrogenation of triglycerides in a gas-liquid slurry system (Boyes et al., 1995).

Figure 6.8.4 Selectivity vs Conversion at 308K

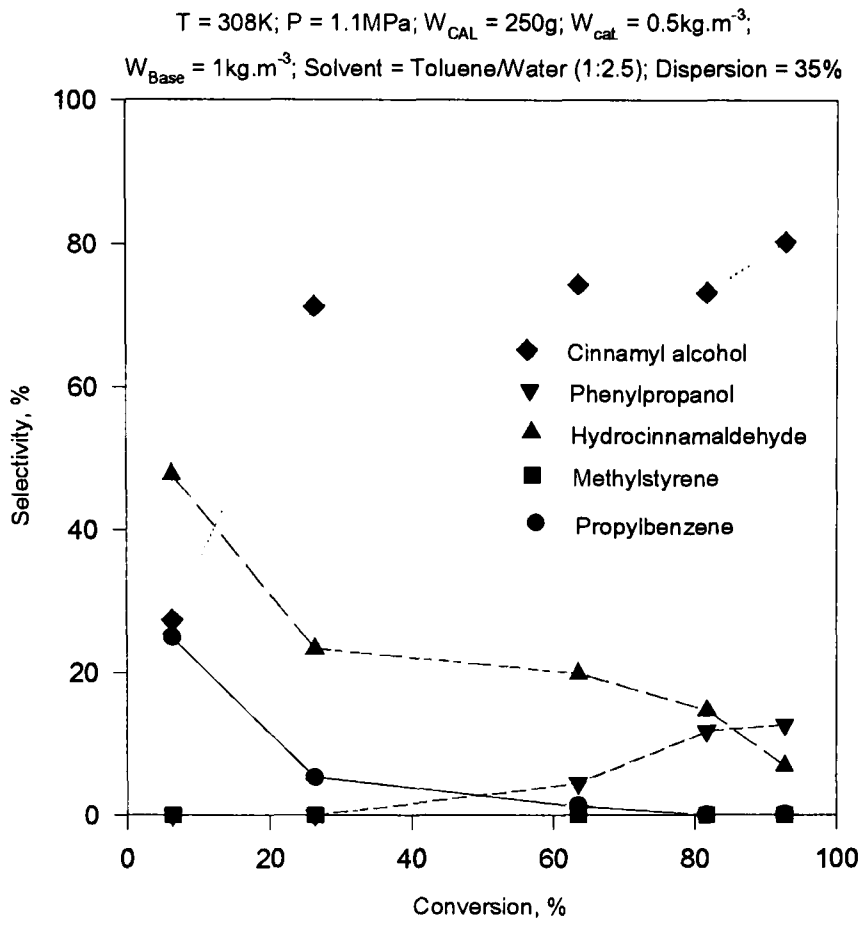

The effect of various factors on the selectivity requires systematic investigation in order to obtain optimal conditions for the clean production of cinnamyl alcohol in the CDC. There are indications that the selective hydrogenation of α,β-unsaturated aldehydes to unsaturated alcohols may benefit from operation under hydrogen diffusion control. This is the case the operating mode of the CDC requires modification in order to promote such a condition.

6.8.4 Kinetics

The hydrogenation of cinnamaldehyde over a platinum/graphite catalyst in toluene/water is both surface reaction rate and mass transfer rate controlled in the stirred batch reactor and the overall rate can be significantly improved in the highly efficient mass transfer CDC (see Section 6.7). In fact the reaction rate per unit of

reaction volume in the CDC was more than ten times that in the stirred batch reactor at the same temperature and pressure, although in the CDC cinnamaldehyde concentration, catalyst loading and base loading were much lower than in the stirred batch reactor. The rate enhancement in the CDC allowed the use of lower catalyst loading and lower base loading without loss of selectivity, but a general conclusion needs more detailed investigation under identical conditions and careful studies under diffusion and kinetically controlled regimes.

Chapter 7 Conclusions and Recommendations

7.1 Conclusions

7.1.1 Hydrodynamic and Mass Transfer Studies in the CDC

1. In general, for the oxygen/water and hydrogen/water systems the flow regimes in the CDC consist mainly of the highly turbulent entrance region (25-40cm) and the less turbulent middle region, although a small-bubble cloud section appears at the end of dispersion when the gas flowrate is high. Large bubbles (4.5mm) prevail in the middle region and high gas holdup (up to 65%) can be achieved due to coalescence.
2. For the hydrogen/organic liquid and hydrogen/organic slurry systems only the entrance and the middle sections were observed. Due to the poor coalescence small bubbles (1-3mm) are dispersed throughout the column but good disengagement of the bubbles from the liquid phase leads to efficient utilization of hydrogen.
3. The minimum liquid inlet velocity for initiating a stable bubble dispersion decreases with an increase in the orifice size and a minimum liquid jet velocity of $2m.s^{-1}$ is essential.
4. Gas holdup increases with an increase in the gas superficial velocity but decreases with an increase in the liquid superficial velocity.
5. Dissolved oxygen concentration along the column increases with an increase in the axial distance from the top of the column and gas flowrate but decreases with liquid flow rate.
6. The volumetric mass transfer coefficient (k_La) increases with gas flowrate but decreases with liquid flowrate.
7. The flow pattern in the liquid phase in the CDC seems to behave as a combination of the continuous stirred tank reactor (C.S.T.R.) and the plug flow reactor (P.F.R).

8. The CDC is a highly efficient gas/liquid and gas/liquid/solid mass transfer device and can also be used in mass transfer controlled gas/liquid and gas/liquid/solid chemical and biochemical reaction processes to accelerate the overall reaction rate leading to high productivity.

7.1.2 Hydrogenation of Cinnamaldehyde over Palladium Catalysts in the STR

1. The hydrogenation of cinnamaldehyde is a parallel-consecutive reaction and the reaction scheme depends significantly on the solvent and the catalyst. Non-polar solvents are better than polar solvents since side reactions are minimized and toluene is the best solvent. Hydrocinnamaldehyde acetals are produced in both primary or secondary alcohol solvents and cinnamaldehyde acetals are formed in primary alcohols but not in the secondary alcohols.
2. When a pre-prepared solution in propan-2-ol is used homogeneous reactions occur due to the formation of long-retention-time products (gas chromatograph) leading to poor selectivity to hydrocinnamaldehyde, and under the same conditions the reaction rates in pre-prepared solutions are greater than in fresh solutions since the reaction mechanism is altered due to the formation of cinnamaldehyde acetals before hydrogenation.
3. Temperature and promoters have significant effects on the product selectivity. Higher temperature decreases the selectivity towards hydrocinnamaldehyde, so a temperature below 323K is preferred when toluene is the solvent. Some metal salts incorporated into the palladium catalysts prevent the further hydrogenation of hydrocinnamaldehyde by blocking some active sites, and potassium acetate and potassium carbonate are best promoters in toluene. Over 97% selectivity towards

hydrocinnamaldehyde has been achieved by the addition of potassium carbonate into in-house-prepared palladium catalysts.

4. Potassium hydroxide and sodium hydroxide are good promoters and enhance substantially the selectivity towards hydrocinnamaldehyde using toluene/water as the solvent medium.
5. The hydrogenation of cinnamaldehyde is first order in hydrogen partial pressure and catalyst loading but zero order in cinnamaldehyde concentration. The following kinetics are obtained: $$R_A = kC_{cat}^{1.0} C_{CAL}^{0} C_{H_2}^{1.0}$$
6. The analysis of activation energy and mass transfer shows that higher values of volumetric mass transfer coefficient (k_La) can be achieved. The reaction is surface reaction rate controlled in toluene, but both mass transfer and surface reaction rate are important in propan-2-ol. With the increase in the temperature mass transfer becomes more important so that the plot of ln(Ra) against 1/T gives a lower slope at higher temperature indicating a lower activation energy.

7.1.3 Hydrogenation of Cinnamaldehyde over Platinum Catalysts in the STR

1. The solvent plays an important role in the selectivity to cinnamyl alcohol. The toluene/water system shows a significant increase in the selectivity to cinnamyl alcohol.
2. Addition of a base such as potassium hydroxide to the reaction system increased greatly the selectivity to cinnamyl alcohol.
3. Temperature has a negative effect on the production of cinnamyl alcohol in the toluene/water system and should be lower than 323K.

4. The reaction rate is proportional to the catalyst loading but independent of the cinnamaldehyde concentration. Addition of a base accelerates the reaction rate in toluene/water system and the rate increases with an increase in the base loading for the range tested.
5. The selectivity to cinnamyl alcohol and the reaction rate are strong functions of the ratio of toluene to water with potassium hydroxide as the promoter and a 1:1 ratio is best; this probably optimize the liquid-liquid interfacial area for the biphasic system.

7.1.4 Hydrogenation of Cinnamaldehyde over Palladium Catalyst s in the CDC

1. Due to efficient mass transfer, equilibrium is achieved readily in the CDC, leading to a constant percentage of hydrocinnamaldehyde acetals in propan-2-ol.
2. The reaction is surface rate controlled and the rate is proportional to the catalyst loading and independent of both the cinnamaldehyde substrate and the products.

7.1.5 Hydrogenation of Cinnamaldehyde over Platinum Catalysts in the CDC

1. Hydrogenation in toluene/water system takes place at a high rate because of efficient mass transfer due to emulsification.
2. In the CDC, lower base loading, lower catalyst loading and lower toluene-to-water ratio can achieve high selectivity to cinnamyl alcohol leading to economic industrial production.

7.2 Recommendations

1. A detailed study of the residence time distribution is required in order to understand more clearly the flow pattern in the CDC.

2. The effects of the addition of promoters, such as potassium hydroxide, potassium acetate and potassium carbonate, on the selectivity towards hydrocinnamaldehyde, and the methods for catalyst preparation and modification need to be studied using palladium catalysts.
3. The hydrogenation of cinnamaldehyde over unmodified and modified palladium catalysts needs to be carried out both in the slurry CDC and in the packed bed CDC (for example, using monolithic catalysts and packing catalysts) using toluene and toluene/water as the solvent media for selectivity, kinetic and mass transfer studies in order to obtain basic information for the industrial production of hydrocinnamaldehyde.
4. The mechanism of the effect of the base on the hydrogenation kinetics over platinum catalysts needs to be studied in order to develop a kinetic expression in toluene/water system and to give an understanding of the interaction of the base with the catalyst and the reactant.
5. Catalyst preparation, characterization and modification including the use of bimetallic catalysts, such as platinum/tin, platinum/cobalt, and platinum modified by potassium hydroxide need to be studied to find a better catalyst system with optimal reaction conditions for the production of cinnamyl alcohol.
6. The hydrogenation of cinnamaldehyde over modified platinum catalysts needs to be carried out both in the slurry CDC and in the packed bed CDC in more detail, such as by varying toluene/water ratio, the catalyst loading and the base loading, for the clean industrial production of cinnamyl alcohol.

7. Careful studies of the reaction are required under both transport control and surface reaction rate control in order to see if there is a genuine benefit to the selectivity from operation under diffusion control for the hydrogenation of α,β-unsaturated aldehydes.

8. Careful observation is required in respect of the distribution in transfer of catalyst between the organic and aqueous phase is required.

Chapter 8 Appendices

8.1 Physical Properties of Materials

8.1.1 General Properties

Oxygen: O_2

M.W. = 32.00kg.kmol^{-1}
m.p. = 54.4K
b.p. = 90.2K
D_{20} = 1.331kg.m^{-3}
n_D^{20} = 1.0003

Hydrogen: H_2

M.W. = 2.016kg.kmol^{-1}
m.p. = 14.0K
b.p. = 20.3K
D_{20} = 0.0838kg.m^{-3}
n_D^{20} = 1.0001

Water: H_2O

M.W. = 18.02kg.kmol^{-1}
m.p. = 273.2K
b.p. = 373.2K
D_{20} = 998.2kg.m^{-3}
n_D^{20} = 1.3330

Methanol: CH_3OH

M.W. = 32.02kg.kmol^{-1}
m.p. = 175.5K
b.p. = 337.9K
D_{20} = 791.3kg.m^{-3}
n_D^{20} = 1.3284

Ethanol: CH_3CH_2OH

M.W. = 46. 02kg.kmol^{-1}
m.p. = 159.1K
b.p. = 351.5K
D_{20} = 789.4kg.m^{-3}
n_D^{20} = 1.3614

Propan-1-ol: $CH_3CH_2CH_2OH$

M.W. = 60.01kg.kmol^{-1}
m.p. = 147.0K
b.p. = 370.4K
D_{20} = 803.8kg.m^{-3}
n_D^{20} = 1.3856

Propan-2-ol: $(CH_3)_2CHOH$

M.W. = 60.01 kg.kmol^{-1}
m.p. = 184.7K
b.p = 355.5K
D_{20} = 785.5 kg.m^{-3}
n_D^{20} = 1.3772

Butan-1-ol: $CH_3(CH_2)_2CH_2OH$

M.W. = 74.02kg.kmol^{-1}
m.p. = 183.9K
b.p. = 390.9K
D_{20} = 809.7kg.m^{-3}
n_D^{20} = 1.3993

Butan-2-ol: $(CH_3)_2CHOHCH_3$

M.W. = 74.02kg.kmol^{-1}
m.p. = 158.5K
b.p. = 372.8K
D_{20} = 806.9kg.m^{-3}
n_D^{20} = 1.3972

Toluene: $C_6H_5CH_3$

M.W. = 92.14 kg.kmol^{-1}
m.p. = 178.2K
b.p. = 383.8K
D_{20} = 865 kg.m^{-3}
n_D^{20} = 1.4960

Heptane: $CH_3(CH_2)_5CH_3$

M.W. = 100.2.kmol^{-1}
m.p. = 182.2K
b.p. = 371.2K
D_{20} = 684kg.m^{-3}
n_D^{20} = 1.3870

Methylcyclohexane:$C_6H_{11}CH_3$

M.W. = 98.2kg.kmol^{-1}
m.p. = 146.8K
b.p. = 374.2K
D_{20} = 770 kg.m^{-3}
n_D^{20} = 1.4220

Cinnamldehyde: $C_6H_5CH=CHCHO$

M.W. = 132.16 kg.kmol^{-1}
b.p. = 521.2K
D_{20} = 1048 kg.m^{-3}
n_D^{20} = 1.6220

Cinnamyl Alcohol: $C_6H_5CH=CHCH_2OH$

M.W. = 134.18 kg.kmol^{-1}
m.p. = 306.2-308.2K
b.p. = 523.2K
D_{20} = 1044 kg.m^{-3}

Hydrocinnamaldehyde: $C_6H_5CH_2CH_2CHO$

M.W. = 134.18 kg.kmol^{-1}
b.p. = 370.2-372.2K.
D_{20} = 1019 kg.m^{-3}
n_D^{20} = 1.5230

Propyl Benzene: $C_6H_5CH_2CH_2CH_3$

M.W. = 120.20 kg.kmol^{-1}
m.p. = 174.2K
b.p. = 432.2K
D_{20} = 862 kg.m^{-3}
n_D^{20} = 1.4910

3-Phenyl Propanol: $C_6H_5CH_2CH_2CH_2OH$

M.W. = 136.19 kg.kmol^{-1}
m.p. = 255.2K
b.p. = 508.2K
D_{20} = 1008 kg.m^{-3}
n_D^{20} = 1.5196

β-Methylstyrene: $C_6H_5CH=CHCH_3$

M.W. = 118.18 kg.kmol^{-1}
b.p. = 448.2K
D_{20} = 911 kg.m^{-3}
n_D^{20} = 1.5500

8.1.2 Vapour Pressure

Water

The vapour pressure of water was evaluated from the relationship by Boublik et al. (1984).

$$\log_{10} p^o = 7.61171 - \frac{1948.271}{249.021 + t} \qquad (8.1.1)$$

where t= temperature, °C,

p^o= vapour pressure, mmHg

Propan-2-ol

The vapour pressure of propan-2-ol was evaluated from the relationship from TRC Thermodynamic Tables: Non-hydrocarbons (Marsh et al., 1993)

$$\log_{10} P^o = 8.11778 - \frac{1580.92}{219.61 + t} \qquad (8.1.2)$$

where t= temperature, °C,

p°= vapour pressure, mmHg.

Toluene

The vapour pressure of toluene was extracted from Data Book on Hydrocarbons: Application to Process Engineering (Maxwell, 1982)

T, K	273	283	293	303	313	323	333	343
P°, mmHg	6.8	12.9	22.1	34.5	58.0	92.0	139.0	204.5

8.1.3 Diffusion Coefficients

The following equation can be used to estimate the diffusional coefficients of non-electrolytes in liquids at low concentrations of the diffusing components (Perry's, 1973)

$$\frac{D_A \mu}{T} = 7.4 \times 10^{-8} \frac{(XM)^{0.5}}{(V^o)^{0.6}} \qquad (8.1.3.1)$$

where D_A = the diffusivity of the solute A at infinite dilution, $cm^2.s^{-1}$

μ = the solution viscosity, cp

T = the temperature, K

X = the association parameter

M = the solvent molecular weight, $g.mol^{-1}$

V^o = the molar volume of the solute at the normal boiling point, $cm^3.mol^{-1}$

For hydrogen, $V^o_{(H2)}$= 14.3$cm^3.mol^{-1}$ and for oxygen $V^o_{(O2)}$=25.6$cm^3.mol^{-1}$.

Table 8.1.3.1 The Association Parameters for Various Solvents

Solvent	Water	Methanol	Ethanol	Unsaturated solvents
X	2.6	1.9	1.5	1.0

The diffusion coefficients of hydrogen in a number of solvents at 293K are estimated from equation (8.1.3.1) and summarized at Table 8.1.3.1.

Table 8.1.3.2 The Diffusion Coefficients of Hydrogen in Various Solvents

Solvent	M, $g.mol^{-1}$	μ, cp	X	$D_A \times 10^5$, $cm^2.s^{-1}$
Water	18.02	1.002	2.6	3.00
Methanol	32.04	0.597	1.9	5.75
Ethanol	46.02	1.189	1.5	3.07
Propan-1-ol	60.11	2.256	1.0	1.51
Propan-2-ol	60.11	2.32	1.0	1.46
Butan-2-ol	74.02	3.632	1.0	1.04
Toluene	92.14	0.583	1.0	7.24

8.2 Analysis of Three Phase Reaction Systems

The analysis of a gas-liquid-solid three-phase slurry system has been discussed in several works (Satterfield, 1970; Shah, 1979; Ramachandran and Chaudhari, 1983; Doraiswamy and Sharma, 1984). In the three-phase slurry system the reaction between a gaseous species and a liquid species is catalysed by a solid-phase catalyst. Three-phase slurry reaction systems can be described by the following reaction scheme:

$$A + \nu B \xrightarrow{Catalyst} \nu_E E \qquad (8.2.1)$$

The species A is a reactant present in the gas phase and B is a non-volatile reactant present in the liquid phase, with the reaction occurring at the surface of a solid catalyst. In some cases both species A and B may be present in the gas-phase. Several steps have to occur before species A can be converted to products on the active sites of the catalyst, which are suspended in the liquid medium:

1. Transport of A from the bulk gas phase to the gas-liquid interface.
2. Transport of A from the gas-liquid interface to the bulk liquid.
3. Transport of A and B from the bulk liquid to the catalyst surface.
4. Intraparticle diffusion of the reactants in the pores of the catalyst.
5. Adsorption of the reactants on the active sites of the catalyst.
6. Surface reaction of A and B to yield the products.

The concentration profile of species A, as it diffuses from the bulk gas to the interior of the catalyst, is shown in Figure 8.2.1. For reversible reactions and volatile products, additional steps, such as desorption of products and transport from the catalyst surface to the bulk liquid and to the gas phase for volatile products, may also become rate controlling.

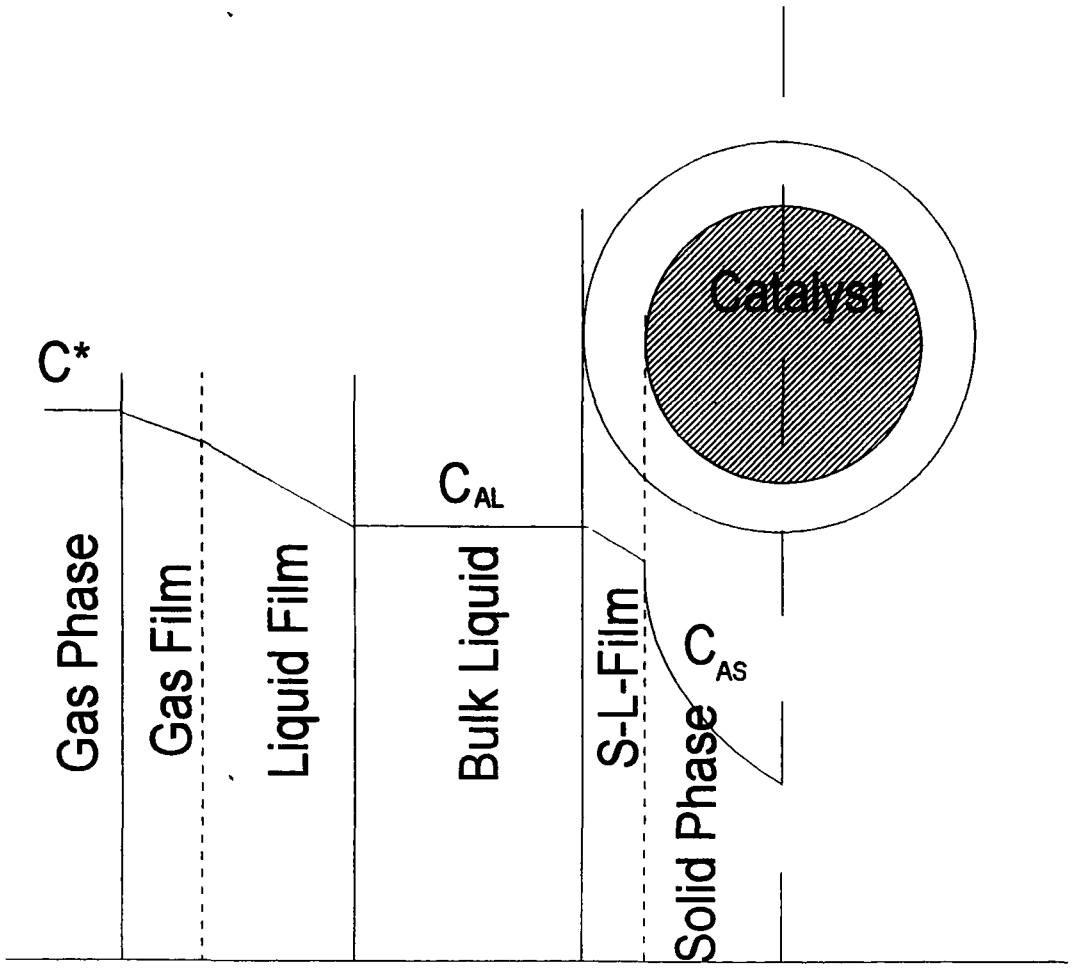

Figure 8.2.1 Concentration Profile in Gas-Liquid-Solid Slurry System

The concentration of the products can be predicted from the global reaction rate at a specific location in the reactor. The rate equations expressed in terms of known bulk concentrations for each individual step can be used to determine the global reaction rate.

8.2.1. Kinetic Models

If the intrinsic kinetics can be represented by the power law model in terms of an overall rate constant and the reaction orders, the rate equation for the reaction scheme (8.2.1) is given as

$$R_a = k_{mn} C_A^m C_B^n \qquad (8.2.2)$$

where k_{mn}, m, n are arbitrary constants valid for a particular system in the range of variables investigated. Here m and n are the reaction orders with respect to A and B,

respectively, and k_{mn} is the rate constant. If the concentration of reactant B is much larger than that of the dissolved gas A the reaction rate can be simplified as

$$R_a = k_m C_A^n \qquad (8.2.3)$$

where k_m is the pseudo mth-order rate constant, and is defined as

$$k_m = k_{mn} C_{BL}^n \qquad (8.2.4)$$

Equation (8.2.3) is valid provided the bulk concentration of species B very much greater than the saturation solubility of A in the liquid.

Since the power law model is mathematically simple and it is more convenient for fitting the experimental data so that only the power law model is used here to analyse the global rate. Although other models, such as the Langmuir-Hinshelwood model may be applied, the analytical procedure is similar to the power law model.

2. Mass Transfer

The number of steps necessary for the reaction to occur in differential reactors can be divided into two categories: (1) overall mass transfer from fluid phase to the catalyst surface and (2) intraparticle diffusion with surface reaction.

(1) Overall Rate of Mass Transfer

Assuming that the film-model is applied the rate of gas-liquid mass transfer is given as

$$R_a = K_L a(C_A^* - C_{AL}) \qquad (8.2.5)$$

where R_a is the rate of mass transfer per unit volume of the reactor in kmol.m^{-3}.s^{-1}; C_A^* is the saturation solubility in kmol.m^{-3}, and C_{AL} is the concentration of species A in the

bulk liquid in kmol.m^{-3}. K_La is the overall gas-liquid mass transfer coefficient and can be related to the individual gas-side and liquid-side mass transfer coefficients as

$$\frac{1}{K_L a} = \frac{1}{Hk_g a} + \frac{1}{k_L a} \qquad (8.2.6)$$

where H = the Henry's Law constant defined

as C_{AG} / C_A^*, kmol.m^{-3}(gas)/[kmol.m^{-3} (liquid)]

C_{AG} = the concentration of A in the bulk gas, kmol.m^{-3}

$k_g a$ = the gas-side mass transfer coefficient, s^{-1}

$k_L a$ = the liquid-side mass transfer coefficient , s^{-1}

a = the gas-liquid interfacial area, m^2.m^{-3}

For sparingly gases, such as hydrogen, and pure gas feed, the term K_La can approximate to k_La.

The rate of mass transfer from the bulk liquid to the surface of the solid catalyst can be expressed as

$$R_a = k_s a_p (C_{AL} - C_{AS}) \qquad (8.2.7)$$

where k_s = the liquid-to-particle mass transfer coefficient , m.s^{-1}

a_p = the external surface area of catalyst particles per unit volume of the reactor, m^2.m^{-3}

C_{AS} = the concentration of A at catalyst surface, kmol.m^{-3}.

For spherical particles the term a_p is given as

$$a_p = \frac{6W}{\rho_p d_p} \qquad (8.2.8)$$

where W = the amount of catalyst per unit volume of the reactor, kg.m^{-3}

ρ_p = the particle density, kg.m^{-3}

d_p = the average particle diameter, m

Combining equations (8.2.5) and (8.2.7), the overall rate of mass transfer of A from the gas phase to the external surface of the catalyst can be expressed as

$$R_a = M_A(C_A^* - C_{AS}) \qquad (8.2.9)$$

where

$$M_A = \left(\frac{1}{K_L a} + \frac{1}{k_s a_p}\right)^{-1} \qquad (8.2.10)$$

The above equation is valid irrespective of the type of kinetic model.

(2) Rate of Chemical Reaction

If the intraparticle diffusional resistance is negligible, the concentration of A is uniform throughout the catalyst particle and equal to C_{AS}, and the rate of reaction per unit volume of the reactor is given by

$$R_a = \eta k_m a_p C_{AS}^m \qquad (8.2.11)$$

For the first-order reaction (m =1), C_{AS} is obtained from equation (8.2.11) as

$$C_{AS} = \frac{R_a}{\eta k_r a_p} \qquad (8.2.12)$$

where k_r is the first order reaction rate constant, m.s^{-1}. Combining (8.2.8), (8.2.9), (8.2.10) and (8.2.12) and rearranging, the following expression is obtained

$$\frac{C_A^*}{R_a} = \frac{1}{K_L a} + \frac{\rho_p d_p}{6W}\left(\frac{1}{k_s} + \frac{1}{\eta k_r}\right) \qquad (8.2.13)$$

For sparingly soluble gases, such as hydrogen the term $K_L a$ can approximate to $k_L a$, so that

$$\frac{C_A^*}{R_a} = \frac{1}{k_L a} + \frac{\rho_p d_p}{6W}\left(\frac{1}{k_s} + \frac{1}{\eta k_r}\right) \qquad (8.2.14)$$

The 5% palladium catalyst on charcoal and the 5% platinum catalyst on graphite used in this research are non-porous and all the metals are deposited on the exterior surface of the supports so that the catalyst effectiveness factor η equals to unity.

For a first-order reaction with respect to A, the reaction and transport parameters can be evaluated by varying the catalyst loading W and the reaction rate Ra. From the straight line plot of $\frac{1}{Ra}$ against $\frac{1}{W}$, $\frac{1}{k_L a}$ can be determined from the intercept and $\left(\frac{1}{k_s a_p} + \frac{1}{k_r a_p}\right)$ from the slope. The value of the liquid-solid mass transfer coefficient k_s can be obtained from a suitable correlation and used to calculate the reaction rate constant k_r by substituting the calculated value into the value of the slope. This study uses the Frössling equation to calculate k_s:

$$Sh = \frac{k_s d_p}{D_A} = 2.0 + 0.76\,\mathrm{Re}^{\frac{1}{2}} Sc^{\frac{1}{3}} \qquad (8.2.15)$$

The Frössling equation is usually used to calculate k_s. For stagnant flow $Sh = 2$ and for turbulent systems the Re and Sc numbers are incorporated as equation (8.2.15).

8.2.3 Calculation on Hydrogenation of Cinnamaldehyde

8.2.3.1 Correction Factor on Reaction Rate Calculation

Table 8.2.1 Correction Factor for Propan-2-ol at 0.1MPa in STR

T, K	P_{prop}, mmHg	P_{H2}, mmHg	x_1*10^4, mol%	H, MPa	ρ_s, kg.m^{-3}	$C_A^* \times 10^3$, kmol.m^{-3}	f_c
273	8.2	751.8	2.03	486.2	801.6	2.71	0.920
283	16.9	743.1	2.15	455.3	793.6	2.84	0.961
293	32.8	727.2	2.26	423.8	785.5	2.95	1
303	60.3	699.7	2.37	389.0	777.0	3.06	1.037
313	105.8	654.2	2.47	348.1	768.3	3.16	1.071
323	178.2	581.8	2.58	297.1	759.3	3.25	1.103
333	288.9	471.1	2.68	231.4	749.9	3.34	1.132
343	453.1	306.9	2.78	145.4	740.2	3.42	1.159

Table 8.2.2 Correction Factor for Propan-2-ol at 0.4MPa in STR

T, K	P_{prop}, mmHg	P_{H2}, mmHg	x_1*10^4, mol%	H, MPa	ρ_s, kg.m^{-3}	$C_A^* \times 10^3$, kmol.m^{-3}	f_c
273	8.2	3031.8	8.14	490.2	801.6	10.85	0.920
283	16.9	3023.1	8.59	463.1	793.6	11.34	0.961
293	32.8	3007.2	9.03	438.1	785.5	11.80	1
303	60.3	2979.7	9.47	414.2	777.0	12.24	1.037
313	105.8	2934.2	9.89	390.3	768.3	12.64	1.071
323	178.2	2861.8	10.31	365.4	759.3	13.02	1.103
333	288.9	2751.1	10.71	337.9	749.9	13.37	1.132
343	453.1	2586.9	11.11	306.3	740.2	13.68	1.159

Table 8.2.3 Correction Factor for Propan-2-ol at 0.6MPa in STR

T, K	P_{prop}, mmHg	P_{H2}, mmHg	x_1*10^4, mol%	H, MPa	ρ_s, kg.m^{-3}	$C_A^* \times 10^3$, kmol.m^{-3}	f_c
273	8.2	4551.8	12.21	490.6	801.6	16.28	0.920
283	16.9	4543.1	12.88	464.0	793.6	17.01	0.961
293	32.8	4527.2	13.55	439.7	785.5	17.70	1.000
303	60.3	4499.7	14.20	417.0	777	18.35	1.037
313	105.8	4454.2	14.84	395.0	768.3	18.96	1.071
323	178.2	4381.8	15.46	372.9	759.3	19.53	1.103
333	288.9	4271.1	16.07	349.7	749.9	20.05	1.132
343	453.1	4106.9	16.67	324.2	740.2	20.52	1.159

Table 8.2.4 Correction Factor for Propan-2-ol at 0.9MPa in STR

T, K	P_{prop}, mmHg	P_{H2}, mmHg	x_1*10^4, mol%	H, MPa	ρ_s, kg.m^{-3}	$C_A^* \times 10^3$, kmol.m^{-3}	f_c
273	8.2	6831.8	18.31	490.9	801.6	24.42	0.920
283	16.9	6823.1	19.33	464.5	793.6	25.52	0.961
293	32.8	6807.2	20.32	440.8	785.5	26.56	1.000
303	60.3	6779.7	21.30	418.9	777	27.53	1.037
313	105.8	6734.2	22.25	398.2	768.3	28.44	1.071
323	178.2	6661.8	23.19	378.0	759.3	29.29	1.103
333	288.9	6551.1	24.11	357.6	749.9	30.07	1.132
343	453.1	6386.9	25.00	336.2	740.2	30.79	1.159

Table 8.2.5 Correction Factor for Toluene at 0.1MPa in STR

T, K	$P_{toluene}$, mmHg	P_{H2}, mmHg	x_1*10^4, mol%	H, MPa	ρ_s, kg.m^{-3}	$C_A^* \times 10^3$, kmol.m^{-3}	f_c
273	6.8	753.2	2.62	378.0	885.5	2.52	0.878
283	12.9	747.1	2.84	346.7	876.2	2.70	0.940
293	22.1	737.9	3.05	318.5	866.9	2.87	1
303	34.5	725.5	3.26	292.5	857.7	3.04	1.059
313	58.0	702.0	3.48	265.6	848.3	3.20	1.116
323	92.0	668.0	3.69	238.1	838.9	3.36	1.172
333	139.0	621.0	3.90	209.3	829.3	3.51	1.225
343	204.5	555.5	4.12	177.6	819.8	3.66	1.277

Table 8.2.6 Correction Factor for Toluene at 0.4MPa in STR

T, K	$P_{toluene}$, mmHg	P_{H2}, mmHg	x_1*10^4, mol%	H, MPa	ρ_s, kg.m^{-3}	$C_A^* \times 10^3$, kmol.m^{-3}	f_c
273	6.8	3033.2	10.49	380.5	885.5	10.08	0.878
283	12.9	3027.1	11.34	351.2	876.2	10.78	0.940
293	22.1	3017.9	12.20	325.6	866.9	11.47	1.000
303	34.5	3005.5	13.05	303.0	857.7	12.15	1.059
313	58.0	2982.0	13.91	282.1	848.3	12.81	1.116
323	92.0	2948.0	14.76	262.7	838.9	13.44	1.172
333	139.0	2901.0	15.62	244.4	829.3	14.06	1.225
343	204.5	2835.5	16.46	226.6	819.8	14.65	1.277

Table 8.2.7 Correction Factor for Toluene at 0.6MPa in STR

T, K	$P_{toluene}$, mmHg	P_{H2}, mmHg	x_1*10^4, mol%	H, MPa	ρ_s, kg.m^{-3}	$C_A^* \times 10^3$, kmol.m^{-3}	f_c
273	6.8	4553.2	15.73	380.8	885.5	15.12	0.878
283	12.9	4547.1	17.01	351.7	876.2	16.18	0.940
293	22.1	4537.9	18.29	326.4	866.9	17.21	1.000
303	34.5	4525.5	19.58	304.1	857.7	18.23	1.059
313	58.0	4502.0	20.86	283.9	848.3	19.21	1.116
323	92.0	4468.0	22.15	265.5	838.9	20.16	1.172
333	139.0	4421.0	23.42	248.3	829.3	21.08	1.225
343	204.5	4355.5	24.69	232.1	819.8	21.97	1.277

Table 8.2.8 Correction Factor for Toluene at 0.9MPa in STR

T, K	$P_{toluene}$, mmHg	P_{H2}, mmHg	x_1*10^4, mol%	H, MPa	ρ_s, kg.m^{-3}	$C_A^* \times 10^3$, kmol.m^{-3}	f_c
273	6.8	6833.2	23.60	381.0	885.5	22.68	0.878
283	12.9	6827.1	25.52	352.1	876.2	24.26	0.940
293	22.1	6817.9	27.44	326.9	866.9	25.82	1.000
303	34.5	6805.5	29.37	304.9	857.7	27.34	1.059
313	58.0	6782.0	31.30	285.1	848.3	28.81	1.116
323	92.0	6748.0	33.22	267.3	838.9	30.25	1.172
333	139.0	6701.0	35.14	250.9	829.3	31.62	1.225
343	204.5	6635.5	37.04	235.7	819.8	32.96	1.277

Table 8.2.9 Correction Factor for Propan-2-ol at 0.3MPa in CDC

T, K	P_{prop}, mmHg	P_{H2}, mmHg	x_1*10^4, mol%	H, MPa	ρ_s, kg.m^{-3}	$C_A^* \times 10^3$, kmol.m^{-3}	f_c
273	8.2	2271.8	6.10	489.7	801.6	8.14	0.920
283	16.9	2263.1	6.44	462.2	793.6	8.51	0.961
293	32.8	2247.2	6.77	436.5	785.5	8.85	1
303	60.3	2219.7	7.10	411.4	777	9.18	1.037
313	105.8	2174.2	7.42	385.7	768.3	9.48	1.071
323	178.2	2101.8	7.73	357.8	759.3	9.76	1.103
333	288.9	1991.1	8.04	326.1	749.9	10.02	1.132
343	453.1	1826.9	8.33	288.5	740.2	10.26	1.159

8.2.3.2 k_s Calculation

Table 8.2.10 k_s for Propan-2-ol over Pd/C in Glass STR

T, K	μ,cp	D_{H2}, m2/s	ρ_s, kg/m^3	Re. No.	Sc.No.	Sh. No.	ks,m/s
273	4.502	7.05E-10	801.6	5698.0	7964.3	1147.7	0.043
283	3.255	1.01E-09	793.6	7801.9	4057.1	1072.7	0.057
293	2.374	1.43E-09	785.5	10586.7	2106.5	1004.4	0.076
303	1.767	1.99E-09	777.0	14071.3	1140.5	943.9	0.099
313	1.340	2.72E-09	768.3	18347.5	642.1	890.1	0.127
323	1.033	3.64E-09	759.3	23521.4	374.2	841.9	0.161
333	0.809	4.79E-09	749.9	29662.3	225.4	798.6	0.201
343	0.642	6.21E-09	740.2	36906.2	139.5	759.3	0.248

Table 8.2.11 k_s for Propan-2-ol over Pd/C in Autoclave

T, K	μ, cp	D_{H2},m^2.s^{-1}	ρ_s,kg.m^{-3}	Re. No.	Sc.No.	Sh. No.	$Sh_{(corr)}$	$Sh_{(mean)}$	k_s, m.s^{-1}
273	4.502	7.05E-10	801.6	8977.3	7964.3	1440.0	481.2	241.6	0.0090
283	3.255	1.01E-09	793.6	12292.1	4057.1	1345.9	449.7	225.9	0.0120
293	2.374	1.43E-09	785.5	16679.6	2106.5	1260.2	421.1	211.6	0.0160
303	1.767	1.99E-09	777.0	22169.6	1140.5	1184.3	395.7	198.9	0.0209
313	1.340	2.72E-09	768.3	28906.8	642.1	1116.8	373.2	187.6	0.0268
323	1.033	3.64E-09	759.3	37058.4	374.2	1056.3	353.0	177.5	0.0340
333	0.809	4.79E-09	749.9	46733.6	225.4	1001.9	334.8	168.4	0.0424
343	0.642	6.21E-09	740.2	58146.5	139.5	952.5	318.3	160.1	0.0524

Table 8.2.12 k_s for Toluene over Pd/C in Autoclave

T, K	μ, cp	D_{H2},m^2.s^{-1}	ρ_s,kg.m^{-3}	Re. No.	Sc.No.	Sh. No.	$Sh_{(corr)}$	$Sh_{(mean)}$	k_s, m.s^{-1}
273	0.766	5.13E-09	885.5	58281.9	168.6	1015.6	339.4	170.7	0.0461
283	0.668	6.1E-09	876.2	66130.4	125.0	979.2	327.2	164.6	0.0528
293	0.583	7.24E-09	866.9	74967.8	92.9	944.6	315.7	158.8	0.0605
303	0.518	8.42E-09	857.7	83479.5	71.7	914.3	305.5	153.8	0.0682
313	0.467	9.65E-09	848.3	91581.3	57.1	887.4	296.5	149.3	0.0758
323	0.422	1.1E-08	838.9	100224.0	45.7	861.9	288.0	145.0	0.0841
333	0.377	1.27E-08	829.3	110903.3	35.7	835.8	279.3	140.6	0.0941
343	0.332	1.49E-08	819.8	124492.7	27.2	808.7	270.2	136.1	0.1066

8.3 Residence Time Distribution (R.T.D.)

8.3.1 R.T.D. Measuring Methods

The backmixing characteristics of various phases in a multi-phase reactor are evaluated by injecting a tracer into the phase of interest at the inlet point and then measuring the residence time distribution (RTD) of the tracer in the exit steam. Shah et al. (1978) thoroughly reviewed the methods for measuring R.T.D. for various phases in gas-liquid contactors and the common tracers and detection methods for a number of different reactor types. Various types of tracer inputs such as step, pulse, sinusoidal, ramp and parabolic are available but step and pulse inputs are the most common ones.

(1) Step Input Method: A tracer is added continuously at a certain point in the reactor and its output is measured on-line or by sampling.

(2) Pulse Input Method - A tracer is injected into the liquid phase as a pulse and the concentration is measured at a certain distance away from the injection point.

Since the pulse input method was mostly used in gas-liquid dispersion studies (Shah et al., 1978) it was also used in this investigation.

8.3.2 Mathematical Analysis

The mixing characteristics are usually expressed by numerical values (Levenspiel, 1972). The most important measure is the centroid of the distribution $\bar{t}$. For a pulse input of tracer into the stream line the corresponding output is termed a **C** curve (Figure 8.3.1). The mean residence time $\bar{t}$ is given by:

$$\bar{t} = \frac{\int_0^\infty t.Cdt}{\int_0^\infty Cdt} \qquad (8.3.1)$$

where C = tracer concentration

t = time

$\bar{t}$ = mean residence time

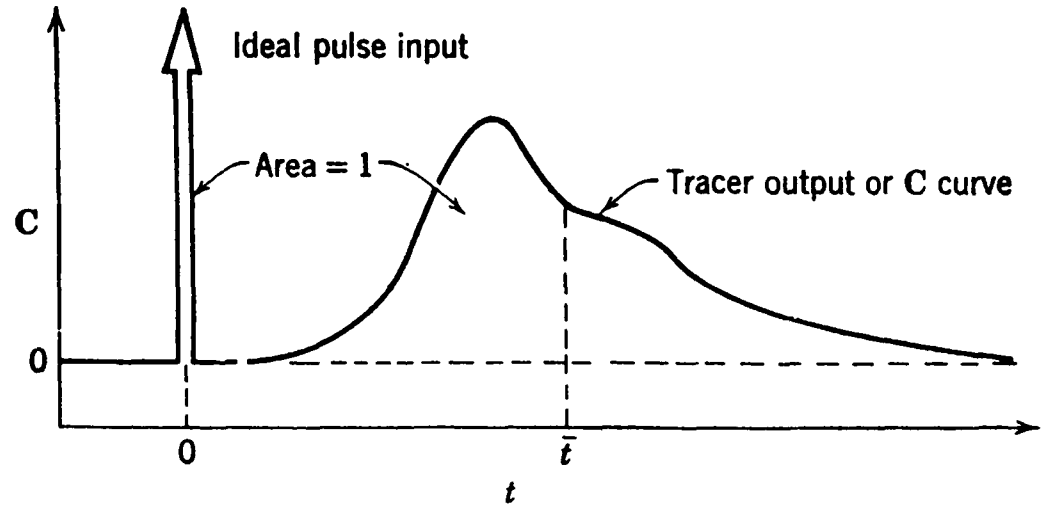

Figure 8.3.1 Typical C Curve Obtained from Pulse Input (Levenspiel, 1972)

For a number of discrete and evenly spaced time intervals the equation (8.3.1) may be written as:

$$\bar{t} \approx \frac{\sum t_i C_i}{\sum C_i} \qquad (8.3.2)$$

The spread or variance of the distribution is expressed as:

$$\sigma^2 = \frac{\int_0^\infty (t-\bar{t})^2 . C dt}{\int_0^\infty C dt} = \frac{\int_0^\infty t^2 . C dt}{\int_0^\infty C dt} - \bar{t}^2 \qquad (8.3.3)$$

where σ^2 = variance

For a number of discrete and evenly spaced time intervals equation (8.3.3) may be written as:

$$\sigma^2 \approx \frac{\sum (t_i - \bar{t})^2 C_i}{\sum C_i} \approx \frac{\sum t_i^2 C_i}{\sum C_i} - \bar{t}^2 \qquad (8.3.4)$$

The axial dispersion coefficient of the liquid phase in a bubble column may be determined by using the mean residence time and the variance. For a closed reactor, a dimensionless variance (σ_θ^2) is defined by :

$$\sigma_\theta^2 = \frac{\sigma^2}{\bar{t}^2} \qquad (8.3.5)$$

8.3.3 Flow Models

8.3.3.1 Ideal Flow Reactors

(1) Plug Flow Reactor (P.F.R.)

This flow is characterized by the facts that the flow through the reactor is orderly with no element of fluid overtaking or mixing with any other element ahead or behind and that all the elements have the same residence time.

(2) Continuously Stirred Tank Reactor (C.S.T.R.)

This reactor is characterized by the fact that all the contents are well stirred and uniform throughout and the exit stream from the reactor has the same composition as the fluid in the reactor.

8.3.3.2 Non-Ideal Flow Models

Although several models are available Deckwer and Schumpe (1987) and Deckwer (1992) suggested that one dimensional axial dispersion model is suitable to describe the mixing characteristics of the liquid phase in bubble columns. The backmixing in the axial dispersion model is characterized by a Fick's law type of diffusion superimposed on a plug flow model (Levenspiel, 1972). This model is usually expressed by the following equation

$$\frac{\partial C}{\partial t} = E\frac{\partial^2 C}{\partial x^2} \qquad (8.3.6.)$$

where C = tracer concentration

t = time

x = axial co-ordination

E = axial dispersion coefficient

Equation (8.3.6) can be expressed in dimensionless form as:

$$\frac{\partial C}{\partial \theta} = \left(\frac{E}{u.L}\right)\frac{\partial^2 C}{\partial z^2} - \frac{\partial C}{\partial z} \qquad (8.3.7)$$

where

$$z = \frac{u.t + x}{L} \qquad (8.3.8)$$

$$\theta = \frac{t}{\bar{t}} = \frac{t.u}{L} \qquad (8.3.9)$$

The axial dispersion coefficient (E) provides a measure of the extent of backmixing and it is usually expressed in the dimensionless form as the Peclet Number (Pe):

$$Pe = \frac{uL}{E} \qquad (8.3.10)$$

where Pe = Peclet Number, --

u = superficial velocity, $m.s^{-1}$

L = characteristic length, m

The Peclet Number can be used to differentiate between the various degrees of backmixing and can be determined for a particular reactor by experiment.

$Pe \rightarrow 0$ complete dispersion (Mixed Flow)

$Pe \rightarrow \infty$ negligible dispersion (Plug Flow)

The axial dispersion model (Equation (8.3.7)) can be solved for different cases. Its solution is dependent on the extent of backmixing and whether the system is closed or open. The extent of dispension can be assessed by the value of E/(u.L): for small

dispersion E/(u.L) ≤ 0.02 and for large dispersion E/(u.L) ≥ 0.2. The equation for a large extent of dispersion should be used if 0.02 ≤ E/(u.L) ≤ 0.2 (Levenspiel, 1972).

(1) Small extents of dispersion

$$\bar{\theta} = 1 \qquad (8.3.11)$$

$$\sigma_\theta^2 = \frac{2}{Pe} \qquad (8.3.12)$$

(2) Large extents of dispersion

1. For open vessel

$$C = \frac{1}{2\sqrt{\pi\theta\left(\frac{1}{Pe_L}\right)}} \exp\left(-\frac{(1-\theta)^2}{4\theta\left(\frac{1}{Pe_L}\right)}\right) \qquad (8.3.13)$$

$$\bar{\theta} = 1 + \left(\frac{2}{Pe_L}\right) \qquad (8.3.14)$$

$$\sigma_\theta^2 = \left(\frac{2}{Pe_L}\right) + 8\left(\frac{1}{Pe_L}\right)^2 \qquad (8.3.15)$$

2. For closed vessel

$$\sigma_\theta^2 = 2\left(\frac{1}{Pe_L}\right) - 2\left(\frac{1}{Pe_L}\right)^2 \left(1 - \exp(-Pe_L)\right)$$

where Pe_L = Peclet Number of the liquid phase, $Pe_L = \frac{u_L L}{E_{Z\,L}}$

E_{ZL} = axial dispersion coefficient of the liquid phase

u_L = superficial liquid velocity

L = length of reactor

8.4 Calculation of Mass Transfer Coefficient

8.4.1 Equilibrium Data

1. Solubility of Oxygen in Water

The solubility of oxygen in water can be expressed as the mole fraction (X_1) at a gas partial pressure of 1 atm (0.1MPa):

$$\ln(X_1) = -66.73538 + \frac{87.47547}{\left(\frac{T}{100}\right)} + 24.45264 \times \ln\left(\frac{T}{100}\right) \qquad (8.4.1)$$

where T = temperature, K

2. Henry's Law Coefficient (*H*)

The Henry's law constant H can be obtained by the following equation

$$H = \frac{p_{O_2}}{X_{O_2}} = \frac{1}{X_1} \qquad (8.4.2)$$

where p_{O_2} = oxygen partial pressure, atm

X_{O_2} = oxygen mole fraction at P_{O_2} atm

3. Oxygen Equilibrium Concentration at Operation Pressure

If C = the total molar concentration of the liquid solution, $kmol.m^{-3}$

C^* = oxygen equilibrium concentration, $kmol.m^{-3}$

ρ_L = the density of the solution, $kg.m^{-3}$

M_m = the average molecular weight, $kg.kmol^{-1}$

X_{O_2} = oxygen equilibrium molar fraction at operating pressure

$$C^* = CX_{O_2} \qquad (8.4.3)$$

and $$C = \frac{\rho_L}{M_m} \qquad (8.4.4)$$

If M = molecular mass of the solute, $kg.kmol^{-1}$

M_s = the molecular mass of the solvent, $kg.kmol^{-1}$

$$M_m = MX_{O_2} + M_s(1 - X_{O_2}) \qquad (8.4.5)$$

Combining equation 8.4.3, 8.4.4 and 8.4.5 and rearrange it,

$$C_A^* = \frac{X_{O_2}\rho_L}{MX_{O_2} + M_s(1 - X_{O_2})} \qquad (8.4.6)$$

Since the concentration of the gas solute in the liquid solution is very small, the mass of the solute is negligible compared to that of the solvent so that

$$MX_{O_2} + M_s(1 - X_{O_2}) \approx M_s(1 - X_{O_2}) \approx M_s \qquad (8.4.7)$$

and the density of the solution could be replaced by the density of the solvent

$$C^* \approx \frac{X_{O_2}\rho_s}{M_s} \qquad (8.4.8)$$

If C_E = oxygen equilibrium concentration, $mg.dm^{-3}$ and replace X_{O_2} with X_I

$$C_E = \frac{32}{18} 1.0 \times 10^6 p_{O_2} X_{O_2} \qquad (8.4.9)$$

where the oxygen partial pressure p_{O_2} (atm) assumed to be equal to the column pressure less the nitrogen partial pressure in the same proportion as in the atmosphere ($p_{O_2} = P - 0.79$).

4. Oxygen Inlet Concentration

Based on the same principle the oxygen inlet concentration C_i in $mg.dm^{-3}$ can be expressed as the following equation

$$C_i = \frac{32}{18} \times 10^6 (1 - 0.79) X_1 = 3.7333 \times 10^5 X_1 \qquad (8.4.10)$$

8.4.2 Hydrodynamic Parameters

1. Bubble Number Present in the Bubble Dispersion

$$n = \frac{3}{2} \varepsilon_g d_c \frac{h_d}{d_b} \qquad (8.4.11)$$

where n = bubble number

ε_g = gas holdup, %

d_c = column diameter, m

h_d = dispersion height, m

d_b = bubble diameter, m

2. Surface Area:

$$A = \frac{3\pi}{2} \varepsilon_g d_c^2 \frac{h_d}{d_b} \qquad (8.4.12)$$

8.4.3 Mass Transfer Parameters

Mass transfer calculations were carried out based on the following assumptions using the plug flow model and the mixed flow model: (1) for sparingly soluble gases the gas phase resistance is negligible, thus the overall liquid phase mass transfer coefficient $K_L a$ equals to the volumetric liquid phase coefficient $k_L a$, (2) the gas equilibrium concentration is constant along the column.

1 Plug Flow

A mass balance for gas component in liquid phase over a differential dispersion volume increment dV yields

$$F_L dC = k_L a(C_E - C)dV \qquad (8.4.13)$$

Equation (8.4.13) can be integrated over the dispersion volume and between the inlet and outlet concentrations and rearranged it to obtain the volumetric mass transfer coefficient

$$(k_L a)_{plug} = \frac{F_L}{V_d} \ln\left(\frac{C_E - C_i}{C_E - C_o}\right) \qquad (8.4.14)$$

where F_L = liquid flowrate, $m^3.s^{-1}$

V_d = dispersion volume, m^3

k_La = volumetric liquid phase mass transfer coefficient, s^{-1}

C_E = gas equilibrium concentration, $mg.dm^{-3}$

C_i = inlet gas concentration, $mg.dm^{-3}$

C_o = outlet gas concentration, $mg.dm^{-3}$

2 Mixed Flow Model

A mass balance for gas component in the liquid phase over the dispersion volume V_d yields

$$F_L(C_o - C_i) = k_L a(C_E - C_o)V_d \qquad (8.4.15)$$

Rearranging equation (8.4.15) gives the volumetric mass transfer coefficient

$$(k_L a)_{mix} = \frac{F_L}{V_d}\left(\frac{C_o - C_i}{C_E - C_o}\right) \qquad (8.4.16)$$

8.5 Total Surface Area Calculation (BET Equation)

The BET equation is derived using a Langmuir approach by assuming an equilibrium between adsorption/condensation and evaporation with a simplifying assumption for multimolecular layers. In the equation, unimolecular layers appear not only to represent the general shape of the actual isotherms, but also to yield reasonable values for the average heat of adsorption in the first layer and for the volume of gas required to form a unimolecular layer on the adsorbent.

To derive this equation, let S_0, S_1, S_2, S_3, ..., S_i, represent the surface area covered by only 0, 1, 2, ..., i, layers of adsorbed molecules. At equilibrium S_0 remains constant since the rate of condensation on the empty surface is equal to the rate of evaporation from the first layer:

$$a_1 P S_0 = b_1 S_1 exp\left(-\frac{E_1}{RT}\right) \qquad (8.5.1)$$

where P is the pressure, E_1 is the heat of adsorption of the first layer, and a_1 and b_1 are constants (pre-exponential terms) which are independent of the number of adsorbed molecules from Langmuir's equation assumptions.

At equilibrium S_1 must also remain constant, and it is defined in a similar manner to equation (8.5.1):

$$a_2 P S_1 = b_2 S_2 exp\left(-\frac{E_2}{RT}\right) \qquad (8.5.2)$$

The rate of condensation on the top of the first layer is equal to the rate of evaporation from the second layer. If condensation is extended to the second and consecutive layers it follows that

$$a_i P S_{i-1} = b_i S_i exp\left(-\frac{E_i}{RT}\right) \qquad (8.5.3)$$

The total surface area (A) of the catalyst is given by

$$A = \sum_{i=0}^{\infty} S_i \qquad (8.5.4)$$

and the total volume adsorbed is

$$V = V_o \sum_{i=0}^{\infty} i S_i \qquad (8.5.5)$$

where V_0 is the volume of the adsorbed gas on one unit area of the adsorbent surface when it is covered with a complete unimolecular layer of the adsorbed gas.

$$\frac{V}{AV_0} = \frac{V}{V_m} = \frac{\sum_{i=0}^{\infty} i S_i}{\sum_{i=0}^{\infty} S_i} \qquad (8.5.6)$$

Simplifying assumptions are made as follows:

$$E_2 = E_3 = \cdots = E_i = E_L \qquad (8.5.7)$$

$$\frac{b_2}{a_2} = \frac{b_3}{a_3} = \cdots = \frac{b_i}{a_i} = g \qquad (8.5.8)$$

where E_L is the heat of liquefaction and g is the appropriate constant. The following relationships can be written:

$$S_1 = yS_0, \text{ where } y = (a_1/b_1)P\, exp(E_1/RT) \qquad (8.5.9)$$

$$S_2 = xS_1, \text{ where } x = (P/g)\, exp(E_L/RT) \qquad (8.5.10)$$

$$S_i = xS_{i-1} = x^{i-1} S_1 = yx^{i-1} S_0 = Cx^i S_o \qquad (8.5.11)$$

where $$C = \frac{y}{x} = \frac{a_1 b_2}{b_1 a_2} \exp[(E_1 - E_L)/RT] \qquad (8.5.12)$$

Substituting into equation (8.5.6) and performing the summation, it follows that

$$\frac{V}{V_m} = \frac{Cx}{(1-x)(1-x-Cx)} \qquad (8.5.13)$$

During adsorption on a free surface with saturation pressure of the gas, an infinite number of layers can be built up on the adsorbent so that $V = \infty$, when the system pressure equals the has saturated pressure and x must be equal to unity. Substituting this result into equation (8.5.12) the isotherm equation is obtained as

$$V = \frac{V_m CP}{(P-P_o)[1+(C-1)(P/P_o)]} \qquad (8.5.14)$$

Rearranging this equation in a linear form the BET equation is obtained:

$$\frac{P}{V(P_o - P)} = \frac{1}{V_m C} + \frac{C-1}{V_m C} \times \frac{P}{P_o} \qquad (8.15)$$

where V_m = volume of adsorbed gas into a monolayer

C = constant, defined by Equation (8.5.12)

P = partial pressure of adsorbed gas in the system (partial pressure of nitrogen in helium/nitrogen gas mixture)

P_o = saturated pressure of the adsorbed gas (vapour pressure of nitrogen at the temperature of the adsorption/desorption process if helium/nitrogen mixture is used)

A straight line can be obtained by a plot of $\frac{P}{V(P_O - P)}$ against $\frac{P}{P_O}$ with a slope $\frac{(C-1)}{V_m C}$ and an intercept $\frac{1}{V_m}$. The value of V_m can be obtained from the slope or the intercept. The total surface area per gramme (S_g) of solid adsorbent can be calculated:

$$S_g = \frac{(V_m N_o)}{V}\alpha \qquad (8.5.16)$$

where N_o = Avogadro Number, 6.023×10^{23}

V = volume per mole of gas at conditions of V_m (since V_m is recorded at STP, $V = 2.4\times10^3$ cm^3.mole^{-1})

α = area occupied by one adsorbed molecule

The value of α can be estimated by the following equation (Emmett and Brunauer, 1937):

$$\alpha = 1.09\left(\frac{M}{\rho N_o}\right)^{2/3} \qquad (8.5.17)$$

where M = molar mass of nitrogen

N_o = Avogadro number

ρ = nitrogen density at 77.4K, 0.808g.cm^{-3}

Therefore the total surface area S_g (cm^2.g^{-1}) can be obtained by using the above equations with nitrogen as the adsorbed gas:

$$S_g = 4.35\times10^4 V_m \qquad (8.5.18)$$

8.6 Tables

Table 8.6.1.1 Calibration of Water Flowrate in 100mm CDC

F_L, %	0	10	20	30	40	50	60	70	80	90	100
F_L, $cm^3.s^{-1}$	0	36.3	258.9	375.0	511.9	692.5	747.5	943.8	1035.7	1234.4	1433.3

Table 8.6.2.1 Gas Holdup and Mass Transfer Measurements

Run	d_o	$T_{wat.}$	T_{air}	P,	P_{O2}	F_L	F_G	DO_1	DO_2	DO_3	DO_4	DO_5	DO_6	H_d	H_{dead}	H_{shut}	ε_g	ε_g	u_{jet}	Re	C_i	C*	k_La	k_La
No.	mm	°C	°C	psig	psig	cm^3/s	cm^3/min	ppm	ppm	ppm	ppm	ppm	ppm	cm	cm	cm	dead	shut	m/s	-	ppm	ppm	plug	mix
M1	10	12	20	10	14	665	400	34.4	35.0	35.5	35.7	36.0	36.2	111	55	60	49.5	54.1	8.5	84713	11.0	46.6	0.10	0.19
M2	10	12	23	11	15	665	600	40.6	41.0	41.6	42.0	42.4	42.8	138	65	71	47.1	51.4	8.5	84713	10.9	46.2	0.16	0.64
M3	10	12	23	11	14	665	800	42.0	42.6	43.1	43.6	44.1	44.6	152	78	85	51.3	55.9	8.5	84713	11.0	46.6	0.20	1.14
M4	10	12	14	10	15	665	1000	44.2	44.7	45.2	45.6	45.0	45.5	152	84	96	55.3	63.2	8.5	84713	11.0	46.6	0.24	2.11
M5	10	12	14	10	20	945	300	26.1	26.2	26.2	26.2	26.2	26.2	38	#	11	#	28.9	12	120382	11.0	46.6	0.24	0.32
M6	10	12	23	10	19	945	400	29.0	30.0	30.6	30.6	30.6	30.6	66	14	22	21.2	33.3	12	120382	11.0	46.6	0.15	0.22
M7	10	11	22	10	19	945	600	35.3	36.3	37.2	38.1	39.5	39.5	130	51	63	39.2	48.5	12	120382	11.1	47.2	0.15	0.36
M8	10	11	22	10	20	945	800	41.4	42.5	43.1	44.0	44.2	44.6	152	83	95	54.6	62.5	12	120382	11.1	47.2	0.26	1.24
M9	10	12	22	10	27	1230	300	24.3	25.2	24.4	24.6	24.7	25.0	42	#	5	#	11.9	16	156688	11.0	46.6	0.26	0.33
M10	10	12	22	10	27	1230	400	26.8	27.8	27.9	28.0	28.0	28.0	60	#	11	#	18.3	16	156688	11.0	46.6	0.21	0.3
M11	10	12	22	10	27	1230	600	30.5	32.1	33.0	33.7	34.6	35.2	138	26	31	18.8	22.5	16	156688	11.0	46.6	0.15	0.27
M12	10	12	22	10	27	1230	800	37.6	38.8	39.4	39.8	40.5	40.8	152	74	84	48.7	55.3	16	156688	11.0	46.6	0.23	0.65
M13	10	12	22	10	27	1230	1000	41.2	41.8	42.5	43.6	43.8	44.2	152	82	101	53.9	66.4	16	156688	11.0	46.6	0.34	1.74
M14	12	11	16	10	13	945	400	29.5	30.8	30.4	30.4	30.4	30.4	48	8	22	16.7	45.8	8.4	100318	11.2	47.4	0.20	0.3
M15	12	11	16	10	13	945	600	33.6	35.1	36.1	37.1	38.1	39.1	126	52	65	41.3	51.6	8.4	100318	11.2	47.4	0.15	0.33
M16	12	11	16	10	13	945	800	39.6	41.3	41.8	42.9	43.6	44.2	152	77	92	50.7	60.5	8.4	100318	11.2	47.4	0.24	1.03
M17	12	11	16	10	17	1230	300	23.2	23.2	23.2	23.2	23.2	23.2	38	#	5	#	13.2	11	130573	11.2	47.4	0.23	0.28
M18	12	11	16	10	17	1230	500	26.8	28.3	29.8	29.8	29.8	29.8	75	6	23	8.0	30.7	11	130573	11.2	47.4	0.17	0.25

Table 8.6.2.1 Gas Holdup and Mass Transfer Measurements (Continued)

M19	12	11	22	10	17	1230	700	29.8	31.9	33.1	34.5	35.3	36.5	144	42	60	29.2	41.7	11	130573	11.2	47.4	0.15	0.3
M20	12	11	22	10	17	1230	900	34.0	35.8	37.1	38.3	39.4	40.0	152	60	70	39.5	46.1	11	130573	11.2	47.4	0.20	0.5
M21	12	11	22	10	17	1230	1000	37.6	39.4	40.1	40.7	41.5	42.0	152	83	102	54.6	67.1	11	130573	11.2	47.4	0.24	0.73
M22	12	11	22	10	19	1370	300	21.2	21.9	21.9	21.9	21.9	21.9	40	#	4	#	10.0	12	145435	11.2	47.4	0.20	0.24
M23	12	11	22	10	19	1370	400	24.3	26.2	26.2	26.2	26.2	26.2	50		10	0.0	20.0	12	145435	11.2	47.7	0.20	0.26
M24	12	11	22	10	19	1370	600	27.7	29.6	30.2	31.4	31.9	31.9	105	7	29	6.7	27.6	12	145435	11.2	47.7	0.14	0.22
M25	12	11	22	10	19	1370	800	30.4	32.8	33.5	34.8	35.8	37.0	152	32	53	21.1	34.9	12	145435	11.2	47.4	0.18	0.35
M26	12	11	22	10	19	1370	1000	36.2	38.0	38.5	39.3	39.9	40.3	152	54	76	35.5	50.0	12	145435	11.2	47.4	0.23	0.59
M27	16	12	20	10	10	945	500	27.9	29.9	31.2	31.4	32.0	32.4	80	27	38	33.8	47.5	4.7	75239	11.0	46.6	0.15	0.24
M28	16	12	20	10	10	945	700	32.8	34.2	35.4	37.0	38.3	39.3	130	56	72	43.1	55.4	4.7	75239	11.0	46.6	0.16	0.38
M29	16	12	20	10	10	945	1000	32.7	35.3	36.8	38.3	39.5	40.5	140	65	73	46.4	52.1	4.7	75239	11.0	46.6	0.17	0.47
M30	16	12	20	10	12	1230	300	21.8	21.8	21.8	21.8	21.8	21.8	38	#	3	#	7.9	6.1	97930	11.0	46.6	0.20	0.24
M31	16	12	20	10	12	1230	500	25.6	27.6	28.0	28.2	28.2	28.2	37	8	21	21.6	56.8	6.1	97930	11.0	46.6	0.30	0.39
M32	16	12	15	10	12	1230	700	27.0	29.2	30.6	32.6	33.5	34.6	124	28	42	22.6	33.9	6.1	97930	11.0	46.6	0.14	0.25
M33	16	12	15	10	12	1230	900	32.2	34.0	35.2	36.7	37.7	38.4	152	57	71	37.5	46.7	6.1	97930	11.0	46.6	0.19	0.42
M34	16	12	15	10	12	1230	950	35.4	36.8	37.3	38.2	39.2	39.8	152	83	99	54.6	65.1	6.1	97930	11.0	46.6	0.21	0.54
M35	16	12	18	10	12	1370	300	14.5	14.7	14.7	14.7	14.7	14.7	37	#	2	#	5.4	6.8	109076	11.0	46.6	0.07	0.07
M36	16	12	18	10	12	1370	500	20.6	21.5	21.1	21.1	21.1	21.1	41	#	8	#	19.5	6.8	109076	11.0	46.6	0.20	0.23
M37	16	12	18	10	12	1370	700	23.3	25.0	25.2	25.8	25.8	25.8	61	2	16	3.3	26.2	6.8	109076	11.0	46.6	0.19	0.24
M38	16	12	18	10	12	1370	900	25.1	26.7	28.2	29.4	30.6	30.6	111	15	31	13.5	27.9	6.8	109076	11.0	46.6	0.13	0.21
M39	16	12	18	10	12	1370	1000	25.4	26.9	28.3	29.6	31.0	32.4	123	21	36	17.1	29.3	6.8	109076	11.0	46.6	0.13	0.21

Table 8.6.2.1 Gas Holdup and Mass Transfer Measurements (Continued)

M40	18	12	20	10	10	945	400	21.3	24.3	23.0	23.0	23.0	23.0	56	19	26	33.9	46.4	3.7	66879	11.0	46.6	0.12	0.15
M41	18	12	20	10	10	945	600	24.5	26.7	29.0	30.4	31.0	31.3	107	41	53	38.3	49.5	3.7	66879	11.0	46.6	0.10	0.15
M42	18	12	20	10	10	945	800	28.3	28.3	30.2	32.0	33.7	33.7	124	55	68	44.4	54.8	3.7	66879	11.0	46.6	0.10	0.17
M43	18	12	20	10	10	945	1000	31.5	34.1	36.5	38.4	40.8	41.2	130	60	75	46.2	57.7	3.7	66879	11.0	46.6	0.18	0.54
M44	18	12	20	10	10	1230	400	18.6	20.0	19.4	19.4	19.4	19.4	47	4	11	8.5	23.4	4.8	87049	11.0	46.6	0.10	0.11
M45	18	12	20	10	10	1230	600	20.8	22.8	24.0	25.6	26.0	26.0	91	19	31	20.9	34.1	4.8	87049	11.0	46.6	0.10	0.13
M46	18	12	20	10	10	1230	800	22.5	24.8	26.2	27.5	29.0	30.0	135	35	48	25.9	35.6	4.8	87049	11.0	46.6	0.10	0.15
M47	18	12	20	10	10	1230	1000	26.8	29.2	30.4	31.9	33.4	34.4	152	68	75	44.7	49.3	4.8	87049	11.0	46.6	0.14	0.24
M48	18	12	20	10	10	1370	400	18.8	20.4	19.8	19.8	19.8	19.8	52	1	13	5.1	25.0	5.4	96957	11.0	46.6	0.11	0.13
M49	18	12	20	10	10	1370	600	20.2	22.6	24.0	25.3	25.3	25.3	90	10	23	11.1	25.6	5.4	96957	11.0	46.6	0.11	0.14
M50	18	12	20	10	10	1370	800	22.4	24.5	26.1	27.5	29.1	29.8	138	27	42	19.6	30.4	5.4	96957	11.0	46.6	0.11	0.16
M51	18	12	20	10	10	1370	1000	25.2	27.3	29.4	31.5	33.0	33.8	152	47	59	30.9	38.8	5.4	96957	11.0	46.6	0.15	0.25
M52	20	12	20	10	10	1230	300	19.3	19.4	19.4	19.4	19.4	19.4	37	#	3	#	8.1	3.9	78344	11.0	46.6	0.15	0.17
M53	20	12	20	10	10	1230	500	23.1	24.9	26.5	26.5	26.5	26.5	67	12	21	17.9	31.3	3.9	78344	11.0	46.6	0.14	0.18
M54	20	12	20	10	10	1230	700	24.0	26.0	28.0	29.8	31.8	31.8	111	27	37	24.3	33.3	3.9	78344	11.0	46.6	0.13	0.21
M55	20	12	20	10	10	1230	900	25.5	28.4	30.6	32.3	34.0	35.2	142	47	55	33.1	38.7	3.9	78344	11.0	46.6	0.15	0.27
M56	20	12	20	10	10	1230	1000	28.4	31.0	32.0	34.1	35.3	36.8	152	69	80	45.4	52.6	3.9	78344	11.0	46.6	0.16	0.33
M57	20	12	20	10	10	1370	400	20.8	21.3	21.3	21.3	21.3	21.3	41	#	8	#	19.5	4.4	87261	11.0	46.6	0.20	0.05
M58	20	12	20	10	10	1370	600	22.4	24.4	26.0	25.7	25.7	25.7	75	9	20	12.0	26.7	4.4	87261	11.0	46.6	0.15	0.19
M59	20	12	20	10	10	1370	800	23.3	25.6	26.5	28.9	30.3	31.0	123	23	37	18.7	30.1	4.4	87261	11.0	46.6	0.12	0.18
M60	20	12	20	10	10	1370	1000	27.1	29.0	30.8	32.5	33.7	34.5	152	59	63	38.8	41.4	4.4	87261	11.0	46.6	0.15	0.28

Table 8.6.5.1 Conversion Data in Blank Experiments

T=303K; P =0.1MPa; W_{CAL}=50kg.m^{-3}

t_S	Conversion	of	Cinnamaldehyde
minute	B1: in Propan-2-ol	B2: in Toluene	B3: in Butan-1-ol
15	0.2	0	0.2
30	0.3	0	0.4
60	0.4	0	0.5
120	0.9	0	0.8
180	1.9	0	1.0

* Only hemiacetal and diacetal were detected.

Table 8.6.5.2 Selectivity vs Catalyst Loading in Toluene

T=303K; P =0.6MPa; W_{CAL}=50kg.m^{-3}

W_{cat}, kg.m^{-3}	S_{HC}, %	S_{PP}, %	S_{PB}, %
2	32.5	64.8	2.7
4	35.1	57.9	7
6	32	58.5	9.5
8	28.1	59.3	12.6
12	33.7	51.1	15.2
15	36.7	48.6	14.7

Table 8.6.5.3 Selectivity vs Catalyst Loading in Propan-2-ol

T=303K; P =0.1MPa; W_{CAL}=50kg.m^{-3}

W_{cat}, kg.m^{-3}	S_{HC}, %	S_{PP}, %	S_{PB}, %
2	52.3	41.6	6.1
4	47.2	49.4	3.5
6	42.6	43.2	14.2
8	31.7	42.9	25.4

Table 8.6.5.4 Selectivity vs Temperature in Toluene

P = 0.6MPa; $W_{cat.}$ = 4kg.m^{-3}; W_{CAL} = 50kg.m^{-3}

T, K	S_{HC}, %	S_{PP}, %	S_{PB}, %
293	35.4	56	8.6
303	35.1	57.9	7
323	28.5	67.8	3.7
343	25.1	73.1	1.8

Table 8.6.5.5 Selectivity vs Temperature in Propan-2-ol

P = 0.6MPa; W_{CAL}=50kg.m^{-3}; $W_{cat.}$ = 4kg.m^{-3}

T, K	S_{HC}, %	S_{PP}, %	S_{PB}, %
303	34.9	50	15.1
313	35.1	50.6	14.3
323	34	49.2	16.8
343	48.1	35.8	16.1

Table 8.6.5.6 Selectivity vs Pressure in Propan-2-ol

T =303K; W_{CAL}=50kg.m^{-3}; $W_{cat.}$ = 4kg.m^{-3}

P, MPa	S_{HC}, %	S_{PP}, %	S_{PB}, %
1.1	37.7	55.9	6.4
0.9	43.1	51	5.9
0.6	40.7	51.7	7.6
0.4	39.5	52.5	8
0.1	47.2	49.4	3.5

Table 8.6.5.7 Selectivity vs Substrate in Toluene

T =303K; P= 0.1MPa; $W_{cat.}$ = 4kg.m^{-3}

W_{CAL}, kg.m^{-3}	S_{HC}, %	S_{PP}, %	S_{PB}, %
10	38.1	60	1.9
20	37.5	54.3	8.2
30	32.3	53.9	13.8
50	29.4	59.2	11.4
80	26.3	61.2	12.6
100	24	62.3	13.7

Table 8.6.5.8 Selectivity vs K^+/Pd Ratio with KAc

T =303K; P= 1.1MPa; W_{CAL}=50kg.m^{-3}; $W_{cat.}$ = 4kg.m^{-3};

K^+/Pd Ratio	X_{conv}, %	S_{HC}, %	S_{PP}, %	S_{PB}, %
0.25	100	38.8	55	5.7
0	100	52.4	46	1.6
1	100	57.9	40.9	1.2
2	100	67.1	32.8	0.1
5	100	77.6	21.7	0.6
10	100	85.2	14.8	0
20	100	84.8	15.2	0

Table 8.6.5.9 Selectivity vs K^+/Pd Ratio with KCl

T =303K; P= 1.1MPa; W_{CAL}=50kg.m^{-3}; $W_{cat.}$ = 4kg.m^{-3};

K^+/Pd Ratio	X_{conv}, %	S_{HC}, %	S_{PP}, %	S_{PB}, %
0.25	100	37.1	55.7	7.2
0.5	100	38.3	55.5	6.2
1	100	39.9	55.9	4.2
2	100	30.4	60.8	8.8
5	100	36	58.8	5.2
10	100	38	57	5

Table 8.6.5.10 Selectivity vs K^+/Pd Ratio with KBr

T =303K; P= 1.1MPa; W_{CAL}=50kg.m^{-3}; $W_{cat.}$ = 4kg.m^{-3};

K^+/Pd Ratio	X_{conv}, %	S_{HC}, %	S_{PP}, %	S_{PB}, %
0.25	61.1	56.2	41.7	2.1
0.5	36.5	60.3	34.9	4.8
1	69.8	55.5	39.2	5.3
2	62.9	45.3	47.6	7
5	86.9	55.8	39	7.4
10	68.2	55.1	39	6

Table 8.6.5.11 Selectivity vs K^+/Pd Ratio with $AlCl_3$

T =303K; P= 1.1MPa; W_{CAL}=50kg.m^{-3}; $W_{cat.}$ = 4kg.m^{-3};

Al^{3+}/Pd Ratio	X_{conv}, %	S_{HC}, %	S_{PP}, %	S_{PB}, %
0.25	100	36	59.3	4.7
0.5	100	40.3	56.5	3.2
1	95.6	43.5	54.6	1.9
2	77	51.4	47.9	0.7
5	60.3	42.6	55.3	2.1
10	5.2	37.9	36	26.1

Table 8.6.5.12 Selectivity vs K^+/Pd Ratio with K_2CO_3*

T =303K; P= 1.1MPa; W_{CAL}=50kg.m^{-3}; $W_{cat.}$ = 4kg.m^{-3};

K^+/Pd Ratio	X_{conv}, %	S_{HC}, %	S_{PP}, %	S_{PB}, %
0.25	100	38.6	57.6	3.8
0.5	98.8	56.2	43.1	0.7
1	100	79.4	18.1	2.5
2	100	82.6	17.3	0.1
5	100	92.1	7.8	0.1
10	100	97.6	2.3	0.1
20	100	97.1	2.8	0.1

* In-house prepared catalyst.

Table 8.7.5.13 Stirring Speed vs Stirrer Setting

Stirrer Setting	Stirring Speed, rpm (in 250 ml Reactor)
2	450
4	850
6	1250
8	1600
10	2000

Table 8.6.5.14 Reaction Rate vs Stirring Speed

T=303K; C_A=50 kg.m^{-3}; W=4 kg.m^{-3}

	250ml STR	500ml STR
N_{stir}, rpm	10^3×Ra kmol.m^{-3}.s^{-1}	10^3×Ra kmol.m^{-3}.s^{-1}
400	0.187	0.284
600	0.287	0.568
800	0.541	0.731
1000	0.618	0.73
1200	0.618	0.728
1400	0.613	0.732

Table 8.6.5.15 Reaction Rate vs Gas Mode

T=303K; C_A=50 kg.m^{-3}; W=4 kg.m^{-3}

10^3×Ra, kmol.m^{-3}.s^{-1}	10^3×Ra, kmol.m^{-3}.s^{-1}
Mode A	Mode B
0.618	0.615
0.618	0.598
0.613	0.618

Table 8.6.5.16 Reaction Rate vs Cinnamaldehyde Concentration

T = 303K; P = 0.1MPa; W_{cat} = 4kg.m^{-3}; Solvent = Toluene

W_{CAL}, kg.m^{-3}	10^3×Ra, kmol.m^{-3}.s^{-1}
10	0.460
20	0.468
30	0.470
50	0.467
80	0.472
100	0.465

Table 8.6.5.17 Homogeneous Reaction Effect on Reaction Rate

T = 303K; P = 0.1MPa; W_{CAL} = 50kg.m^{-3}; Solvent = Propan-2-ol

$W_{cat.}$, kg.m^{-3}	10^3×Ra, kmol.m^{-3}.s^{-1}	10^3×Ra, kmol.m^{-3}.s^{-1}
	Pre-prepared	Fresh
2	0.255	0.230
3	0.462	-
4	0.620	0.475
5	0.693	-
6	0.922	0.687
8	-	0.987

Table 8.6.5.18 Reaction Rate vs Catalyst Loading in Pre-prepared Solution

P = 0.1MPa; W_{CAL} = 50kg.m^{-3}; Solvent = Propan-2-ol

	10^3×Ra, kmol.m^{-3}.s^{-1}					
W_{cat}, kg.m^{-3}	273k	283K	293K	303K	313K	323K
2	0.0451	0.111	0.187	0.255	0.423	0.493
3	0.076	0.15	0.363	0.462	0.667	0.722
4	0.099	0.213	0.447	0.62	0.818	0.977
5	0.118	0.228	0.488	0.693	1.162	1.433
6	0.134	0.31	0.633	0.922	1.44	1.71

Table 8.6.5.19 Reaction Rate vs Catalyst Loading in Fresh Solution

T = 303K; P = 0.1MPa; W_{CAL} = 50kg.m^{-3}; Solvent = Propan-2-ol

$W_{cat.}$, kg.m^{-3}	10^3×Ra, kmol.m^{-3}.s^{-1}
2	0.23
4	0.475
6	0.687
8	0.987

Table 8.6.5.20 Reaction Rate vs Catalyst Loading in Fresh Solution

T = 303K; P = 0.6MPa; W_{CAL} = 50kg.m^{-3}; Solvent = Toluene

$W_{cat.}$, kg.m^{-3}	10^3×Ra, kmol.m^{-3}.s^{-1}
2	0.347
4	0.73
6	1.237
8	1.353
12	2.09
15	2.377

Table 8.6.5.21 Reaction Rate vs Temperature in Pre-prepared Solution

T = 303K; P = 0.1MPa; W_{CAL} = 50kg.m^{-3}; Solvent = Propan-2-ol

T, K	ln(Ra)	ln(Ra)	ln(Ra)	ln(Ra)	ln(Ra)
323	-7.614	-7.234	-6.93	-6.55	-6.37
313	-7.767	-7.313	-7.11	-6.76	-6.54
303	-8.274	-7.681	-7.32	-7.27	-6.99
293	-8.604	-	-7.65	-7.62	-7.36
283	-9.109	-8.807	-8.45	-8.38	-8.08
273	-10.103	-9.489	-9.22	-9.04	-8.92
$W_{cat.}$, kg.m^{-3}	2	3	4	5	6

Table 8.6.5.22 Reaction Rate vs Temperature in Fresh Solution

W_{CAL} = 50kg.m^{-3}; Solvent = Propan-2-ol

T, K	ln(Ra)	ln(Ra)
343	-	-5.135
323	-7.286	-5.911
313	-7.491	-6.614
303	-7.652	-7.688
293	-8.09	-
283	-8.534	-
P =	0.1MPa	0.6MPa

Table 8.6.5.23 Reaction Rate vs Temperature in Fresh Solution

W_{CAL} = 50kg.m^{-3}; Solvent = Toluene

T,K	ln(Ra)	ln(Ra)	ln(Ra)
293	-8.501	-7.996	-7.575
303	-7.283	-6.903	-6.312
323	-5.604	-5.543	-5.094
343	-4.412	-3.981	-3.638
P =	0.4 MPa	0.6 MPa	0.9 MPa

Table 8.6.5.24 Reaction Rate vs Pressure in Fresh Solution

T = 303K; W_{CAL} = 50kg.m^{-3}; $W_{cat.}$ = 4kg.m^{-3}; Solvent = Propan-2-ol

P, MPa	Ra×10^{3}, kmol.m^{-3}
1.1	2.862
0.9	2.123
0.6	1.482
0.4	0.848
0.1	0.475

Table 8.6.5.25 Reaction Rate vs Pressure in Fresh Solution

W_{CAL} = 50kg.m^{-3}; $W_{cat.}$ = 4kg.m^{-3}; Solvent = Toluene

P, MPa	Ra×10^3, kmol.m^{-3}	Ra×10^3, kmol.m^{-3}	Ra×10^3, kmol.m^{-3}	Ra×10^3, kmol.m^{-3}
0.1	-	0.1867	-	-
0.4	0.2033	0.6867	2.6	12.13
0.6	0.3367	1.005	3.917	18.67
0.9	0.5133	1.815	6.132	26.31
T =	293K	303K	323K	343K

Table 8.6.5.26 Reaction Rate vs Hydrocinnamaldehyde Concentration

T = 303K; P= 0.1MPA; W_{CAL} = 50kg.m^{-3}; $W_{cat.}$ = 4kg.m^{-3}; Solvent = Toluene

W_{HC}, kg.m^{-3}	Ra×10^3, kmol.m^{-3}
0	0.475
5	0.462
10	0.484
25	0.468

Table 8.6.5.27 k_s Calculation in Propan-2-ol

W_{CAL} = 50kg.m^{-3}; $W_{cat.}$ = 4kg.m^{-3}; Solvent = Propan-2-ol (Pre-prepared)

1/(W-0.5)	C_A^*/Ra	C_A^*/Ra	C_A^*/Ra	C_A^*/Ra	C_A^*/Ra	C_A^*/Ra
0.67	60.09	25.66	16.09	12.00	7.46	6.59
0.40	35.79	18.97	8.12	6.63	4.74	4.50
0.29	27.46	13.31	6.60	4.94	3.86	3.33
0.22	22.90	12.44	6.04	4.41	2.72	2.27
0.18	20.22	9.16	4.66	3.32	2.19	1.90
T =	273K	283K	293K	303K	313K	323K

Table 8.6.5.28 k_s Calculation in Toluene

T = 303K; P=0.6MPa; W_{CAL} = 50kg.m^{-3}; Solvent = Toluene

$W_{cat.}$, kg,m^{-3}	Ra×10^3, kmol.m^{-3}	C_A^*/Ra
2	0.3467	50.3
4	0.73	25
6	1.237	14.75
8	1.353	13.49
12	2.09	8.73
15	2.377	7.68

Table 8.6.6.1 Calibration of Liquid Flowmeter in the 50mm Glass CDC

$F_{L,read}$, $L.min^{-1}$	0	4	6	8	10	12	14
$F_{L,actual}$, $L.min^{-1}$	0	3.04	4.96	7.25	9.80	11.47	13.59

Table 8.6.6.2 Calibration of Break Vessel Volume in the 50mm Glass CDC

h, cm	3.6	5	6.5	8	9.5	11	12.5	14.1
V_B, dm^3	1.5	2	2.5	3	3.5	4	4.5	5
h, cm	15.7	17.2	18.5	19.9	21	22.4	23.8	
V_B, dm^3	5.5	6	6.5	7	7.5	8	8.5	

Table 8.6.6.3 Selectivity vs Temperature over Pd/C in the CDC

P = 0.3MPa; W_{cat} = 4kg.m^{-3}; W_{CAL} = 50kg.m^{-3}; $H_{disp.}$=120cm

T, K	X_{conv}, %	S_{HC}, %	(DA%)	S_{PP}, %	S_{PB}, %
293	100	53.3	(60.2)	42.0	4.7
313	100	54.5	(70.8)	41.5	4.0
323	100	60.2	(83.7)	38.0	1.8
348	100	63.5	(88.5)	32.8	3.7

Table 8.6.6.4 Selectivity vs Catalyst Loading over Pd/C in the CDC

T = 293K; P = 0.3MPa; W_{CAL} = 50kg.m^{-3}; $H_{disp.}$=120cm

$W_{cat.}$, kg.m^{-3}	X_{conv}, %	S_{HC}, %	(DA%)	S_{PP}, %	S_{PB}, %
2	100	60.2	(48.9)	38.2	1.6
4	100	53.3	(60.2)	42.0	4.7
8	100	52.2	(66.2)	45.4	2.4

Table 8.6.6.5 Rate vs Temperature over Pd/C in the CDC

P = 0.3MPa; Wcat. = 4kg.m^{-3}; W_{CAL} = 50kg.m^{-3}; $H_{disp.}$=120cm

T, K	$10^3 \times 1/T$	$Ra \times 10^3$, $kmol.m^{-3}.s^{-1}$	ln(Ra)
343	2.92	2.726	1.003
323	3.1	1.162	0.150
313	3.19	0.732	-0.312
293	3.41	0.204	-1.592

Table 8.6.6.6 Rate vs Catalyst Loading over Pd/C in the CDC

T = 293K; P = 0.3MPa; W_{CAL} = 50kg.m^{-3}; $H_{disp.}$=120cm

W_{cat}, kg.m^{-3}	Ra×10^{3}, kmol.m^{-3}.s^{-1}
2	0.1352
4	0.2035
6	0.3829
8	0.5023

Table 8.6.6.7 C_A^* /Ra vs 1/W over Pd/C in the CDC

T = 293K; P = 0.3MPa; W_{CAL} = 50kg.m^{-3}; $H_{disp.}$=120cm

W, kg.m^{-3}	1/W	Ra×10^{3}, kmol.m^{-3}	C_A^*/Ra
2	0.5	0.1352	54.5
4	0.25	0.2035	36.21
6	0.167	0.3829	19.24
8	0.125	0.5023	14.67

Table 8 6.7.1 Selectivity vs Toluene/Water Ratio

T = 288K; P = 0.9MPa; W_{CAL} = 50kg.m^{-3}; W_{Base} = 50kg.m^{-3};
$W_{cat.}$ = 10kg.m^{-3}; Solvent = Toluene/Water

W, kg.m^{-3}	$X_{conv.}$, %	S_{PB}, %	S_{MS}, %	S_{HC}, %	S_{PP}, %	S_{COL}, %
10.0	99.32	0	0.89	1.37	28.10	69.64
5.0	51.91	1.75	1.44	1.33	14.77	80.70
2.0	99.77	0	0.60	0.92	17.69	80.56
1.0	99.02	0	0.38	2.79	15.30	81.53
0.5	99.65	0	0.52	1.03	21.99	76.46
0.2	99.51	0	0.57	1.50	30.04	67.89
0.1	96.88	0	0.55	0.70	35.17	63.58

Table 8.6.7.2 Selectivity vs Catalyst Loading

T = 303K; P = 0.9MPa; W_{CAL} = 50kg.m^{-3};
W_{Base} = 50kg.m^{-3}; Solvent = Toluene/Water (2:1)

W, kg.m^{-3}	$X_{conv.}$, %	S_{COL}, %	S_{HC}, %	S_{PP}, %	S_{MS}, %	S_{PB}, %
5	78.76	94.18	3.21	1.94	0.10	0.57
10	68.89	93.08	5.14	1.29	0.20	0.30
20	95.90	90.73	3.43	5.27	0.26	0.31
30	92.42	95.38	2.90	1.72	0.00	0.00

Table 8.6.7.3 Selectivity vs Cinnamaldehyde Concentration

T = 288K; P = 0.9MPa; W_{Base} = 50kg.m^{-3};
$W_{cat.}$ = 10kg.m^{-3}; Solvent = Toluene/Water (1:1)

W_{CAL}, kg.m^{-3}	$X_{conv.}$, %	S_{COL}, %	S_{HC}, %	S_{PP}, %	S_{MS},%	S_{PB}, %
10	100	27.47	0.56	71.49	0.18	0.28
30	100	72.46	0.3	26.95	0.18	0.12
50	100	81.64	2.79	15.32	0.25	0
50	99.58	83.79	0.9	15.16	0.15	0
75	100	90.57	1.27	8.05	0.11	0
100	100	86.38	0.98	12.45	0.18	0

Table 8.6.7.4 Selectivity vs Cinnamaldehyde Concentration

T = 303K; P = 0.9MPa; W_{Base} = 50kg.m^{-3};
$W_{cat.}$ = 10kg.m^{-3}; Solvent = Toluene/Water (1:1)

W_{CAL}, kg.m^{-3}	$X_{conv.}$, %	S_{PB}, %	S_{MS},%	S_{HC}, %	S_{PP}, %	S_{COL}, %
30	90.31	0.06	0.16	1.17	9.73	88.88
50	96.58	0.07	0.47	1.95	9.28	88.23
100	97.2	0.05	0.19	1.7	6.32	91.74

Table 8.6.7.5 Selectivity vs Base loading at 333K in Water

T = 333K; P = 1.1MPa; W_{CAL} = 50kg.m^{-3}; $W_{cat.}$ = 20kg.m^{-3}; Solvent = Water

W_{Base}, kg.m^{-3}	X_{conv}, %	S_{PB}, %	S_{MS}, %	S_{HC}, %	S_{PP}, %	S_{COL}, %
10	98.65	1.22	9.04	6.46	12.41	70.86
5	97.59	0.54	14.32	9.99	12.12	63.02
1	97.23	0.84	8.49	19.74	20.58	50.34

Table 8.6.7.6 Selectivity vs Base loading at 373K in Water

T = 373K; P = 1.1MPa; W_{CAL} = 50kg.m^{-3}; $W_{cat.}$ = 20kg.m^{-3}; Solvent = Water

W_{Base}, kg.m^{-3}	X_{conv}, %	S_{PB}, %	S_{MS}, %	S_{HC}, %	S_{PP}, %	S_{COL}, %
15	98.68	0.65	34.54	1.05	48.3	15.46
10	100	1.16	45.09	1.05	24.41	28.28
5	98.06	0.87	34.88	1.29	22.35	40.61

Table 8.6.7.7 Selectivity vs Base loading at 373K in Propan-2-ol/Water

T = 373K; P = 1.1MPa; W_{CAL} = 50kg.m^{-3};
$W_{cat.}$ = 20kg.m^{-3}; Solvent = Propan-2-ol/Water

W_{Base}, kg.m^{-3}	X_{conv}, %	S_{PB}, %	S_{MS}, %	S_{HC}, %	S_{PP}, %	S_{COL}, %	S_{aldol}, %
50	98.76	0.10	2.77	0.55	5.62	85.17	5.79
25	96.49	4.98	20.74	4.46	24.58	42.06	3.18
10	66.88	5.40	2.27	22.96	12.06	52.32	5.00
5	74.62	0.96	0.31	22.24	11.45	64.46	0.57
1	47.88	0.41	0.00	13.17	12.12	75.92	0.39

Table 8.6.7.8 Base loading Effect at 303K in Toluene/Water (2:1)

T = 303K; P = 0.9MPa; W_{CAL} = 50kg.m^{-3}; $W_{cat.}$ = 10kg.m^{-3};
Solvent = Toluene/Water (2:1)

W_{Base}, kg.m^{-3}	X_{conv}, %	S_{PB}, %	S_{MS}, %	S_{HC}, %	S_{PP}, %	S_{COL}, %
50	68.78	0	0.00	5.16	1.29	93.53
10	71.53	0	0.00	7.70	3.52	88.77
2	58.01	0	0.00	13.39	5.72	80.89
None	11.11	8.07	1.79	35.03	3.21	51.91

Table 8.6.7.9 Base loading Effect at 303K in Toluene/Water (1:1)

T = 303K; P = 0.2MPa; W_{CAL} = 50kg.m^{-3}; $W_{cat.}$ = 10kg.m^{-3};
Solvent = Toluene/Water (1:1)

W_{Base}, %	X_{conv}, %	S_{PB}, %	S_{MS}, %	S_{HC}, %	S_{PP}, %	S_{COL}, %
5.0	28.63	3.62	0.72	9.15	4.98	81.53
2.0	48.58	1.89	0.18	13.83	5.15	78.95
1.0	31.67	3.84	0.30	15.85	5.99	74.02
0.5	29.36	8.04	1.39	27.99	5.72	58.86

Table 8.6.7.10 Base loading Effect at 303K in Toluene/Water (1:1)

T = 303K; P = 0.9MPa; W_{CAL} = 50kg.m^{-3}; $W_{cat.}$ = 10kg.m^{-3};
Solvent = Toluene/Water (1:1)

W_{Base}, kg.m^{-3}	X_{conv}, %	S_{PB}, %	S_{MS}, %	S_{HC}, %	S_{PP}, %	S_{COL}, %
10.0	100	0.01	1.00	0.60	5.78	92.61
5.0	96.58	0.07	0.47	1.95	9.28	88.23
3.0	100	0.04	0.20	0.45	11.07	88.24
1.0	93.2	0.37	0.28	11.21	16.49	71.65
0.4	49.28	0.72	0.28	34.61	18.08	46.32
0.1	36.64	2.21	0.84	39.39	23.44	34.12

Table 8.6.7.11 Selectivity vs Temperature in Water

T = 303K; P = 0.9MPa; W_{CAL} = 50kg.m^{-3};
$W_{cat.}$ = 10kg.m^{-3}; Solvent = Water

T, K	X_{conv}, %	S_{PB}, %	S_{MS}, %	S_{HC}, %	S_{PP}, %	S_{COL}, %
293	90.43	0.43	0.92	12.26	10.44	75.95
323	87.81	2.65	9.51	11.53	9.12	67.19
333	97.59	0.54	14.32	9.99	12.12	63.02
343	98.54	0.58	20.15	6.75	14.40	58.12
373	98.06	0.87	34.88	1.29	22.35	40.61

Table 8.6.7.12 Selectivity vs Temperature with Toluene/Water (1:1)

P = 0.9MPa; W_{CAL} = 50kg.m^{-3}; $W_{cat.}$ = 50kg.m^{-3};
W_{Base} = 50kg.m^{-3} ; Solvent = Toluene/Water (1:1)

T, K	X_{conv}, %	S_{PB}, %	S_{MS}, %	S_{HC}, %	S_{PP}, %	S_{COL}, %
353	100	1.08	8.73	13.23	14.94	62.03
323	100	0.04	1.95	2.34	14.04	81.63
303	100	0.05	0.46	0.32	14.32	84.32

Table 8.6.7.13 Selectivity vs Temperature with Toluene/Water (14:1)

P = 1.1MPa; W_{CAL} = 50kg.m^{-3}; $W_{cat.}$ = 20kg.m^{-3};
W_{Base} = 0.5kg.m^{-3} ; Solvent = Toluene/Water (14:1)

T, K	X_{conv}, %	S_{PB}, %	S_{MS}, %	S_{HC}, %	S_{PP}, %	S_{COL}, %
373	60.45	0.46	0.14	39.74	14.44	45.22
343	78.05	0.18	0	25.97	19.4	54.46
313	93.18	1.4	0.23	7.23	17.63	73.51

Table 8.6.7.14 Selectivity vs Temperature with Toluene/Water (5:1)

P = 1.1MPa; W_{CAL} = 50kg.m^{-3}; $W_{cat.}$ = 20kg.m^{-3}; W_{Base} = 2.5kg.m^{-3};
Solvent = Toluene/Water (5:1)

T, K	X_{conv}, %	S_{PB}, %	S_{MS}, %	S_{HC}, %	S_{PP}, %	S_{COL}, %
373	80.61	0.64	0.69	34.6	20.13	43.93
343	77.26	0.23	0.21	30.93	18.95	49.68
313	56.52	2.44	0.57	23.07	22.1	51.82

Table 8.6.7.15 Selectivity vs Temperature with Toluene/Water (2:1)

P = 1.1MPa; W_{CAL} = 50kg.m^{-3}; $W_{cat.}$ = 20kg.m^{-3}; W_{Base} = 5kg.m^{-3}; Solvent = Toluene/Water (2:1)

T, K	X_{conv}, %	S_{PB}, %	S_{MS}, %	S_{HC}, %	S_{PP}, %	S_{COL}, %
373	37.62	4.73	0.61	52.65	8.55	33.45
343	98.27	0.1	0.44	14.72	42.12	42.62
313	39.04	0.5	0.75	5.93	45.36	47.46

Table 8.6.7.16 Selectivity vs Pressure at 288K

T = 288K; W_{CAL} = 50kg.m^{-3}; $W_{cat.}$ = 10kg.m^{-3}; W_{Base} = 50kg.m^{-3}; Solvent = Toluene/Water (1:1)

P, MPa	X_{conv}, %	S_{PB}, %	S_{MS}, %	S_{HC}, %	S_{PP}, %	S_{COL}, %
0.2	56.96	0.65	0.55	5.06	4.29	89.46
0.5	100	0.76	0.32	2.04	24.45	72.43
0.99	100	0	0.25	2.79	15.32	81.64
1.1	100	0.46	0.23	0.55	17.38	81.38

Table 8.6.7.17 Selectivity vs Pressure at 303K

T = 303K; W_{CAL} = 50kg.m^{-3}; $W_{cat.}$ = 20kg.m^{-3}; W_{Base} = 50kg.m^{-3}; Solvent = Toluene/Water (2:1)

P, MPa	X_{conv}, %	S_{PB}, %	S_{MS}, %	S_{HC}, %	S_{PP}, %	S_{COL}, %
0.3	76.65	0	0.33	1.23	7.14	91.31
0.6	79	0	0	5.75	3.75	90.5
0.9	68.78	0	0	5.16	1.29	93.53

Table 8.6.7.18 Rate vs. Toluene/Water Ratio

T = 288K; P = 0.9MPa; W_{CAL} = 50kg.m^{-3}; $W_{cat.}$ = 10kg.m^{-3}; W_{Base} = 50kg.m^{-3})

Ratio	Ra×10^{3}, kmol.m^{-3}.s^{-1}
10	0.1255
5	0.1491
2	0.2200
1	0.2742
0.5	0.2000
0.2	0.1850
0.1	0.1833

Table 8.6.7.19 Rate vs. Catalyst Loading

T = 303K; P = 0.9MPa; W_{CAL} = 50kg.m^{-3}; W_{Base} = 50kg.m^{-3}; Solvent = Toluene/Water (2:1)

$W_{cat.}$, kg.m^{-3}	Ra×10^{3}, kmol.m^{-3}.s^{-1}
5	0.1850
10	0.3962
20	0.7663
30	1.1120

Table 8.6.7.20 Rate vs. Pressure

W_{CAL} = 50kg.m^{-3}; W_{Base} = 50kg.m^{-3}; Solvent = Toluene/Water (2:1)

P, MPa	Ra×10^{3}, kmol.m^{-3}.s^{-1} (288K)	Ra×10^{3}, kmol.m^{-3}.s^{-1} (303K)
0.2	0.0688	-
0.3	-	0.186
0.5	0.1347	-
0.6	-	0.3282
0.9	0.2742	0.5312
1.1	0.3287	-

Table 8.6.7.21 Rate vs. Base Loading in Water

P = 1.1MPa; W_{CAL} = 50kg.m^{-3}; $W_{cat.}$ = 20kg.m^{-3}; Solvent = Water

W_{Base}, %	T, K	Ra×10^{3}, kmol.m^{-3}.s^{-1}
1.5	333	0.2670
1	333	0.3562
0.5	333	0.4707
1	373	0.5020
0.5	373	0.3784
0.1	373	0.2418

Table 8.6.7.22 Rate vs. Cinnamaldehyde Concentration

P = 0.9MPa; $W_{cat.}$ = 10kg.m^{-3}; W_{Base} = 50kg.m^{-3}; Solvent = Toluene/Water (1:1)

W_{CAL}, kg.m^{-3}	Ra×10^{3}, kmol.m^{-3}.s^{-1}	Ra×10^{3}, kmol.m^{-3}.s^{-1}
10	0.2298	0.3042
30	0.2398	-
30	0.2332	0.2912
50	0.2375	0.2974
75	0.2345	-
100	0.2432	0.3012
T =	288K	303K

Table 8.6.7.23 Rate vs. Temperature

P = 1.1MPa; $W_{cat.}$ = 10kg.m^{-3};
W_{CAL} = 50kg.m^{-3}; W_{Base} = 50kg.m^{-3}

	ln(Ra)	ln(Ra)
293	-2.24	-
303	-	-2.60
323	-1.12	-1.63
333	-0.64	-
343	-0.40	-
353	-	-0.61
373	0.27	-

8.7 Figures

Figure 8.7.1.1 Calibration Chart for Flowmeter in the 100mm CDC

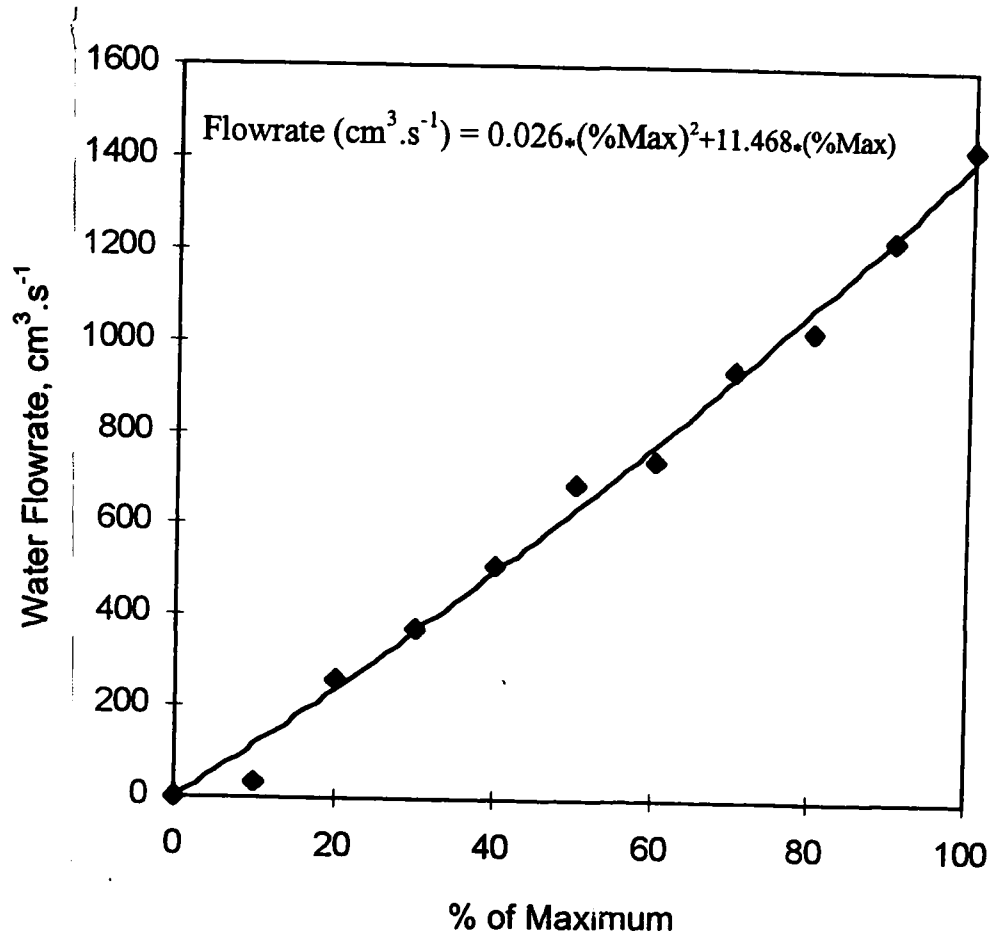

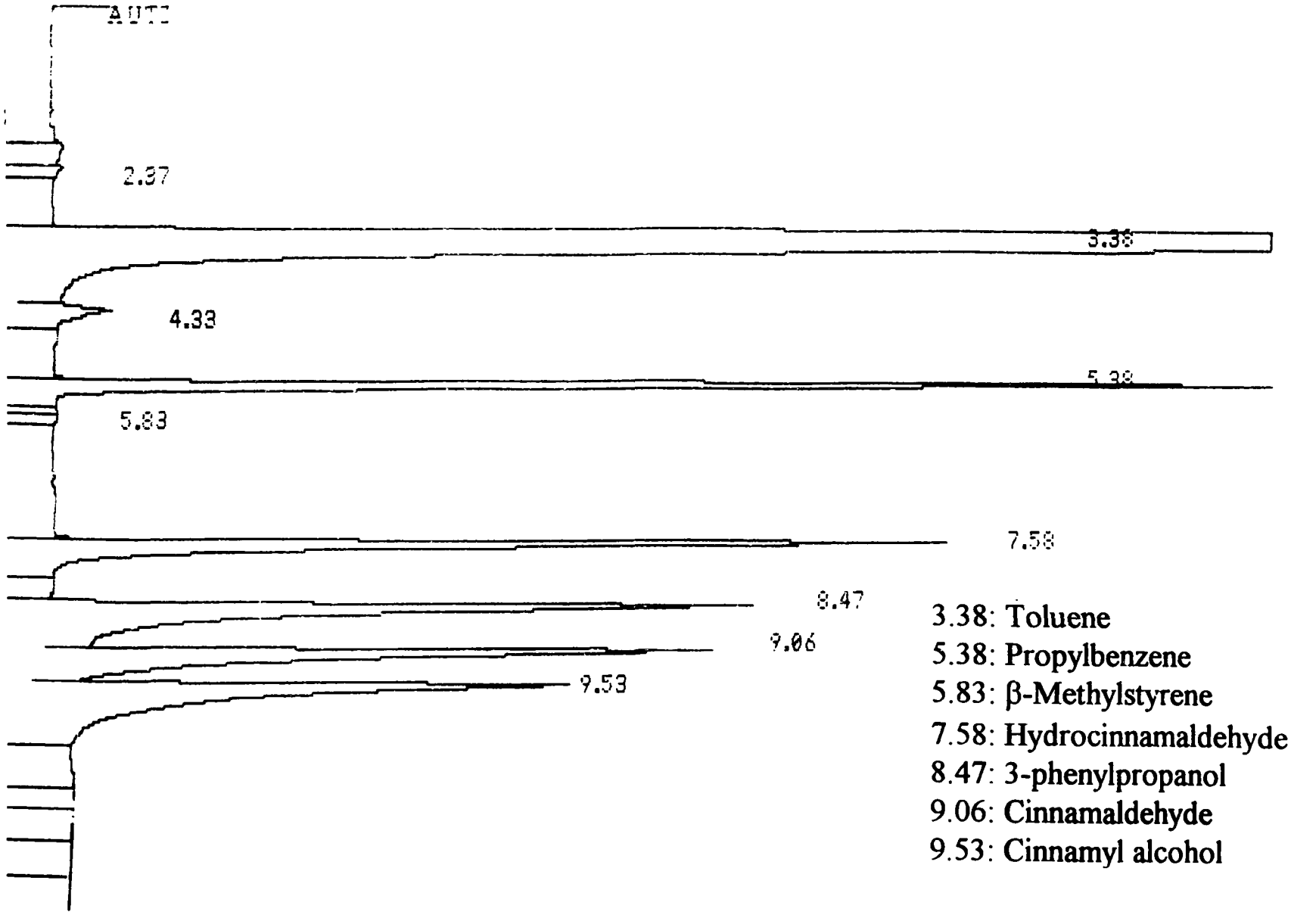

Figure 8.7.5.1 Gas Chromatogram of Standards in Toluene

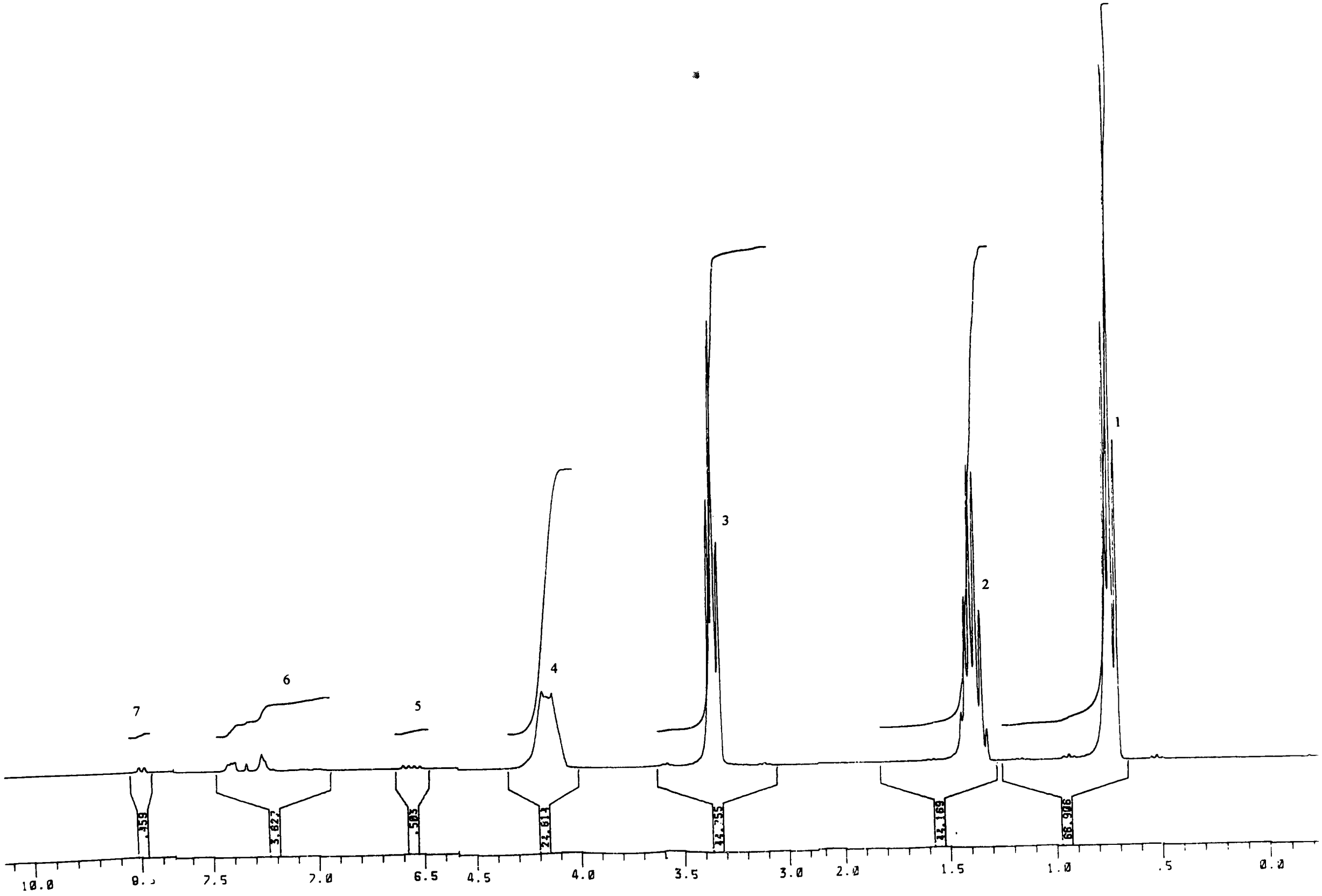

Figure 8.7.5.2 NMR Spectrum of the Initial Sample of Hydrogenation of Cinnamaldehyde in Ethanol

1: $-\underline{C}H_3$ $-\underline{C}H_3$ 2: $-\underline{C}H_2CH_3$ $-\underline{C}H_2CH_3$ 3: $-C(-O\underline{C}H_2-)(-O\underline{C}H_2-)$ 4: $-\underline{C}H=C\underline{H}C\underline{H}-$ (O—, O—) 5: $-\underline{C}H=\underline{C}H-$ 6: 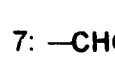 7: $-CHO$

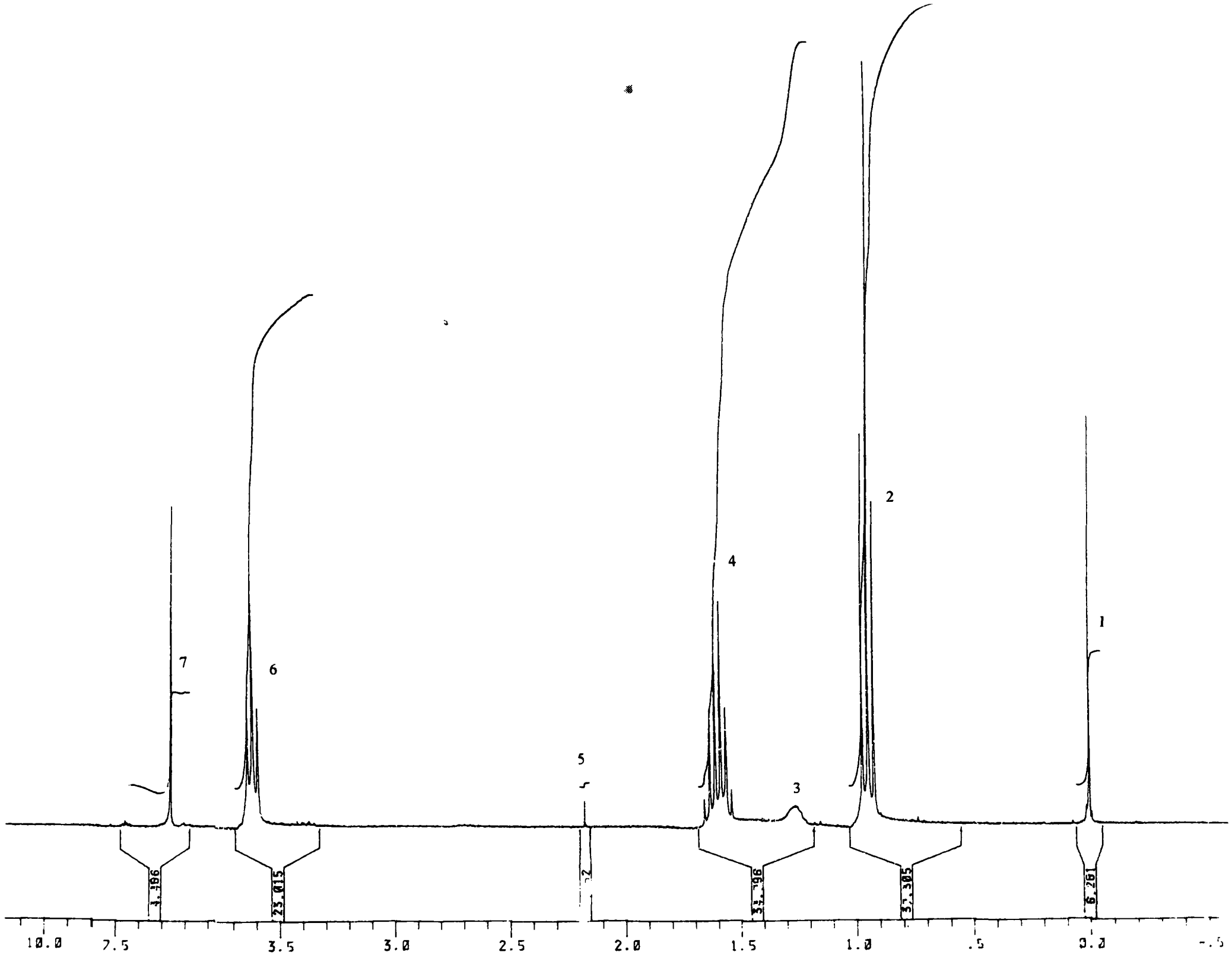

Figure 8.7.5.3 NMR Spectrum of the Final Sample of Hydrogenation of Cinnamaldehyde in Ethanol

1: $C\underline{D}Cl_3$ 2: $-C\underline{H}_3$ / $-C\underline{H}_3$ 3: 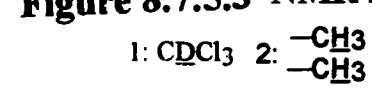 4: $-C\underline{H}_2CH_3$ / $-C\underline{H}_2CH_3$ 5: 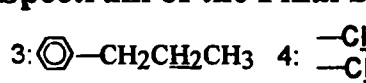 6: 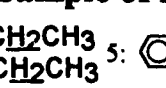 7: 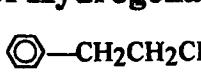

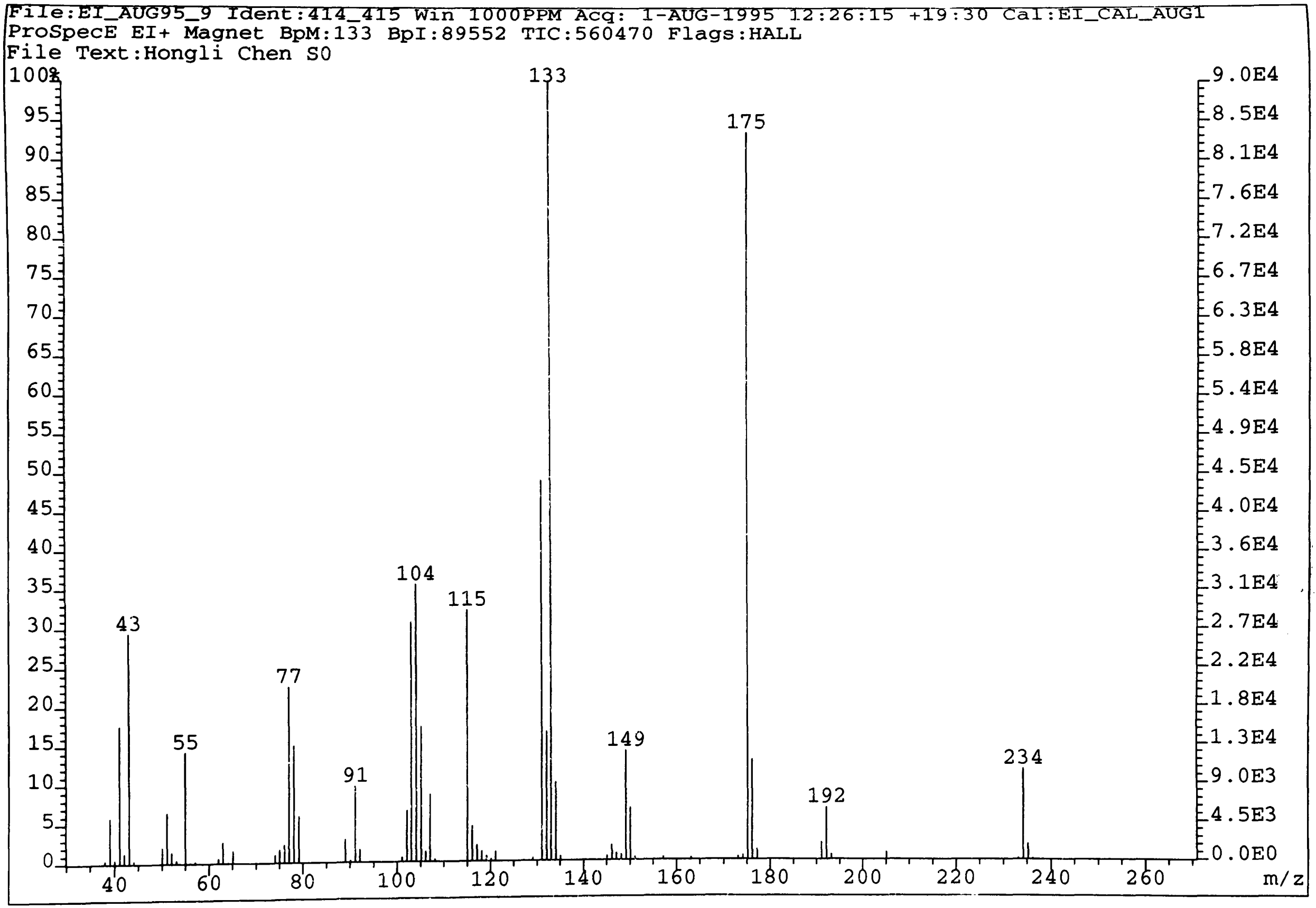

Figure 8.7.5.4 Mass Spectrum of Cinnamaldehyde Diacetal in Propan-1-ol

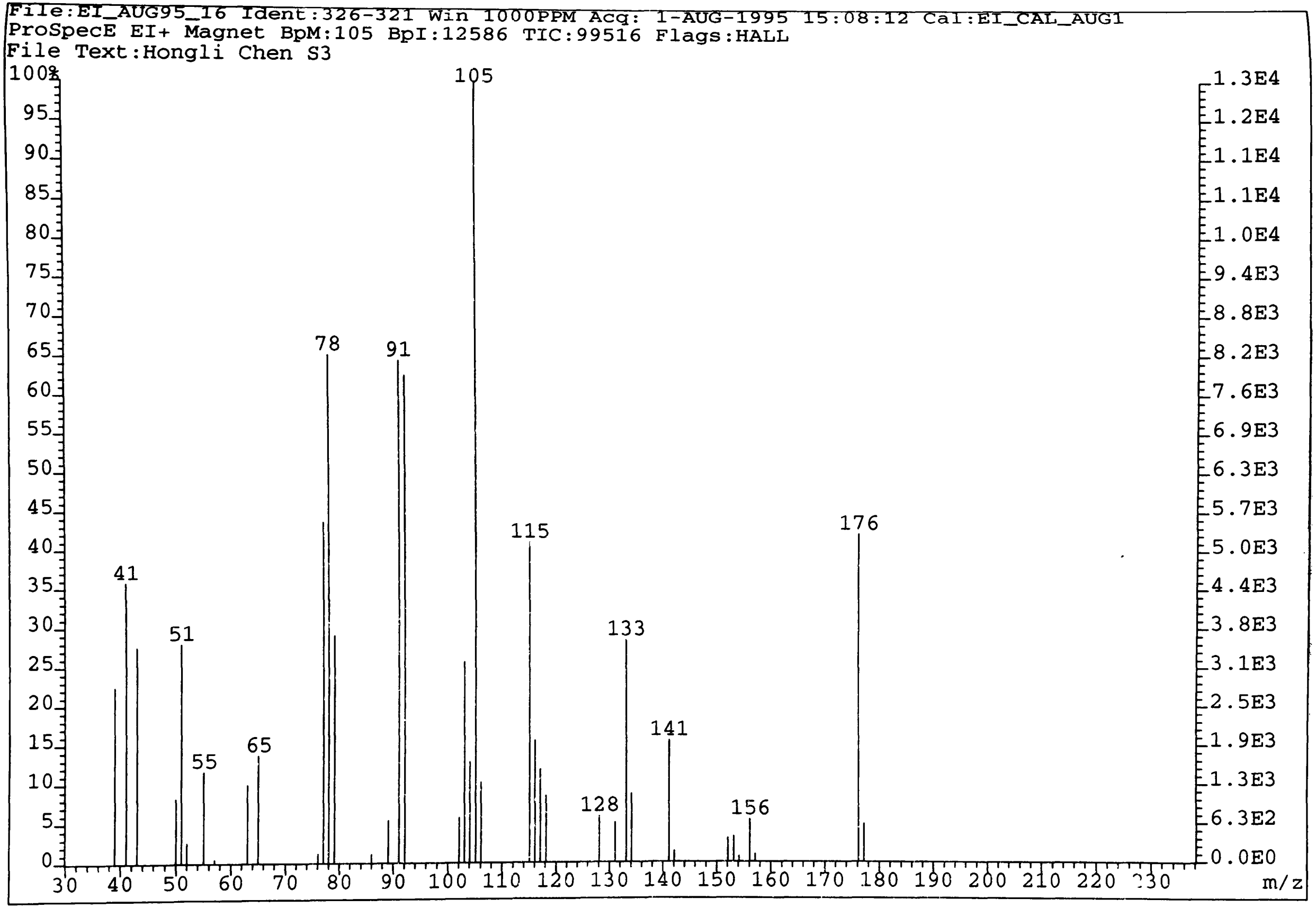

Figure 8.7.5.5 Mass Spectrum of Hydrocinnamaldehyde Hemiacetal in Propan-1-ol

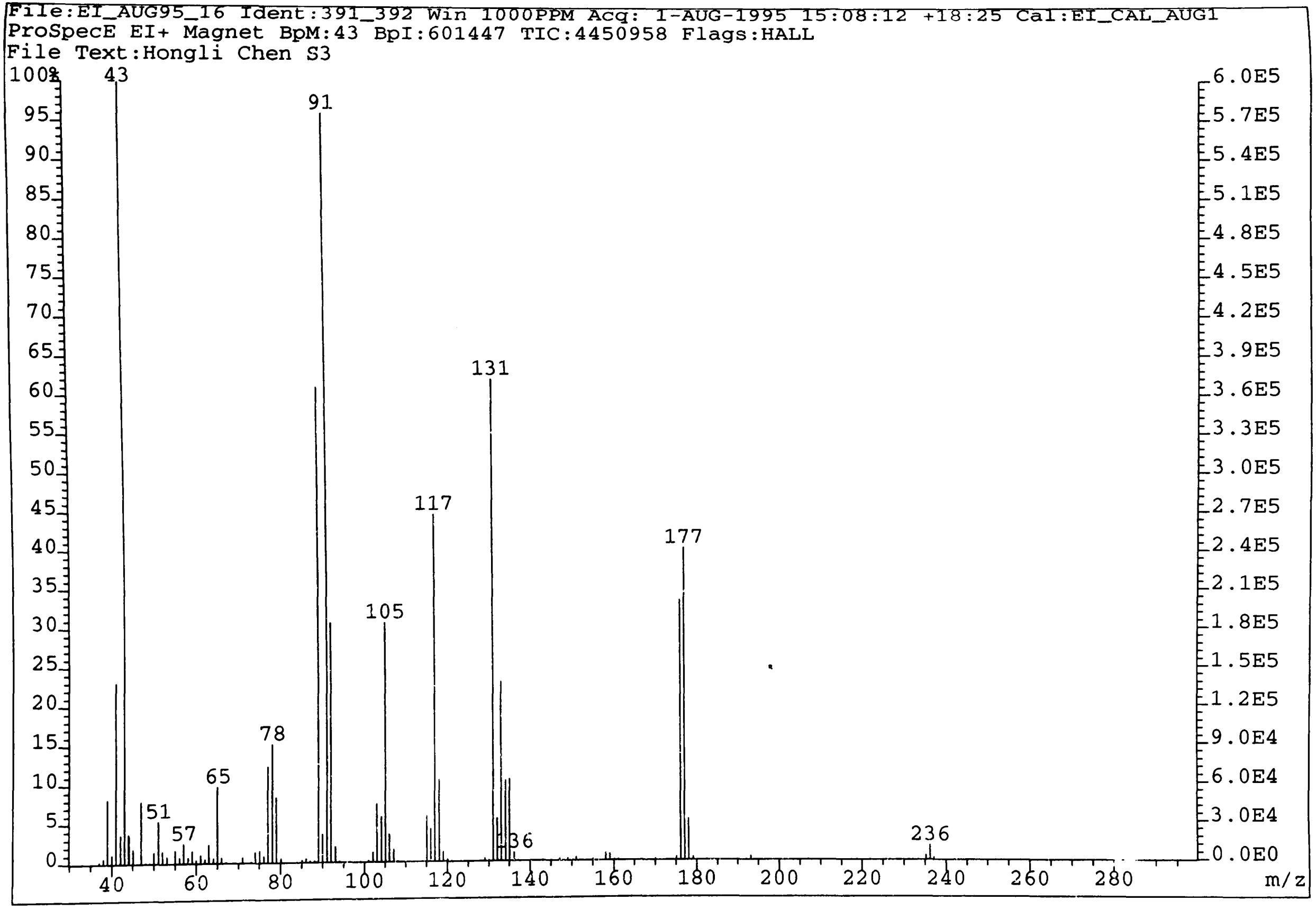

Figure 8.7.5.6 Mass Spectrum of Hydrocinnamaldehyde Diacetal in Propan-1-ol

Figure 8.7.5.7 Selectivity vs Conversion in Methanol over Pd/C

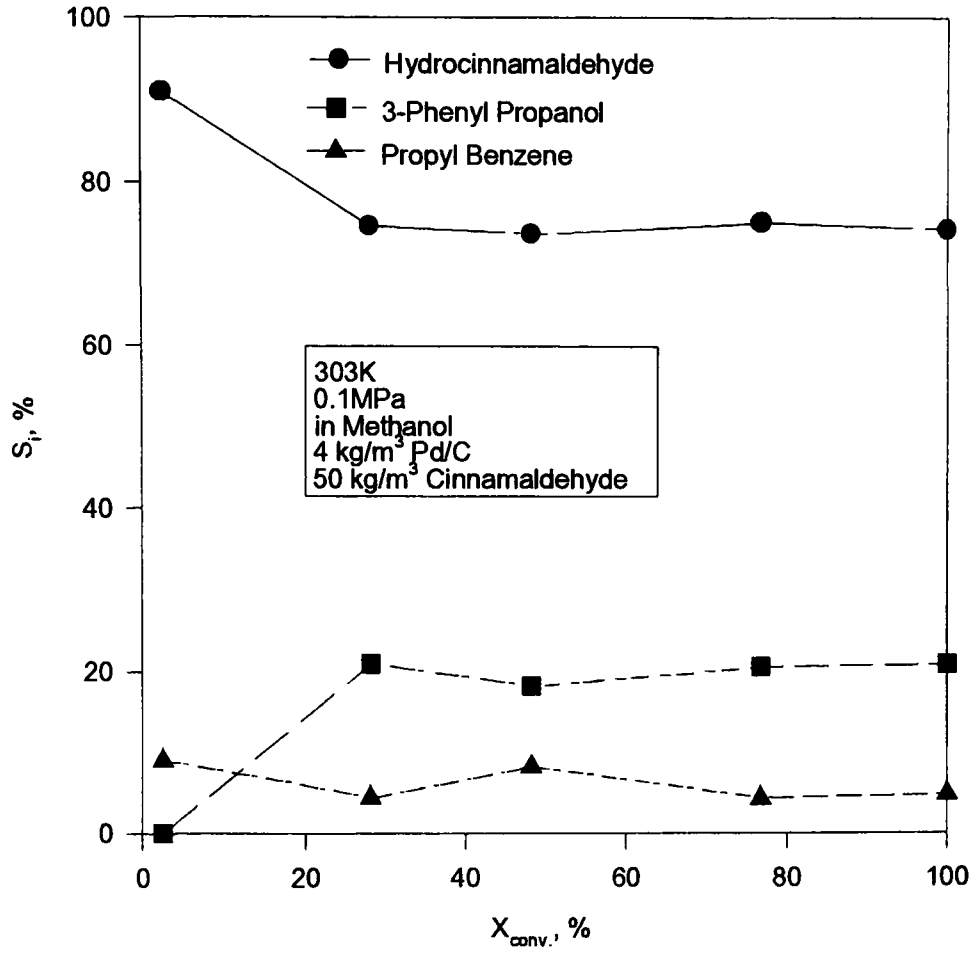

F Figure 8.7.5.8 Selectivity vs Conversion in Ethanol over Pd/C

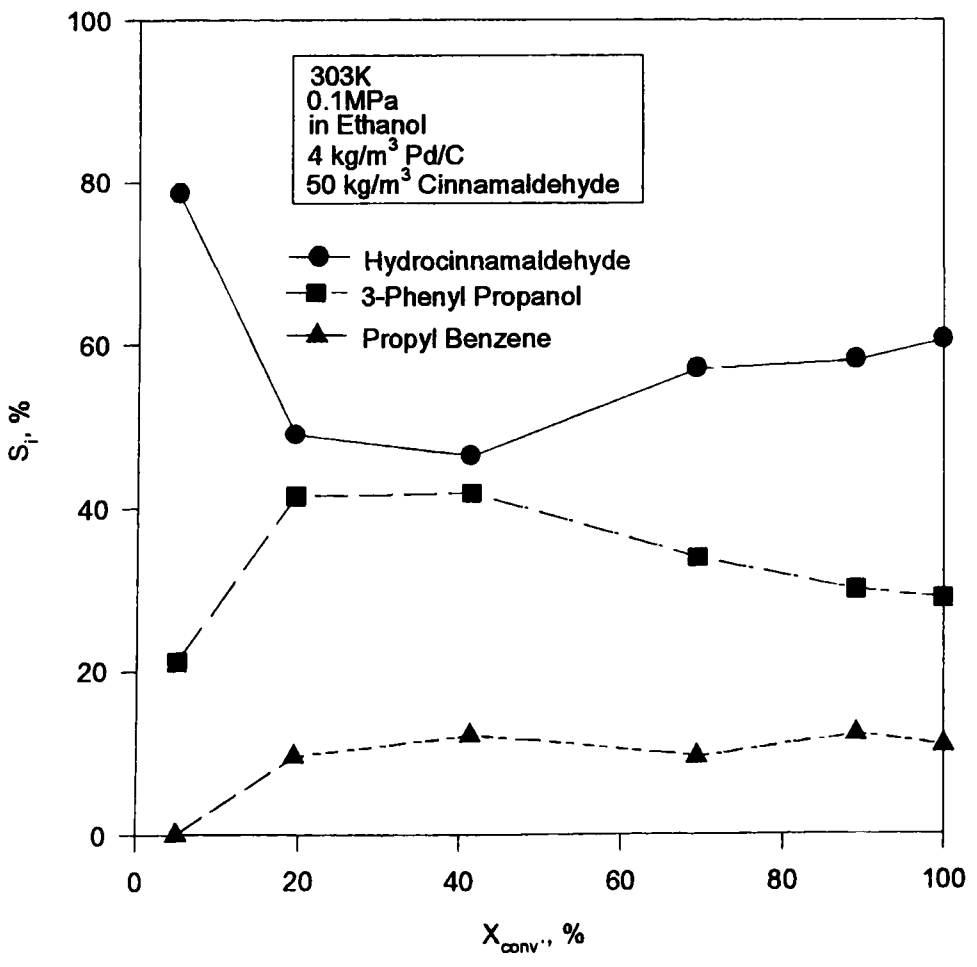

Figure 8.7.5.9 Selectivity vs Conversion in Propan-1-ol over Pd/C

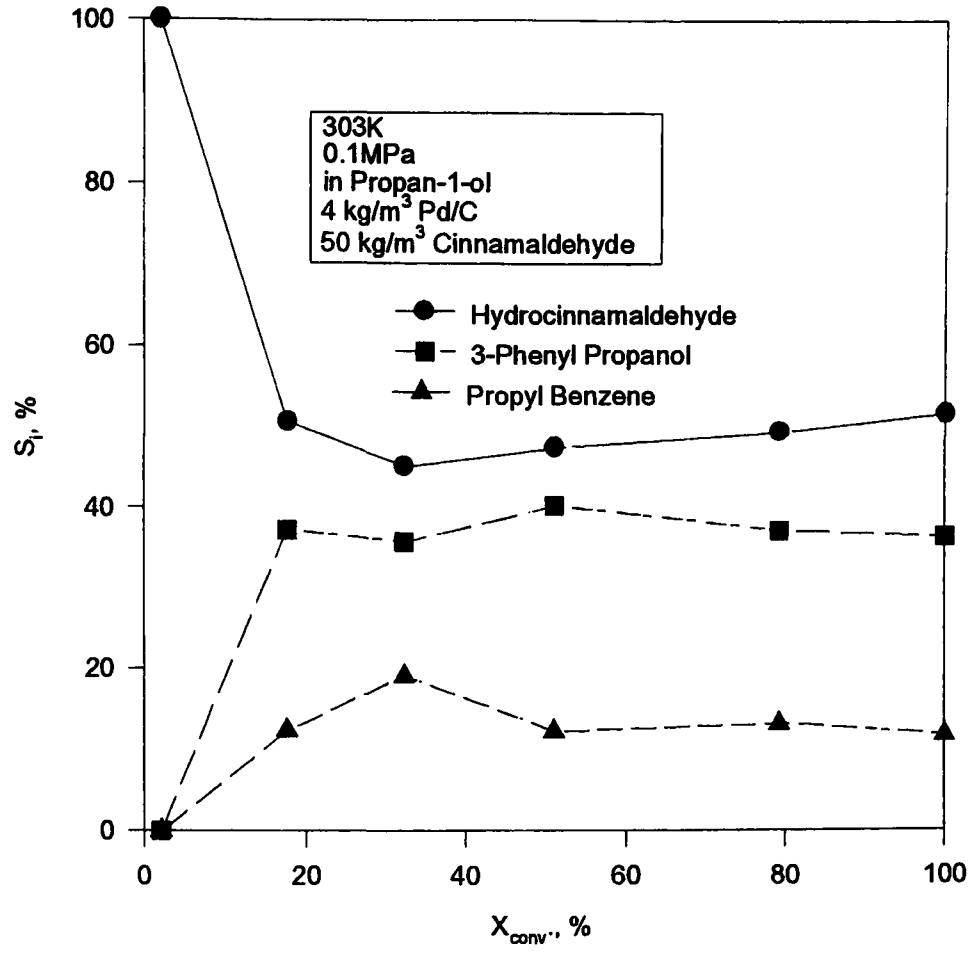

Figure 8.7.5.10 Selectivity vs Conversion in Propan-2-ol over Pd/C

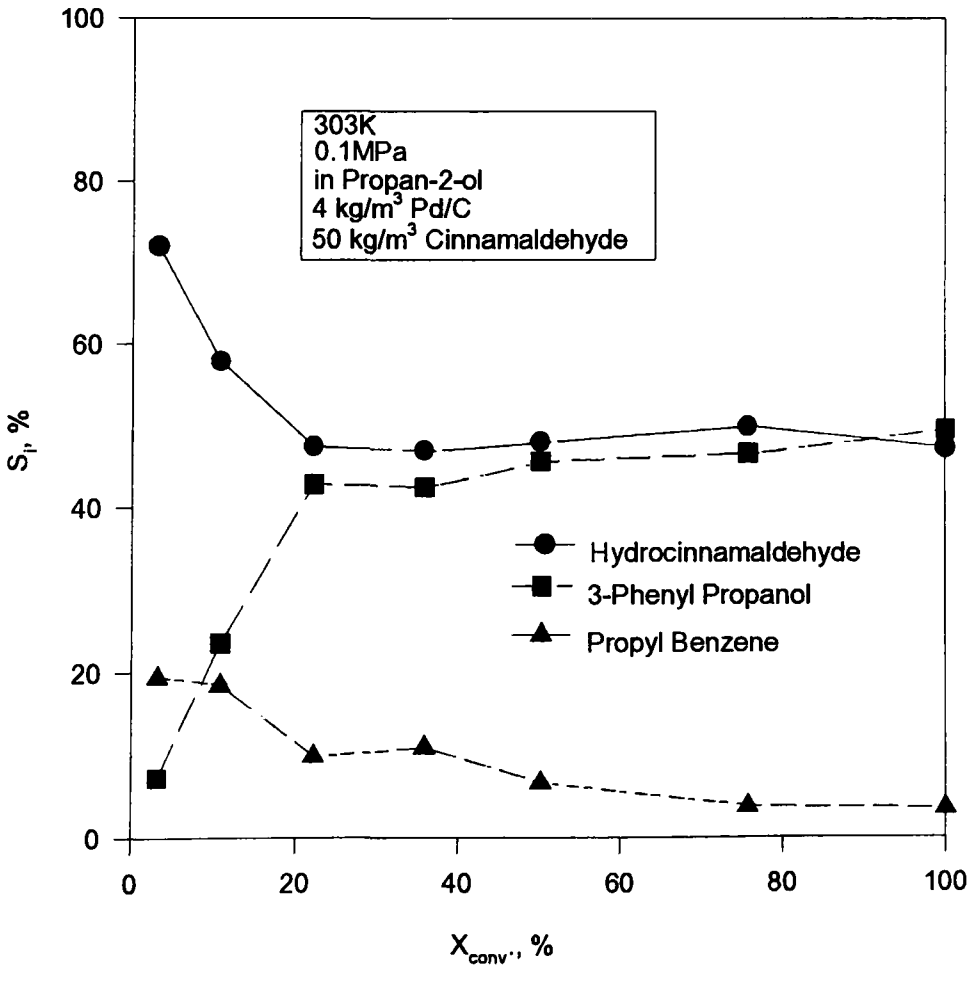

Figure 8.7.5.11 Selectivity vs Conversion in Butan-1-ol over Pd/C

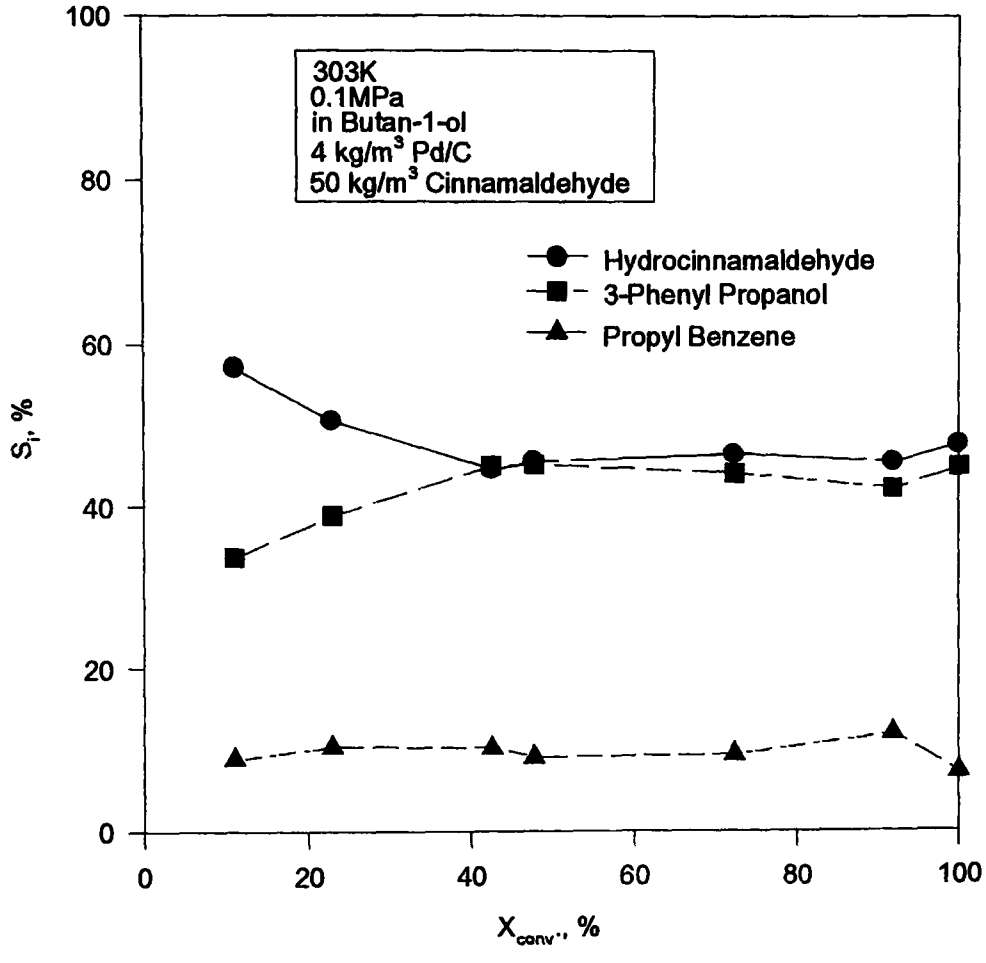

Figure 8.7.5.12 Selectivity vs Conversion in Butan-2-ol over Pd/C

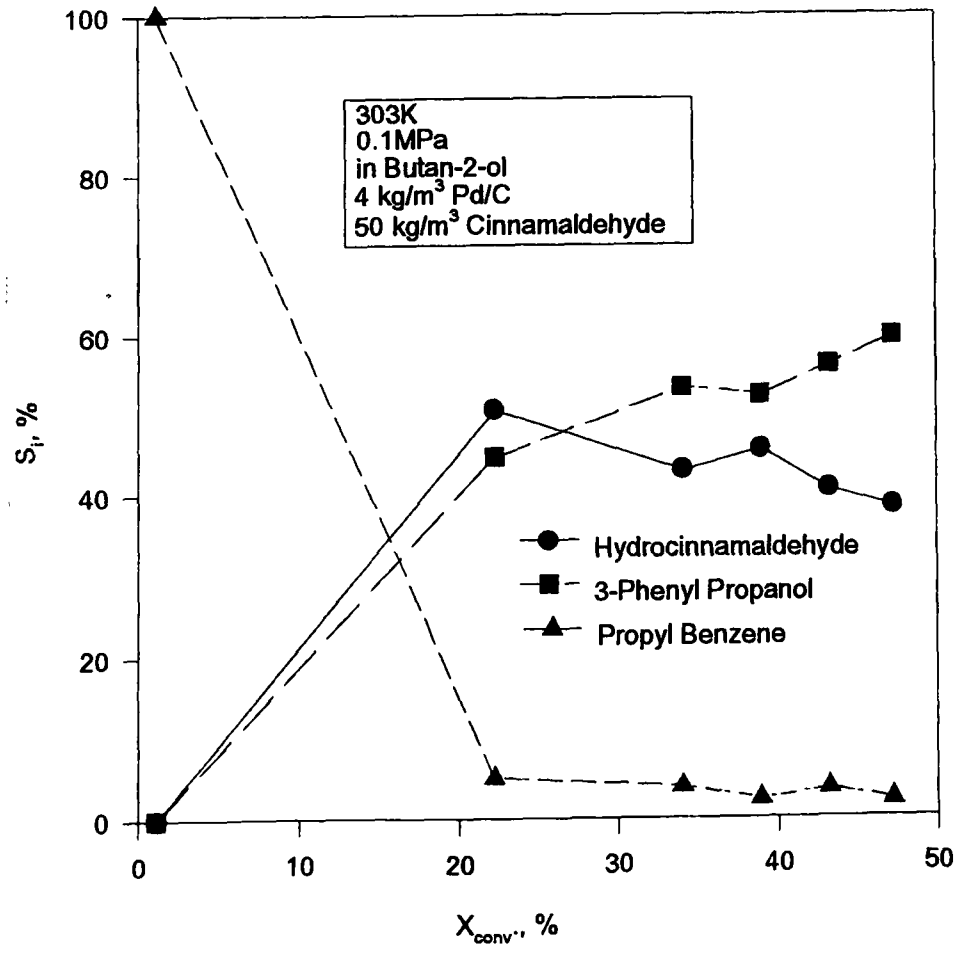

Figure 8.7.5.13 Selectivity vs Conversion in Toluene over Pd/C

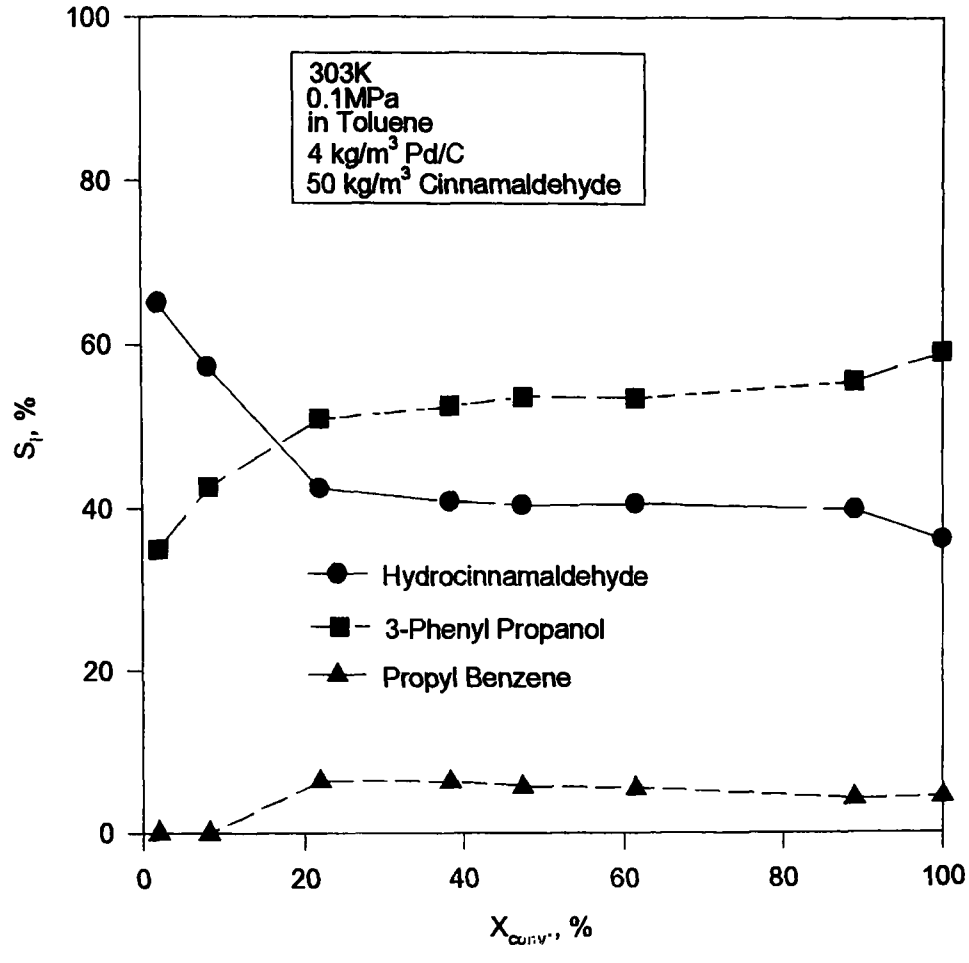

Figure 8.7.5.14 Selectivity vs Conversion in Heptane over Pd/C

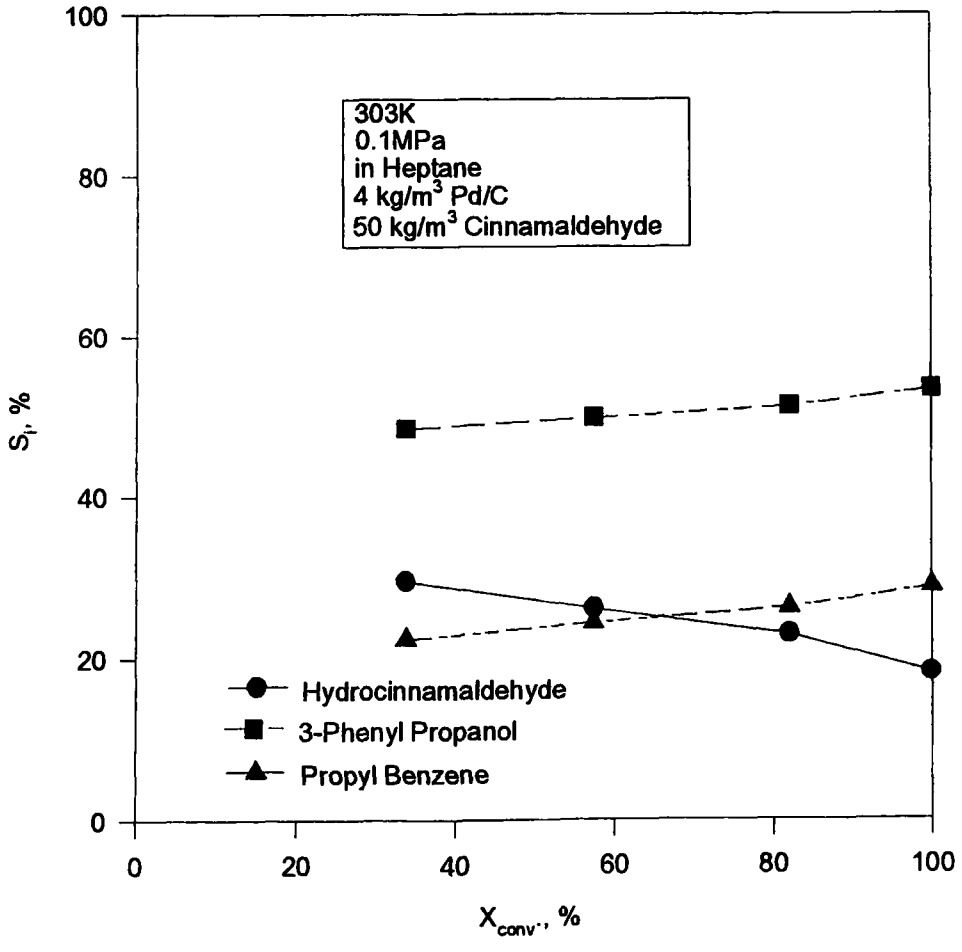

Figure 8.7.5.15 Selectivity vs Conversion in Methylcyclohexane over Pd/C

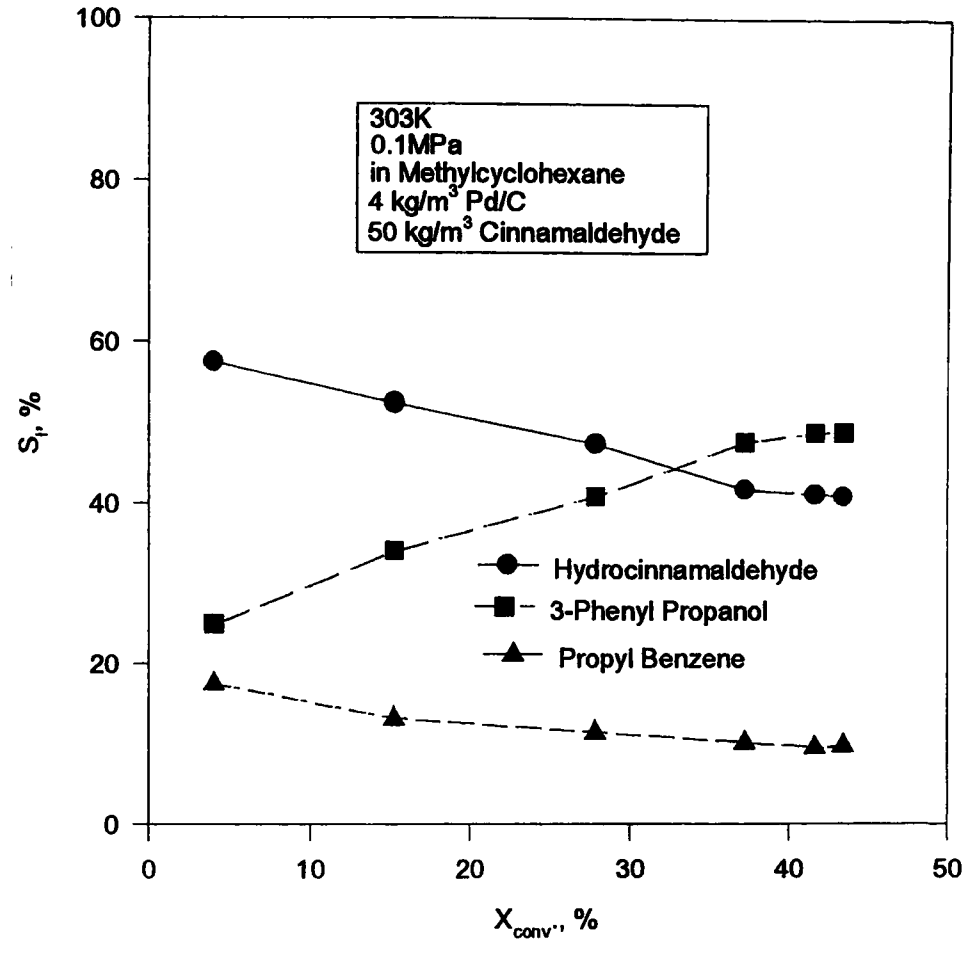

Figure 8.7.5.16 Selectivity vs Conversion in Decalin over Pd/C

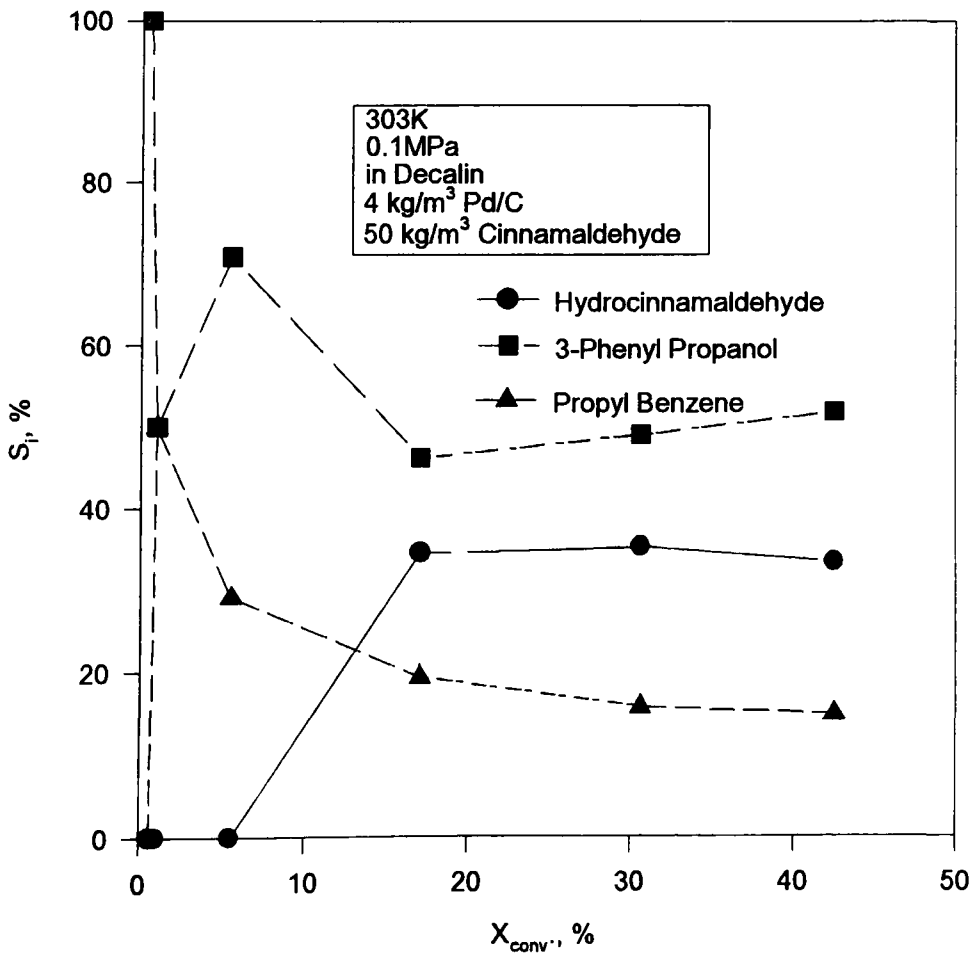

Figure 8.6.5.17 Selectivity vs Pressure in Toluene over Pd/C

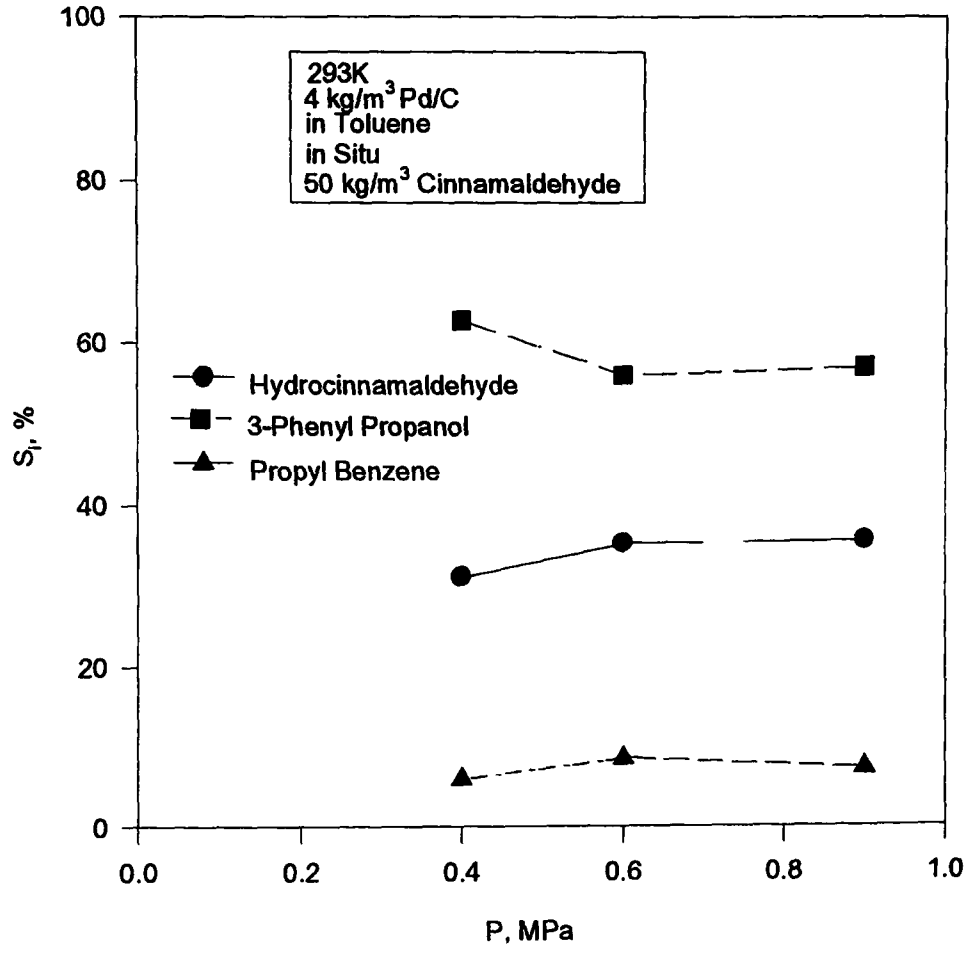

Figure 8.6.5.18 Selectivity vs Pressure in Toluene over Pd/C

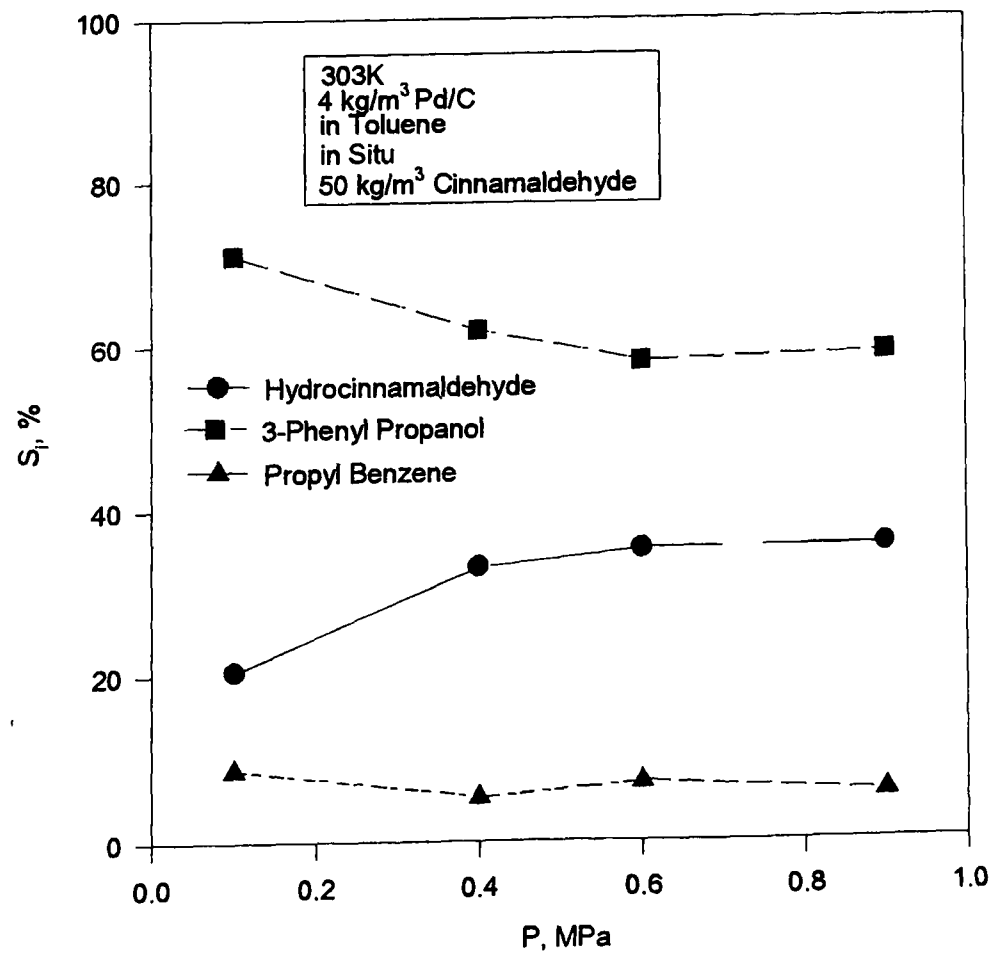

Figure 8.6.5.19 Selectivity vs Pressure in Toluene over Pd/C

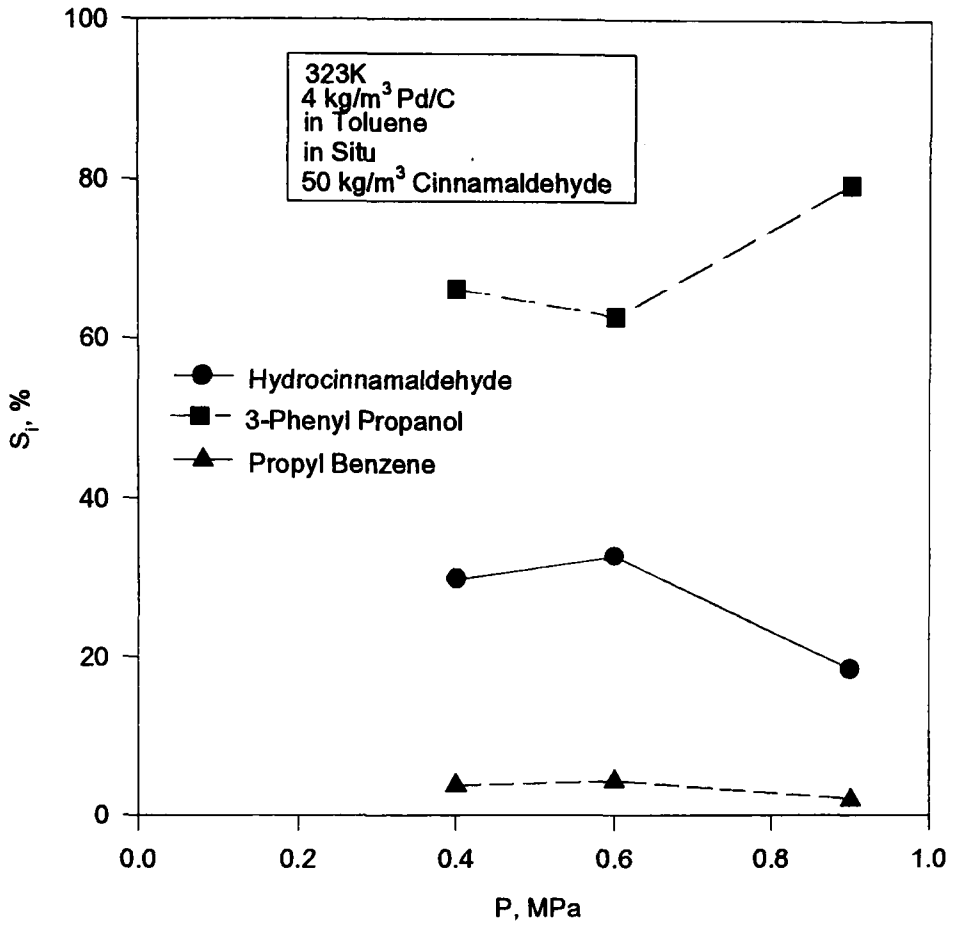

Figure 8.6.5.20 Selectivity vs Pressure in Toluene over Pd/C

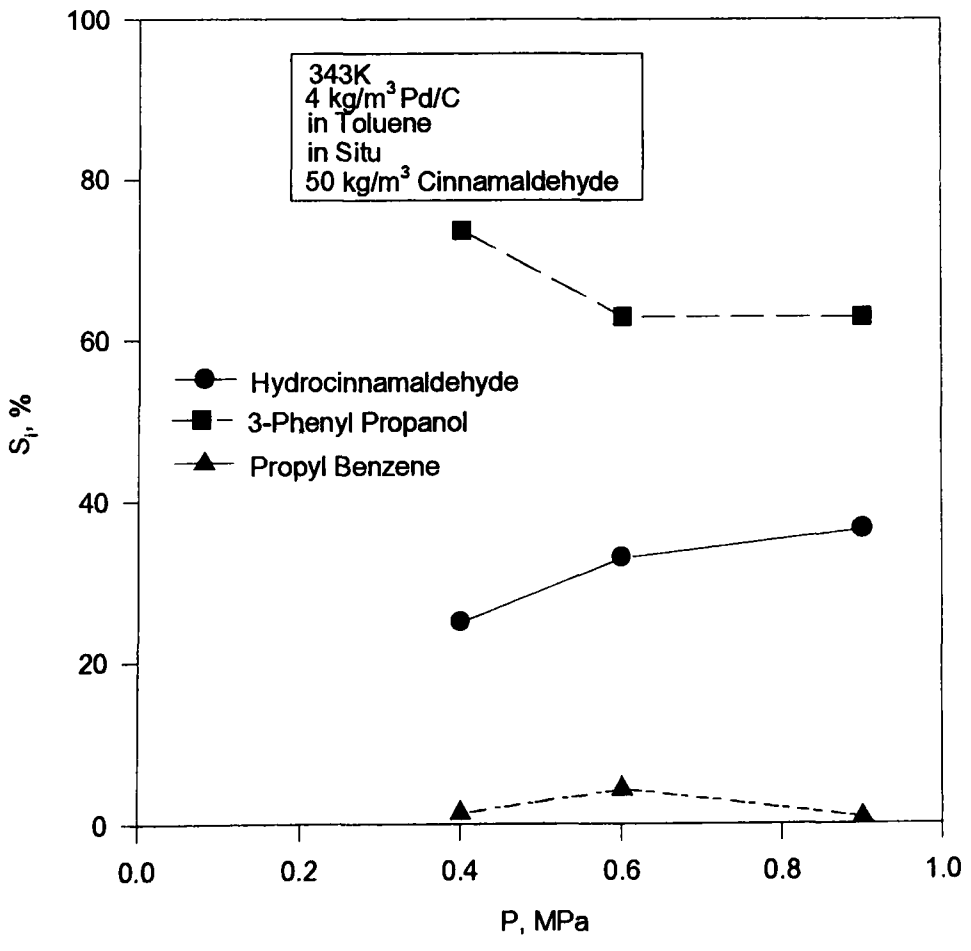

Figure 8.7.5.21 Selectivity vs Ratio of K^+/Pd with KCl

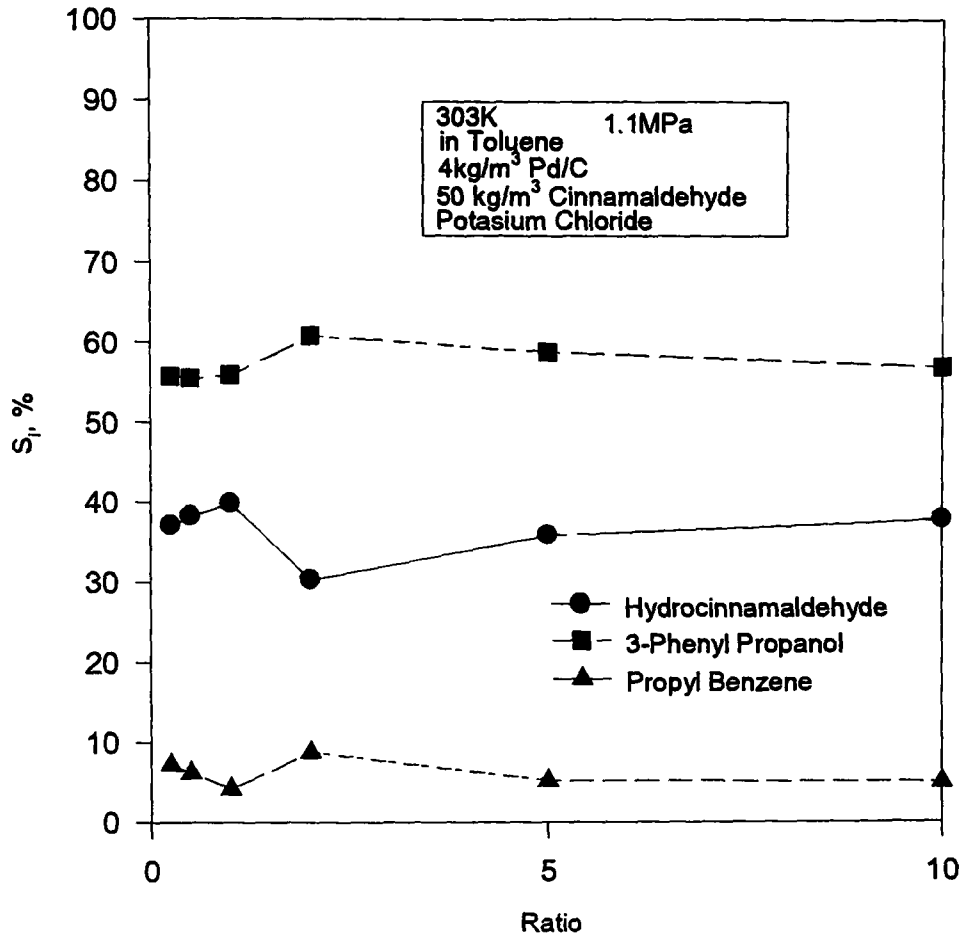

Figure 8.7.5.22 Selectivity vs Ratio of K^+/Pd with KBr

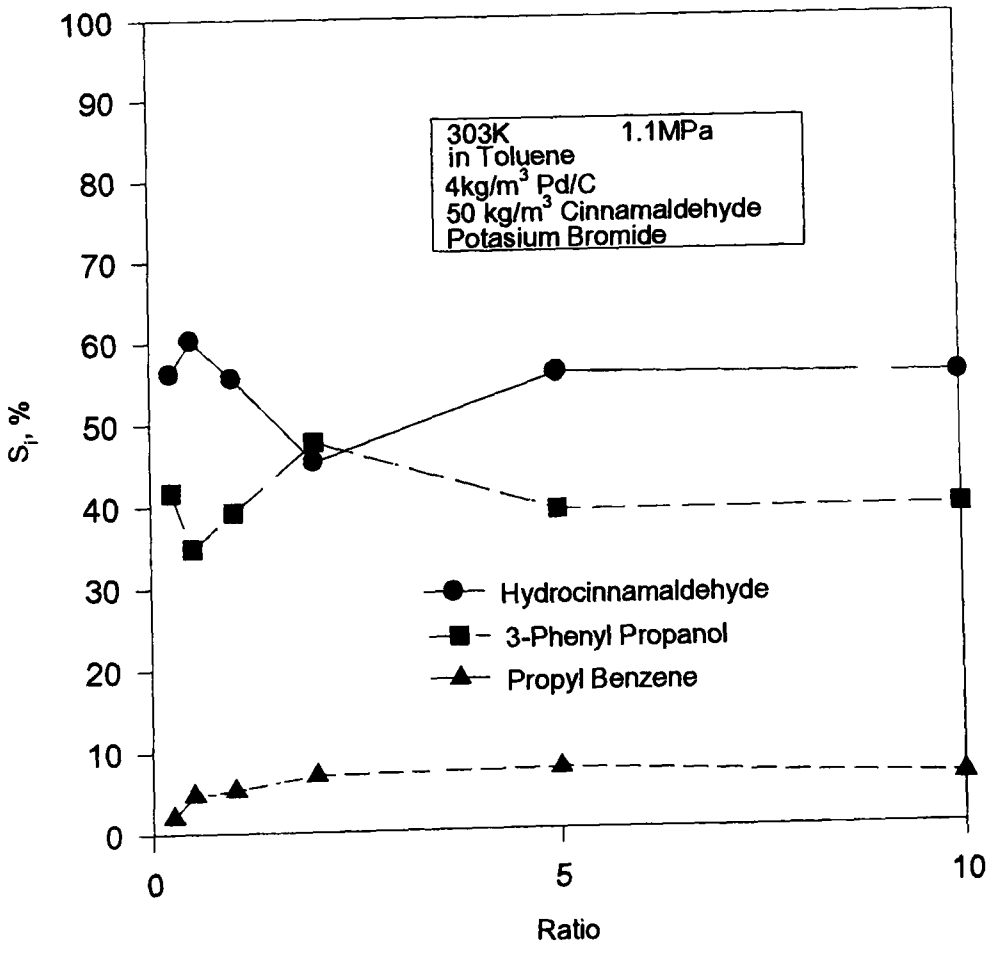

Figure 8.7.5.23 Selectivity vs Ratio of Ag^+/Pd wiith $AgNO_3$

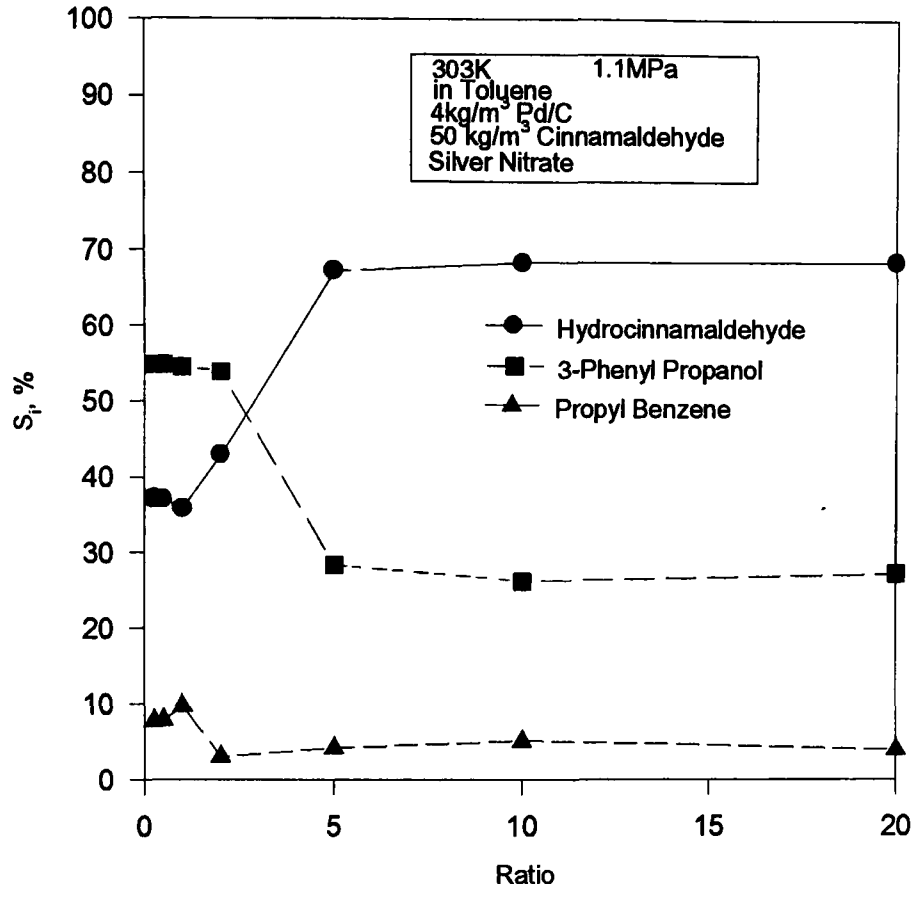

Figure 8.7.5.24 Selectivity vs Ratio of Al^+/Pd with $AlCl_3$

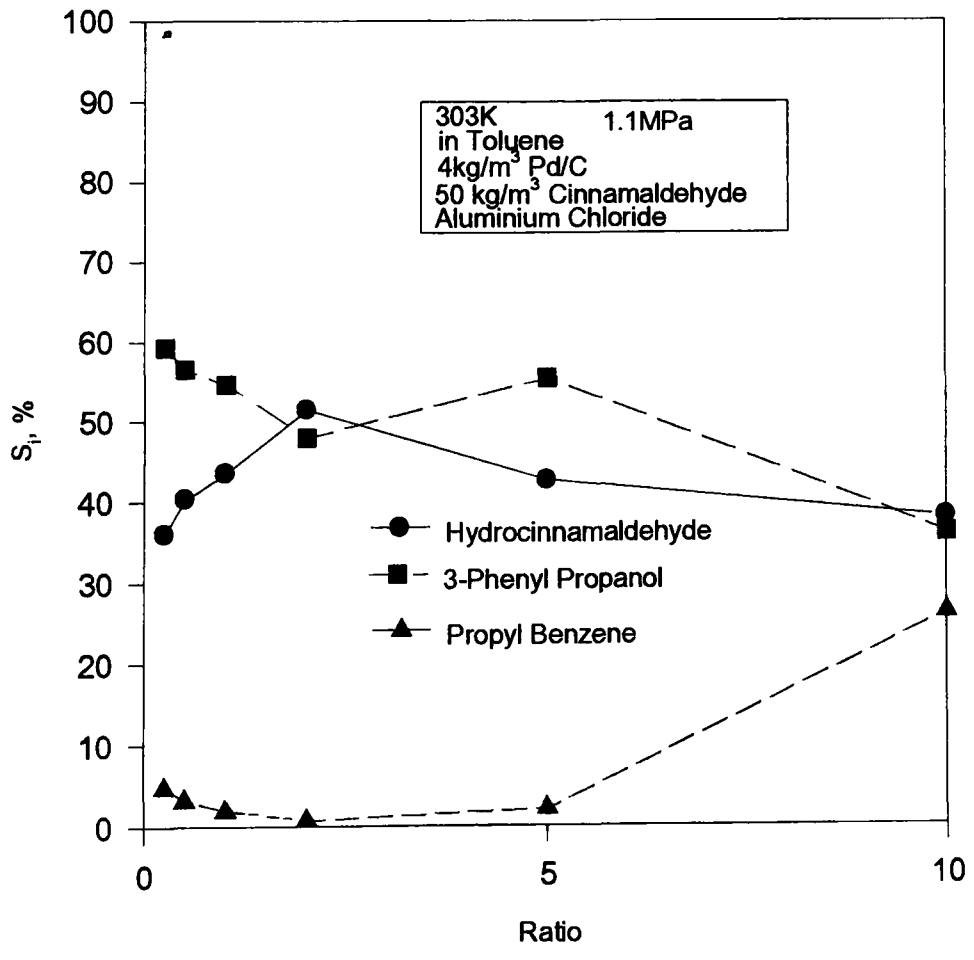

Figure 8.7.5.25 Stirring Speed vs Setting

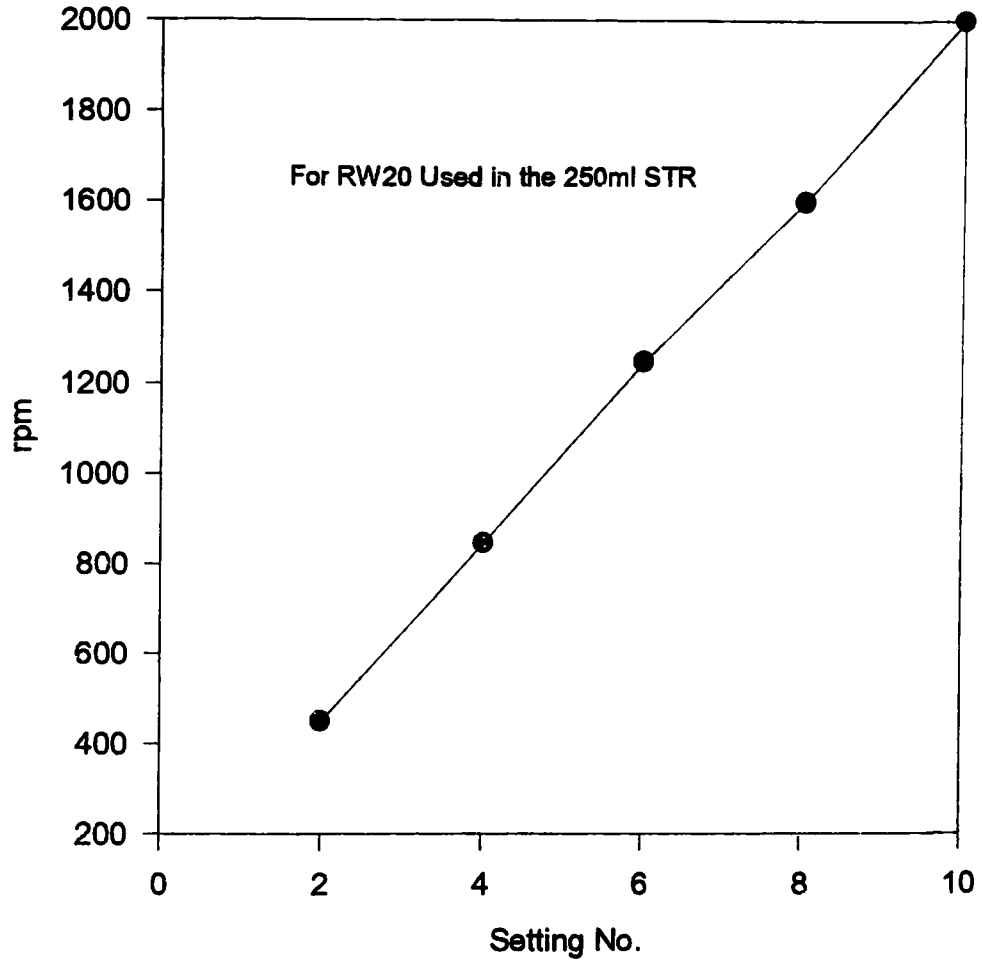

Figure 8.7.6.1 Calibration of Liquid Flowmeter in the 50mm CDC

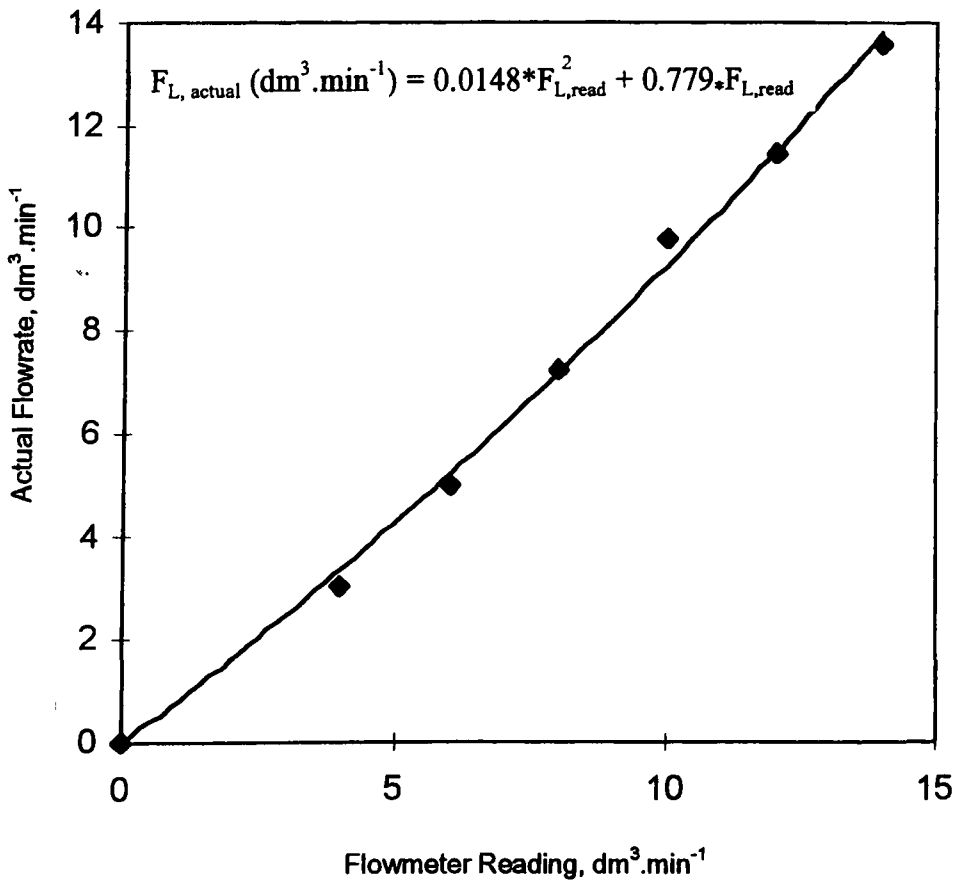

Figure 8.7.6.2 Calibration of Break Vessel in the 50mm CDC

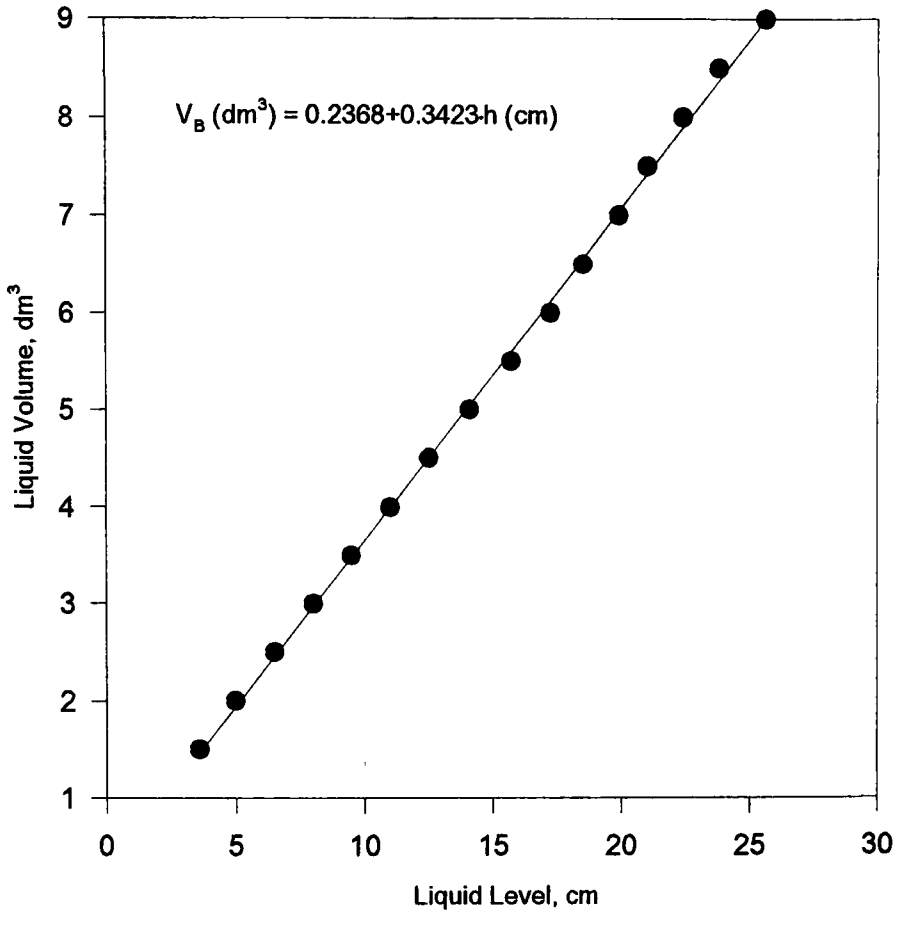

Nomenclature

A: Arrhenius constant, --

a: gas-liquid interfacial area per unit volume dispersion, m^2/m^3

A_{HC} = the GC peak area of hydrocinnamaldehyde

A_i= the GC peak area of component i

A_j= the GC peak area of component j

a_{photo} = interfacial area measured by photography

$a_{sulfite}$ = interfacial area measured by sulphite method

ΔC_L = logarithmic-mean concentration driving force, kg/m^3

C_A^*: equilibrium concentration of hydrogen at the gas-liquid interface, $kmol/m^3$

C_A: cinnamaldehyde concentration, $kmol/m^3$

C_{CAL} = cinnamaldehyde concentration, $kmol/m^3$

C_{cat} = catalyst concentration, $kmol/m^3$

C_{H2} = hydrogen concentration, $kmol/m^3$

C_i = dissolved oxygen concentration at column inlet, kg/m^3

C_o = dissolved oxygen concentration at column outlet, kg/m^3; initial phenol concentration, kg/m^3

D_{20} = density at 293K

D_A = diffusivity of gas, m^2/s

d_b = bubble diameter, m

D_C = column diameter, m

d_I = impeller diameter, m

DO_{in} = dissolved oxygen concentration at inlet, kg/m^3

DO_{out} = dissolved oxygen concentration at outlet, kg/m^3

$d_{orifice}$ = orifice diameter, m

d_p: catalyst particle diameter, m

D_T = reactor diameter, m

d_{vs} = volume-to-surface mean bubble diameter defined by equation 2.3.1

E_{ZL} = axial dispersion coefficient, m^2/s

E = activation energy, kJ/mol; energy dissipated, W

e = energy supplied by agitator/gas bubbling to liquid per unit mass, m^2/s^3

E_A: activation energy, kJ/mol

E_{app} = apparent activation energy, kJ/mol

F_G = volumetric gas flowrate, ml/min

f_i= the correction factor of component I

F_L = volumetric liquid flowrate, m^3/s

$F_{L,\,actual}$ = actual flowrate of flowmeter, m^3/s

$F_{L,\,read}$ = flowmeter reading, dm^3/min

Fr_b = Froude number defined by $Fr_b = \dfrac{u_g^2}{g\varepsilon_g^2 d_b}$

g = gravity acceleration, m/s^2

h = liquid level in break vessel, cm; axial distance from top of the column, cm

H: Henry's constant, $Pa.m^3/kg\ mol$

H_{c1} = clear liquid level in the deadleg, m

H_{c2} = clear liquid level in the column, m

H_d = dispersion height in reactor, m

H_g = gas height in the deadleg, m

H_i = impeller position from reactor bottom, m

K_m^* = absorption-reaction parameter defined by equation 2.3.6

K = constant; adsorption constant

k = rate constant

k_1, k_2 = parallel reaction rate constant to cinnamyl alcohol and hydrocinnamaldehyde, respectively

k_L = liquid-side mass transfer coefficient, m/s

k_La: volumetric gas-liquid phase coefficient, 1/s

k_m = rate constant

k_r: surface reaction rate constant, m/s

k_s: liquid-solid mass transfer coefficient, m/s

L = dimensional length, m

m = a constant (see equation 2.2.17 & 2.3.8); reaction order

M_{min} = minimum liquid jet momentum, m^2/s

n = a constant (see equation 2.2.17 & 2.3.8)

n_D^{20} = infraction index at 293K

N_m = minimum speed of agitation for particle suspension (see Equation 2.2.1), rev/s

N_p = power number defined by equation 2.2.7, -

N_{stir} = stirring speed, rev/s

O_{2input} = oxygen input, kg

P = power consumption for agitation of an aerated liquid, W; Reactor Pressure, MPa

Pe = Peclet number, = uL/E_{ZL}

P_o = power consumption for agitation of a gas-free liquid, W

Q = pumping capacity of impeller, m^3/s

Q_G = volumetric flowrate of gas, m^3/s

R: gas constant, 8.314 J/(mol. K)

R_A: initial hydrogen takeup rate per unit volume of dispersion, $kmol/(s.m^3)$

Re: Reynolds number, $Re=nd_I^2\rho_L/\mu_L$, --

R_{heat} = heat rate of oven, K/min

R_o = initial reaction rate, $kmol/m^3.s$

S_{actals}: selectivity of acetals in the product, %

Sc: Schmit number, $Sc=\mu_L/(\rho_L D_A)$, --

S_{COL}: selectivity of cinnamyl alcohol in the product, %

Sh: Sherwood number, $Sh=k_s d_p/D_A$, --

S_{HC}: selectivity of hydrocinnamaldehyde in the product, %

S_i: selectivity of component i in the product, %

S_j: selectivity of component j in the product, %

S_{MS}: selectivity of β-methylstyrene in the product, %

S_{other}: selectivity of other components in the product, %

S_{PB}: selectivity of propyl benzene in the product, %

S_{PP}: selectivity of 3-phenyl propanol in the product, %

St_m = Stanton number defined by equation 2.3.5

T: temperature, K

T_{reduce} = catalyst reduction temperature, K

u = characteristic velocity, m/s

u_c = circulation velocity, m/s

u_G = superficial gas velocity, m/s

u_{jet} = liquid inlet jet velocity, m/s

u_L = superficial liquid velocity, m/s

$u_{o,min}$ = minimum liquid jet velocity for a stable bubble dispersion in CDC, m/s

V_B = slurry volume in the break vessel, litre

V_c = clear liquid volume in the reservoir, m^3

V_d = dispersion volume in the reservoir, m^3

V_L = volume of liquid in reactor, m^3

V_R = reactor volume, m^3

W = catalyst weight, g; catalyst loading, kg/m^3

w' = percentage catalyst loading, g (catalyst)/100g (solution) (see Equation 2.2.1)

W_{base} = base loading, kg/m^3(liquid)

W_{CAL} = initial cinnamaldehyde loading, kg/m^3(liquid)

W_{cat} = catalyst loading, kg/m^3(liquid)

W_{HC} = initial hydrocinnamaldehyde loading, kg/m^3 (liquid)

$X_{conv.}$ = conversion of a reactant, %; total conversion of cinnamaldehyde, %

X_{actals}: mole fraction of acetals in the product, %

X_{CAL}: mole fraction of cinnamaldehyde in the product, %

X_{COL}: mole fraction of cinnamyl alcohol in the product, %

X_{conv}: total conversion of cinnamaldehyde, %

X_{HC}: mole fraction of hydrocinnamaldehyde in the product, %

X_i: mole fraction of component i in the product, %

X_j: mole fraction of component j in the product, %

$X_{L\text{-}S}$: % liquid-solid mass transfer resistances, %

X_{MS}: mole fraction of β-methylstyrene in the product, %

X_{other}: mole fraction of other components in the product, %

X_{PB}: mole fraction of propyl benzene in the product, %

X_{PP}: mole fraction of 3-phenyl propanol in the product, %

α = a constant (see equation 2.2.17 & 2.3.8)

σ = liquid surface tension, kg/s^2

β_2 = a constant defined by equation 2.2.1

η_c: catalyst effectiveness factor, --; for spherical particles with metal on external surface, $\eta_c=1$

ε_g = gas holdup, %

ν_L = kinematic viscosity, m^2/s

ρ_g = gas density, kg/m^3

ρ_L: liquid density, kg/m^3

ρ_p: particle density, kg/m^3

$\rho_{S\text{-}L}$ = slurry density defined by equation 2.2.10, kg/m^3

τ = gas phase residence time, s

μ_L: liquid viscosity, $kg/(m.s^2)$

w = catalyst mass per unit volume of reactor, kg/m^3

N.B. in Section 2.2 the c.g.s units are mainly used

Abbreviations

b.p = boiling point

c = column

CAL = cinnamaldehyde

CDC = cocurrent downflow contactor

C.S.T.R.= continuous stirred tank reactor

COL = cinnamyl alcohol

G = gas

HC = hydrocinnamaldehyde

L = liquid

m.p = melting point

m.w = molecular weight

MS = β-methylstyrene

PB = propyl benzene

P.F.R = plug flow reactor

PP = 3-phenyl propanol

RTD = residence time distribution

T= tank

References

Akita, K. and Yoshida, F., Bubble Size, Interfacial Area, and Liquid-Phase Mass Transfer Coefficient in Bubble Columns, Ind. Eng. Chem. Proc. Des. Dev., 13, 1974, 84.

Anderson, J.R., Structure of Metallic Catalysis, Academic Press, London, 1975.

Arai, M., Usui, K. and Nishiyama, Y., Preparation of Alumina-supported Platinum Catalyst at Ambient Temperature for Selective Synthesis of Cinnamyl Alcohol by Liquid-phase Cinnamaldehyde Hydrogenation, J. Chem. Soc., Chem. Commun., 1993, 1853.

Archer, A., Determination of Cinnamaldehyde, Coumarin and Cinnamyl Alcohol in Cinnamon and Cassia by High-performance Liquid Chromatography, J. of Chromatography, 447, 1988, 272.

Arrigo, J. T., Christensen, N. J., Chrysler, R. L., and Sparks, A. K., Hydrogenation of Cinnamic Aldehydes, US Patent 3,520,935, 1970.

Astarita, G., Mass Transfer with Chemical Reaction, Elsevier, Amsterdam, 1967.

Bailey, J.E., and Ollis, D. F., Biochemical Engineering Fundamentals, 2nd Edition, McGraw Hill, New York, 1986.

Bakhanova, E.N., Astakhova, A.S., and Khiedekel, M.L., USSR Patent 264,352, 1972.

Baltzly, R., Studies on Catalytic Hydrogenation I. The Influence on Reaction Rates of the Metal-Carrier Ratio of Solvents and Acidity, J. Org. Chem, 41, 1976, 920.

Bando, Y., Kuraishi, M., Nishimura, M., Hattori, M. and Asada, T., Cocurrent Downflow Bubble with Simultaneous Gas-Liquid Injection Nozzle, J. Chem. Eng. Japan, 21, 1988, 607.

Bando, Y., Nishimura, M, Ichikawa, C., Takeshita, I. and Kuraishi, M., Gas-Liquid Contactor Using Gas Entrainment by Liquid Flowing Downward into Downcomer, J.

Chem. Eng. Japan, 22, 1989, 660.

Barker, J.J., and Treybal, R.E., Mass Transfer Coefficients for Solids Suspended in Agitated Liquids, AIChE J., 6, 1960, 289.

Bates, R.L., Fondy, P.L., and Corpstein, R.R., An Examination of Some Geometric Parameters of Impeller Power, Ind. Eng. Chem. Proc. Des. Dev., 2, 1963, 310.

Beccat, P., Bertolini, J.C., Gauthier, Y., Massardier, J. and Ruiz, P., Crotonaldehyde and Methylcrotonaldehyde Hydrogenation and Platinum (III) and Platinum-Iron (Pt80Fe20) (III) Single Catalysts, J. Catal., 126, 1990, 451.

Begovich, J. M. and Watson, J.S., Hydrodynamic Characteristics of Three Phase Fluidized Beds, Fluidization, Proceedings of the Second Engineering Fundamental Conference, 1978, 190.

Blackmond, D.G., Oukaci, R., Blanc, B., Gallezot, P., Geometric and Electronic Effects in the Selective Hydrogenation of α,β-Unsaturated Aldehydes over Zeolite-Supported Metals, J. Catal., 131, 1991, 401.

Blenk, Loop Reactors, in "Advances in Biochemical Engineering", Vol. 13, Springer-Verlag, Berlin, 1979.

Bond, G.C., Heterogeneous Catalysis: Principles and Applications, Second Edition, Clarendon Press, Oxford, 1987.

Boublik, T., The Vapour Pressure of Pure Substances, Physical Science Data 17, Elsevier, New York, 1984.

Boyes, A.P., and Ellis, S.R.M., Gas Liquid Contactor, U.K. Patent 1,596,738A, 1976.

Boyes, A.P., Chughtai, A, Lu, X.X, Raymahasay, S., Sarmento, S., Tilston, M.W. and Winterbottom, J.M., The Cocurrent Downflow Contactor (CDC)-Chemically Enhanced Mass Transfer and Reaction Studies for Slurry and Fixed Bed Catalytic Hydrogenation, Chem. Eng. Sci., 47, 1992, 3729.

Briens, C.L., Huynh, L.X., Large, J.F., Catros, A., Bernard, J.R. and Bergougnou,

M.A., Hydrodynamics and Gas-Liquid Mass Transfer in a Downward Venturi-Bubble Column Combination, Chem. Eng. Sci., 47, 1992, 3549.

Buckling, C.J., Halling, P.J., Kirkwood, R.C., and Bell, G., Clean Synthesis of Effective Chemicals, AFRC-SERC Clean Technology Unit, Swilndon, 1992.

Caga, T., Shutt, E., and Winterbottom, J.M., The Comparison of Reduced Palladium Oxide and Its Behaviour as a Catalyst for Liquid Phase Hydrogenation, J. Catal., 44, 1976, 271.

Calderbank, P.H. and Young, M.B., The Continuous-Phase Heat and Mass Transfer Properties of Dispersions, Chem. Eng. Sci., 16, 1961, 39.

Calderbank, P.H., Gas Absorption from Bubbles, Chem. Engrs., 47, 1967, CE203.

Calderbank, P.H., Physical Rate Processes in Industrial Fermentation, Part I. The Interfacial Area in Gas-Liquid Contacting with Mechanical Agitation, Trans. Instn. Chem. Engrs., 36, 1958, 443.

Carothes, W.H., and Adames, R., Platinum Oxide as a Catalyst in the Reduction of Organic Compounds II: Reduction of Aldehydes--Activation of the Catalyst by Salts of Certain Metals, J. Am. Chem. Soc., 45, 1923, 1071.

Chapman, C. M., Nienow, A.W., Cooke, M., and Middleton, J.C., Particle-Gas-Liquid Mixing in Stirred Vessel, Part III Three Phase Mixing, Chem. Eng. Res. Dev., 61, 1983, 167.

Chaudhari, R.V., and Gholap, R.V., Gas-Liquid Mass Transfer in "Dead-End" Autoclave Reactors, Can. J. Chem. Eng. 65, 1987, 744.

Chaudhari, R.V., and Ramachandran, P.A., Three Phase Slurry Reactors, AIChE J., 26, 1980, 177.

Chen, Y.Z., Wei, S.W., Wu, K.J., Effect of Promoter on Selective Hydrogenation of α,β-unsaturated Aldehydes over Cobalt Borides, Applied Catalysis A: General. 99, 1993, 85.

Chisti, M.Y., Airlift Bioreactors, Elsevier, London, 1989.

Chughtai, A., The Development of A Packed Bed CDCR, PhD Thesis, University of Birmingham, 1993.

Clark, N.N. and Flemmer, R.L.C., On Vertical Downward Two-Phase Flow, Chem. Eng. Sci., 39, 1984, 170.

Clift, R., Clean Technology: The Idea and Practice, Clean Tech 96, London, 19-21 June, 1996.

Clift, R., Clean Technology--an Introduction, J. Chem. Tech. Biotechnol., 62, 1995, 321-326.

Clift, R., On Cradles, Graves and Possible Lives, Professor Roland Clift's Inaugural Lecture, University of Surrey, Surrey, 11 January 1995.

Cocco, G., Enzo, S., Galvagno, S., Poltarzewki, Z., and Pietropaolo, X-Ray-Scattering Structural Investigation of Pt and Pt-Sn Catalysts Supported on Nylon, J. Chem. Soc., Faraday Trans. 81, 1985, 321.

Coq, B., Figueras, F., Geneste, P., Moreau, C., Moreau, P. and Warawdekar, M., Hydrogenation of α,β-unsaturated Carbonyls: Acrolein Hydrogenation on Group VIII Metal Catalysts, J. of Mol. Catal., 78, 1993, 201.

Coq, B., Kumbhar, P.S., Moreau, C., Moreau, P., and Figueras, F., Zirconia-Supported Monometallic Ru and Bimetallic Ru-Sn, Ru-Fe Catalysts: Role of Metal Support Interaction in the Hydrogenation of Cinnamaldehyde, J. Phys. Chem., 98, 1994, 10180.

Coq., B., Kumbhar, P. S., Moreau, C., Moreau, P. and Warawdekar, M.G., Liquid Phase Hydrogenation of Cinnamaldehyde over Supported Ruthenium Catalysts: Influence of Particle Size, Bimetallics and Nature of Support, J. of Mol. Catal., 85, 1993, 215.

Cowan, K.D. and Eisenbraun, E.J., A Convenient Sampling Device for Low Pressure Hydrogenation Vessels, Chem. Ind., 1976, 416.

Cvetanovic, R.J., and Amenomiya, Y., A Temperature Programmed Desorption Technique for Investigation of Practical Catalysts, Catal. Rev.-Sci. Eng., 6, 21(1972)

Dankwerts, P. V., Gas-Liquid Reactions, McGraw-Hill, New York, 1970.

Darensbourg, D.J., Stafford, N.W., Joó, F., and Reibenspies, J.H., Water-Soluble Organometallic Compounds: The Regio-selective Catalytic Hydrogenation of Unsaturated Aldehydes to Saturated Aldehydes in an Aqueous Two-Phase Solvents System Using 1,3,5-Triaza-7-Phosphaadamantantane Complexes of Rhodium, J Organometallic Chemistry, 488, 1995, 99.

Deckwer, W. D., Louisi, Y., Zaidi, A. and Ralek, M., Hydrodynamic Properties of the Fischer-Tropsch Slurry Process, Ind. Eng. Chem. Proc. Des. Dev., 19, 1980, 699.

Deckwer, W.D., Adler I. and Zaid, A., A Comprehensive Study on CO_2-Interphase Mass Transfer in Vertical Cocurrent and Countercurrent Gas Flow, Can. J. Chem. Eng., 56, 1978, 43.

Deckwer, W.D., Bubble Column Reactors, John Wiley and Sons, London, 1992.

Doraiswamy, L.K., and Sharma, M.M., Heterogeneous Reactions, Volume 2, Wiley Interscience, London, 1984.

Dunkel, M., Eckhardt, D. J., and Stern, A., Hydrogenation of Cinnamaldehyde, US Patent 3,520,934, 1970.

Duveen, R. F., Buss Loop Reactor, The Centre for Professional Advancement, 1993.

Eilerman, R.G., Kirk-Othmer Encyclopaedia of Chemical Technology, 3rd Edition, Vol.6, A Wiley-Interscience Publication, 1979, 142.

Eilerman, R.G., Kirk-Othmer Encyclopaedia of Chemical Technology, 4th Edition, Vol.6, A Wiley-Interscience Publication, 1985, 344.

Emmett, P.H., and Brunauer, S., The Use of Low-temperature Van Der Waals Adsorption Isotherms in Determining the Surface Area of Fe Synthetic NH_3 Catalysts,

J. Am. Chem. Soc., 59, 1937, 1553.

Evinc, F., Absorption of Gases in a Cocurrent Downflow Column, MSc Thesis, University of Birmingham, 1982.

Fair, J.R., Designing Gas-sparged Reactors, Chem. Eng. J., 74, 1967, 67.

Falconer, J.C. and Schwarz, J.A., Temperature-Programmed Desorption and Reaction Applications to Supported Catalysts, Catal. Rev.-Sci. Eng., 25, 1983, 141.

Fieser, L.F., and Fieser, M., Organic Chemistry, Reinhold Publishers Corporation, New York, 1956.

Fogler, A.S., Elements of Chemical Reaction Engineering, Prentice-Hall, New Jersey, 1986.

Fouilloux, P., in Heterogeneous Catalysis and Fine Chemicals (M.Guisnet, J. Barrault, C. Bouchoule, D. Duprez, C. Montassier and G. Perot. eds.), Elsevier, Amsterdam, 1988, 23.

Freidel, L., Herbrechtsmeier, P., and Steiner, R., Mean Gas Holdup in Downflow Bubble Columns, Ger. Chem. Eng., 3, 1980, 342.

Frössling, N., The Evaporation of Falling Drops, Gerlands Beitr. Geophysik, 52, 1958, 170.

Fujie, K., Takaine, M., and Kuboto, H., Flow and Oxygen Transfer in Cocurrent Gas-Liquid Downflow, J. Chem. Eng. Japan, 13, 1980, 188.

Gallezot, P., Giroir-Fendler, A. and Richard, D., Chemioselectivity in the Catalytic Hydrogenation of Cinnamaldehyde: Effect of Metal Particle Morphology, Catalysis Letters, 5, 1990, 175.

Gallezot, P., Giroir-Fendler, A., and Richard, D., Chemioselectivity in Cinnamaldehyde Hydrogenation Induced by Shape Selectivity Effects in Pt-Y Zeolite Catalysts, Catalysis Letters, 5, 1990, 169.

Gallezot, P., Giroir-Fendler, A., and Richard, D., Selectivity Control in Cinnamaldehyde Hydrogenation by Metal Catalysts of Precise Structure and Morphology, in "Catalysis of Organic Reactions" (W. Poscoe, ed.), Marcel Dekker, New York, 1991, 1.

Gallezot, P., in "Proceedings of the 6th International Zeolite Conference" (D. Olson and A.Bisio, eds.), Butterworths, Guildford, 1984, 352.

Gallezot, P., Richard, D., and Bergeret, G., in "New Catalytic Materials" (E.T.K. Baker, ed.), ACS Symposium Series, American Chemical Society, Washington, DC, 437, 1990, 150.

Galvagno, S., Capannelli, G., Neri, G., Donato, A., and Pietropaolo, R., Hydrogenation of Cinnamaldehyde over Ru/C Catalysts: Effect of Ru Particle Size, J. Mol. Catal., 64, 1991, 237.

Galvagno, S., Donato, A., Neri, G., and Pietropaolo, R., Liquid Phase Hydrogenation of Benzonitrile over Pt and Pt-Sn Catalysts, J. Mol. Catal., 58, 1990, 215.

Galvagno, S., Donato, A., Neri, G., Pietropaola, R., and Capannelli, G., Selective Hydrogenation of Cinnamaldehyde over Ru-Sn catalysts, J. Mol. Catal., 78, 1993, 227.

Galvagno, S., Donato, A., Neri, G., Pietropaolo, R., and Capannelli, D, Hydrogenation of Cinnamaldehyde over Platinum Catalysts: Influence of Addition of Metal Chlorides, J. of Mol. Catal., 49, 1989, 223.

Galvagno, S., Donato, A., Neri, G., Pietropaolo, R., and Pietropaolo, D., Hydrogenation of Cinnamaldehyde over Platinum Catalysts: Influence of Addition of Metal Chlorides, J. Mol. Catal., 49, 1989, 223.

Galvagno, S., Donato, A., Neri, G., Pietropaolo, R., and Poltarzewski, Z., Nitrobenzene Hydrogenation on Pt-Sn Catalysts, J. Mol. Catal., 42, 1987, 379.

Galvagno, S., Poltarzewski, Z., Donato, A., Neri, G., and Pietropaolo, R., Liquid Phase Hydrogenations over Platinum-Tin Catalysts, J. Chem. Soc., Chem. Commun., 1986, 1729.

Galvagno, S., Poltarzewski, Z., Donato, A., Neri, G., and Pietropaolo, R., Liquid Phase Hydrogenations over Platinum-Tin Catalysts, J. Mol. Catal., 35, 1986, 365.

Gholap, R.V., Kolhe, D.S., and Chaudhari, R.V., A New Approach for the Determination of Liquid-Solid Mass Transfer Coefficients in Multiphase Reactors, Chem. Eng. Sci., 42, 1987, 1689.

Giroir-Fendler, A., Richard, D., and Gallezot, P., Chemioselectivity in the Catalytic Hydrogenation of Cinnamaldehyde: Effect of Metal Particle Morphology, Catalysis Letters, 5, 1990, 175.

Giroir-Fendler, A., Richard, D., and Gallezot, P., Preparation of Pt-Ru Bimetallic Particles on Functionalized Carbon Supports by Co-exchange, J. Chem. Soc., Faraday Discuss., 92, 1991, 69.

Giroir-Fendler, A., Richard, D., and Gallezot, P., Selectivity in Cinnamaldehyde Hydrogenation of Group VIII Metals Supported on Graphite and Carbon, in "Heterogeneous Catalysis and Fine Chemicals" (M. Guisnet, J. Barrault, C. Bouchoule, D. Duprez, C. Montassier and G. Pérot, ed.), Elsevier, Amsterdam, 1988, 171

Goupil, D., Fouilloux, P., and Maurel, R., Activity and Selectivity of Pt-Fe Alloys for the Liquid Phase Hydrogenation of Cinnamaldehyde to Cinnamyl Alcohol, React. Kinet. Catal. Lett., 35,1987, 185.

Govier, G.W. and Aziz, K., The Flow of Complex Mixtures in Pipes, Van Nostrand Reinhold, New York, 1972.

Gray, J.I., and Russell, L.F., Hydrogenation Catalysts-Their Effect on Selectivity, J. Am. Oil Chem. Soc., 56, 1979, 36.

Greenwood, T.S., Loop Reactors for Hydrogenation, Chem. Ind., 3, 1986, 94.

Gregg, S.J., and Sing, K.S.W., Adsorption, Surface Area and Porosity, Academic Press, London, 1967.

Grosselin, J.M., Mercier, C., Allmang, G., and Grass, F, Selective Hydrogenation of α,β-unsaturated Aldehydes in Aqueous Organic Two-Phase Solvent Systems Using

Ruthenium or Rhodium Complexes of Sulfonated Phosphines, Organometallics, 1991, 2126.

Guisnet, M., Heterogeneous Catalysts and Fine Chemicals, Elsevier, Amsterdam, 1988.

Harriot, P., Mass Transfer to Particles, Part I Suspended in an Agitated Tank, AIChE J., 8, 1962, 93.

Herbrechtsmeier, P. and Schafer, H., Development of a Cascade Downflow Reactor as a High Performance Equipment for Physical Absorption and Desorption Processes, Ger. Chem. Eng., 5, 1982, 369.

Herbrechtsmeier, P., Schafer, H. and Steiner, R., Gas Absorption in Downflow Bubble Columns for the Ozone-water System, Ger. Chem. Eng., 4, 1981, 258.

Herbrechtsmeier, P., Schafer, H. and Steiner, R., Influence of Operating Parameters on Interfacial Area in Downflow Bubble Columns, Ger. Chem. Eng., 8, 1985, 57.

Hikita, H., Asai, S., Tanigawa, K., Segawa, K., and Kitao, M., Gas Holdup in Bubble Column, Chem. Eng. J., 20, 1980, 59.

Hills, J.H. and Darton, R.C., The Rising Velocity of a Large Bubble in a Bubble Swarm, Trans. Inst. Chem. Eng., 54, 1976, 248.

Hills, J.H., Radial Nonunformity of Velocity and Voidage in a Bubble Column, Trans. Inst. Chem. Engrs, 52, 1974, 1.

Hills, J.H., The Operation of a Bubble Column at High Throughputs I: Gas Holdup Measurements, Chem. Eng. J., 12, 1976, 89.

Hoffman, N.E., Kanakkanettt, A.T., and Schneider, R.F., Palladium-Catalyzed Decarbonylation of Trans-α-Substituted Cinnamaldehyde, J. Org. Chem., 27, 1962, 2687.

Holfman, H., Reaction Engineering Problems in Slurry Reactors, in "Mass Transfer with Chemical Reaction in Multiphase Systems", Vol.2. Three-Phase Systems (E.

Alper ed.), Nijhoff, Amsterdam, 1983.

Hotta, K., and Kubomatsu, T., Liquid Phase Selective Hydrogenation of An Aliphatic α,β-unsaturated Aldehyde over Raney Cobalt Catalyst Modified with Ferrous Chloride, Bull. Chem. Soc. Japan., 42, 1969, 1447.

Hughmark, G.A., Mass Transfer for Suspended Solid Particles in Agitated Liquids, Chem. Eng. Sci., 24, 1969, 291.

Hularni, A., Shah, Y.T. and Schumpe, A., Hydrodynamics and Mass Transfer in Downflow Bubble Column, Chem. Eng. Commun., 24, 1983, 307.

Innes, W.B., Catalyst Carriers, Promoters, Accelerators, Poisons, and Inhibitors in Catalysis, P.H. Emmett, Reinhold, New York, 1954.

Isaeva, V., Derouault, A., and Barrault, J., Synthesis of Ru, Rh and Pd Complexes Immobilized on Modified Supports: Investigation of the Hydrogenation of Cinnamaldehyde, Bull. Soc. Chim. Fr., 133,1996, 351.

Issacs, B.H., and Petersen, E.E., The Effect of Drying Temperature on the Temperature-Programmed Reduction Profile of a Platinum-Rhenium/Alumina Catalyst, J. Catal., 77, 1982, 43.

Jacbs, P.A., Linart, J-P., Nijs, H., and Uytterhoeven, J.B., Redox Behaviour of Transition Metal Ions in Zeolites. Part 5- Method of Quantitative Determination of Bidisperse Distribution of Metal Particle Sizes in Zeolites, J. Chem. Soc., Faraday Trans. I, 73, 1977, 1745.

Jack, J., Loop Reactor for Bulk Pharmaceuticals, Presented in Novel Chemistry to Neat Process, Nottingham, March 1996.

Jiang, X., Li, B., Zhang, L., Fundamentals of Theories and Applications of Gas-Liquid Reactions, Hydrocarbon Process Press, Beijing, 1990.

Johnson, A.I. and Huang, C.J., Mass Transfer Studies in an Agitated Vessel, AIChE J.,

2, 1965, 412.

Joshi, J.B. and Sharma, M.M., Mass Transfer Characteristics of Horizontal Sparged Contactors, Trans. IChemE., 54, 1976, 42.

Joshi, J.B., Pandit, A.B. and Sharma, M.M., Mechanically Agitated Gas-Liquid Reactors, Chem. Eng. Sci., 37, 1982, 813.

Kastanek, F., Kratochvil, J., and Rylek, M., Mass Transfer Coefficient in Bubble Reactors without Mechanical Mixing, Column., Coll. Czechoslov. Chem. Commun., 42, 1977, 3459.

Katayama, M., Mukai, Y., and Taniguchi, H., High Performance Liquid Chromatographic Determination of Cinnamaldehyde, Analysis, 115, 1990, 9.

Kato, Y. and Nishiwaki, A., Longitudinal Dispersion Coefficient of a Liquid in a Bubble Column, Int. Chem. Eng., 12, 1972, 182.

Kato, Y., Fukuda, T., and Tanaka, S., The Behaviour of Suspended Particles and Liquid in bubble Columns, J. Chem. Eng. Japan, 5, 1972, 112.

Khan, Z., Catalytic Hydrogenation in a Cocurrent Downflow Contactor Reactor, PhD Thesis, University of Birmingham, 1995.

Kirkwood, R.C. and Longley, A.J., Clean Technology and the Environment, Blackie Academic and Professional, London, 1994.

Kirkwood, R.C., Environment and Human Influence, in "Clean Technology and The Environment" (R.C. Kirkwood and A.J. Longley, eds.), Blackie Academic and Professional, London, 1994.

Kolbel, H., Borcherers, E. and Langemann, H., Größenverteilung der Gas-blasen in Blasensäulen, Chem.-Ing.-Tech., 33, 1961, 668.

L'Homme, G.A., Introduction to Gas-Liquid-Solid Systems, in "Mass Transfer with Chemical Reaction in Multiphase Systems", Vol.2. Three-Phase Systems (E. Alper ed.), Nijhoff, Amsterdam, 1983.

Lee, H.H., Heterogeneous Reactor Design, Butterworth Publishers, Boston, 1985.

Leuteritz, G.M., Increasing the Profitability of Gas-Liquid Reactions through the Use of Loop Reactor Plants, Presented at International Meeting for Chemical Technology ACHIEMA 85, 13th June, Frankfurt, Germany, 1985.

Levenspiel, O., Chemical Reaction Engineering, 2nd Edition, John Wiley and Sons, New York, 1972.

Levich, G., Physicochemical Hydrodynamics, Prentice-Hall, New York, 1962.

Levins, D.M., and Glastonbury, J.R., Applications of Kolmogoroff's Theory to Particle-Liquid-Mass Transfer in Agitated Vessels, Chem. Eng. Sci., 27, 1972, 537.

Li, G., Li, T., and Xu, Y., Pt/ML (M = Rb, Sr) as Highly Selective and Active Catalysts for Cinnamaldehyde Hydrogenation to Cinnamyl Alcohol, J. Chem. Soc., Chem. Commun., 1996, 497.

Linek, V., and Vacek, V., Chemical Engineering Use of Catalysed Sulphite Oxidation Kinetics for the Determination of Mass Transfer Characteristics of Gas-Liquid Contactors, Chem. Eng. Sci., 36, 1991, 1747.

Lockett, M.J., and Kirkpatrick, R.D., Ideal Bubbly Flow and Actual Flow in Bubble Columns, Trans. Inst. Chem. Engrs., 53, 1975, 267.

Lu, X.X., A Study of the Characteristics of a Novel Cocurrent Downflow Bubble Column Contactor for Use as a Three Phase Reactor, PhD Thesis, University of Birmingham, 1988.

Lu, X.X., Boyes, A.P., and Winterbottom, J.M., Operating and Hydrodynamic Characteristics of a Cocurrent Downflow Bubble Column Reactor, Chem. Eng. Sci., 49, 1994, 5719.

Luong, H.T., and Volesky, B., Mechanical Power Requirements of Gas-Liquid Agitated Systems, AIChE J., 25, 1979, 893

Marinelli, T. B. L. W., Vleeming, J. H. and V. Ponec, Reactions of Multifunctional

Organic Compounds-hydrogenation of Acrolein of Modified Pt-Catalysts, Proceedings of the 10th International Congress on Catalysis, 19-24 July, 1992, 1211.

Marsh, K. N., Wilhoit, R. C., and Gammon, B. E., TRC Thermodynamic Tables : Non-Hydrocarbons, Thermodynamics Research Centre, Texas, 1993.

Martin, G.O., Gas-Inducing Agitator, Ind. Eng. Chem. Proc. Des. Dev., 11, 1972, 397.

Maxted, E.B., and Akhtar, S., Metallic Salts as Promoters in Hydrogenation with Platinum Oxide Catalysts, J. Chem. Soc., Chem. Commun., 1959, 3130.

Maxted, E.B., The Poisoning of Metallic catalysts, Adv. Catal., 3, 1951, 129.

Maxwell, J.B., Data Book on Hydrocarbons: Application to Process Engineering, D. Van Nostrand Company, New York, 1982.

McMurry, J., Organic Chemistry, Second Edition, Brooks/Cole Publisher, California, 1988.

Mercadante, L., Neri, G., Milone, C., Donato, A. and Galvagno, S., Hydrogenation of α, β-unsaturated Aldehydes over Ru/Al_2O_3 Catalysts, J. Mol. Catal., 105, 1996, 93.

Middleton, J.C., Gas-Liquid Dispersion and Mixing, in "Mixing in the Process Industries" (N. Harnby, M.F. Edwards, And A.W. Nienow ed.), Butterworth, London, 1985.

Miller, D.N., Gas Holdup and Pressure Drop in Bubble Column Reactor, Ind. Eng. Chem. Proc. Des. Dev., 19, 1980, 371.

Millman, W.S., and Smith, G.V., in "Catalysis in Organic Synthesis"(G.V. Smith, Ed.), Academic Press, New York, 1977.

Minot, C., and Gallezot, P., Competitive Hydrogenation of Benzene and Toluene--Theoretical Study of Their Adsorption on Ruthenium, Rhodium, and Palladium, J. Catal., 123, 1990, 341.

Miyauchi, T., and Shyu, C.N., Flow of Fluids in Gas-Liquid Columns, Kagaku

Kogaku, 34, 1970, 958.

Mongold, E.C., Coal Liquefaction and Gasification Technology, Ann Arbor Science, 1992.

Murthy, A,.K.S., Design of Agitated Tank Reactors, The Centre for Professional Advancement, 1993.

Nagata, S., Mixing Principles and Applications, Wiley, New York, 1975.

Nagel, O., and Kurten, H., Untersuchungen zum Dispergieren im Turbulenten Scherfeld, Chem. Ing. Tech., 48, 1976, 513.

Nagel, O., Kurten, H., and Hegner, B., Design of Gas-liquid Reactor: Mass Transfer Area and Input of Energy from Two-Phase Momentum, Heat, and Mass Transfer in Chemical Process and Energy Engineering Systems, ed. F. Durst, G. U.Tsiklauri, and N.H. Afgan, Hemisphere Publisher,, 1979, 835.

Nemerow, N. L. and Dasgupta, A., Industrial and Hazardous Waste Water Treatment, Van Nostrand Reihold, New York, 1991.

Neri, G., Milone, C., Donato, A., Mercadante, L. and Visco, A. M., Selective Hydrogenation of Citral over Pt-Sn Supported on Activated Carbon, J. Chem. Tech. Biotechnol., 60, 1991, 83.

Nienow, A.W., Agitated Vessel Particle-Liquid Mass Transfer: A Comparison between Theories and Data, Chem. Eng. J., 9, 1975, 153.

Nishikawa, M., Yonezawa, Y., Kayama, T., Koyama, K., and Nagata, S., Study on Gas Holdup in Gas-Liquid Sprouted Vessel, J. Chem. Eng. Japan, 9, 1976, 214.

Nitta, Y., Hiramatsu, Y., and Imanaka, T., Effects of Preparation Variables of Supported-Cobalt Catalysts on the Selective Hydrogenation of α,β-unsaturated Aldehydes, J. Catal., 126, 1990, 235.

Nitta, Y., Ueno, K., and Imanaka, T., Selective Hydrogenation of α,β-unsaturated Aldehydes on Cobalt-Silica Catalysts Obtained from Cobalt Chrysotile, Appl. Catal.,

56, 1989, 9.

Noller, N. and Lin, W.M., Activity and Selectivity of Ni-Cu/Al_2O_3 Catalysts for Hydrogenation of Crotonaldehyde and Mechanism of Hydrogenation, J. Catal., 85, 1984, 25.

Nottenkamper, R., Steiff, A. and Weinspach, P.M., Experimental Investigation of Hydrodynamics of Bubble Columns, Ger. Chem. Eng., 6, 1983, 147.

Ohkawa A, Bubble Size, Interfacial area and Volumetric Liquid-Phase Mass Transfer Coefficient in Downflow Bubble Columns With Gas Entertainment by a Liquid Jet, J. Chem. Eng. Japan, 20, 1987, 99.

Ohkawa, A., Gas Holdup in Downflow Bubble Column with Gas Entrainment by a Liquid Jet, J. Chem. Eng. Japan, 18, 1985, 172.

Oldshue, J.Y., Mixing in Hydrogenation Processes, Chem. Eng. Prog., 76, 1980, 60.

Patterson, H. B. W., Hydrogenation of Oil and Fats, Applied Science, London, 1983.

Pauling, L., The Chemical Bond, Cornell University Press, Ithaca, New York, 1967.

Perry, R.H., and Chilton, C.H., Chemical Engineers Handbook, 5th ed. McGraw Hill, New York, 1984.

Perry, R.H., and Green, P. Chemical Engineers Handbook, 6th ed. McGraw Hill, New York, 1988.

Phillips, J., Gallezot, P., and Bergeret, G., Cinnamaldehyde Hydrogenation: Dual Catalytic Chemistry of Iron-Rhodium/Grafioil Catalysts, J. Mol. Catal., 78, 1993, 295.

Poltarzewski, Z., Galvagno, S., Pietropaolo, R., and Staiti, P., Hydrogenation of α,β-unsaturated Aldehydes over Pt-Sn/nylon, J. Catal., 102, 1986, 190.

Poscoe, W. E. and Stenberg, J.F., in "Catalysis in Organic Synthesis" (W.H. Jones ed.), Academic Press, New York, 1980.

Quicker, G. and Deckwer, W.D., Gasgehalt und Phasengrenzfläche in Begasten

Kohlenwasserstoffen, Chem.-Ing.-Tech., 53, 1981, 474.

Rajadhyahsha, R.A., and Karwa, S. L., Solvent Effects in Catalytic Hydrogenation, Chem. Eng. Sci., 41, 1986, 1765.

Ram, N. M., Christman, R.F. and Cantor, K. P., Significance and Treatment of Volatile Organic Compounds in Water Suppliers, Lewis Publishers, Michigan, 1990.

Ramachandran, P. A. and Chandhari, R.V., Three Phase Catalytic Reactors, Gordon & Breach Science Publication, New York, 1983.

Ranz, W.E. and Marshall, W.R., Evaporation from Drops, Chem. Eng. Prog., 48, 1952, 141.

Raymahasay, S., Report on Triglyceride Hydrogenation in a Cocurrent Downflow Contactor, SERC Report, School of Chemical Engineering, University of Birmingham, 1989.

Reith, T., Renken, S., and Israel, B.A., Gas Holdup and Axial Mixing in the Fluid Phase of Bubble Columns, Chem. Eng. Sci., 23, 1968, 619.

Richard, D., and Gallezot, P., in "Preparation of Catalysts", Vol. IV (B. Delmon, P. Grange, P.A. Jacobs, and G. Poncelet, eds.), Elsevier, Amsterdam, 1987, 71.

Richard, D., Fouilloux, P., and Gallezot, P., Proceedings of the 9th International Congress on Catalysis, Calgary (eds.: M.J. Phillips and M. Ternan), vol.3, 1988, 1074.

Richard, D., Fouilloux, P., and Gallezot, P., Proceedings of the 8th International Congress on Catalysis, Verlag Chemie, Weinheim, 1984, 659.

Richard, D., Gallezot, P., Neibecker, D., and Tkatchenko, I., Characterization and Selectivity in Cinnamaldehyde Hydrogenation of Graphite-Supported Platinum Catalysts Prepared from Zero-Valent Platinum Complex, Catal. Today, 6, 1989, 171.

Richard, D., J. Ockelford, A. Giroir-Fendler and P. Gallezot, Composition and Catalytic Properties in Cinnamaldehyde Hydrogenation of Charcoal-Supported , Platinum Catalysts Modified by $FeCl_2$ Additives, Catalysis Letters, 3, 1989, 53.

Richardson, J.T., Principles of Catalyst Development, Plenum, New York, 1989.

Rylander, P. N., Catalysts in Use: Catalytic Hydrogenation over Noble Metals, AIChE J., 1980, 46.

Rylander, P. N., Himelstein, N., and Kilroy, M., Hydrogenation of α,β-unsaturated Aldehydes, Engelhard Ind. Tech. Bull., 4, 1963, 49.

Rylander, P.N. and Greenfield, Catalysis in Organic Synthesis, Academic Press, New York, 1977.

Rylander, P.N., and Himelstein, N., Selective Hydrogenation of α,β-Unsaturated Aldehydes, Engelhard Ind. Tech. Bull., 4, 1963, 131.

Rylander, P.N., and Steele, D.R., Selectivity in Platinum Metal Catalysed Hydrogenations, Engelhard Ind. Tech. Bull., 5, 1965, 113.

Rylander, P.N., Catalytic Hydrogenation in Organic Syntheses, Academic Press, New York, 1979.

Rylander, P.N., Catalytic Hydrogenation over Platinum Metals, Academic Press, New York, 1967.

Rylander, P.N., Hydrogenation Methods, Academic Press, New York, 1990.

Sarmento, S.M., A Systemic Investigation of the Hydrodynamic and Mass Transfer Characteristics of the Co-current Downflow Contactor Operation in Fixed Bed Mode, PhD Thesis, University of Birmingham, 1995.

Satagopan, V. and Chandalia, S.B., Selective Aspects In The Multi-Phase Hydrogenation Of α,β-Unsaturated Aldehydes Over Supported Noble Metal Catalysts: Part I, J. Chem. Tech. Biotechnol., 59, 1994, 257.

Satagopan, V. and S. B. Chandalia, Selective Aspects in the Multi-Phase Hydrogenation of α,β- unsaturated Aldehydes over Supported Noble Metal Catalysis: Part II., J. Chem. Tech. Biotechnol., 60, 1994, 17.

Satterfield, C.N., Mass Transfer in Heterogeneous Catalysis, MIT Press, Cambridge, 1970.

Schröder, U., and Andersson B., Influence of Oxygen in the Gas Phase Hydrogenation of 2-Ethyl-Hexaenal, J. Catal, 132, 1991, 402.

Schröder, U.and L.D. Verdier, Influence of Oxygen and Iron in the Liquid-Phase Hydrogenation of α,β- unsaturated Aldehydes, J Catal., 142, 1993, 490.

Shah, Y. T., Gas-Liquid-Solid Reactor Design, McGraw-Hill, New York, 1979.

Shah, Y. T., Kelkar, B. G., Godbole, S.P., and Deckwer, W. D., Design Parameter Estimation for Bubble Column Reactors, AIChE J., 28, 1982, 353.

Shah, Y. T., Stiegel, G.J. and Sharma, M.M., Backmixing in Gas-Liquid Reactors, AIChE J., 24, 1978, 369.

Shah, Y.T., Kulkarni, A.A., Weiland, J.H. and Carr, N.L., Gas Holdup in Two- and Three-Phase Downflow Bubble Columns, Chem. Eng. J., 26, 1983, 95.

Smith, J.M., Chemical Engineering Kinetics, McGraw Hill, New York, 1981.

Steiner, R., Operating Characteristics of Special Bubble Column Reactors, Chem. Eng. Progress, 21, 1987, 1.

Stiles, A.B., Catalyst Manufacture: Laboratory and Commercial Catalyst Preparations, Marcel Deckker Inc, New York, 1993.

Subba Rao, D. and Taneja, V.K., Third European Conference on Mixing, April 1979.

Suckling, C.J., Halling, P.J., Kirkwood, R.C. and Bell, G., Clean Synthesis of Effect Chemicals, SERC Clean Technology Unit, Swindon, 1992.

Sulidis, A. T., Application of the Cocurrent Downflow Bubble Column Contactor (CDC) for Use as a Photocatalytic Reactor and Assorted Mass Transfer Studies, PhD Thesis, University of Birmingham, 1995.

Tarhan, M.M., Catalytic Reactor Design, McGraw Hill , New York, 1983.

Tauster, S.J., Fung, S.C., and Garten, R.L., Strong Metal-Support Interactions: Group VIII Noble Metals Supported on TiO_2, J. Am. Chem. Soc., 100, 1978, 170.

Tilston, M.W., The Development of a Swirlflow CDC, PhD Thesis, University of Birmingham, 1990.

Timmermans, J., Physico-chemical Constants of Pure Organic Compounds, New York, Elsevier Publishing Company, 1950.

Treybal, R.E., Mass Transfer Operations, Third Edition, McGraw Hill, 1981.

Tronconi, E., Crisafulli, C., Galvagno, S., Donato, A., Neri, G., and Pietropaolo, R., Kinetics of Liquid-Phase Hydrogenation of Cinnamaldehyde over a Pt-Sn/ Nylon Catalyst, Ind. Eng. Chem. Res. 29, 1990, 1766.

Tuley, W. F., and Adams, R.J., Reduction of Cinnamaldehyde to Cinnamic Alcohol in the Presence of Platinum Oxide-Platinum Black and Promoters, J. Am. Chem. Soc., 45, 1925, 3061.

Turner, E.E, and Harris, M.M., Organic Chemistry, Longman, New York, 1952, 74.

Vannice, M.A., and Sen, B., Metal Support Effects on the Intramolecular Selectivity of Crotonaldehyde Hydrogenation over Platinum, J. Catal., 115, 1989, 65.

Vasalos, I.A., Bild, E.M., Rundell, D.N. and Tatterson, D.F., Experimental Techniques for Studying Fluid Dynamics of H-COAL Reactor, Coal Processing Technology, CEP Technical Manual, 6, 1980, 226.

Wagstaff, N., Prins, R., Alloy Formation and Metal Oxide Segregation in Pt-Re/γ-Al_2O_3 Catalysts as Investigated by Temperature-Programmed Reduction, J. Catal., 59, 1979, 434.

Wallis, G.B., One-Dimensional Two-Phase Flow, McGraw Hill, New York, 1969.

Weiseiler, W. and Rösch, S., Interfacial Area and Bubble Size Distribution in Gas/Liquid Jet Reactor, Ger. Chem. Eng., 1, 1978, 212.

Whitmore, F.C., Organic Chemistry, D Van Nostrand Company Inc., New York, 1955, 199.

Wiemeijer, A., Kieboom, A.P.G., and Bekkum, H. van, Selective Hydrogenation of Citronellal to Citronellol over Ru/TiO_2 as Compared to Ru/SiO_2, Appl. Catal. 25, 1986, 181.

Willett, J.E., Gas Chromatography, Wiley, New York, 1988.

Winterbottom, J.M., Private Communication, The University of Birmingham, 1998.

Yagi, H. and Yoshida, F., Gas Absorption by Newtonian and Nonnewtonian Fluids in Sparged Agitated Vessels, Ind. Eng., Chem. Proc. Des. Dev., 14, 1975, 488.

Yamagiwa, K., Kusabiraki, D. and Ohkawa, A., Gas Holdup and Gas Entrainment Rate in Downflow Bubble Column with Gas Entrainment by a Liquid Jet Operating at High Liquid Throughput, J. Chem. Eng. Japan, 23, 1990, 22.

Yong, C.L., Solubility Data Series, Volume 5/6, Hydrogen and Deuterium, Pergamon Press, Oxford, 1981.

Yoshida H,. and Iwasawa, Y., Cooperative Behaviour of Two Kinds of Reaction Sites and Reaction Mechanisms for Deuteration of Acrolein on SMSI-Pt/Nb_2O_5 Catalysts, J. Catal., 125, 1990, 227.

Young, D.M., and Crowell, A.D., Physical Adsorption of Gases, Butterworths, London, 1962.

Yu, W-Y., Liu, H.F, and Tao, Q., Modification of Metal Cations to Metal Cluster in Liquid Medium, J. Chem. Soc., Chem. Commun., 1996, 1773.

Yung, C.N., Wong, C.W. and Chang, C. L., Gas Holdup and Aerated Power Consumption in Mechanical Stirred Tanks, Can. J. Chem. Eng., 57, 1979, 672.

Zahrandnik, J. and Kastanek, F., Gas Holdup in Uniformly Aerated Bubble Column Reactors, Chem. Eng. Commun., 3, 1979, 413.

Zhang, L. and Li, B., Effect of Temperature and Electrolyte on Gas Holdup, Chemical Reaction Engineering and Technology, 6, 1990, 103

Zhang, L. Zhou, R., Jiang, X., Li, B. and Zu Y. , Studies on Gas Holdup in a Bubble Column Operated at Elevated Temperatures, Ind. Eng. Chem. Res., 27, 1988, 1910.

Zhang, L., Experimental Results, Private Communication with Dr J. M. Winterbottom, University of Birmingham, 1995.

Zhang, L., Experimental Results, Private Communication with Dr J. M. Winterbottom, University of Birmingham,1996.

Zhang, L., Winterbottom, J.M. and Boyes, A,P., Raymahasay, S., Studies on Catalytic Hydrogenation of Cinnamaldehyde over Pd/C Catalysts, J. Chem. Tech. Biotechnol., 72, 1998, 264.

Zhang, L., Winterbottom, J.M. and Boyes, A.P., Catalytic Hydrogenation of Cinnamaldehyde over Pd/C in a Stirred Tank Reactor, EuropaCAT-II, MAASTRICH, 3-8 September 1995.

Zhang, L., Winterbottom, J.M. and Boyes, A.P., Selective Hydrogenation of Cinnamaldehyde over Pd/C with Metal Promoters, The 1997 Jubilee Research Event, Nottingham, 7-9 April 1997.

Zhang, L., Winterbottom, J.M. and Boyes, A.P., Studies on Catalytic Hydrogenation of Cinnamaldehyde, Clean Tech, London, 19-21 June 1996.

Zwietering, T.N., Suspending of Solid Particles in Liquid by Agitators, Chem. Eng. Sci., 8, 1958, 244.